



## SOCIAL SUPPORT AND MENTAL HEALTH OF EMPLOYEES

Dr Mallikarjun H. Krishnakar  
PDF Fellow, Dept. of Psychology, Gulbarga  
University, Kalaburagi.

### ABSTRACT:

*The aim of the present study is to examine the Influence of Social Support on Mental Health of Employees selected from Gulbarga District. The Sample consists of 200 (of different occupations and gender) employees. The sample was administered with Social support questionnaire and Mental Health Inventory. And the data were subjected the t-test. The results revealed that social support produces differences in mental health of employees and there is a significant difference in Mental Health between the male and female sample.*

**KEYWORDS :** Mental Health , male and female sample.

### INTRODUCTION:

Social support is a concept that is generally understood in an intuitive sense, as the help from other people in a difficult life situation. One of the

first definitions was put forward by (Cobb, 1976). He defined social support as 'the individual belief that one cared for and loved, esteemed and valued, and belongs to a network of communication and mutual obligations'.

Social Support is one of the most important factors in predicting the physical health and well-being of everyone, ranging from childhood through older. The absence of social support shows some disadvantage among the impacted individuals. In most cases, it can predict the deterioration of physical and mental health among the victims.

The Oxford dictionary defines support, in part, as to keep from falling or giving way, give courage, confidence, or power of endurance to apply with necessities. What presumably social support from the border concept is that it necessarily involves the presence and products of stable human relationships.

The initial social support given is also a determining factor in successfully overcoming life stress. The presence of social support significantly predicts the individual's ability to cope with stress. Knowing that they are valued by others is an important psychological factor in helping them to forger the negative aspects of their thinking more positively about their environment. Social support not only helps to improve a person's well-being, it affects the immune system as well.

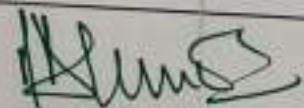
According to WHO (1974), "Health is not merely the absence of disease, but a state of complete physical, mental, spiritual and social well being. This definition seems to equate health with all round well being. It highlights health as a positive goal rather than just a neutral state of 'no disease' and indicates that this is to be achieved by personal and social change as well as by medical advance. As a definition, it contains almost as many new problems as it tries to solve. Its idealistic, even utopian nature

Available online at [www.lbp.world](http://www.lbp.world)

S. G. Gomballi

**IQAC Co-ordinator**

Smt. V.G. Women's Degree College  
KALABURAGI



**PRINCIPAL**

Smt. V.G. Degree College for Women  
GULBARGA



SELF-CONCEPT AND EMOTIONAL INTELLIGENCE OF STUDENTS

Dr. Mallikarjun H. Krishnakar

PDF Fellow, Dept.of Psychology, Gulbarga University, Kalaburagi.

ABSTRACT:

The major aim of the present study was to assess the Self-concept and Emotional intelligence of Degree college student. The sample of 100 (50 Boys Girls & 50 Government private students) students was chosen from Gulbarga district on whom the Self-Concept and Emotional intelligence Scales were administered. After scoring, the data were subjected to t-test. The results revealed that there is significant difference in Self-concept and Emotional intelligence of the sample subgroups. The study also revealed significant gender differences in the amount of self-concept and Emotional intelligence.

KEYWORDS: Emotional intelligence , Self-concept.

1. INTRODUCTION:

A. Self-Concept:

The self-concept is the accumulation of knowledge about the self, such as, beliefs regarding personality traits, physical characteristics, abilities, values, goals, and roles. Beginning in infancy, children acquire and organize information about them as a way to enable them to understand the relation between the self and their social world. This developmental process is a direct consequence of children's emerging cognitive skills and their social relationships with both family and peers.

During early childhood, children's self-concepts are less differentiated and are centered concrete characteristics, such as physical attributes, possessions, and skills. During middle childhood, the self-concept becomes more integrated and differentiated as the child engages in social comparison and more clearly perceives the self as consisting of internal, psychological characteristics. Throughout later childhood and adolescence, the self-concept becomes more abstract, complex, and hierarchically organized into cognitive mental representations or self-schemas, which direct the processing of self-relevant information.

Self-concept is one of the most important variables within the motivational (Núñez, Pienda González-García, González-Pumariega, Rods, Alvarez and González Torre, 1998). As noted by Malo, Bataller, Houses, Gras and Gonzalez (2011), the self is a psychological construct studied from almost all areas of psychology (Baumeister, Campbell, Krueger and Vohs, 2003; Gergen, 1984, Palacios and Zabala, 2007, Stevens 1996). Thus, Sanchez (2009) believes that the self is responsible for many successes and failures, as it promotes a positive self-esteem, promoting safety and personal trust to develop skills. Broadly speaking, we could identify components are self-knowledge (Sanchez, 2009): (a) recognize what emotions you are feeling and why they feel, (b) Understanding the links between thoughts, feelings, words and actions; (c) Understand how emotions influence the performance and actions, (d) Know the intra-personal characteristics, that is, the ethical and moral values, goals, etc.. (E) Identify interpersonal skills, and finally, (f) Recognize attitudes and behavioral characteristics.



Available online at www.ibp.world

S.G. Gounbali

IQAC Co-ordinator

Smt. V.G. Women's Degree College

KALABURAGI

[Handwritten signature]

PRINCIPAL

Smt. V.G. Degree College for Women  
GULBARGA



# ĀRYAVĀIDYAN

A QUARTERLY JOURNAL ON AYURVEDA AND ALLIED SCIENCES

ISSN 0970 - 4006

Vol. XXXI, No. 2

November 2017 - January 2018



लाभानां श्रेय आरोग्यम्  
*Of all the gifts,  
the most precious is health*

*S. G. Gonnaballi*

**IQAC Coordinator**  
Smt. Veeramma Gangasiri  
College for Women  
Kalaburagi - 585 102



Vaidyaratnam P.S. Varier's  
**Arya Vaidya Sala, Kottakkal, Kerala**

*[Handwritten Signature]*

**PRINCIPAL**  
Smt. Veeramma Gangasiri  
College for Women  
Kalaburagi - 585 102



# Study on macro and micro nutrients content in the leaves of *Murraya koenigii* (L.) Spreng.

Mohanraj Pattar, Santoshkumar Teerthe, Ashwini A. and Kerur B. R.

**ABSTRACT:** A macro and micro nutrients content analysis was carried out in leaves of *Murraya koenigii* (L.) Spreng., an indigenous medicinal plant, collected from different places of North Karnataka. The leaves were digested with Conc. HCl, deionized water and ash (25:25:1:950) and the contents of macro and micro nutrients and harmful heavy metals such as Potassium (K), Calcium (Ca), Magnesium (Mg), Iron (Fe), Molybdenum (Mo), Copper (Cu), Manganese (Mn), Zinc (Zn), Aluminium (Al), Vanadium (V), Cadmium (Cd) and Titanium (Ti) were determined by analytical Atomic absorption spectrometry (AAS) technique. The experimental results confirmed the presence of mineral nutrients which are beneficial to the human body, within limits. The heavy metals like Cd and Al, which are harmful to human body were within the limits but concentration of Al was absent in the leaves collected from Shahapur and Kappathgudda. The data obtained in this study may help in the synthesis of new drugs with various combinations of plants that can cure many diseases.

**Key words:** *Murraya koenigii* (L.) Spreng., Macro and Micro nutrients, Atomic absorption spectroscopy.

## Introduction

Medicinal plants are the richest bioresource of drugs of traditional systems of medicine. They play an important role in meeting the global health care needs. Medicinal plants supply minerals, vitamins and certain hormone precursors in addition to protein and energy to the body.<sup>1,2</sup> According to the survey reported by World Health Organization (WHO), about 80% of the world's population depends the traditional medicinal plants in direct or indirect ways to overcome their illness. The traditional medicine system uses indigenous medicinal plants widely as home remedies to improve the health and to prevent or cure various life style disorders. It depends on the mineral nutrient contents of the plants. The concentration level of the mineral nutrients in the plant plays an important role in chemical, biological, biochemical, metabolic, catabolic and enzymatic reactions in the living organism which will lead to the formation of active organic constituents<sup>3</sup> and these mineral nutrients by the geochemical characteristics of the soil and environmental

conditions.<sup>4</sup> During the past few decades, a significant increase in the use of traditional medicine is seen due to their minimal side effect, easy availability and acceptability.<sup>5</sup>

Essential macro and micro nutrients in indigenous medicinal plants have been investigated by many researchers to strengthen the importance of mineral nutrients content analysis with respect to human health.<sup>6</sup> Macro nutrients include carbohydrates, fats and proteins which are the structural and energy giving caloric components. Whereas the micro nutrients are the vitamins, minerals, trace elements, phytochemicals and antioxidants.

Human body requires a number of mineral nutrients to maintain a good health.<sup>7</sup> In this context several attempts have been made to determine the mineral nutrient contents of indigenous medicinal plants using different elemental analysis techniques from various countries all over the world.<sup>8</sup>

In the present study, leaves of *Murraya koenigii* Spreng., a commonly available garden plant was

S. V. Gounkhal  
IOAO Coordinator  
Smt. Veeramma Gangasiri  
College for Women  
Kalaburagi - 585 102

PRINCIPAL  
Smt. Veeramma Gangasiri  
College for Women  
Kalaburagi - 585 102

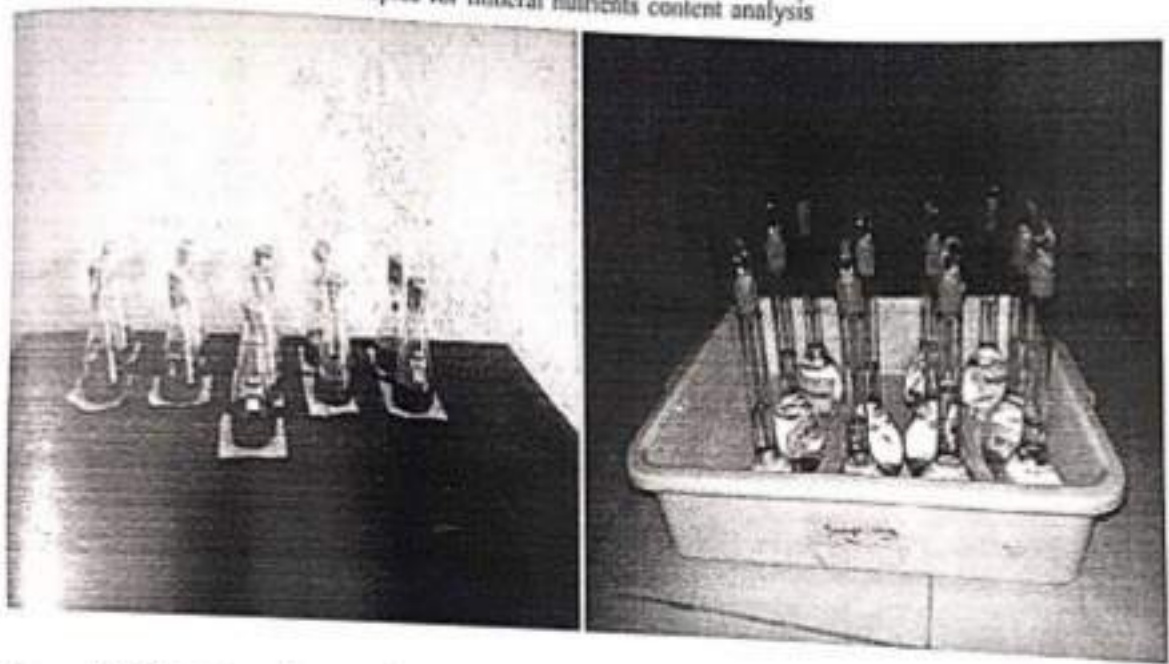




concentrated HCL, double distilled water and 1gm of ash in the ratio 25: 25:1. The mixed solution was then stirred for few minutes and was then filtered using Whatman filter paper 41. A 950 ml of double distilled water was added to the filtered solution to make it 1000 ml solution. The same procedure was repeated for all other plant material samples. (The prepared solutions are as shown in Figure 3) The same solution was used for the measurement of mineral nutrients content analysis using AAS technique.

Determination of elements: The mineral nutrients such as K, Ca, Mg, Fe, Mo, Cu, Mn, Zn, Al, V, Cd and Ti in the leaves of *Murraya koenigii* (L.) Spreng. plant samples were analyzed using analytical atomic absorption spectrophotometer. It is manufactured by Thermo Scientific™ with a model No. i CETM-3000 series and it is equipped with dedicated flame, furnace or combined flame and furnace option. Air-C<sub>2</sub>H<sub>2</sub> and N<sub>2</sub>O-C<sub>2</sub>H<sub>2</sub> flame was used for determination mineral nutrients content. The instrument was operated with

Figure 3  
Samples for mineral nutrients content analysis



conditions shown in Table 1. Calibration has been carried out using different hollow-cathode lamps for Al, Cu, Mg, Zn, and Cd employed as radiation source and calibrated using 100 ml standard solutions in equal ratio. A detector measures the wavelengths of light transmitted by the sample, and compares them to the wavelengths which originally passed through the sample. Atoms of each element will emit a characteristic spectral line. Every atom has its own distinct pattern of wavelengths at which it will absorb energy, due to the unique configuration of electrons in its outer shell. This enables the qualitative analysis of a sample. The absorption wavelength for the detection of each element within its linear working

range and correlation coefficient was calibrated for the analysis. A monochromator was used to select the specific wavelength of light that is absorbed by the sample and to exclude other wavelengths. The selection of the specific wavelength of light allows for the determination of the specific element of interest when it is in the presence of other elements. Figure 4 shows the instrument processes of an atomic absorption spectrometer.

**Results and discussion**

Table 2, 3 and 4 shows the concentrations of essential macro nutrients, essential micro nutrients and harmful heavy metals measured in the leaves of *Murraya koenigii* (L.) Spreng.

Smt. Veeramma Gangasiri  
IQAC Coordinator  
Smt. Veeramma Gangasiri  
College for Women  
Kalaburagi - 585102

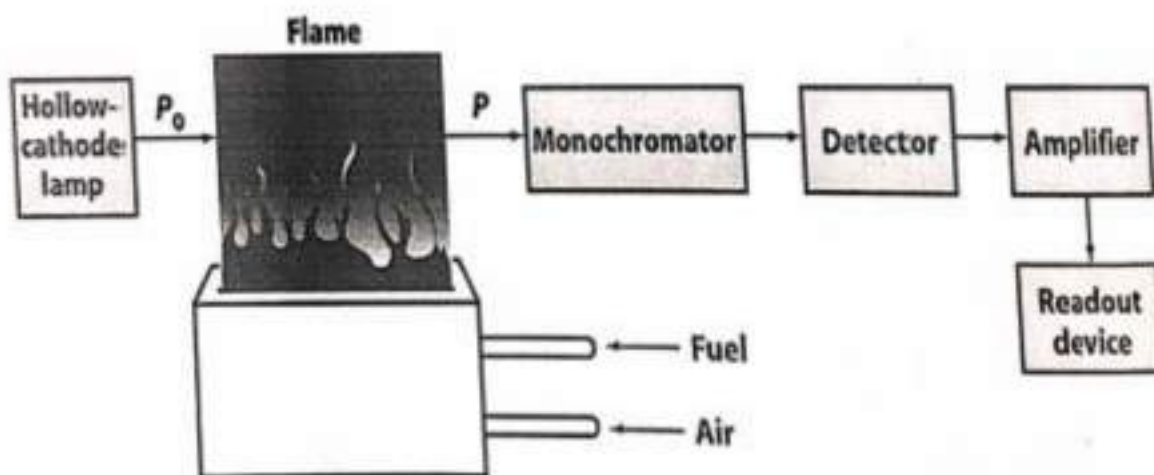
Smt. Veeramma Gangasiri  
PRINCIPAL  
Smt. Veeramma Gangasiri  
College for Women  
Kalaburagi - 585102



Table 1  
Operating parameter for working elements

Elements Flow	Wavelength (nm)	Slit width (nm)	Lamp Current	Flame Type	Fuel Flow (L/min)	Characteristic Conc. (mg/L)	Burner Height (mm)
Mg	285.2	0.5	75%	Air-C <sub>2</sub> H <sub>2</sub>	1.2	0.0170	7
Al	309.3	0.5	100%	N <sub>2</sub> O-C <sub>2</sub> H <sub>2</sub>	4.3	12.0442	11
K	766.5	0.5	100%	Air-C <sub>2</sub> H <sub>2</sub>	1.2	0.0567	7
Mn	279.5	0.2	75%	Air-C <sub>2</sub> H <sub>2</sub>	1.0	0.0860	7
Fe	248.3	0.5	75%	Air-C <sub>2</sub> H <sub>2</sub>	0.9	0.2344	7
Cr	357.9	0.5	100%	N <sub>2</sub> O-C <sub>2</sub> H <sub>2</sub>	4.2	0.6196	8
Ca	422.7	0.5	100%	N <sub>2</sub> O-C <sub>2</sub> H <sub>2</sub>	4.2	0.2340	11
Cu	324.8	0.5	75%	Air-C <sub>2</sub> H <sub>2</sub>	1.1	0.1119	7
Zn	213.9	0.2	75%	Air-C <sub>2</sub> H <sub>2</sub>	1.2	0.0333	7
Cd	228.8	0.5	50%	Air-C <sub>2</sub> H <sub>2</sub>	1.2	0.0344	7
Si	251.6	0.5	75%	N <sub>2</sub> O-C <sub>2</sub> H <sub>2</sub>	4.9	2.698	11
Mo	313.3	0.5	75%	N <sub>2</sub> O-C <sub>2</sub> H <sub>2</sub>	4.7	3.6551	11
V	318.5	0.5	75%	N <sub>2</sub> O-C <sub>2</sub> H <sub>2</sub>	4.7	4.2067	11
Ti	365.4	0.5	75%	N <sub>2</sub> O-C <sub>2</sub> H <sub>2</sub>	4.7	45.6638	11

Figure 4  
Instrument processes of an Atomic absorption spectrometer



S.G. Gounballe  
 IQAC Coordinator  
 Smt. Veeramma Gangasiri  
 College for Women  
 Kalaburagi - 585 102

*[Signature]*  
 BRINGIBAL  
 Smt. Veeramma Gangasiri  
 College for Women  
 Kalaburagi - 585 102



Table 2

Essential macro nutrients concentration (mg/L) of *Murraya koenigii* (L.) Spreng. leaves

Sl. No.	Mineral	Bidar	Kalaburagi	Shahapur	Sandur	Kappathgudda
1.	K	16.2793	17.1518	17.5753	17.3008	17.0827
2.	Ca	68.1831	73.779	75.9759	71.6995	74.3512
3.	Mg	6.8058	7.0280	7.3278	7.0660	7.2192

Table 3

Essential micro nutrients concentration (mg/L) of *Murraya koenigii* (L.) Spreng. leaves

Sl. No.	Mineral	Bidar	Kalaburagi	Shahapur	Sandur	Kappathgudda
1.	Zn	0.1071	0.0744	0.2086	0.1192	0.1198
2.	Fe	8.8503	3.1464	1.1948	3.7004	6.1110
3.	Cu	0.0364	0.0460	0.0919	0.0298	0.0527
4.	Mn	0.3240	0.2419	0.2840	0.1145	0.3217
5.	Mo	2.3720	2.808	2.5465	2.4943	2.2794
6.	V	1.9062	2.0665	2.0436	1.7820	1.9617
7.	Ti	4.6044	4.7605	4.9615	2.2708	2.8988

Table 4

Harmful heavy metals concentration (mg/L) of *Murraya koenigii* (L.) Spreng. leaves

Sl. No.	Mineral	Bidar	Kalaburagi	Shahapur	Sandur	Kappathgudda
1.	Cd	0.0095	0.0188	0.0097	0.0044	0.0040
2.	Al	0.5249	0	0	0.3495	1.7302

**Essential macro nutrients**

**Calcium (Ca)**

The concentration of calcium was found in all the collected leaves of *Murraya koenigii* (L.) Spreng. and it was the highest compared to all other macro nutrients. It could be due to the fact that the soil of North Karnataka region contains maximum amount of calcium and the same is reflected in the medicinal plants. The level of calcium varied from 68.1831-75.9759 mg/l in all samples. Figure 5 shows the calcium concentration in the leaves of *Murraya koenigii* (L.) Spreng., the least for Bidar and the highest is of Shahapur. Calcium is essential for all organisms, used in cell walls, bones etc. It helps in the transport of long chain fatty acids which helps in

preventing high blood pressure, heart diseases, cardiovascular diseases, repair worn out cells, strong teeth in humans, building of RBCs and body mechanism. That is why calcium has been extensively used for the treatment of various diseases.

**Potassium (K)**

The concentration of potassium was found in all the collected leaves of *Murraya koenigii* (L.) Spreng. and was the second dominant essential macro nutrient. The presence of high amount of the K concentration in the leaves could be due to the botanical structure as well as the mineral composition of the soil and also other factors like the use of fertilizers, water irrigation and geological conditions of the region. The level of K varied from 16.2793-17.5753 mg/L

S. P. Goudhalli  
 P.O. Coordinator  
 Smt. Veeramma Gangasiri  
 College for Women  
 Kalaburagi - 585 102

PRINCIPAL  
 Smt. Veeramma Gangasiri  
 College for Women  
 Kalaburagi - 585 102





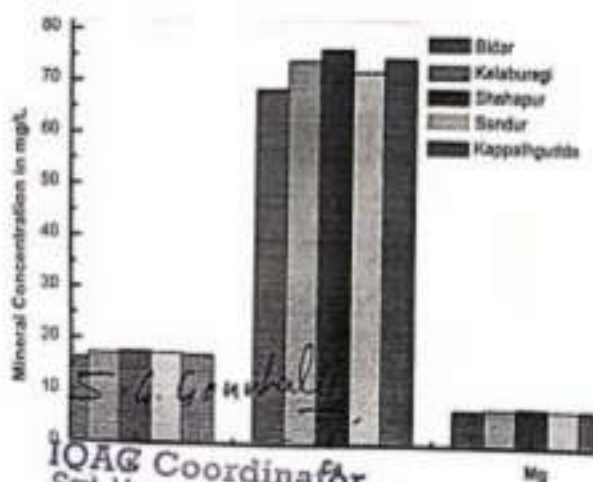
samples collected from different places of North Karnataka region. The mineral concentration level is same as the Ca i.e. mineral concentration is least for Bidar and highest for Shahapur (Figure 5). Potassium is essential for all organisms with the possible exception of blue green algae. It is a major cation and is important in nerve action. Potassium reduces the blood pressure but moderately toxic to mammals when injected intravenously.

### Magnesium (Mg)

The concentration of magnesium was also found in all collected leaves and was the third dominant mineral. The level of Mg was varied from 6.8058-7.3278 mg/L in all samples collected from different places of North Karnataka region. Like Ca and K the mineral concentration level of Mg was almost same for the leaves collected from different places which can be seen in Figure 5. Magnesium works with calcium to help transmitting nerve impulses in the brain. Magnesium has calming effect and helps in the nervous system of those peoples, suffering from depression. In blood, its quantity is 2-4 mg/100 ml. Magnesium plays an important role in the phosphorylation reactions of glucose and its metabolism. Its deficiency has been implicated in insulin resistance, carbohydrate intolerance, dyslipidemia and complications of diabetes.

Figure 5

Comparative study of essential macro nutrients in the leaves of *Murraya koenigii* (L.) Spreng.



### Essential micro nutrients

#### Zinc (Zn)

The concentration of zinc was found in all the collected leaves of *Murraya koenigii* (L.) Spreng. and their level was in the range of 0.0744-0.2086mg/L. The mineral nutrient concentration of Zn was in very small amount. Several biological roles of Zn have been reported and over 200 proteins and enzymes contain Zn and produce important role in DNA synthesis, brain development, steroidogenesis, bone formation, wound healing. (Figure 6)

#### Iron (Fe)

Iron is an essential mineral to prevent anemia and cough associated with angiotensin converting enzyme (ACE) inhibitors. The mineral concentration of Fe was in the range of 1.1948-8.8503 mg/L. For the synthesis of hemoglobin Fe is necessary. For the normal growth and development Fe is required in human body.<sup>12</sup> Iron deficiency is the most prevalent nutritional deficiency in humans.<sup>13</sup> (Figure 6)

#### Copper (Cu)

The mineral concentration of copper was 0.0298 mg/L in leaves of *Murraya koenigii* (L.) Spreng. of Sandur and 0.0527 mg/L in leaf sample of Kappathgudda. Copper plays an important role in the treatment of chest wounds, to prevent inflammation in arthritis and similar diseases. It is required for some essential enzymes such as super oxide dismutase, cytochrome oxidase, lysyl oxidase, etc. Excess consumption of Cu results in dermatitis, metallic taste in the mouth, hair and skin discoloration etc. Copper play role in some neurological conditions like Alzheimer's disease, Wilson's disease, etc.<sup>14</sup> (Figure 6)

#### Manganese (Mn)

The mineral concentration of manganese was 0.1145mg/L in leaves of *Murraya koenigii* (L.) Spreng. of Sandur and 0.3240mg/L in leaf sample of

IOAG Coordinator  
Smt. Veeramma Gangasiri  
College for Women  
Kalaburagi - 585 102

PRINCIPAL  
Smt. Veeramma Gangasiri  
College for Women  
Kalaburagi - 585 102



Bidar, Mn can help to assist the body in metabolizing protein and carbohydrates. (Figure 6)

### Molybdenum (Mo)

The concentration of molybdenum was found in all the collected leaves of *Murraya koenigii* (L.) Spreng. and it varied from 2.2794-2.808 mg/L. Molybdenum is a rare mineral, but it is essential for human body for various metabolic processes. The amount of Mo in the plant depends on the soil content in the growing area. Molybdenum is stored in the body, particularly in the liver, kidneys, glands and bones. It is also found in the lungs, spleen, skin and muscles. About 90% of the molybdenum eaten in foods is eliminated by the body through the urine. (Figure 6)

### Vanadium (V)

The concentration of vanadium was found in all the collected leaves of *Murraya koenigii* (L.) Spreng. that varied from 1.7820-2.0665 mg/L. Vanadium affects carbohydrate metabolism including glucose transport, glycolysis, glucose oxidation and glycogen synthesis.<sup>14</sup> At a dose of 100 mg/day vanadyl sulfate improves insulin sensitivity.<sup>15</sup> Its possible mechanism of action in glycemic control is thought to be primarily insulin sensitive with up regulation of insulin receptors. (Figure 6)

### Titanium (Ti)

The concentration of titanium was found in all the collected leaves of *Murraya koenigii* (L.) Spreng. and it varied from 2.2708-4.7605 mg/L. Titanium is a physically promotive trace mineral. The function of Ti is not known yet. It is harmless to our body. (Figure 6)

### Harmful heavy metals

#### Cadmium (Cd)

The concentration of cadmium was found in all the collected leaves of *Murraya koenigii* (L.) Spreng. and their level was in the range of 0.0040-0.0188 mg/L. The mineral concentrations of leaves collected from different place of North Karnataka were very low and within the permissible limit set by WHO. Cadmium is a non-essential harmful heavy metal which biochemically replaces zinc and causes high blood pressure. It also damages the kidney and liver<sup>16</sup> and causes a disease known as Itai-itai. (Figure 7)

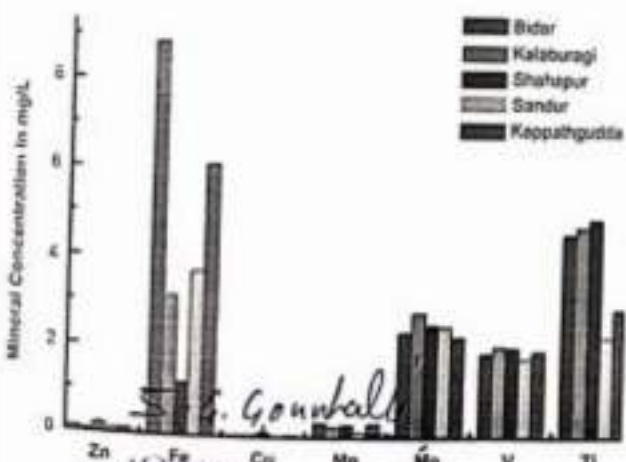
#### Aluminium (Al)

The concentration of aluminium was not found in all the leaves of *Murraya koenigii* (L.) Spreng. It was present in the leaves collected from Bidar, Sandur and Kappathgudda in the range of 0.3495-1.7303 mg/L. The concentration of Al was high in the leaves collected from Kappathgudda and was totally absent in Kalaburagi and Shahapur. Aluminium is usually not harmful. Some studies show that aluminium may develop Alzheimer's disease, but other studies have not found this to be true. (Figure 7)

In the present study 12 mineral nutrients viz. Macro nutrients, micro nutrients and harmful heavy metals concentration were determined and found varying from place to place. These mineral nutrients help us to prevent and cure various diseases and are very essential for human health.

Figure 6

Comparative study of essential micro nutrients in the leaves of *Murraya koenigii* (L.) Spreng.



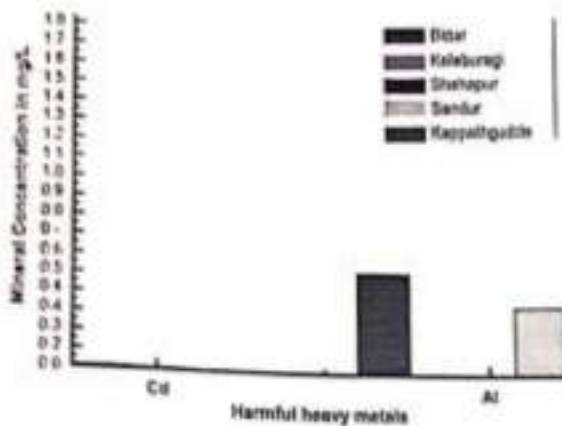
Smt. Veeramma Gangasiri College for Women Kalaburagi - 585 102

*[Signature]*  
**PRINCIPAL**  
 Smt. Veeramma Gangasiri College for Women Kalaburagi - 585 102



Figure 7

Comparative study of harmful heavy metals in the leaves of *Murraya koenigii* (L.) Spreng.



### Conclusion

The present study on macro and micro nutrients content in the leaves of *Murraya koenigii* (L.) Spreng. reveals the presence of various mineral nutrients attributed to the presence of the minerals of the soil, the different botanical structure of the medicinal plant or soil, environmental factors including atmosphere and pollution, season of collection sample, age of indigenous medicinal plant and soil conditions in which plant grows. From this study it is also verified that the leaves of *Murraya koenigii* (L.) Spreng. contains concentration of micro nutrients viz. copper and zinc along with macro and other micro nutrients, which are required for the metabolism as per the recommendations of WHO.<sup>14-18</sup> The data obtained in the present study will be helpful in the synthesis of new modern drugs with various combinations of plants which can be used to cure many diseases. However, more detailed study of chemical composition of the indigenous medicinal plants is required which is progressive in this direction.

### References

1. Faizul Haq and Rahat Ullah, Comparative determination of trace elements from *Azadirachta indica*, *Rheum australe* and *Ternstroemia* by using atomic absorption spectroscopy.

Kalaburagi - 585 102

International Journal of Biosciences (IJB)  
No. 5, P 77-82, 2011.

2. Anlia B.S., Akpun E. J., Okon P. A. and Umoren I. Nutritive and anti-nutritive evaluation of sweet potatoes (*Ipomoea batatas*) leaves. Pakistan Journal of Nutrition, 5: 166-168, Asian Network for Scientific Information, 2006.

3. Serfar-Armah Y., Nyarko B. J. B., Akaho E. H. K., Kyere A. W. K., Osae S., Oppong-Benchie K. and Osae E. K. J. Activation analysis of some essential elements in five medicinal plants used in Ghana, Journal of Radioanalytical and Nuclear Chemistry, 250 (1), 173-176, Springer Science+Business Media, Netherlands, 2001.

4. Tolonen M., Vitamins and minerals in health and nutrition, P 240, Ellis Harwood Ltd., Chichester, England, 1990.

5. Raut O. P., Acharya R., Gupta R., Mishra S. K. and Sahoo R. et. A, International Journal of Applied biology and pharmaceutical technology, Vol. 4, Issue - 1, 2013.

6. Subramanian R., Subramaniyan P. and Raj V., Asian Pacific Journal of Tropical Biomedicine, S 555-558, Elsevier, Amsterdam, Netherlands, 2012.

7. Loznik A., Soltyk K., Ostapczuk P. and Fijalek Z., The Science of the Total Environment, 289, 33, Elsevier, Amsterdam, Netherlands, 2002.

8. Rivier L. and Bruhn J. G., Editorial. J. Ethnopharmacol. (1979) 1 110.1016/0378-8741(79)90013-8.

9. Subramanian R., Gayathri S., Rathnavel C. and Raj V., Analysis of mineral and heavy metals in some medicinal plants collected from local market, Asian Pacific Journal of Tropical Biomedicine, 2 (1), S74-S78, Elsevier, Amsterdam, Netherlands, 2012.

10. Dushenkov V., Kumar P. B. A. N., Motto H. and Raskin I., Rhizofiltration: The Use of Plants to Remove Heavy Metals from Aqueous Streams, Environmental Science Technology, Vol. No. 29, Pages 1239-1245, American Chemical Society, United States, 1995.

11. Santosh T., Mohanraj P., Sharanabasappa and Kerur B. R., Accumulation of Elements in Homemade Herbal Medicinal plants, International Journal of Pure & Applied Physics, Vol. 13, No. 1, P 50-53, Research India Publications, Delhi, 2017.

12. Kayu I. and Incekara N., Turkish Journal of Weed Science, 3: 56, Huseyin ONEN, Turkey, 2000.

13. Reddy M. B., Chidambaram M. V. and Buter G. W., Iron Transport in Microbes, Plants and Animals, VCH, New York, 1987.

PRINCIPAL  
Smt. Veeramma Gangasiri  
College for Women  
Kalaburagi - 585 102



14. Onyamboko N. V., Benentariya H., Robberecht H. and Deelstra H., *Atomic absorption spectrometric determination of selenium, zinc and copper in different vegetables from Zaire*, Belgian Journal Food Chemistry Biotechnology, 45: 21, 1990.

15. Hunt J. R., *Bioavailability of Fe, Zn and other Trace Minerals for Vegetarian Diets*, The American Journal of Clinical Nutrition, 78: 633-39, American Society for Nutrition, United States, 1994.

16. Neil P.O., *Minor Element and Environmental Problems*, 2<sup>nd</sup> Edn., Environmental Chemistry, 1993.

17. Thunus L. and Lejeune R., *Handbook on Metals in Clinical and Analytical Chemistry*, Marcel Dekker, New York, 1994.

18. World Health Organization, *Quality Control Methods for Medicinal Plant Materials*, WHO Press, Geneva, Switzerland, 1998.

**Authors**  
Mohanraj Pattar, H.K.E Society's, M S I Degree College of Arts, Science and Commerce, Kalaburagi- 585102, Karnataka. E-mail: mohanrajpattar@gmail.com  
Anishkumar Teerthe, Department of Physics, Gulbarga University, Kalaburagi- 585 106, Karnataka.  
Suhwini A., Department of Physics, Gulbarga University, Kalaburagi- 585 106, Karnataka.  
Kerur B. R., Department of Physics, Gulbarga University, Kalaburagi- 585 106, Karnataka. E-mail: kerurbrk@hotmail.com

Kottakkal Ayurveda Series: 72



**Medicinal Plants**  
of Arya Vaidya Sala Herb Garden  
Udayan P.S. and Indira Balachandran  
Price: ₹ 240/-

This comprehensive handbook provides detailed information on the 1025 medicinal plant species with details of their names in different languages, places where they grow naturally, parts used in medicines and important uses for the benefit of professionals, students, herb collectors, farmers, etc. The handbook lists the plants alphabetically by their Latin names; information on groups of plants such as nakṣatravana (plants representing 27 stars), daśamūla (ten roots), daśapuṣpa (ten flowers) triphala (three myrobalans), trikaṭu (three myrobalans), etc. is also included in the book. Indices of common names, glossary of medicinal terms and list of reference are also provided.

S.G. Gounballi  
IQAC Coordinator  
Smt. Veeramma Gangasiri  
College for Women  
Kalaburagi - 585102

**PRINCIPAL**  
Smt. Veeramma Gangasiri  
College for Women  
Kalaburagi - 585102

## DETERMINATION OF MAJOR AND TRACE ELEMENTS OF TRADITIONAL MEDICINAL PLANTS OF GULBARGA REGION

Mohanraj Pattar<sup>1,2</sup>, Santoshkumar Teerthe<sup>2</sup>, B R Kerur<sup>2</sup>

<sup>1</sup>H.K.E Society's, M S Irani Degree College of Arts, Science & Commerce, Kalaburagi -585102, Karnataka, India

<sup>2</sup>Department of Physics, Gulbarga University, Kalaburagi, Karnataka, India – 585 106

Email: [kerurbrk@gmail.com](mailto:kerurbrk@gmail.com)

### ABSTRACT

The elemental analysis was carried out for 13 different traditional medicinal plants are known to occur naturally and abundant in Gulbarga of North Karnataka region using Atomic Absorption Spectrophotometer (AAS) technique. A total of 12 elements were measured in the collected traditional medicinal plants; out of these 12 elements, the concentration of Ca, K, Mg and V was found to be in the range of Ca[52-80 mg/L], K[6-20 mg/L], Mg[6-7.5 mg/L] and V[0.4 – 1.5 mg/L], while the other elements such as Al, Mn, Fe, Cu, Zn, Cd, Mo, and Ti were less than 1 mg/L. The results were compared and correlated with multi-elemental analysis technique i.e., Scanning Electron Microscopy-Energy Dispersive x-ray Spectroscopy (SEM-EDX) for the confirmation of presence of elements in the collected medicinal plants. The results of SEM-EDX also confirmed the determined elements and are at the same level. The data obtained from the study can be used to evaluate the potentiality of these plants and also in deciding the dosage of Ayurvedic drug for the treatment of various diseases.

**Keywords:** Traditional Medicinal Plants, Trace elements, AAS technique and SEM-EDX.

### INTRODUCTION

The traditional medicinal plants play an important role in the traditional medicine system. According to the survey reported by World Health Organization (WHO), about 80% of the world's population consumes traditional medicinal plants in direct and indirect ways to treat their

diseases. Medicinal plants have been using for curing and preventing of the various diseases. The curing and prevention property of the medicinal plants depends on their chemical composition. The level of the elements in the plants varies by the characteristics of the soil and also





environmental conditions [1, 2, 3, 4 and 5]. During the past decade, it has seen a significant increase in the use of traditional medicine due to their minimal side effect, availability and acceptability [6].

Essential major and trace elements in traditional medicinal plants have been investigated by many researchers to strengthen the importance of elemental analysis with respect to human health. The human body requires a number of elements to maintain a good health. Several attempts have been made to determine the elemental compositions of traditional medicinal plants using different elemental analysis techniques from many countries all over the world [7, 8].

In the present study, 13 different traditional medicinal plants were selected from Gulbarga of North Karnataka region which are known to occur naturally and in abundant in this region. These traditional medicinal plants are used to prevent and cure various diseases by the local traditional practitioners (Nati Vaidhya). Hence an attempt has been made to determine the elemental constituents of the selected traditional medicinal plants using AAS technique. This technique measures the concentrations of elements. Atomic absorption is so sensitive that it can measure down to ppb (parts per billion) or ppm (parts per million) of a gram ( $\mu\text{g dm}^{-3}$  or  $10^{-6}$ ) in a sample. The technique makes use of the wavelengths of light specifically absorbed by an element present in the sample. They correspond to the energies needed to promote electrons from one energy level to another, i.e., higher energy level. Atomic absorption spectroscopy has many uses in different areas such as clinical analysis, Environmental analysis, Pharmaceuticals, Industry, Mining and Agriculture [9, 10]. SEM-EDX,

among the various analytical techniques used for elemental analysis, is highly qualified for the identification and the quantification of different elements in various samples of biological and environmental importance [11]. Besides, a powerful tool for such analysis the method is non-destructive and is more advantageous in multi-elementary analysis compared to other existing methods such as ICP-AES, ICP-MS, AAS and INAA.

### Materials and Methods:

#### Sample Collection:

Table.1 shows the profile of the selected traditional plants collected from Gulbarga of North Karnataka region. About a few kg of each plant material was collected and then collected materials were washed in deionized water to eliminate contamination due to dust and environmental pollution. The washed plant materials were dried in shade for a months and then grinded to a fine powder which was further used for the major and trace elemental analysis.

#### Sample preparation for elemental analysis:

A 10 gm of powder was taken in a silica crucible and then kept in an oven for 2-3 hours at  $250-350^{\circ}\text{C}$  to get ash. The obtained ash was used for preparation of solution. The solution was prepared by mixing of concentrated HCL, double distilled water and 1gm of ash in the ratio 25: 25:1. The mixed solution was then stirred for few minutes; it was then filtered using watt man filter paper 41. A 950 ml of double distilled water was added to the filtered solution to make it 1000 ml solution. The same procedure was repeated for all other plant material samples [12]. The obtained solutions were finally used







for the measurement of trace elemental analysis using AAS technique.

#### Determination of elements:

The elements such as Mg, Al, K, Mn, Fe, Cr, Ca, Cu, Zn, Cd, Si, Mo, V and Ti in the plant samples were analyzed using atomic absorption spectrophotometer. It is manufactured by Thermo Scientific™ with a model No. iCETM-3000 series and it is equipped with dedicated flame, furnace or combined flame and furnace option. Air – C<sub>2</sub>H<sub>2</sub> and N<sub>2</sub>O- C<sub>2</sub>H<sub>2</sub> flame was used for determination elemental content. The absorption wavelength for the determination of each element with its linear working range and correlation coefficient were calibrated for the analysis.

## RESULTS & DISCUSSION

The botanical as well as local name of the plant, part used, coding of the samples and medicinal uses are listed in Table 1. Table. 2 show the measured elemental concentration of the traditional medicinal plant collected from Gulbarga of North Karnataka region.

#### Calcium (Ca)

The concentration of Ca is found in all the collected medicinal plants and the concentration of calcium is highest when compared to all other elements. The presence of high amount of the calcium concentration in medicinal plants could be due to the fact that the soil of this region. Gulbarga of North Karnataka region contains maximum amount of calcium in the soil and the same one is reflected in the medicinal plants. The level of calcium is varied from 52 – 80 mg/L in all samples. The levels of concentration

are also verified by considering the SEM-EDX results. It helps in preventing and curing all bone related issues. It also helps to repair worn out cells, strong teeth in humans, building of RBCs and body mechanism. Therefore it has been extensively used for treatment of various diseases.

#### Potassium (K)

The concentration of potassium (K) is found in all collected medicinal plants and it is the second dominant element when compared to all other elements. The presence of high amount of the K concentration in medicinal plants could be due to botanical structure as well as the mineral composition of the soil and also other factors like use of fertilizers, water irrigation and geological conditions of the region. The level of K is varied from 6 – 20 mg/L in all samples. The results of SEM-EDX technique also show the presence of potassium element at higher level which can be seen in figure 2.

#### Magnesium (Mg)

The concentration of Magnesium (Mg) is found in all collected medicinal plants and it is the third dominant element when compared to all other elements. The level of Mg is varied from 6 – 7.5 mg/L in all samples. The presence of Magnesium element is also reflected in SEM-EDX and its concentration level is in accordance with the AAS technique which can be seen in figure 2. Magnesium works with calcium to help transmitting nerve impulse in the brain. Magnesium has calming effect and works on the nervous system of those peoples, suffering from depression. In blood its quantity is 2-4mg/100ml [19]. Magnesium has an important role in the phosphorylation reactions of glucose and its me-





tabolism. Its deficiency has been implicated in insulin resistance, carbohydrate intolerance, dyslipidemia and complications of diabetes.

#### Vanadium (V)

The concentration of Vanadium (V) is found in all collected medicinal plants and it varied from 0.4411– 1.4762 mg/l. in all collected samples. Vanadium affects carbohydrate metabolism including glucose transport, glycolysis, glucose oxidation, and glycogen synthesis [13]. At a dose of 100 mg/day vanadyl sulfate improves insulin sensitivity [14]. Its possible mechanism of action in glycemic control is thought to be primarily insulin mimetic with up regulation of insulin receptors.

The other elements such as Al, Mn, Fe, Cu, Zn, Cd, Mo, and Ti were also determined in the present study but the concentration of these elements is found to be comparatively less. The above said elements were compared and correlated with SEM-EDX and are found to be simi-

lar. Figure 3, shows the concentration few major and trace elements of *Datura metal* L. (Solanaceae). The variation in elemental concentration is mainly attributed to the differences in botanical structure, as well as in the mineral composition of the soil in which the plants grow. Other factors which are also responsible for variation in elemental contents are preferential absorability of the plant and climatological conditions [18]. These determined elements are very essential for the human health. These elements are within the permissible limits and help to prevent and cure various diseases. From this study it is also verified that the medicinal plants viz., *Murrayakoenigii*, *Lawsonianermis*, *Datura metal*, *Acalyphaindia*, *Mirabilis jalapa*, *Gymnemasylvestre* and *Tylophora india* contains trace elemental concentration of copper and zinc along with major and other trace elements, which are the required nutrients for the metabolism as per the recommendations of WHO [15-17].

#### Tables and Figures:

**Table 01:** Profile of the traditional medicinal plants and their medicinal uses

S.No	Botanical name	Local name	Coding	Part	Medicinal use
1	<i>Abutilonindicum</i> (L)	<i>Tutti</i> <i>Vibutigida</i>	TU	Leaf	Diuretic, infected skin and dysentery.
2	<i>Murrayakoenigii</i> (L.) Spreng	<i>Karibevu</i>	KA	Leaf	Anti-diabetic, antioxidant, antimicrobial, anti-inflammatory and hair treatments
3	<i>Tinosporacordifolia</i>	<i>Amrita balli</i>	AM	Leaf	Immune booster, general tonic, Chronic fevers, Upper respiratory,
4	<i>Lawsonianermis</i> L. (Lythraceae).	<i>Madarangi</i> ,	MA	Leaf	Jaundice, amoebic dysentery and sore throats.
5	<i>Datura metal</i> L. (Solanaceae),	<i>Umatta</i>	UN	Leaf	Rheumatism, Asthma, control of dandruff.
6	<i>Adathodkrasica</i> Nees. (Acanthaceae).	<i>Adusoge</i>	AD	Leaf	Cough, Spiny outgrowths of piles to control bleeding.





7	<i>Acalypha indica</i> L. (Euphorbiaceae)	<i>Kuppigada</i>	KU	Leaf	Constipation, Scabies, Eczema, and Urinary problems.
8	<i>Plumbago zeylanica</i> L. (Plumbaginaceae),	<i>Bili chitramuda</i>	BI	Root	Pile, elephantiasis and rheumatic pain.
9	<i>Balanites roxburghii</i> Planch. (Simarubaceae)	<i>Ingudi</i>	IN	Leaf	Jaundice, intestinal worm infections, leukoderma, psychiatric disorders.
10	<i>Barleria prionites</i> L. (Acanthaceae),	<i>Mullugoranti</i>	MU	Leaf	Scabies, respiratory diseases, tooth ache and joint pains.
11	<i>Mirabilis jalapa</i> L. (Nyctaginaceae),	<i>Sanjemallige</i>	SA	Leaf	Wound healing, abscesses and inflammation.
12	<i>Gymnema sylvestre</i> (Asclepiadaceae)	<i>Kodapatri</i>	KO	Leaf	Diabetes, metabolic syndrome, weight loss and cough.
13	<i>Tylophora indica</i> (Asclepiadaceae)	<i>Aadamuttakaballi</i>	AA	Root & Leaf	Cough, asthma, bronchitis, dysentery, diarrhea, wounds, ulcer, hemorrhoids, malignant tumor, and leukemia

**Table 02:** Concentration of elements (in mg/l.) in the traditional medicinal plants collected from Gulbarga.

S. No	Botanical name	Coding	Mg	Al	K	Mn	Fe	Ca	Cu	Zn	Cd	Mo	V	Ti
1	<i>Abutilon indicum</i> (L)	TU	7.48 17	0	18.07 94	0.10 74	0.30 72	76.59 54	0	0.19 48	0.00 36	0.53 14	0.44 11	0
2	<i>Murrayakoenigii</i> (L.) Spreng	KA	7.02 80	0	17.15 18	0.24 19	3.14 64	73.77 79	0.04 60	0.07 44	0.01 88	0.16 39	0.70 94	1.73 25
3	<i>Tinospora cordifolia</i>	AM	6.90 69	0	19.59 53	0.46 77	0.52 91	71.99 77	0	0.03 74	0.00 73	0	0.84 77	0.65 97
4	<i>Lawsonia inermis</i> L. (Lythraceae),	MA	7.28 17	0	12.26 85	0.25 39	1.45 74	78.20 88	0.01 35	0.08 53	0.00 08	0	1.44 01	0
5	<i>Datura metel</i> L. (Solanaceae),	UN	7.18 55	0	20.08 02	0.22 33	1.05 44	80.40 63	0.00 55	0.07 61	0.01 32	0	0.97 52	0
6	<i>Adathodavasicana</i> Nees. (Acanthaceae),	AD	7.05 82	0	15.21 56	0.21 17	1.83 10	78.95 19	0	0.13 54	0.02 13	0	1.17 39	0
7	<i>Acalypha indica</i> L. (Euphorbiaceae)	KU	7.21 65	1.38 96	17.06 68	0.24 15	4.00 92	78.37 28	0.00 66	0.13 16	0.00 86	0	1.29 96	2.55 03
8	<i>Plumbago zeylanica</i> L. (Plumbaginaceae),	BI	7.53 61	0.57 86	18.18 69	0.24 81	1.02 17	53.13 60	0	0.09 38	0.00 02	0.26 50	1.30 24	0.63 45





9	<i>Balanites roxburghii</i> Planch. (Simarubaceae)	IN	6.94 88	0.68 73	6.153 6	0.16 06	0.47 61	76.81 92	0	0.04 01	0	0.59 87	1.31 79	1.82 17
10	<i>Barleria prionites</i> L. (Acanthaceae)	MU	7.42 21	0.24 43	18.82 29	0.08 47	0.99 37	79.04 60	0	0.06 18	0.01 43	0.65 44	1.39 29	3.93 78
11	<i>Mirabilis jalapa</i> L. (Nyctaginaceae)	SA	7.51 32	2.49 91	18.25 89	0.19 31	0.70 03	78.54 45	0.00 54	0.09 93	0.01 04	0.72 66	1.28 74	3.47 99
12	<i>Gymnomysylvestre</i> (Retz.) R.Br. ex Schult. (Asclepiadaceae)	KO	7.19 39	3.07 92	16.88 41	0.55 15	1.27 41	70.66 04	0.01 38	0.07 29	0.00 46	0.64 93	1.47 62	3.77 41
13	<i>Tylophora indica</i> (Asclepiadaceae)	AA	6.74 28	2.38 62	13.28 19	0.22 65	0.38 03	72.49 58	0.03 97	0.08 26	0.00 97	0.52 73	1.54 03	0.76 07

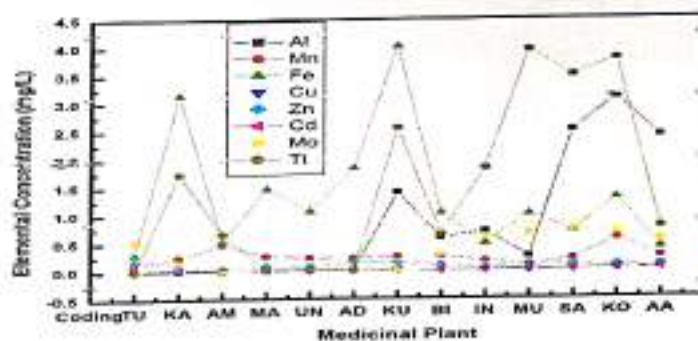
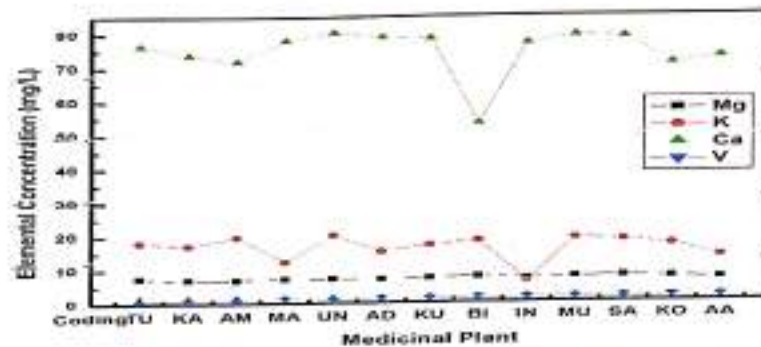


Fig. 1: Elemental concentration versus medicinal plants





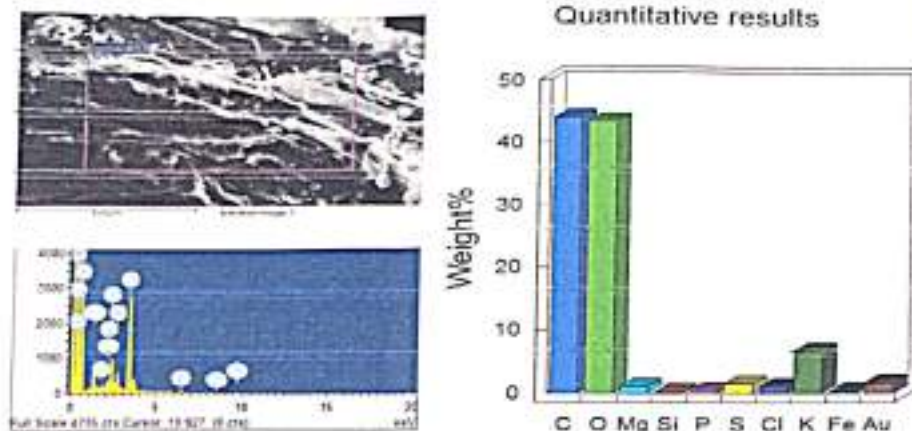


Fig. 2: SEM-EDX for Datura metal L. (Solanaceae)

## CONCLUSIONS

The present study of an elemental analysis of the medicinal plant reveals the presence of various elements but the concentration of the elements are at different levels reflecting the impact of natural processes. This variation in elemental concentration in the medicinal plants is mainly attributed to the differences in botanical structure, mineral composition of the soil and the climatic conditions in which the plants grow. The data obtained from the study can be used to evaluate the potentiality of these plants and also in deciding the dosage of ayurvedic drug prepared from these plants in the treatment of various diseases.

## REFERENCES

1. Lozak, A., Soltyk, K., Ostapczuk, P., Fijalek, Z. Determination of selected trace elements in herbs and their infusions, *The Science of the Total Environment*, 2002 Apr 22;289(1-3):33-40.
2. World Health Organization, WHO Guidelines on Good Agricultural and Collection Practices (GACP) for Medicinal Plants, WHO Press, Geneva, Switzerland 2003.
3. World Health Organization, Monographs on Selected Medicinal Plants, Vol.1-3, WHO Press, Geneva, Switzerland 2007.
4. World Health Organization, Quality Control Methods for Medicinal Plant Materials, WHO Press, Geneva, Switzerland 1998.
5. World Health Organization, Traditional Medicine Growing Needs and Potential - WHO Policy Perspectives on Medicines, No. 002, May 2002
6. O P Raut, R Acharya, R Gupta, S K Mishra and R Sahoo et., *International Journal of Applied Biliogy and pharmaceutical technology*, Vol. 4, Issue - 1. A (2013)
7. Santoshkumar S Teerthe, Mohanraj Pattar, Sharanabasappa and B R Kerur, *Elemental Contents in Ayurvedic Medicinal plants Using AAS Technique*, *Jl. Of Instrum.Soc. of India*, (2017),45(2), 110-112, 2015. ISSN: 0970-9983.





8. R. Subramanian P. Subbramaniyan and V.Raj, Determination of some minerals and trace elements in two tropical medicinal plants, *Asian Pacific Journal of Tropical Biomedicine* (2012), S 555-S 558
9. R Subramanian, S Gayathri, C Rathnavel, V Raj, Analysis of mineral and heavy metals in some medicinal plants collected from local market, *Asian Pacific Journal of Tropical Biomedicine*(2012) 2 (1), S74-S78
10. Dushenkov V, Kumar PBAN, Motto H, Raskin I, Rhizofiltration: The Use of Plants to Remove Heavy Metals from Aqueous Streams, *Environmental Science Technology* (1995) Vol. No. 29, Pages 1239-1245.
11. Ramamurthy N and Kannan S. Romanian, SEM-EDS analysis of soil and plant (*Calotropis gigantea* Linn) collected from an Industrial village, Cuddalore Dt, Tamil Nadu, India, *J Biophys* 2009; 19(3): 219-226.
12. Santosh T, Mohanraj P, Sharanabasappa and B. R. Kerur, Accumulation of Elements in Homemade Herbal Medicinal plants, *International Journal of Pure & Applied Physics*. (2017) Vol. 13, No. 1, PP.50-53.
13. Ngugi P, Njagi J, Kibiti C, Maina D, Ngeranwa J, et al. (2012) Trace elements content of selected Kenyan anti-diabetic medicinal plants. *Int J Curr Pharm Res* 4: 39-42.
14. O'Connell B Select vitamins and minerals in the management of diabetes. *Diabetes Spectra*(2001) 14: 133-148.
15. Hunt, J.R. Bioavailability of Fe, Zn and other Trace Minerals for Vegetarian Diets. *Am. J. Clin. Nutr.* 1994,78: 633-39.
16. Thunus L, Lejeune R. *Handbook on Metals in Clinical and Analytical Chemistry*. Marcel Dekker, New York, 1994.
17. World Health Organization, *Quality Control Methods for Medicinal Plant Materials*, WHO Press, Geneva, Switzerland 1998.
18. Ram Lokhande , Pravin Singare , Mahadeo Andhale. Study on Mineral content of Some Ayurvedic Indian Medicinal Plants by Instrumental Neutron Activation Analysis and AAS Techniques. *HEALTH SCIENCE JOURNAL*, (2010), VOLUME 4, ISSUE 3.
19. David M. Greenberg, Salvatore P. Lucia, Myrtle A. Mackey and Elma V. Tufts. The magnesium content of the plasma and the red corpuscles in human blood. *J. Biol. Chem.* 1933, 100:139-148.

**Source of Support: Nil**

**Conflict Of Interest: None Declared**

How to cite this URL: B R Kerur et al: Determination Of Major And Trace Elements Of Traditional Medicinal Plants Of Gulbarga Region. *International Ayurvedic Medical Journal* {online} 2017 {cited December, 2017} Available from: [http://www.iamj.in/posts/images/upload/\\_pdf](http://www.iamj.in/posts/images/upload/_pdf)





## A study on major and trace elements in some traditional medicinal plants using AAS technique

<sup>1</sup>Mohanraj Pattar, <sup>2</sup>Santoshkumar Teerthe, <sup>3</sup>BR Kerur

<sup>1</sup>H.K.E.Society's, MS Inani Degree College of Arts, Science & Commerce, Kalaburagi, Karnataka, India

<sup>2,3</sup>Department of Physics, Gulbarga University, Kalaburagi, Karnataka, India

### Abstract

The elemental analysis was carried out for 13 different traditional medicinal plants collected from Gulbarga of North Karnataka region using Atomic Absorption Spectrophotometer (AAS) technique. A total of 12 elements were measured in the collected traditional medicinal plants; out of these 12 elements, the concentration of Ca, K, Mg and V was found to be in the range of Ca[52-80 mg/L], K[6-20 mg/L], Mg[6-7.5 mg/L] and V[1.2-2.3 mg/L], while the other elements such as Al, Mn, Fe, Cu, Zn, Cd, Mo, and Ti were less than 1 mg/L. These results were correlated with multi-elemental analysis technique SEM-EDX.

**Keywords:** traditional medicinal plants, trace elements, AAS technique and SEM-EDX

### 1. Introduction

The traditional medicinal plants play an important role in the traditional medicine system. According to the survey reported by World Health Organization (WHO), about 80% of the world's population consumes traditional medicinal plants in direct and indirect ways to treat their diseases. Medicinal plants have been using for curing and preventing of the various diseases. The curing and prevention property of the medicinal plants depends on their chemical composition. The level of the elements in the plants varies by the characteristics of the soil and also environmental conditions [1, 2, 3, 4, 5]. During the past decade, it has seen a significant increase in the use of traditional medicine due to their minimal side effect, availability and acceptability [6].

Essential major and trace elements in traditional medicinal plants have been investigated by many researchers to strengthen the importance of elemental analysis with respect to human health. The human body requires a number of elements to maintain a good health. Several attempts have been made to determine the elemental compositions of traditional medicinal plants using different elemental analysis techniques from many countries all over the world [7, 8].

In the present study, the different traditional medicinal plants, which are used to prevent and cure various diseases, were selected from Gulbarga of North Karnataka region and the selected plants were investigated for their elemental constituents using AAS technique. This technique measures the concentrations of elements. Atomic absorption is so sensitive that it can measure down to ppb (parts per billion) or ppm (parts per million) of a gram ( $\mu\text{g dm}^{-3}$  for 10<sup>-6</sup>) in a sample. The technique makes use of the wavelengths of light specifically absorbed by an element present in the sample. They correspond to the energies needed to promote electrons from one energy level to another, i.e., higher energy level. Atomic absorption spectroscopy has many uses in different areas such as clinical analysis, Environmental analysis, Pharmaceuticals, Industry, Mining and Agriculture [9, 10].

SEM-EDX, among the various analytical techniques used for elemental analysis, is highly qualified for the identification and the quantification of different elements in various samples of biological and environmental importance [11]. Besides a powerful tool for such analysis the method is non-destructive and is more advantageous in multi-elementary analysis compared to other existing methods such as ICP-AES, ICP-MS, AAS and INAA.

### 2. Materials and Methods

#### 2.1 Sample Collection

Table 1 shows the profile of the selected traditional plants collected from Gulbarga of North Karnataka region. About a few kg of each plant material was collected and then collected materials were washed in distilled water to eliminate contamination due to dust and environmental pollution. The washed plant materials were dried in shade for 4 months and then grinded to a fine powder which was further used for the major and trace elemental analysis.

#### 2.2 Sample Preparation for Elemental Analysis

A 10 gm of powder was taken in a silica crucible and then kept in an oven for 2-3 hours at 250-350° C to get ash. The obtained ash was used for preparation of solution. The solution was prepared by mixing of concentrated HCL, double distilled water and 1gm of ash in the ratio 25:25:1. The mixed solution was then stirred for few minutes, it was then filtered using what man filter paper 41. A 950 ml of double distilled water was added to the filtered solution to make a 1000 ml solution. The same procedure was repeated for all other plant material samples [12]. The obtained solutions were finally used for the measurement of trace elemental analysis using AAS technique.

#### 2.3 Determination of Elements

The elements such as Mg, Al, K, Mn, Fe, Cr, Ca, Cu, Zn, Cd, Se, Mo, V and Ti in the plant samples were analyzed using

S.G. Gomballi  
IQAC Co-ordinator  
Smt. V.G. Women's Degree College  
KALABURGI

PRINCIPAL  
Smt. V.G. Degree College for Women  
KALABURGI



atomic absorption spectrophotometer. It is manufactured by Thermo Scientific™ with a model No. IC17M-3000 series and it is equipped with dedicated flame, furnace or combined flame and furnace option. Air - C<sub>2</sub>H<sub>2</sub> and N<sub>2</sub>O- C<sub>2</sub>H<sub>2</sub> flame was used for determination elemental content. The instrument was operated with the conditions shown in Table. 2. The absorption wavelength for the determination of each element with its linear working range and correlation coefficient were calibrated for the analysis.

### 3. Results & Discussion

The images of leaves of the traditional medicinal plants are shown in Fig. 1. The botanical as well as local name of the plant, part used, coding of the samples and medicinal uses are listed in Table. 1. Table. 3 show the measured elemental concentration of the traditional medicinal plant collected from Gulbarga of North Karnataka region.

#### Calcium (Ca)

The concentration of Ca is found in all the collected medicinal plants and the concentration of calcium is highest when compared to all other elements. The presence of high amount of the calcium concentration in medicinal plants could be due to the fact that the soil of this region, Gulbarga, North Karnataka region contains maximum amount of calcium and the same one is reflected in the medicinal plants. The level of calcium is varied from 52 - 80 mg/l in all samples. It helps in preventing and curing all bone related issues. It also helps to repair worn out cells, strong teeth in humans, building of RBC's and body mechanism. Therefore it has been extensively used for treatment of various diseases.

#### Potassium (K)

The concentration of potassium (K) is found in all collected medicinal plants and it is the second dominant element when compared to all other elements. The presence of high amount

of the K concentration in medicinal plants could be due to botanical structure as well as the mineral composition of the soil and also other factors like use of fertilizers, water irrigation and geological conditions of the region. The level of K is varied from 6 - 20 mg/L in all samples.

#### Magnesium (Mg)

The concentration of Magnesium (Mg) is found in all collected medicinal plants and it is the third dominant element when compared to all other elements. The level of Mg is varied from 6 - 7.5 mg/L in all samples. Magnesium works with calcium to help transmitting nerve impulse in the brain. Magnesium has calming effect and works on the nervous system of those peoples, suffering from depression. In blood its quantity is 2-4mg/100ml. Magnesium has an important role in the phosphorylation reactions of glucose and its metabolism. Its deficiency has been implicated in insulin resistance, carbohydrate intolerance, dyslipidemia and complications of diabetes.

#### Vanadium (V)

The concentration of Vanadium (V) is found in all collected medicinal plants and it varied from 1.2 - 2.3 mg/l in all collected samples. Vanadium affects carbohydrate metabolism including glucose transport, glycolysis, glucose oxidation, and glycogen synthesis [13]. At a dose of 100 mg/day vanadyl sulfate improves insulin sensitivity [14]. Its possible mechanism of action in glycemic control is thought to be primarily insulin mimetic with up regulation of insulin receptors.

The other elements such as Al, Mn, Fe, Cu, Zn, Cd, Mo, and Ti were also determined in the present study but the concentration of these elements is found are comparatively less. It depends on the botanical structure of the medicinal plant or soil. These elements also help to prevent and cure various diseases and are very essential for the human health.

### 4. Tables and Figures

Table 1: Profile of the traditional medicinal plants and their medicinal uses

S. No	Botanical name	Local name	Coding	Part	Medicinal use
1	<i>Abutilon indicum</i> (L.)	Tutti Vibutigida	TU	Leaf	Diuretic, infected skin and dysentery.
2	<i>Murraya koenigii</i> (L.) Spreng	Karibevu	KA	Leaf	Anti-diabetic, antioxidant, antimicrobial, anti-inflammatory and hair treatments
3	<i>Tinospora cordifolia</i>	Amrita balli	AM	Leaf	Immune booster, general tonic, Chronic fevers, Upper respiratory.
4	<i>Lawsonia inermis</i> L. (Lythraceae),	Madarangi,	MA	Leaf	Jaundice, amoebic dysentery and sore throats.
5	<i>Datura metel</i> L. (Solanaceae),	Umatta	UN	Leaf	Rheumatism, Asthma, control of dandruff.
6	<i>Adathoda vasica</i> Nees (Acanthaceae),	Adusoge	AD	Leaf	Cough, Spiny outgrowths of piles to control bleeding.
7	<i>Acalypha indica</i> L. (Euphorbiaceae)	Kappigida	KU	Leaf	Constipation, Scabies, Eczema, asthma and Urinary problems.
8	<i>Plumbago zeylanica</i> L. (Plumbaginaceae),	Bili chitrannada	BI	Root	Pile, elephantiasis and rheumatic pain.
9	<i>Balaaites roxburghii</i> Planch. (Simarubaceae)	Ingudi	IN	Leaf	Jaundice, intestinal worm infections, leukoderma, psychiatric disorders.
10	<i>Barleria prionites</i> L. (Acanthaceae),	Mulligoranti	MU	Leaf	Scabies, respiratory diseases, tooth ache and joint pains.
11	<i>Mirabilis jalapa</i> L. (Nyctaginaceae),	Sanjemallige	SA	Leaf	Wound healing, abscesses and inflammation.
12	<i>Gymnema sylvestre</i> (Asclepiadaceae)	Kudapatri	KO	Leaf	Diabetes, metabolic syndrome, weight loss and cough.
13	<i>Tylophora indica</i> (Asclepiadaceae)	Aadu mittada balli	AA	Root & Leaf	Cough, asthma, bronchitis, dysentery, diarrhea, wounds, ulcer, hemorrhoids, malignant tumor, and leukemia

Table 2: Operating parameter for working elements

Elements	Wavelength (nm)	Slit width (nm)	Lamp Current	Flame Type	Fuel Flow (L/min)	Characteristic Conc. mg/L	Burner Height (mm)
Mg	285.2	0.5	75%	Air-C <sub>2</sub> H <sub>2</sub>	1.2	0.0170	7
Al	309.3	0.5	100%	N <sub>2</sub> O-C <sub>2</sub> H <sub>2</sub>	4.3	12.0442	11
K	766.5	0.5	100%	Air-C <sub>2</sub> H <sub>2</sub>	1.2	0.0567	7
Mn	279.5	0.2	75%	Air-C <sub>2</sub> H <sub>2</sub>	1.0	0.0860	7
Fe	248.3	0.5	75%	Air-C <sub>2</sub> H <sub>2</sub>	0.9	0.2344	7
Ca	422.7	0.5	100%	N <sub>2</sub> O-C <sub>2</sub> H <sub>2</sub>	4.2	0.2340	11
Cu	324.8	0.5	75%	Air-C <sub>2</sub> H <sub>2</sub>	1.1	0.1119	7
Zn	213.9	0.2	75%	Air-C <sub>2</sub> H <sub>2</sub>	1.2	0.0333	7
Cd	228.8	0.5	50%	Air-C <sub>2</sub> H <sub>2</sub>	1.2	0.0344	7
Mo	313.3	0.5	75%	N <sub>2</sub> O-C <sub>2</sub> H <sub>2</sub>	4.7	3.6551	11
V	318.5	0.5	75%	N <sub>2</sub> O-C <sub>2</sub> H <sub>2</sub>	4.7	4.2067	11
Ti	305.4	0.5	75%	N <sub>2</sub> O-C <sub>2</sub> H <sub>2</sub>	4.7	45.6638	11

Table 3: Concentration of elements (in mg L<sup>-1</sup>) in the traditional medicinal plants collected from Gulbarga

S. No	Botanical name	Coding	Mg	Al	K	Mn	Fe	Ca	Cu	Zn	Cd	Mo	V	Ti
1	<i>Absolom indicum</i> (L.)	YU	7.4817	0	18.0794	0.1074	0.3072	76.5954	0	0.1048	0.0036	2.3730	1.8851	0.4551
2	<i>Murraya koenigii</i> (L.) Spreng	KA	7.0280	0	17.1518	0.2419	3.1464	73.7779	0.0460	0.0744	0.0188	2.2808	2.0665	4.7605
3	<i>Thaunpora conditiosa</i>	AM	6.9069	0	19.3953	0.4677	0.5291	71.9977	0	0.0374	0.0073	2.5380	2.1404	1.2515
4	<i>Lavonina inermis</i> L. (Lythraceae)	MA	7.2817	0	12.2685	0.2539	1.4574	78.2088	0.0135	0.0853	0.0008	2.5437	2.2929	0
5	<i>Datura metel</i> L. (Solanaceae)	UN	7.1855	0	20.0802	0.2233	1.0544	80.4063	0.0055	0.0761	0.0132	2.3948	2.2706	0
6	<i>Adathoda vasika</i> Nees. (Acanthaceae)	AD	7.0582	0	15.2156	0.2117	1.8310	78.9519	0	0.1354	0.0213	2.5630	2.3034	0
7	<i>Aclypha indica</i> L. (Euphorbiaceae)	KU	7.2165	1.3896	17.0665	0.2415	4.0092	78.3728	0.0066	0.1316	0.0086	0.1084	1.2996	2.5503
8	<i>Plumbago zeylanica</i> L. (Plumbaginaceae)	BI	7.5361	0.5786	18.1869	0.2481	1.0217	53.1360	0	0.0938	0.0002	0.2650	1.3024	0.6345
9	<i>Salanthes muburgii</i> Planch. (Simarubaceae)	IN	6.9488	0.6873	6.1536	0.1606	0.4761	76.8192	0	0.0401	0	0.5987	1.3179	1.8217
10	<i>Barleria prionites</i> L. (Acanthaceae)	MU	7.4221	0.2443	18.8229	0.0847	0.9937	79.0460	0	0.0618	0.0143	0.6544	1.3029	3.9378
11	<i>Abrabilis jalapa</i> L. (Nyctaginaceae)	SA	7.5132	2.4991	18.2589	0.1931	0.7003	78.5445	0.0054	0.0993	0.0104	0.7266	1.2874	3.4799
12	<i>Gynema sylvestre</i> (Retz.) R.Br. ex Schult. (Asclepiadaceae)	KO	7.1939	3.0792	16.8841	0.5515	1.2741	70.6604	0.0138	0.0729	0.0046	0.6493	1.4762	3.7741
13	<i>Tylophora indica</i> (Asclepiadaceae)	AA	6.7428	2.3862	13.2819	0.2265	0.3803	72.4958	0.0397	0.0826	0.0097	0.5273	1.5403	0.7607

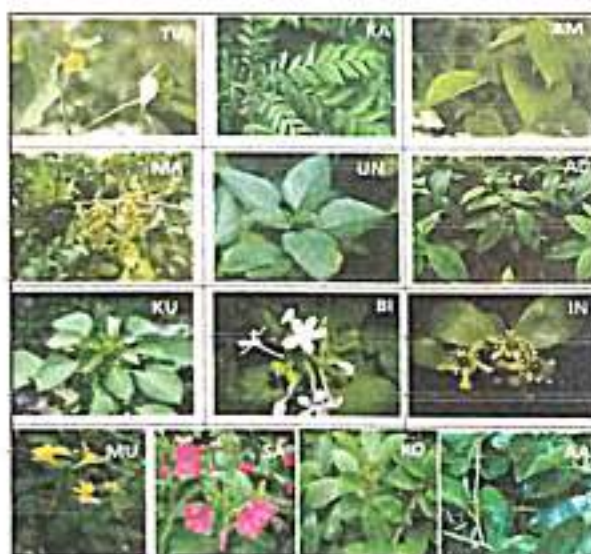


Fig 1: Leaves of Different traditional medicinal plants

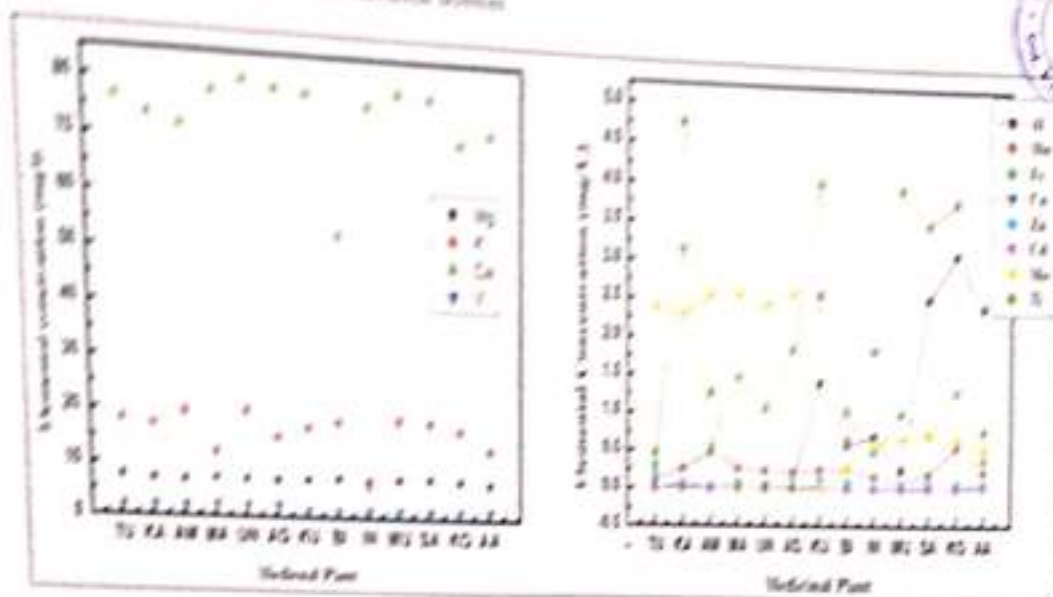


Fig 2: Elemental concentration in dried medicinal plants

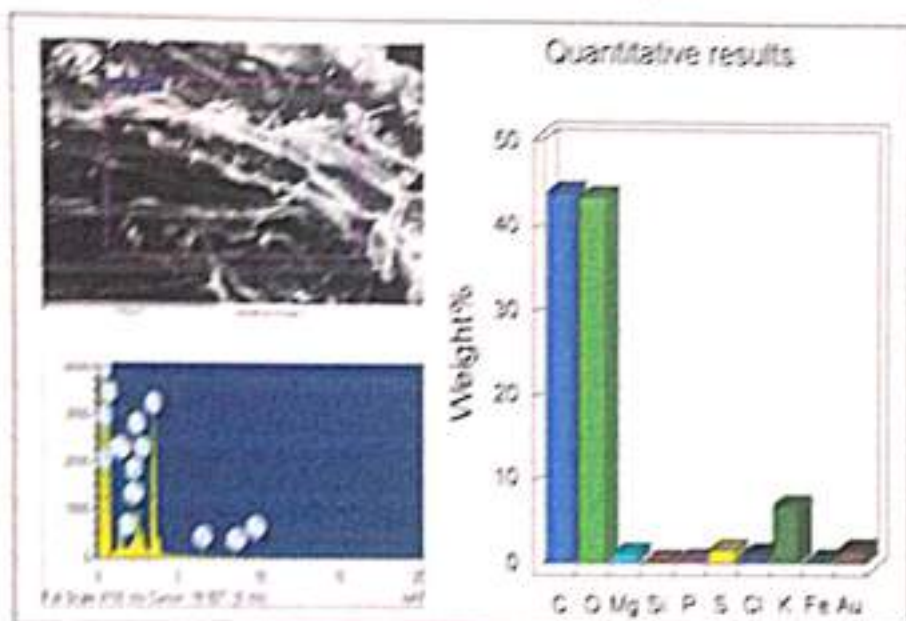


Fig 3: SEM-EDX for Ficus metal L. (Solanaceae)

**5. Conclusions**

The present study of elemental analysis of the medicinal plant reveals the presence of various elements but the concentration of the elements such as Ca, K, Mg and V is found to be significantly high. This is attributed to the presence of the said elements the soil surrounding of the nature and the different botanical structure of the medicinal plant. From this study it is also verified the medicinal plants viz. *Moraya kromigii*, *Laurusus inermis*, *Datura metal*, *Asalypha indica*, *Mirabilis jalapa*, *Crysanema sylvestre* and *Tylophora indica* contains trace elemental concentration of copper and zinc along with copper and other trace elements, which are the required nutrients for the metabolism as per the recommendations of WHO<sup>[1-11]</sup>. The other elements such as Al, Mn, Fe, Cd, Mo, and Ti were determined in the present study but the

concentration of these elements is found to be comparatively less. The data obtained in present study will be helpful in the synthesis of new modern drugs with various combinations of plants which can be used to cure many diseases. The results were correlated with SEM-EDX and are found to be similar as shown in figure 1, for *Ficus metal L.* (Solanaceae). However, more detailed analysis of chemical composition of these traditional medicinal plants is required and work is progressive in this direction.

**6. References**

1. Lissak A, Soltyk K, Ostapczuk P, Fijalik Z. Determination of selected trace elements in herbs and their infusions. *The Science of the Total Environment*. 2002; 289(1-3):31-40.





2. World Health Organization, WHO Guidelines on Good Agricultural and Collection Practices (GACP) for Medicinal Plants, WHO Press, Geneva, Switzerland, 2003.
3. World Health Organization, Monographs on Selected Medicinal Plants. WHO Press, Geneva, Switzerland. 2007, 1-3.
4. World Health Organization, Quality Control Methods for Medicinal Plant Materials, WHO Press, Geneva, Switzerland, 1998.
5. World Health Organization, Traditional Medicine Growing Needs and Potential - WHO Policy Perspectives on Medicines, 2002.
6. Raut OP, Acharya R, Gupta R, Mishra SK, Sahoo R, et. International Journal of Applied biology and pharmaceutical technology. 2013; 4(1).
7. Santoshkumar Teerthe S, Mohanraj Pattar, Sharanabasappa, Kerur BR. Elemental Contents in Ayurvedic Medicinal plants Using AAS Technique, JI Of Instrum.Soc. of India. 2017; 45(2):110-112. ISSN: 0970-9983.
8. Subramanian R, Subbramaniyan P, Raj V. Determination of some minerals and trace elements in two tropical medicinal plants, Asian Pacific Journal of Tropical Biomedicine. 2012; S555-S558.
9. Subramanian R, Gayathri S, Rahnavel C, Raj V, Analysis of mineral and heavy metals in some medicinal plants collected from local market, Asian Pacific Journal of Tropical Biomedicine. 2012; 2(1):S74-S78.
10. Dushenkov V, Kumar PBAN, Motto H, Baskin I. Rhizofiltration: The Use of Plants to Remove Heavy Metals from Aqueous Streams, Environmental Science Technology. 1995; 29:1239-1245.
11. Ramamurthy N, Kannan S. Romanian, SEM-EDS analysis of soil and plant (*Calotropis gigantea* Linn) collected from an Industrial village, Cuddalore Dt, Tamil Nadu, India, J Biophys. 2009; 19(3):219-226.
12. Santosh T, Mohanraj P, Sharanabasappa, Kerur BR. Accumulation of Elements in Homemade Herbal Medicinal plants, International Journal of Pure & Applied Physics. 2017; 13(1):50-53.
13. Ngugi P, Njagi J, Kibiti C, Maina D, Ngeranwa J, et al. Trace elements content of selected Kenyan anti-diabetic medicinal plants. Int J Curr Pharm Res. 2012; 4:39-42.
14. O'Connell B. Select vitamins and minerals in the management of diabetes. Diabetes Spectra. 2001; 14:133-148.
15. Hunt JR. Bioavailability of Fe, Zn and other Trace Minerals for Vegetarian Diets. Am. J Clin. Nutr. 1994; 78:633-39.
16. Thunus L, Lejeune R. Handbook on Metals in Clinical and Analytical Chemistry. Marcel Dekker, New York, 1994.
17. World Health Organization, Quality Control Methods for Medicinal Plant Materials, WHO Press, Geneva, Switzerland, 1998.



# International Journal of Research in Pharmacy and Pharmaceutical Sciences

Peer Reviewed Journal, Refereed Journal, Indexed Journal

ISSN: 2455-698X, Impact Factor: RJIF 5.22

UGC Approved Journal, UGC Journal No.: 48760

## *Publication Certificate*

This certificate confirms that "Mohanraj Pattar" has published manuscript titled "A study on major and trace elements in some traditional medicinal plants using AAS technique".

Details of Published Article as follow:

Volume : 2  
Issue : 6  
Month : Nov-Dec  
Year : 2017  
Page Number : 86-90

Certificate No.: 2-6-29

Date: 01-11-2017

Yours Sincerely,



Nikhil Gupta

Publisher

International Journal of Research in Pharmacy and Pharmaceutical Sciences

[www.pharmacyjournal.in](http://www.pharmacyjournal.in)

Tel: 9999888931

International Journal of Research in Pharmacy and Pharmaceutical Sciences

Email: [ijpps.research@gmail.com](mailto:ijpps.research@gmail.com) Website: [www.pharmacyjournal.in](http://www.pharmacyjournal.in)

# Certificate of Publication

International Recognized Multidisciplinary Research Journal

## Indian Streams Research Journal

ISSN 2230-7850

Impact Factor : 4.1625(UIF)



RNI: MAHMUL 2011/38595

This is to certify that our review board accepted research paper of Dr./Shri./Smt.: **Muqem Miyan** Topic: ಭಾರತೀಯ ಜಾನಪದ ಸಂಗೀತ. College:- Smt. V. G. Degree College For Women, Kalaburagi. The research paper is original & innovative. It is done double blind peer reviewed. Your article is published in the month of Jan year 2017.



258/34, Raviwar Peth, Solapur-413005 Maharashtra India  
Contact Detail: +91-0217-2372010 / 9595-359-435  
e-Mail: ayisrj2011@gmail.com  
Website: www.isrj.org

*S.G. Gounbali*  
**IQAC Co-ordinator**  
Smt. V.G. Women's Degree College,  
KALABURAGI

Authorised Signature

**H.N. Jagtap**  
Editor-in-Chief

**PRINCIPAL**  
Smt. V.G. Degree College for Women,  
KALABURAGI

## ಭಾರತೀಯ ಜಾನಪದ ಸಂಗೀತ

**Muqem Miyan**

Lecturer in Hindustani Music ,

Smt.V.G.Degree College for Women , Kalaburagi.

ಭಾರತ ಪ್ರಾಚೀನ ಕಾಲದಿಂದ ಶ್ರೇಷ್ಠ ಸಂಗೀತಗಾರರ ನೆಲೆಬಿಡಲಾಗಿದೆ. ಭಾರತದ ಕರ್ನಾಟಕ ರಾಜ್ಯವು ಅನೇಕಾನೇಕ ಸುಪ್ರಸಿದ್ಧ ಸಂಗೀತಗಾರರ ನೆಲೆಯಾಗಿದೆ. ಪುರಂದರದಾಸರು, ವಿಜಯದಾಸರು, ಕನಕದಾಸರು ಮುಂತಾದ ದಾಸವರೇಣ್ಯರ ಜೊತೆಗೆ ಬಸವೇಶ್ವರರು, ಅಕ್ಕಮಹಾದೇವಿ, ನಿಜಗುಣ ಶಿವಯೋಗಿಗಳು ಇತ್ಯಾದಿ ಅನೇಕ ಶ್ರೇಷ್ಠ ಸಂತ-ಸಂಗೀತಜ್ಞರು ಆಗಿ ಹೋಗಿದ್ದಾರೆ.

ಭಾರತೀಯ ಸಂಗೀತದ ಚರಿತ್ರೆಯಲ್ಲಿ ನಮ್ಮ ನಾಡಿನ ಕೊಡುಗೆ ಅತ್ಯಂತ ಮಹತ್ವಪೂರ್ಣವಾದದ್ದು. ಭಾರತೀಯ ಸಂಗೀತದ ಎರಡು ಪದ್ಧತಿಗಳು ಅಂದರೆ, ಹಿಂದೂಸ್ತಾನಿ ಹಾಗೂ ಕರ್ನಾಟಕ ಸಂಗೀತ ಪದ್ಧತಿಗಳು ಪ್ರಚಾರದಲ್ಲಿ ಎಂದಿನಿಂದ ಬಂದವೋ, ಅಂದಿನಿಂದ ಸ್ವಾಭಾವಿಕವಾಗಿ ದಕ್ಷಿಣ ಭಾರತದಲ್ಲೆಲ್ಲ ಕರ್ನಾಟಕ ಸಂಗೀತದ ಪ್ರಚಾರ ವಿಶೇಷವಾಗಿತ್ತು. ಪ್ರಚಾರದಲ್ಲಿ ಹೀಗಿದ್ದರೂ ಸುಮಾರು ಎರಡುನೂರು ವರ್ಷಗಳಿಂದ ಕರ್ನಾಟಕದಲ್ಲಿ ಹಿಂದೂಸ್ತಾನಿ ಸಂಗೀತದ ಪ್ರವೇಶ ಆದುದನ್ನು ನೋಡಿದರೆ ಅದು ಅತ್ಯಂತ ವೈಶಿಷ್ಟ್ಯಪೂರ್ಣವೆನಿಸುತ್ತದೆ. ಕರ್ನಾಟಕದಲ್ಲಿ ಹಿಂದೂಸ್ತಾನಿ ಪ್ರಚಾರ ವಿಶೇಷ ರೂಪದಿಂದ ಬ್ರಿಟಿಷ್ ಕಾಲದಿಂದಲೇ ಆಗಲು ಪ್ರಾರಂಭವಾಯಿತು ಎಂದು ಕಂಡುಬರುತ್ತದೆ.

ಬ್ರಿಟಿಷ್ ಕಾಲದಲ್ಲಿ ಕರ್ನಾಟಕ ದೇಶವನ್ನು ಉತ್ತರ ಕರ್ನಾಟಕ ಹಾಗೂ ದಕ್ಷಿಣ ಕರ್ನಾಟಕ ಎಂದು ವಿಭಜಿಸಲಾಗಿತ್ತು. ದಕ್ಷಿಣ ಕರ್ನಾಟಕದ ಭಾಗವೆಂದರೆ ಇಂದಿನ ಪಳೆಯ ಮೈಸೂರು ರಾಜ್ಯ. ಈ ಭಾಗವು ಮೈಸೂರಿನ ರಾಜಮನೆತನದವರ ಆಡಳಿತದಲ್ಲಿತ್ತು. ಉತ್ತರ ಕರ್ನಾಟಕದ ಭಾಗವನ್ನು ಬ್ರಿಟಿಷರ ಆಡಳಿತದಲ್ಲಿದ್ದ ಮುಂದೆ ವಿಭಾಗಕ್ಕೆ ಹೋಡಿಸಲಾಗಿತ್ತು.

ಮೈಸೂರು ಆಸ್ಥಾನದ ದೊರೆಗಳಾದ ಮುಮ್ಮಡಿ ಕೃಷ್ಣರಾಜ ಒಡೆಯರರು, ನಾಲ್ವಡಿ ಕೃಷ್ಣರಾಜ ಒಡೆಯರರು ಹಾಗೂ ಶ್ರೀ ಜಯಚಾಮರಾಜ ಒಡೆಯರರು ಸ್ವತಃ ಸಂಗೀತಜ್ಞರೂ, ಸಂಗೀತ ಕಲೆಯ ಮೋಹಕರೂ ಆಗಿದ್ದರು.

ಕರ್ನಾಟಕದಲ್ಲಿ ಹಿಂದೂಸ್ತಾನಿ ಸಂಗೀತದ ಜೊತೆಗೆ ಜಾನಪದ ಸಂಗೀತವೂ ದೆಳೆಯಿತು. ನಮ್ಮ ರಾಜ್ಯದಲ್ಲಿಯೇ ಜಾನಪದ ಸಂಗೀತದ ಬೆಳವಣಿಗೆಯ ಸಂಪೂರ್ಣ ವಿವರಣೆ ಈ ಕೆಳಗೆ ನೀಡಲಾಗಿದೆ.

ಪ್ರಾಚೀನ ಕಾಲದಿಂದಲೇ ಮಾನವನ ಸಂಬಂಧವು ನಿಸರ್ಗದೊಡನೆ ಅನ್ಯೋನ್ಯವಾಗಿದ್ದರಿಂದ, ಅವನ ಪ್ರತಿಯೊಂದು ಕ್ರಿಯೆಯು ಪ್ರಾಕೃತಿಕವಾಗಿತ್ತು. ಯಾವುದೇ ಪರಿಸ್ಥಿತಿಯಲ್ಲಿ ಅವನು ನಿಸರ್ಗದ ಮೊರೆಹೋಗುತ್ತಿದ್ದ. ಇದರಿಂದಾಗಿ ಅವನ ಮನೋಭಾವಗಳು ಸಂಗೀತದ ರೂಪ ಧರಿಸಿ ಹೊರಬರುತ್ತಿದ್ದವು. ಆ ಕಾಲದಲ್ಲಿಯೇ ಸಂಗೀತದಲ್ಲಿ ಸಹಜತೆ ಅಧಿಕವಾಗಿತ್ತು. ಕಾಲಕ್ರಮೇಣ ಮಾನವನು ನಿಸರ್ಗದ ಮೇಲೆ ಪ್ರಭುತ್ವ ಸ್ಥಾಪಿಸಲು ಪ್ರಾರಂಭಿಸಿದನು. ಕಾರಣ ಅವನು ಮೊದಲಿನಂತೆ ನಿಸರ್ಗದ ಮೊರೆಹೋಗುವುದನ್ನು ಕಡಿಮೆಮಾಡಲಾರಂಭಿಸಿದನು. ಇದರ ಪರಿಣಾಮವಾಗಿ ಪ್ರಕೃತಿಯ ಜೊತೆಗೆ ಅವನ ಸಂಬಂಧ ಕಡಿಮೆಯಾಗಿ ಅವನ ಜೀವನದಲ್ಲಿ ಕೆಲವು ಪರಿವರ್ತನೆಗಳು ಆಗಲಾರಂಭಿಸಿದವು. ಈ ಪರಿವರ್ತನೆಗಳ ಪ್ರಭಾವವು ಅವನು ನಿರ್ಮಿಸಿದ ಸಂಗೀತದ ಮೇಲೆಯೂ ಕಂಡುಬರಲು ಪ್ರಾರಂಭಿಸಿತು.

ಯಾವುದೇ ಒಂದು ದೇಶದ ಜಾನಪದ ಸಂಗೀತವು ದೇಶದ ಸಂಸ್ಕೃತಿಯನ್ನು ಪ್ರತಿನಿಧಿಸುತ್ತದೆ. ಸಂಗೀತದಲ್ಲಿಯೇ ಸಾತ್ವಿಕ ಭಾವವು ದೋಷ ಸಂಗೀತ ಅಥವಾ ಜಾನಪದ ಸಂಗೀತದ ಮಾಧ್ಯಮದಿಂದ ವ್ಯಕ್ತ ಮಾಡಲ್ಪಡುತ್ತದೆ. ಜೀವನ ಹಾಗೂ ಸಂಗೀತದ ನೈಸರ್ಗಿಕ ಸಂಬಂಧದ ಪರಿಚಯ ಯಾವ ರೀತಿ ನಮಗೆ ಜಾನಪದ ಸಂಗೀತದಲ್ಲಿ ದೊರಕುತ್ತದೆಯೋ ಆ ರೀತಿ ಶಾಸ್ತ್ರೀಯ ಸಂಗೀತದಲ್ಲಿ ದೊರಕಲಾರದು. ಜಾನಪದ ಗೀತೆಗಳಿಗೆ ಸಹಜ ಅಥವಾ ದೋಷಗೀತ ಎಂದು ಹೇಳಲಾಗುತ್ತದೆ. ಈ ಗೀತದ ಪ್ರಕಾರವು ಅತ್ಯಂತ ಸರಳವಾಗಿದ್ದು ಕೇವಲ ಅನುಕರಣ ಮಾತ್ರದಿಂದಲೇ ಕಲಿಯಲು ಸಾಧ್ಯ. ಯಾವುದೇ ಪ್ರಕಾರದ ಶಾಸ್ತ್ರೀಯ ಬಂಧನ ಹಾಗೂ ನಿಯಮಗಳು ಇದರಲ್ಲಿ ಇರದಿದ್ದ ಕಾರಣ ಜನಸಾಮಾನ್ಯರು ಇದನ್ನು ಸುಲಭವಾಗಿ ಗ್ರಹಿಸಲು



Folk Musics in India



ಸಾಧ್ಯ

ಲೋಕ ಜೀವನದ ಅತ್ಯಂತ ಸುಂದರವಾದ ಪ್ರತಿಬಿಂಬವು ಜಾನಪದ ಸಂಗೀತದಲ್ಲಿ ಕಂಡುಬರುತ್ತದೆ. ಎಕೆಂದರೆ ಜಾನಪದ ಗೀತೆಗಳಲ್ಲಿ 'ಶಬ್ದ' ಹಾಗೂ 'ಸ್ವರಗಳ' ಸಂಯೋಜನೆಯಲ್ಲಿ ಕೃತ್ರಿಮತೆ ಇರುವುದಿಲ್ಲ. ಗೀತೆಗಳಲ್ಲಿ ಲೋಕ ಜೀವನದ ಅತ್ಯಂತ ಸರಳವಾದ ಪರಿಚಯವಿರುತ್ತದೆ. ಅವು ಮಾನವನ ಬಾಹ್ಯ ಜೀವನದ ಜೊತೆಗೆ ಅವನ ಮಾನಸಿಕ ಭಾವನೆಗಳನ್ನು ಕೂಡ ಸ್ಪಷ್ಟಪಡಿಸುತ್ತದೆ. ಜಾನಪದ ಗೀತೆಗಳು ಸಂಕ್ಷಿಪ್ತವಾಗಿಯೂ, ಸರಳವಾಗಿಯೂ, ಸ್ಪಷ್ಟವಾಗಿಯೂ, ಅನುಭೂತಿಮಯವಾಗಿಯೂ ಹಾಗೂ ಸಂಗೀತಮಯವಾಗಿಯೂ ಇರುತ್ತವೆ. ಜಾನಪದ ಗೀತೆಗಳ ಮುಖ್ಯ ಉದ್ದೇಶವು ಜನ ಮನರಂಜನೆಗಾಗಿದ್ದು ವೇದಕಾಲದಿಂದ 'ದೇಶಿ' ಸಂಗೀತ ಎಂಬ ನಾಮ ಧರಿಸಿ ಪ್ರಸಾರಕ್ಕೆ ಬಂದವು. ಬೃಹದ್ದೇಶಿ ಎಂಬ ಗ್ರಂಥದ ಕರ್ತೃ 'ಮತಂಗ' ಮುನಿಯು 'ದೇಶಿ' ಸಂಗೀತ ಅರ್ಥಾತ್ ಜಾನಪದ ಸಂಗೀತದ ಬಗೆಗೆ ಸಾಕಷ್ಟು ವಿವರಣೆ ನೀಡಿದ್ದಾನೆ. ರಾಮಾಯಣ, ಮಹಾಭಾರತ ಕಾಲದಲ್ಲಿಯೂ ವಿವಿಧ ಸಂದರ್ಭಗಳಲ್ಲಿ ಜಾನಪದ ಗೀತೆಗಳನ್ನು ಹಾಡಲಾಗುತ್ತಿತ್ತು ಎನ್ನುವುದರ ಬಗೆಗೆ ಉಲ್ಲೇಖ ಸಿಗುತ್ತವೆ.

**ಜಾನಪದ ಗೀತೆಗಳ ವೈಶಿಷ್ಟ್ಯತೆ**

ಜಾನಪದ ಗೀತೆಗಳು ವಿಶೇಷವಾಗಿ ನಾಲ್ಕು ಅಥವಾ ಐದು ಸ್ವರಗಳಲ್ಲಿ ಹಾಡಲ್ಪಡುತ್ತವೆ. ಈ ಗೀತೆಗಳೂ ಲಯಬದ್ಧವಾಗಿದ್ದು ಲಯದ ವಿವಿಧ ಪ್ರಕಾರಗಳೂ ಇದರಲ್ಲಿ ಕಂಡುಬರುತ್ತವೆ. ಜಾನಪದ ಗೀತೆಗಳಲ್ಲಿ ಯೋಜಿಸಿದ ಸ್ವರಗಳು 'ಶಬ್ದ' ಹಾಗೂ 'ಸಮಯ'ವನ್ನು ಅನುಸರಿಸುತ್ತವೆ. ಶಾಸ್ತ್ರೀಯ ಸಂಗೀತದ ಉತ್ತಮ ಜಾನಪದ ಸಂಗೀತದಿಂದಲೇ ಆಯಿತು ಎಂದು ಹೇಳಲಾಗುತ್ತದೆ. ಜಾನಪದ ಗೀತೆಗಳು ವಿಶೇಷವಾಗಿ ಸಾಮೂಹಿಕ ರೂಪದಲ್ಲಿ ಹಾಡಲ್ಪಡುತ್ತಿದ್ದು, ಇವುಗಳ ಜೊತೆಗೆ ಪ್ರಾದೇಶಿಕ ಪಕ್ಕ ವಾದ್ಯಗಳ ಉಪಯೋಗವೂ ಕೂಡಾ ಮಾಡಲಾಗುತ್ತದೆ.

**ಕರ್ನಾಟಕದಲ್ಲಿ ಜಾನಪದ ಸಂಗೀತ**

ಕರ್ನಾಟಕದಲ್ಲಿ ಜಾನಪದ ಸಂಗೀತದ ಅನೇಕ ಪ್ರಕಾರಗಳು ಕಂಡು ಬರುತ್ತವೆ. ಅವುಗಳು ಈ ಕೆಳಗಿನಂತಿವೆ.

- 1.ಸಾಂಪ್ರದಾಯಿಕ ಹಾಡುಗಳು: ಮನುಷ್ಯನ ಜೀವನದಲ್ಲಿ ಜನನ, ನಾಮಕರಣ, ಕರ್ಣವೇಧ, ವಿವಾಹ, ಮರಣ ಮುಂತಾದ ಸಂದರ್ಭಗಳಲ್ಲಿ ಹಾಡಲ್ಪಡುವ ಗೀತೆಗಳು ಈ ಗೀತ ಪ್ರಕಾರದಲ್ಲಿ ಬರುತ್ತವೆ. ಈ ಮೇಲೆ ನಮೂದಿಸಿರುವ ಎಲ್ಲ ಸಮಾರಂಭಗಳು ಸಾಂಪ್ರದಾಯಿಕವಾದ ರೂಢಿಗಳು, ಪದ್ಧತಿಗಳು, ಆಚರಣೆಗಳು ಆಗಿವೆ. ಈ ಸಮಾರಂಭಗಳಲ್ಲಿ ಹಾಡುವ ಗೀತೆಗಳನ್ನು ಸಾಂಪ್ರದಾಯಿಕ ಜಾಜಪದ ಗೀತೆಗಳು ಎಂದು ಕರೆಯಲಾಗುತ್ತದೆ.
- 2.ಸುಗ್ಗಿಯ ಹಾಡುಗಳು: ಈ ಗೀತೆಯ ಪ್ರಕಾರವು ಕರ್ನಾಟಕದಲ್ಲಿ ಅತ್ಯಂತ ಲೋಕಪ್ರಿಯವಾಗಿದೆ. ಸುಗ್ಗಿಯ ಹಾಡುಗಳಿಂದ ಒಡಗೂಡಿ ಸುಗ್ಗಿಯ ಕಾಲದಲ್ಲಿ ವಿಶೇಷ ಪ್ರಕಾರದ ಉತ್ಸವವನ್ನು ಆಚರಿಸಲಾಗುತ್ತದೆ. ಧೂದೇವಿಯ ಸ್ತುತಿ, ಮಳೆರಾಯನ ಆರಾಧನೆ ನಂತರ ಹೊಲದಲ್ಲಿದ್ದ ಧಾನ್ಯ ರಾಶಿ ನೋಡಿ ಆಗುವ ಅನಂದೋಲ್ಲಾಸ ಹಾಗೂ ರೈತ ಸಮಾಜದಲ್ಲಿ ದಿನಂಪ್ರತಿ ನಡೆಯುವ ಘಟನೆಗಳ ವರ್ಣನೆ ಈ ಗೀತೆಗಳ ವಸ್ತುಗಳಾಗಿರುತ್ತವೆ. ಬಹುಶಃ ಸುಗ್ಗಿಯ ಸಮಯದಲ್ಲಿ ರೈತ ಸಮುದಾಯವು ಸಂಪೂರ್ಣವಾಗಿ ಉಲ್ಲಾಸಭರಿತವಾಗಿರುವುದರಿಂದ ಬಹಳಷ್ಟು ವಿಶೇಷ ಹಾಡುಗಳು ಜಾನಪದ ಲೋಕವೇ ಅತ್ಯರ್ಥಪಡುವ ಹಾಗೆ ಒಳ್ಳೆಯ ಸುಗ್ಗಿಯ ಗೀತೆಗಳು ಹೊರಹೊಮ್ಮಿವೆ. ಇವುಗಳು ರೈತ ಸಮುದಾಯವನ್ನು ಈ ಸಮಯದಲ್ಲಿ ಮಹದಾನಂದದಲ್ಲಿ ಇಡುವುದರಲ್ಲಿ ಯಶಸ್ವಿಯಾಗಿವೆ.
- 3.ಪೌರಾಣಿಕ ಗೀತೆಗಳು: ಪುರಾಣ ಕಥೆಗಳ ಮೇಲೆ ಆಧಾರಗೊಂಡ ಗೀತೆಗಳು ಈ ಪ್ರಕಾರವಾಗಿವೆ. ಉದಾಹರಣೆಗೆ ರಾಮ, ಕೃಷ್ಣ ಹಾಗೂ ಪಾಂಡವರ ಪರಾಕ್ರಮದ ಕಥೆ, ಶ್ರೀ ಕೃಷ್ಣಲೀಲಾ ಮುಂತಾದ ಸಂಗತಿಗಳು ಈ ಗೀತೆಗಳ ವಸ್ತುಗಳಾಗಿರುತ್ತವೆ.
- 4.ಕಸಬಿನ ಹಾಡುಗಳು: ದೈನಂದಿನ ಕಾರ್ಯ ಮಾಡುವಾಗ ಶ್ರಮಪರಿಹಾರಾರ್ಥವಾಗಿ ಹಾಗೂ ಸ್ವೂರ್ತಿಗಾಗಿ ಕೆಲವು ಗೀತೆಗಳನ್ನು ಹಾಡಲಾಗುತ್ತದೆ. ಹಳ್ಳಿ ಜನರ ದೈನಂದಿನ ಕೆಲಸಗಳಾಗಿರುವ ಕುಟ್ಟುವುದು, ಬೀಸುವುದು, ಹೆಣೆಯುವುದು, ಇತ್ಯಾದಿಗಳಲ್ಲಿ ಈ ಕಸಬಿನ ಹಾಡುಗಳನ್ನು ಹಾಡಲಾಗುತ್ತದೆ. ಇವುಗಳಲ್ಲಿ ಗೋಪಾಲಕರ ಗೀತೆಗಳು, ಅಂಬಿಗರ ಹಾಡುಗಳು, ಕಮ್ಮಾರರ ಹಾಡುಗಳು, ಅಗಸರ ಹಾಡುಗಳು, ಕಲ್ಲುಕುಟಿಗರ ಹಾಡುಗಳು ಈ ಪ್ರಕಾರದ ಅನೇಕ ಪಾರಿಶಿಕ ಶ್ರಮಗಳ ಕಾರ್ಯದಲ್ಲಿ ಹಾಡುವ ಗೀತೆಗಳು ಇದರಲ್ಲಿ ಒಳಗೊಂಡಿವೆ.
- 5.ನೀತಿ ಹಾಡುಗಳು: ಜನರಿಗೆ ನೀತಿಪಾಠ ಕಲಿಸುವುದಕ್ಕಾಗಿ ಅನೇಕ ಗೀತೆಗಳ ರಚನೆಗಳಾದವು. ನಿತ್ಯ ಜೀವನದಲ್ಲಿ ಹೇಗಿರಬೇಕು, ಹೇಗೆ ದಾಂಧಪ್ಪುವುದೇಕೆ, ಹೇಗೆ ಪಾರಮಾರ್ಥವನ್ನು ಸಾಧಿಸಬೇಕು, ಹೇಗೆ ತ್ಯಾಗ ಮಾಡುವುದನ್ನು ಕಲಿಯಬೇಕು ಹಾಗೂ ಮುಂತಾದವು. ಇವುಗಳಲ್ಲದೆ ಧರ್ಮ, ಸುಡಿ, ನಡತೆ ಇತ್ಯಾದಿ ಸಂಗತಿಗಳನ್ನು ಬೋಧಿಸಿ ಜನರ ಕಲ್ಯಾಣಕ್ಕಾಗಿ ಈ ಗೀತೆಗಳು ರಚಿಸಲ್ಪಟ್ಟಿವೆ. ಕನ್ನಡದಲ್ಲಿಯೆ ವಚನ ಸಾಹಿತ್ಯದ ಕೆಲವು ಛಾಂದಸು ಇಂತಹ ಹಾಡುಗಳಿಗೆ ಒಂದು ಉತ್ತಮ ನಿದರ್ಶನ ಎಂದು ಹೇಳಬಹುದು.
- 6.ಜೋಗುಳ ಹಾಡುಗಳು: ತಾಯಂದಿರು ತಮ್ಮ ಮಕ್ಕಳಿಗೆ ಹಾಲುಣಿಸುವಾಗ ಹಾಗೂ ಅವರನ್ನು ಮಲಗಿಸುವುದಕ್ಕಾಗಿ ಹಾಡು ಹೇಳುತ್ತಾರೆ. ಇವುಗಳನ್ನೇ ಜೋಗುಳದ ಹಾಡುಗಳೆಂದು ಕರೆಯಲಾಗಿದೆ. ಈ ಹಾಡುಗಳು ಕೂಡಾ ಹೆಚ್ಚಿನ ಜನಪ್ರಿಯತೆಯನ್ನು ಪಡೆದುಕೊಂಡಿವೆ.
- 7.ಪವಾಡದ ಹಾಡುಗಳು: ಈ ಹಾಡುಗಳಲ್ಲಿ ಕೂರ, ಪರಾಕ್ರಮೀ ವೀರರ ವರ್ಣನೆ, ರಾಜರ ವರ್ಣನೆ, ಪ್ರಸಿದ್ಧ ವ್ಯಕ್ತಿಗಳ ವರ್ಣನೆ ಮುಂತಾದ ವಿಷಯಗಳು ವರ್ಣಿಸಲ್ಪಡುತ್ತವೆ.

ಇದರ ಹೊರತಾಗಿ ಶೃಂಗಾರದ ಹಾಡುಗಳು, ಒಗಟಿನ ಹಾಡುಗಳು, ಭಕ್ತಿ ಹಾಡುಗಳು, ಆರತೀ ಹಾಡುಗಳು ಅಲ್ಲದೇ ಶಕ್ತಿ ಪೂಜೆ, ಕಾಳಿ ಪೂಜೆ, ಪೈಶಾಚಿಕ ಪೂಜೆ ಮುಂತಾದ ಸಂದರ್ಭಗಳಲ್ಲಿ ಹಾಡುವ ಹಾಡುಗಳಲ್ಲದೇ ಹಸ್ತ ಸಾಮುದ್ರಿಕ ಹೇಳುವಾಗ ಹಾಡುವ ಗೀತೆ, ಕೊರವಂಜಿ ಹಾಡು, ಗಿಡಮೂಲಿಕೆ ಔಷಧ ಪ್ರಯೋಗ ಮಾಡುವಾಗ ಹಾಡುವ ಹಾಡುಗಳು ಮುಂತಾದ ಅನೇಕ ಜಾನಪದ ಗೀತೆಗಳ ಪ್ರಕಾರಗಳು ಕರ್ನಾಟಕದಲ್ಲಿ ಪ್ರಚಲಿತ ಇವೆ.

**ಆಧಾರ ಗ್ರಂಥಗಳು:**

- 1.ಪ್ರೊ. ಬಿ.ಡಿ. ಬಾಲಕ - ಭಾರತೀಯ ಸಂಗೀತದ ಚರಿತ್ರೆ, ಕನ್ನಡ ಅಧ್ಯಯನ ಪೀಠ, ಪಠ್ಯಪುಸ್ತಕ ನಿರ್ದೇಶನಾಲಯ, ಕರ್ನಾಟಕ ವಿಶ್ವವಿದ್ಯಾಲಯ, ಧಾರವಾಡ.
- 2.ಡಾ. ಎಂ.ಎಚ್. ಕೃಷ್ಣ - ಕನ್ನಡ ನಾಡಿನ ಚರಿತ್ರೆ, ಕರ್ನಾಟಕ ಕಲೆಗಳು (ಮೂರನೇ ಭಾಗ), 1972.
- 3.ಎಂ.ಜಿ.ಬಿರಾದಾರ - 'ಕಲಾ ಗಂಗಾ' ಪ್ರಸಾರಾಂಗ, ಗು.ವಿ.ಗು., 1990.

www.deccanjournals.com

ISSN - 2347 - 8896

Indexed with International  
ISSN Directory, Paris

Impact Factor - 2.2



# ಡೆಕ್ಕನ್ ಕನ್ನಡ ಅವರಣಿ ಪ್ಲಾಟೋ

Deccan Kannada  
Literary Plateau

Indexed with International  
ISSN Directory, Paris

VOLUME : 4 • ISSUE : 7 • JAN 2017

Founder Editor : Prof. Vyasa Kumar Surjan

Chief Editor : Dr. Shanappa S. Nalagi



## ಸಂಗೀತದಲ್ಲಿ ರಾಗ ಚಿಹ್ನೆ

ಮುಕೇಶ್ ಮಿಯಾನ್

ಭಾರತೀಯ ಸಂಗೀತದಲ್ಲಿ ಆಧ್ಯಾತ್ಮದ ಪವಿತ್ರತೆ ಇದೆ. ಮನಃಶಾಸ್ತ್ರದ ವಿಶ್ಲೇಷಣೆಯೂ ಕೂಡಾ ಇದೆ. ತತ್ವಶಾಸ್ತ್ರದ ಆಳವಿದೆ ಹಾಗೂ ಸೌಂದರ್ಯ ಬೋಧನೆ ಇದೆ. ಸಂಗೀತ, ಆಧ್ಯಾತ್ಮ, ಯೋಗಾಸನ ಮತ್ತು ವ್ಯಾಯಾಮ ಒಂದಕ್ಕೊಂದು ಪೂರಕವಾಗಿವೆ. ಆಧ್ಯಾತ್ಮವೆಂದರೆ ಧರ್ಮ, ಅರ್ಥ, ಕಾಮ ಹಾಗೂ ಮೋಕ್ಷಗಳ ಪ್ರಾಪ್ತಿಯಾಗಿದೆ. ಅಂದರೆ ಧರ್ಮದ ಆಚರಣೆಯಿಂದ ಸಂಪತ್ತನ್ನು ಗಳಿಸಬೇಕು. ಈ ಸಂಪತ್ತಿನಿಂದ ನಮ್ಮ ಮನೋಕಾಮನೆಗಳನ್ನು ಅಥವಾ ಆಸೆ ಆಕಾಂಕ್ಷೆಗಳನ್ನು ಈಡೇರಿಸಿಕೊಳ್ಳಬೇಕು. ಹೀಗೆ ನಡೆದುಕೊಂಡಾಗ ಮೋಕ್ಷಕ್ಕೆ ದಾರಿ ಸುಗಮ ಎಂದು ಅನುಭವಿಗಳ ಅಭಿಪ್ರಾಯವಾಗಿದೆ. ಅರ್ಥಾತ್ ಇವೆಲ್ಲವುಗಳ ಪ್ರಾಪ್ತಿ ಎಂದತ್ತಾಗುತ್ತದೆ. ಇದರ ಅಂತರ್ಗತವಾಗಿ ಸತ್ಯ, ಅಹಿಂಸೆ, ಪ್ರೀತಿ, ಪ್ರೇಮ, ಸದ್ಭಾವನೆ, ಸಹಬಾಳ್ವೆ, ಸಮಚಿತ್ತ ಇವುಗಳನ್ನು ಆಧ್ಯಾತ್ಮ ಬೋಧಿಸುತ್ತದೆ. ಸನ್ಮಾರ್ಗದಿಂದಲೇ ಆತ್ಮ ಪರಮಾತ್ಮನಲ್ಲಿ ಲೀನವಾಗುವುದು ಸಾಧ್ಯ ಎಂಬುದು ಈ ಮೇಲಿನ ವಿವರಣೆಯಿಂದ ತಿಳಿದುಬರುತ್ತದೆ.

ಆಧ್ಯಾತ್ಮದ ತಳಹದಿಯನ್ನು ಪಡೆದುಕೊಂಡಿರುವ ಸಂಗೀತದ ಸಹಾಯದಿಂದ ಅನೇಕ ರೋಗರುಜಿನಗಳನ್ನು ವಾಸಿ ಮಾಡಬಹುದು. ಜೀವನದಲ್ಲಿ ಅಸಮಾಧಾನ, ಅಸಹಾಯಕತೆ, ಅಶಾಂತಿ, ಮಾನಸಿಕ ಒತ್ತಡ ರಕ್ತದೊತ್ತಡ, ನಿದ್ರೆಗೇಡಿತನ ಮುಂತಾದವುಗಳು ಹೀಗೆ ಆಧುನಿಕ ಜೀವನದಲ್ಲಿ ಸಾಮಾನ್ಯವಾಗಿವೆ. ಆಧುನಿಕ ಜನರ ಜೀವನವನ್ನುವುದು ರೋಗದ ತವರು ಮನೆವಾಗಿದೆ. ಈ ಎಲ್ಲ ರೋಗಗಳನ್ನು ಓಡಿಸಿ, ಮಾನಸಿಕ ಹಾಗೂ ದೈಹಿಕ ಒತ್ತಡವನ್ನು ಸಮತೋಲನದಲ್ಲಿಡುವ ಮಹಾದಿವ್ಯ ಔಷಧಿಯು ಸಂಗೀತದಲ್ಲಿದೆ ಎನ್ನುವುದನ್ನು ಅರಿತು ಜನರು ಸಂಗೀತಕ್ಕೆ ಮೊರೆಹೋಗಿದ್ದುಂಟು ಹಾಗೂ ಈಗಲೂ ಮೊರೆಹೋಗುತ್ತಿದ್ದಾರೆ. ಅಷ್ಟೇ ಅಲ್ಲ ಇತ್ತೀಚೆಗೆ ಪಾರ್ಶ್ವವಾಯು ಪೀಡಿತ ರೋಗಿಗಳನ್ನು ಈ ಸಂಗೀತದಿಂದ ಗುಣಪಡಿಸುತ್ತಿದ್ದಾರಲ್ಲದೇ, ವಿವಿಧ ರಾಗ ಮಾಲಿಕೆಗಳ ಮೂಲಕ ರೋಗಿಗಳ ಮೇಲೆ ಚಿಕಿತ್ಸೆ ಕೂಡ ನಡೆಸುತ್ತಿದ್ದಾರೆ. ಶ್ವಾಸಕೋಶದ ತೊಂದರೆ ಅಸ್ಥಮಾ, ತಲೆನೋವು ಕಾಯಿಲೆ, ಯಾವುದೇ ಇರಲಿ ಸಂಗೀತದ ಶೃತಿ ಅದನ್ನು ವಾಸಿ ಮಾಡಿ ಬಿಡುತ್ತದೆ. ಸರಿಯಾದ ಸ್ವರದಲ್ಲಿ ಹಾಡಿದರೆ ಸಮಸ್ಯೆ ತಾನೇ ತಾನಾಗಿ ದೂರವಾಗುತ್ತದೆ. ಬೇರೆ ಬೇರೆ ರಾಗಗಳು, ಪ್ರಾಣಾಯಾಮದ ಬೇರೆ ಬೇರೆ ರೀತಿಗಳಂತೆ ಕೆಲಸ ಮಾಡುತ್ತವೆ. ತತ್ತರಿಣಾಮವಾಗಿ ಶ್ವಾಸಕೋಶಕ್ಕೆ ಸಂಬಂಧಪಟ್ಟ ಅಸ್ಥಮಾದಂತಹ ಕಾಯಿಲೆಗಳು ವಾಸಿಯಾಗುತ್ತವೆ. ತಲೆನೋವು, ನಿದ್ರಾತೂನ್ಯತೆಗೂ ಸಂಗೀತ ರಾಮಬಾಣ. ಅಸ್ಥಮಾ ರೋಗಕ್ಕೆ ರಾಗ ದರಬಾರಿ ಕಾನಡಾ ರಾಮಬಾಣವಾದರೆ, ರಾಗ ವಸಂತ ತಲೆನೋವನ್ನು ಹೊಡೆದೊಡಿಸುತ್ತದೆ. ರೋಗಿ ಸ್ವತಃ ಹಾಡುವುದರಿಂದ ಬಹಳಷ್ಟು ಹಚ್ಚಿನ ಲಾಭವಾಗುತ್ತದೆ. ಅಂದರೆ ಶೇಕಡಾ 75 ರಷ್ಟು ರೋಗವು ಗುಣವಾಗುತ್ತದೆ. ಬೇರೆಯವರ ಗಾಯನವನ್ನು ಕೇಳುವುದರಿಂದ ರೋಗವು ಶೇಕಡಾ 25 ರಷ್ಟು ಪ್ರಯೋಜನ ಉಂಟಾಗುತ್ತದೆ. ನೃತ್ಯವೂ ಕೂಡಾ ಕಾಯಿಲೆಗಳಾಗಿರುವ ಆರ್ಥರೈಟಿಸ್ ಹಾಗೂ ಸ್ಪಾಂಡಿಲೈಟಿಸ್‌ಗಳನ್ನು ಗುಣಪಡಿಸುತ್ತದೆ. ಸಂಗೀತವು ಕೇಂದ್ರ ನರಮಂಡಲದ ಮೇಲೆ ನೇರವಾಗಿ ಪರಿಣಾಮ ಬೀರುತ್ತದೆ. ನೂರಕ್ಕೆ ತೊಂಬತ್ತರಷ್ಟು ಜನ ಸಂಗೀತದಿಂದ ಮಾನಸಿಕ ಶಾಂತಿಯನ್ನು ಹೊಂದಿದ್ದಾರೆ. ಸಂಗೀತದಲ್ಲಿರುವ ಈ ಎಲ್ಲ ಗುಣಗಳನ್ನು ಅರಿತುಕೊಂಡೆ "ನನ್ನ

ಮುಕೇಶ್ ಮಿಯಾನ್, ಉಪನ್ಯಾಸಕರು, ಹಿಂದೂಸ್ಥಾನಿ ಸಂಗೀತ, ಶ್ರೀಮತಿ ವಿ.ಪಿ. ಮಹಿಳಾ ದಿಗ್ರಿ ಕಾಲೇಜು, ಕಲಬುರಗಿ

ರೋಗವು ಸಂಗೀತದಿಂದ ಬೇಗ ಗುಣವಾದಷ್ಟು ಮತ್ತು ಔಷಧದಿಂದ ಗುಣವಾಗಿಲ್ಲ ಎಂದು ರಾಷ್ಟ್ರಪಿತ ಮಹಾತ್ಮಾ ಗಾಂಧೀಜಿಯವರು ಹೇಳಿದ್ದಾರೆ. ಅಂದರೆ ಸಂಗೀತದ ಪ್ರಭಾವದ ಪರಿಣಾಮದಿಂದ ಮಾನಸಿಕ ವಿಷಯಗಳು, ದೈಹಿಕ ರಕ್ತಿ, ರಕ್ತದೊತ್ತಡ ಇತ್ಯಾದಿಗಳು ಸಮತೋಲನದಲ್ಲಿರುತ್ತವೆ ಮತ್ತು ಆರೋಗ್ಯಕರವಾಗಿರುತ್ತವೆ.

ಸಂಗೀತ ಸಾಧನೆ ಮಾಡುವಾಗ ಸಂಗೀತಗಾರರು ಪ್ರತಿದಿನ ವಿಳಂಬ ತಾಸು, ಅರ್ಧ ಪದ್ಯಾಸನ ಅಥವಾ ಪದ್ಯಾಸನದಲ್ಲಿ ಬೆನ್ನು ಬಾಗಿಸದೆ ಸರಳವಾಗಿ ಕುಳಿತು ಒಂದೇ ಶ್ವಾಸದಲ್ಲಿ ಮಂದ್ರ, ಮಧ್ಯ ಅಥವಾ ತಾರ ಸಪ್ತಕಗಳ ಸ್ವರಗಳನ್ನು ಐದಾರು ನಿಮಿಷಗಳವರೆಗೆ ಹಚ್ಚುವುದೆಂದರೆ, ಯೋಗದಿಂದ ಸ್ವರ - ಸಿದ್ಧಿಯಿಲ್ಲವೆ? ನೃತ್ಯವು ಸಂಪೂರ್ಣವಾಗಿ ಯೋಗಾಸನದ ಮೇಲೆ ಅವಲಂಬಿಸಿದೆ. ನೃತ್ಯದಲ್ಲಿ ಈ ಕಡೆಯಿಂದ ಆಕಡೆ ಹೆಜ್ಜೆ ಹಾಕುತ್ತಾ ಓಡಾಡುತ್ತಿರುತ್ತಾರೆ. ಮುಂದೆ, ಹಿಂದೆ, ಎಡಕ್ಕೆ, ಬಲಕ್ಕೆ, ಮೇಲೆ, ಕೆಳಗೆ, ಬಾಗುತ್ತಾ ವಿಳಂಬ ಇರುತ್ತಾರೆ. ತಮ್ಮ ಎರಡೂ ಕಾಲುಗಳನ್ನು ಅಗಲ ಮಾಡಿ ನೆಲಕ್ಕೆ ಕೂಡುತ್ತಾರೆ. ಚಕ್ರದಂತೆ ಸುತ್ತುತ್ತಾರೆ. ಎರಡೂ ಕೈಗಳನ್ನು ಭುಜಗಳನ್ನು ಹಿಂದೆ ಮುಂದೆ ಸರಿಸುತ್ತಾರೆ. ಕುತ್ತಿಗೆಯನ್ನು ಅಲ್ಲಾಡಿಸುತ್ತಾ ಎರಡೂ ಹುಬ್ಬುಗಳನ್ನು ವಿರಿಸುವುದು. ಇಳಿಸುವುದು ಹಾಗೂ ನೇತ್ರ ಚಲನವಲನ ಮಾಡುತ್ತಾರೆ. ಹೀಗೆ ತಮ್ಮ ಶರೀರದ ಎಲ್ಲ ಅಂಗಾಂಗಗಳ ಚಲನವಲನ ಪ್ರತಿದಿನ ಐದರಿಂದ ಹತ್ತು ಶಾಸುಗಳವರೆಗೆ ಮಾಡುತ್ತಾರೆ. ಅಂದರೆ ಯೋಗಾಸನದಲ್ಲಿ ಕಾಣುವ ಎಲ್ಲಾ ಅಂಶಗಳನ್ನೂ ಕೂಡಾ ನೃತ್ಯದಲ್ಲಿ ನೋಡುತ್ತೇವೆ. ಸಂಗೀತವು ಮನಸ್ಸಿಗೆ ಅಖಂಡ ಶಾಂತಿಯನ್ನು ಕೊಡುತ್ತದೆ. ಸಂಗೀತದಲ್ಲಿರುವ ಯೋಗ ಆರೋಗ್ಯಭಾಗ್ಯ ನೀಡುತ್ತದೆ. ಇದರಿಂದ ಮನುಷ್ಯ ಯಾವಾಗಲೂ ಚಟುವಟಿಕೆಯಿಂದ ಇರುತ್ತಾನೆ. ಇದರಿಂದ ಶಲೆನೋವು, ಬೆನ್ನು ನೋವು, ಹೊಟ್ಟೆನೋವು, ಸೊಂಟನೋವು, ಕೈಕಾಲು ಹರಿಯುವುದು, ಆಲಸ್ಯ, ಮುಂತಾದವುಗಳು ಮಾಯವಾಗುತ್ತವೆ ಎಂದು ಹೇಳಬಹುದು. ಹೃದಯಾಘಾತ ಹಾಗೂ ಮಾನಸಿಕ ರೋಗಿಗಳಿಗೆ ಕೂಡಾ ಸಂಗೀತವೇ ರಾಮಬಾಣ. ಇದನ್ನು ಹೇಳುವುದಿಲ್ಲ. ಶಾಸ್ತ್ರ ಸಮ್ಪ್ರದಾಯದಂತೆ ಹಾಡಿದರೆ ರೋಗಿ ನಿರೋಗಿಯಾಗುತ್ತಾನೆ ಅನ್ನುತ್ತದೆ ಶಾಸ್ತ್ರ. ಈ ಪದ್ಧತಿಗೆ "ರಾಗ ಚಿಕಿತ್ಸೆ" ಅಥವಾ "ಸಂಗೀತ ಚಿಕಿತ್ಸೆ" ಎಂಬ ಹೆಸರುಗಳಿಂದ ಕರೆಯುವರು.

ಹಳ್ಳಿಯಲ್ಲಿ ತಾಯಂದಿರು ತಮ್ಮ ಮಗು ಆಳುವುದನ್ನು ನಿಲ್ಲಿಸದಿದ್ದರೆ, ತೊಟ್ಟಲಲ್ಲಿ ಮಲಗಿಸಿಯೋ ಅಥವಾ ಶೋಡೆಯ ತೊಟ್ಟಲ ಮೇಲೆ ಮಲಗಿಸಿಯೋ ಜೋಗುಳ ಹಾಡುತ್ತಿದ್ದರು ಹಾಗೂ ಹಾಡುತ್ತಿರುವರು. ಜೋಗುಳ ಪದ ಆಲಿಸುತ್ತ ಮಗು ನಿದ್ರೆಗೆ ಶರಣಾಗುತ್ತದೆ. ಜೋಗುಳ ಪದಗಳಲ್ಲಿ ಕರ್ಣಸುಖ ನೀಡುವ ಕೋಮಲ ರವ್ಯಗಳುಂಟು. ಈ ಪ್ರಯೋಗವನ್ನು ಜಗತ್ತಿಗೆ ನೀಡಿದ ಕೀರ್ತಿ ಭಾರತದ್ದು. ಭಾರತದ ಜೋಗುಳ ಪದ ಪ್ರಥಮ ಧರಪಿ ಎಂದು ಕರೆಯಲಾಗುತ್ತದೆ. ಇದರಿಂದಾಗಿ ಮುಂದೆ ಅನೇಕ ಧರಪಿಗಳು ಹುಟ್ಟಿಕೊಂಡವು ಎಂದು ಡಾ|| ಪುಟ್ಟರಾಜ ಗವಾಯಿ ಅವರು ಹೇಳಿದ್ದಾರೆ. ಈ ಕಾರಣದಿಂದಾಗಿಯೇ ಆರೋಗ್ಯ ಕೇಂದ್ರ, ಆಸ್ಪತ್ರೆ, ಪುಸ್ತಕಾಲಯ, ಗುಡಿ-ಗುಂಡಾರ, ಮಂದಿರಗಳಲ್ಲಿ ಮಧುರವಾದ ಸಂಗೀತ ಆಳವಡಿಸುವರು. ಆಸ್ಪತ್ರೆಗಳಲ್ಲಿ ದಾಖಲಾಗಿರುವ ರೋಗಿಗಳು ಬೇಗನೆ ಗುಣಮುಖವಾಗಲಿ ಎಂಬ ಉದ್ದೇಶದೊಂದಿಗೆ ಸಂಗೀತವನ್ನು ಆಳವಡಿಸಲಾಗಿರುತ್ತದೆ.

ಸಂಗೀತಕ್ಕೂ ಮನಸ್ಸಿಗೂ ಅತ್ಯಂತ ನಿಕಟ ಸಂಬಂಧವಿದೆ. ಸಂಗೀತ ಚಿತ್ತ ಅಂದರೆ ಮನವನ್ನು ರಂಜಿಸಬೇಕು. ಚಿತ್ತರಂಜನದಿಂದ ಶಾಂತಿ ಲಭಿಸುತ್ತದೆ. ಇದಕ್ಕೆ ಯೋಗಾಸನದಲ್ಲಿ ಸಮಾಧಿ ಸುಖ ಎನ್ನುವರು. ಸಂಗೀತ ನವರಸಗಳ ಸಂಪತ್ತು, ಸಂಗೀತಗಾರನಲ್ಲಿ ಭಾವ ಪಕ್ಷ ಮತ್ತು ಕಲಾ ಪಕ್ಷ ಸಮ್ಮಿಶ್ರಣ ಉಂಟು. ಸಂಗೀತವು ಮಾನವನ ಚಂಚಲ ಮನಸ್ಸಿಗೆ ಕಡಿವಾಣ ಹಾಕುತ್ತದೆ. ಸಂಗೀತವು ಮಾನವನ ಕುಲಕ್ಕೆ ಒಂದು ಶಾಶ್ವತ ಸುಖವನ್ನು ತಂದು ಕೊಡುತ್ತದೆ. ಸಂಗೀತ ಎಂಬುದು ಕಲುಷಿತ, ಕದಡಿದ ಮನವನ್ನಾಳುವ ದೊರೆ. ಶಾಸ್ತ್ರೀಯ ಸಂಗೀತ ಸಿಹಿ ನೀರು ಇದ್ದಂತೆ, ಲಘು ಶಾಸ್ತ್ರೀಯ ಸಂಗೀತ ಪಾಯಸ ಇದ್ದಂತೆ, ಭಾರತೀಯ ಸಂಗೀತ ಅಮರ. ಸಂಗೀತದಲ್ಲಿ ಬದುಕಿನ ಭುಗೆಯ ಮಧುರ ನಿನಾದದ ಮರ್ಮವಿದೆ.

ಈ ಮೇಲೆ ಹೇಳಿದ ಅಂಶಗಳನ್ನು ಗಮನಿಸಿದಾಗ ಸಂಗೀತಗಾರನಲ್ಲಿ ಸಂಗೀತ, ಸಾಹಿತ್ಯ, ಗಣಿತ, ಯೋಗಾಸನ, ವ್ಯಾಯಾಮ, ಆಧ್ಯಾತ್ಮ ಹಾಗೂ ವೈಜ್ಞಾನಿಕ ದೃಷ್ಟಿ ಇದೆ ಎನ್ನುವುದರಲ್ಲಿ ಸಂಶಯವಿಲ್ಲ. ಹಿಂದೂಸ್ತಾನಿ





ಜನಗಣತಿಯು ಜನಜನಿತವಾದ ಮತ್ತು ಸರ್ಕಾರದ ಮೇಲೆ ಸಂಪೂರ್ಣವಾಗಿರುವುದು ಅದರ ಮಹತ್ವವನ್ನು ತಿಳಿಸುತ್ತದೆ. ಈ ಕೃತಿ ಸರ್ಕಾರದ ಮೇಲೆ ಜನರ ಅಭಿಮತವನ್ನು ತಿಳಿಸುವುದು ಮತ್ತು ಸರ್ಕಾರದ ಮೇಲೆ ಜನರ ಅಭಿಮತವನ್ನು ತಿಳಿಸುವುದು.

ಕ್ರ. ಸಂಖ್ಯೆ	ಜನಗಣತಿ	ಕಾರಣಗಳು	ಒಂದು ಸಂಖ್ಯೆ
1	ಅಂತಿಮ ಭೇದನೆ ಕೇಂದ್ರ	ಅಧಿಕಾರ, ಸಂಯೋಜನೆ, ಅಧ್ಯಯನ, ಅತಿ ರಕ್ಷಣಾತ್ಮಕ, ಮಾನವ ಕಾರಣಗಳು	ಬೆಂಗಳೂರು
2	ಅಧಿಕಾರ	ಅಧ್ಯಯನದ ಮೂಲಕ, ಸರ್ಕಾರದ ನಿರೀಕ್ಷೆ	ಬೆಂಗಳೂರು
3	ಅಧಿಕಾರ ಬಹು	ಅಧಿಕಾರ	ಬೆಂಗಳೂರು
4	ಅಧಿಕಾರ, ಅಧಿಕಾರ	ಸಂಯೋಜನೆ, ಅಧ್ಯಯನ, ಸಂಯೋಜನೆ, ಅಧಿಕಾರ, ಅಧಿಕಾರ, ಅಧಿಕಾರ, ಅಧಿಕಾರ	ಬೆಂಗಳೂರು
5	ಅಧಿಕಾರ ಮತ್ತು	ಅಧಿಕಾರ, ಅಧಿಕಾರ, ಅಧಿಕಾರ	ಬೆಂಗಳೂರು
6	ಅಧಿಕಾರ, ಅಧಿಕಾರ	ಅಧಿಕಾರ, ಸಂಯೋಜನೆ, ಅಧ್ಯಯನ, ಅಧಿಕಾರ	ಬೆಂಗಳೂರು
7	ಅಧಿಕಾರ ಮತ್ತು	ಅಧಿಕಾರ, ಅಧಿಕಾರ, ಸರ್ಕಾರದ ನಿರೀಕ್ಷೆ	ಬೆಂಗಳೂರು
8	ಅಧಿಕಾರ	ಅಧಿಕಾರ	ಬೆಂಗಳೂರು
9	ಅಧಿಕಾರ ಮತ್ತು	ಅಧಿಕಾರ, ಅಧಿಕಾರ	ಬೆಂಗಳೂರು
10	ಅಧಿಕಾರ	ಅಧಿಕಾರ, ಅಧಿಕಾರ ಮತ್ತು	ಬೆಂಗಳೂರು
11	ಅಧಿಕಾರ	ಅಧಿಕಾರ, ಅಧಿಕಾರ, ಅಧಿಕಾರ	ಬೆಂಗಳೂರು
12	ಅಧಿಕಾರ, ಅಧಿಕಾರ	ಅಧಿಕಾರ, ಅಧಿಕಾರ, ಅಧಿಕಾರ, ಅಧಿಕಾರ	ಬೆಂಗಳೂರು
13	ಅಧಿಕಾರ	ಸಂಯೋಜನೆ, ಅಧ್ಯಯನ, ಅಧಿಕಾರ	ಬೆಂಗಳೂರು
14	ಅಧಿಕಾರ	ಅಧಿಕಾರ, ಅಧಿಕಾರ ಮತ್ತು	ಬೆಂಗಳೂರು
15	ಅಧಿಕಾರ	ಅಧಿಕಾರ, ಅಧಿಕಾರ ಮತ್ತು	ಬೆಂಗಳೂರು

ಈ ಮೇಲೆ ನಮೂದಿಸಿರುವ ರಾಗಗಳು ಆಯಾ ಸಮಯಕ್ಕೆ ಅನುಗುಣವಾಗಿ ಒಳ್ಳೆಯ ಸಂಗೀತ ಡಿಪಾಲು  
 ನಿರ್ಮಿಸಿ ನಿಮಿಷ ಬೆಳಗ್ಗೆ ಹಾಗೂ ರಾತ್ರಿ 30 ನಿಮಿಷ ಕೇಳಿದರೆ, ದೈಹಿಕ ಹಾಗೂ ಮಾನಸಿಕ ಆರೋಗ್ಯ, ಸುಖ,  
 ಸಂತೋಷ, ನಮ್ಮಡಿ ಜೀವನ ನಡೆಸಬಹುದು. ಇದು ನಮ್ಮ ಜೀವನ ಶೈಲಿಯಲ್ಲಿ ಅಳವಡಿಸಿಕೊಳ್ಳುವುದರಿಂದ  
 ನಮ್ಮ ಪ್ರಸ್ತುತ ಜೀವನ ಶೈಲಿಯನ್ನು ಬದಲಾಯಿಸಿ ಆಯುಷ್ಯವೂ ವೃದ್ಧಿಮಾಡಿಕೊಳ್ಳುವ ಸದವಕಾಶ ನಮಗಿದೆ.

**ಆಧಾರ ಗ್ರಂಥಗಳು:**

1. ಪ್ರೊ. ಬಿ.ಡಿ. ಪಾಠಕ - ಧಾರತೀಯ ಸಂಗೀತದ ಚರಿತ್ರೆ, ಕನ್ನಡ ಅಧ್ಯಯನ ಪೀಠ, ಪಠ್ಯಪುಸ್ತಕ  
ನಿರ್ದೇಶನಾಲಯ, ಕರ್ನಾಟಕ ವಿಶ್ವವಿದ್ಯಾಲಯ, ಧಾರವಾಡ.
2. ಶ್ರೀ ಮೃತ್ಯುಂಜಯಸ್ವಾಮಿ ಪುರಾಣಿಕಮಠ - ಹಿಂದೂಸ್ತಾನಿ ಸಂಗೀತ.
3. ವಸಂತ - ಸಂಗೀತ ವಿಶಾರದ.
4. ಡಾ|| ಶಂಭು ಬಳಗಾರ ಮತ್ತು ಡಾ|| ಬಸವರಾಜ ಜಿಗಳೂರ (ಸಂಪಾದಕರು) || ಗಾನ ಗಂಧರ್ವ, 2011.



## SYNTHESIS AND CHARACTERIZATION OF SILVER NANOPARTICLES USING *PSIDIMUM GUAJAYA* LEAVES

\*Rayindra B. K. and N. G. Patil

Department of P. G. Studies and Research in Botany,  
Gulbarga University, Gulbarga-585106, Karnataka, India  
\*Author for Correspondence: rayindrabk@rediffmail.com

### ABSTRACT

*Psidium guajava* is a small tree in the family Myrtaceae plant is commonly known as guava. India is the largest producer of guavas. The most frequently eaten species, and the one often simply referred to as "the guava", is the apple guava. This plant was formerly included in *Psidium*. In the present study, the aqueous leaves extract of *Psidium guajava* was used to synthesize silver nanoparticles. 5 ml of aqueous leaf extract was added to 50 ml 1 mM Silver nitrate. After 12 hours of incubation at room temperature, the formation of stable dark brown color indicated the synthesis of AgNPs. Synthesized silver nanoparticles were characterized using UV-VIS Spectroscopy, XRD, and TEM.

**Key words:** AgNO<sub>3</sub>, PDA, *Psidium guajava* leaves, and Mercuric chloride etc.

### INTRODUCTION

Nanoparticles, generally considered as particles with a size up to 100 nm, exhibit completely new or improved properties as compared to the bulk material that they are collected based on particular characteristics such as size, distribution, and morphology [Wildenberg 2005]. Nanoparticles of noble metals, such as gold, silver and platinum are broadly applied in many fields and also directly come in contact with the human body, such as champans, soaps, detergents, shoes, cosmetic products, and tooth paste, besides medical and pharmaceutical applications [Parveen *et al.*, 2012]. In present days, nanoparticles based on their electrical, optical, magnetic, chemical and mechanical properties are used in various areas, such as the medical sector for diagnosis, antimicrobial, drug delivery and also they are also used in the electronic and optoelectronic industry [Phillips *et al.*, 2011, Raveendran and Gulians 2009] in the chemical sector for catalysis [Du Nam and Leal 2008] for environmental protection [Kim *et al.*, 2010] and energy conversion [Rayindra and Rajash 2014]. Nanoparticle synthesis is generally carried out by physical and chemical methods, such as laser sblation, pyrolysis, chemical or physical vapour deposition, lithography electro deposition, sol gel etc., which are costliest, human hazardous, and not eco friendly. Because of the use of toxic and hazardous reagents emits toxic byproducts in environment. Compared to physical and chemical methods, the green synthesis is low cost, ecofriendly, competent, and fast method for producing nanoparticles. Currently, there is a growing need to develop environmentally benevolent nanoparticles synthesis processes that do not use toxic chemicals in the synthesis protocol. So the researchers in the field of nanoparticles synthesis and assembly have turned to biological inspiration [Song *et al.*, 2009].

In biosynthesis, many prokaryotic and eukaryotic micro organisms such as bacteria, fungi, yeast, and macro organisms like plants are using nanomaterial synthesis either intra or extracellularly. Compare to micro organisms' plants are the rich source of nature and are easily available in nature and also their enzymatic activity is more. Grounding on these potential properties we selected plant extract for synthesis of Silver nanoparticles. In the present work, we used *Psidium guajava* leaves extract for AgNPs synthesis. *Psidium guajava* it is an evergreen flowering plant belongs to family Myrtaceae. Because of its evergreen properties, easy availability and more metabolic rate we selected *Psidium guajava* for silver nanoparticles synthesis.

S. G. Gowthalli  
IQAC Co-ordinator  
Smt. V.G. Women's Degree Collge,  
KALABURGI

PRINCIPAL  
Smt. V.G. Degree Collge for Women,  
KALABURGI





## Research Article

### MATERIALS AND METHODS

#### Materials

Silver nitrate ( $\text{AgNO}_3$ ), *Psidium guajava* leaves, and Mercuric chloride,

#### Methodology

##### Sample collection

Fresh leaves of *Psidium guajava* were collected in sterilized polythene bag from Gulbarga University campus kalaburgi. And brought to Mycology and Plant pathology Laboratory and stored in laboratory conditions for further studies.

##### Preparation of leaf extract

Collected sample *Psidium guajava* leaves were surface sterilized, and dried under shade. Dried leaves were cut into small pieces and grinded to powder. 10 gram of *Psidium guajava* leaves powder boiled in 200 ml of distilled water for 10 minutes then filtered it with whatman No. 1 filter paper. The prepared plant extract solution was cooled at 4° C and stored in laboratory condition (Fig. 1) for further experimental work.

##### Green synthesis of silver nanoparticles

50 ml. of 1 mM aqueous solution of silver nitrate ( $\text{AgNO}_3$ ) was taken in 100 ml. conical flask. Then the prepared leaf extract solution with various concentrations from 5, 10, and 15 ml. was added separately and agitated at room temperature. Control treatment (without Silver nitrate, only plant extract and distilled water) was also run along with experimental flask.(Fig. 2) After 24, 48 and 72 hours of time interval culture filtrate and Silver nitrate solutions turned colourless to dark brown colour due to reduction of Silver nitrate to Silver ions.

##### Characterization of synthesized silver nanoparticles

###### UV-Visible spectroscopy

UV-Visible spectroscopy is simplest way to confirm the formation of nanoparticles. The reduction of Silver ions was confirmed by qualitative testing of supernatant by UV-Visible spectrophotometer. The UV-Visible spectroscopy measurements were performed on Elico spectral photometer as a resolution of 1nm from 200 to 800 nm with distilled water as blank reference.

###### XRD study

Powdered sample was used for X-ray diffraction; analysis for silver nanoparticles was performed by using monochromatic Cu  $\text{K}\alpha$  radiation ( $\lambda=1.5406 \text{ \AA}$ ) operated at 40 kV and 30 mA at 2 $\theta$  angle pattern. The Coherently diffracting Crystallography domain size of the Silver nano particle was calculated from the width of the XRD peaks using scherrer formula.

###### TEM analysis

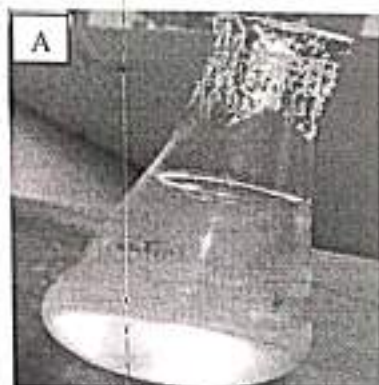
Samples were prepared for Transmission electron microscopic Analysis (IIT Mumbai) TEM Technique was employed to see the size and shape of the synthesized silver nanoparticles, the dilute drops of suspension were allowed to dry slowly on carbon-coated grids for TEM measurement

### RESULTS AND DISCUSSION

It was observed that there is variation in the particle sizes around 30% of particles in 25 nm range and 25% in 30 nm range and 20% in 35 nm ranges. The particles range from 12 nm least to 75 nm high, the TEM image suggests that the particles are polydispersed and are rounding spherical in shape.

Three different concentrations that are 5 ml, 10 ml, and 15 ml of *Psidium guajava* leaves extracts screened for Biological synthesis of Silver nanoparticles. Plant extract was treated with 1 Mm Silver nitrate in 100 ml conical flask the reduction of silver ion into silver nanoparticles during exposure to plant extract was followed by changing color, colorless to dark brown. It is known that silver nanoparticles exhibits brown color in aqueous solution due to excitation of surface plasmon vibrations in Silver nanoparticles. Interestingly, 10 ml and 15 ml concentration plant extracts were changed the color within 24 hours from colorless to brown whereas 5 ml concentration plant extract changed the color within 72 hours the UV VIS-Spectroscopy of the synthesized silver nanoparticles were in the range of 420,425, and 430 respectively.( Fig. 3)





(A) 250ml plant extract

Fig 1: Aqueous plant extract of *Psidium guajava*

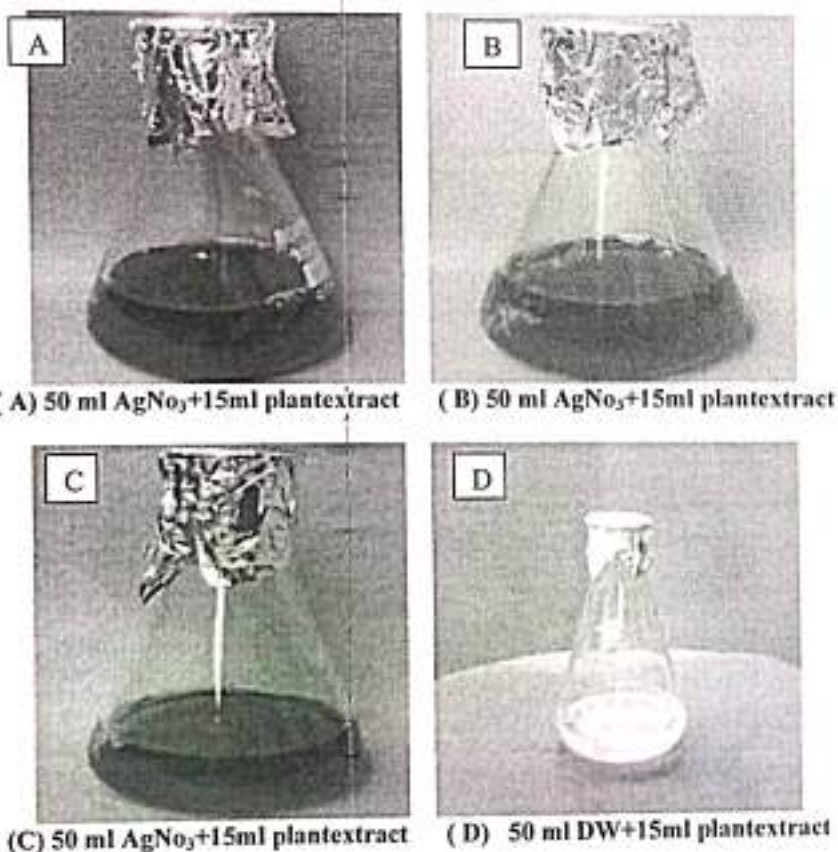
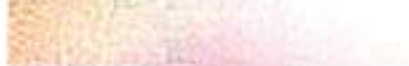


Fig 2: Biosynthesis of silver nanoparticles-color change reaction: conical flask containing the aqueous plant extract of *Psidium guajava*







Research Article

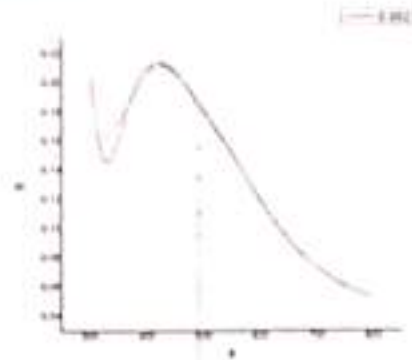


Fig 3: UV-Vis spectrum of silver nanoparticles synthesized using *Psidium guajava* plant extract. UV-Vis spectra recorded as function of time of reaction of an aqueous solution of 1mM silver nitrate solution with the plant filtrate. The time of reaction is indicated next to the respective curves

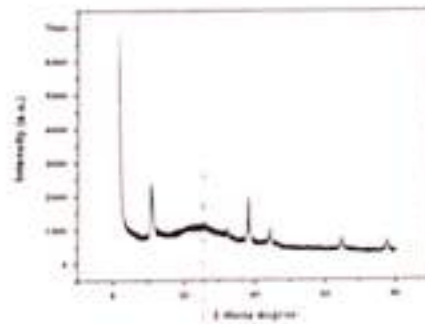


Fig 4: XRD analysis, peaks assigned to the corresponding diffraction signals (111), (200), (220), and (311) facets of Silver

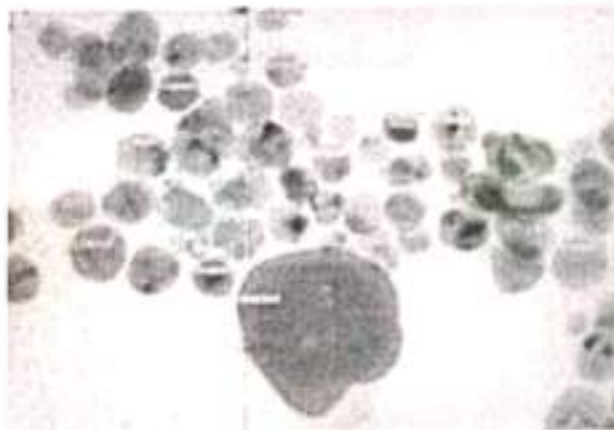


Fig 5: Transmission electron microscopic photographs of synthesized silver nanoparticles from *Psidium guajava*





### Research Article

**Table 1: UV-VIS Spectrum analysis shows time interval for changing color of plant extracts**

Plant extracts & concentration	Time taken for reduction	UV – peaks in nm	Colour
<i>Psidium guajava</i> 5 ml	72 hours	430-490	Colorless- Brown
<i>Psidium guajava</i> 10 ml	24 hours	420-470	Colorless- Brown
<i>Psidium guajava</i> 15 ml	24 hours	420-470	Colorless- Brown

#### XRD study

Obtained Silver nanoparticles were purified by repeated centrifugation at 3000 rpm for 40 minutes by redispersing silver nanoparticles pellet into 10 ml double distilled water. After drying silver nanoparticles in room temperature structure and composition analysis was carried out by XRD (Fig. 4) The crystallite domain size was calculated by the width of the XRD peaks using Scherer formula  $D = 0.96 \lambda / \beta \cos \theta$ , where D is crystalline domain size perpendicular to reflecting planes,  $\lambda$  is the x-ray wavelength,  $\beta$  is the full width at half maximum and  $\theta$  is the diffraction angle.

The average particle size was 30-35 nm. XRD analysis, peaks assigned to the corresponding diffraction signals (111), (200), (220), and (311) facets of Silver. The mean particle diameter of silver nanoparticles was calculated from the XRD pattern according to the line width of the (111) plane.

#### TEM Analysis

Sample was prepared for Transmission electron microscopic Analysis (IIT Mumbai) TEM Technique was employed to see the size and shape of the synthesized silver nanoparticles; it was observed that there is variation in the particle sizes around 30% of particles in 25 nm range and 25% in 30 nm range and 20% in 35 nm ranges. The particles range from 12 nm least to 75 nm high, the TEM image suggests that the particles are polydispersed (Fig. 5) and are rounding spherical in shape.

#### Conclusion

In the present study Silver nanoparticles were Green synthesized using *Psidium guajava* plant extract. The plant extract in different concentration i.e. 5 ml 10 ml and 15 ml are challenged with 1mM Silver nitrate; change of mixture from color less to dark brown indicates the synthesis of Silver nanoparticles in the reaction mixture. And the crystallite domain size of synthesized silver nano particles was measured 30-35 nm by XRD analysis, shape and size of the silver nanoparticles was studied by TEM analysis. Results conclude that *Psidium guajava* plant extract is potential producer of Silver nano particles.

#### ACKNOWLEDGEMENT

Authors wish to thank to Gulbarga University Gulbarga, Karnataka, India. And also thankful to USIC and Physics departments (G.U.G) for UV spectrum and XRD analysis and IIT Mumbai for TEM analysis

#### REFERENCES

- Ju-Nam Y and Lead JR (2008). Manufactured nanoparticles: An overview of their chemistry, interactions and potential environmental implications. *Science of the total environment* **400**, 396-414.
- Kim K, Jun, B, Kim J and Kim W (2010). Effects of embedding non-absorbing nanoparticles in organic photovoltaics on power conversion efficiency. *Solar Energy Materials and Solar Cells* **94** 1835-1839.
- Parveen S, Misra R and Sahoo SK (2012). Nanoparticles: a boon to drug delivery, therapeutics, diagnostics and imaging. *Nanomedicine: Nanotechnology, Biology and Medicine* **8** 147-166.
- Phillips J, Bowen W, Cagin E, Wang W (2011). Electronic and Optoelectronic Devices Based on Semiconducting Zinc Oxide. *Comprehensive Semiconductor Science and Technology* **6** 101-127.
- Raveendran Shiju N and Gulants, VV (2009). Recent developments in catalysis using nanostructured materials. *Applied Catalysis A: General* **356** 1-17.
- Ravindra B K., A H Rajasab (2014). A comparative study on biosynthesis of silver nanoparticles using four different fungal species. *Academic Sciences IJPPS* **6**(1).





*International Journal of Innovative Research and Review* ISSN: 2347 - 4424 (Online)  
An Online International Journal Available at <http://www.cibtech.org/ijer.htm>  
2017 Vol. 5 (4) October-December, pp.72-77/Ravindra and Patil

**Research Article**

**Song JY, Jang HK and Kim BS (2009).** Biological synthesis of gold nanoparticles using *Magnolia kobus* and *Diospyros kaki* leaf extracts, *Process Biochemistry* **44** 1133-1138.

**Van den Wilkenberg W (2005).** Roadmap Report on Nanoparticles, W&W Espuna s.l. Avda, Diagonal 361.





Research Article

## SYNTHESIS AND CHARACTERIZATION OF SILVER NANOPARTICLES USING ANNONA SQUAMOSA LEAVES

\*Ravindra B. K., N.G. Patil

Department of P. G. Studies and Research in Botany,  
 Gulbarga University, Gulbarga-585135, Karnataka, India  
 \*Author for Correspondence: [ravindra01shukla@gmail.com](mailto:ravindra01shukla@gmail.com)

### ABSTRACT

*Annona squamosa* is a small, well-branched tree or shrub. It is commonly called as Sitaphal. The plant bears edible fruits called sugar-apples or sweetseps. It tolerates a tropical climate. In the present study, the aqueous leaves extract of *Annona squamosa* was used to synthesize silver nanoparticles. 5 ml of aqueous leaf extract was added to 50 ml 1mM Silver nitrate. After 72 hours of incubation at room temperature, the formation of stable dark brown color indicated the synthesis of AgNPs. Synthesized silver nanoparticles were characterized using UV-VIS Spectroscopy, XRD, and TEM.

**Key words:** AgNO<sub>3</sub>, PDA, Ravistin, *Annona squamosa* leaves, and Mercuric chloride etc.

### INTRODUCTION

Nanoparticles, generally considered as particles with a size up to 100 nm, exhibit completely new or improved properties as compared to the bulk material that they are collected based on particular characteristics such as size, distribution, and morphology [Willenberg, 2005]. Nanoparticles of noble metals, such as gold, silver and platinum are broadly applied in many fields and also directly come in contact with the human body, such as shampoos, soaps, detergents, shoes, cosmetic products, and tooth paste, besides medical and pharmaceutical applications [Parveen et al., 2012]. In present days, nanoparticles based on their electrical, optical, magnetic, chemical and mechanical properties are used in various areas, such as the medical sector for diagnosis, antimicrobial, drug delivery and also they are also used in the electronic and optoelectronic industry [Phillips et al., 2011], Raveendran and Guiliano 2009] in the chemical sector for catalysis [Ji-Nam and Lead, 2008] for environmental protection [Kim et al., 2010] and energy conversion [Ravindra and Ratasab, 2014]. Nanoparticle synthesis is generally carried out by physical and chemical methods, such as laser ablation, pyrolysis, chemical or physical vapour deposition, lithography, electro deposition, sol gel etc., which are costliest, human hazardous, and not eco friendly. Because of the use of toxic and hazardous reagents emits toxic byproducts in environment. Compared to physical and chemical methods, the green synthesis is low cost, ecofriendly, competent, and fast method for producing nanoparticles. Currently, there is a growing need to develop environmentally benevolent nanoparticles synthesis processes that do not use toxic chemicals in the synthesis protocol. So the researchers in the field of nanoparticles synthesis and assembly have turned to biological inspiration [Song et al., 2009].

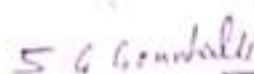
In biosynthesis, many prokaryotic and eukaryotic micro organisms such as bacteria, fungi, yeast, and macro organisms like plants are using for nanomaterial synthesis either intra or extracellularly. Compare to micro organisms' plants are the rich source of nature and are easily available in nature and also their enzymatic activity is more. Grounding on these potential properties we selected plant extract for synthesis of Silver nanoparticles. In the present work, we used *Annona squamosa* leaves extract for AgNPs synthesis. *Annona squamosa* it is a small tropical tree belongs to family Annonaceae. Plant is widely grown, Because of its evergreen properties, easy availability and more metabolic rate we selected *Annona squamosa*, for silver nanoparticles synthesis.

### MATERIALS AND METHODS

#### Materials

Silver nitrate (AgNO<sub>3</sub>), *Annona squamosa* leave, and Mercuric chloride

Centre for Info Bio Technology (CIBTech)

  
**S.G. Gondalli**  
 IQAC Co-ordinator  
 Smt. V.G. Women's Degree College,  
 KALABURAGI

  
**PRINCIPAL**  
 Smt. V.G. Degree College for Women,  
 KALABURAGI



## Research Article

### Methodology

#### Sample collection

Fresh leaves of *Annona squamosa* were collected in sterilized polythene bag from Gulbarga University campus. And brought to Mycology and Plant pathology Laboratory and stored in laboratory conditions for further studies.

#### Preparation of leaf extract

Collected sample *Annona squamosa* leaves were surface sterilized, and dried under shade. Dried leaves were cut into small pieces and grinded to powder. 10 gram of *Annona squamosa* leaf powder boiled in 200 ml of distilled water for 10 minutes then filtered it with whatman No.1 filter paper. (Fig. 1) The prepared plant extract solution was cooled at 4° C and stored in laboratory condition for further experimental work.

#### Green synthesis of silver nanoparticles

50 mL of 1 mM aqueous solution of silver nitrate ( $\text{AgNO}_3$ ) was taken in 100 mL conical flask. Then the prepared leaf extract solution with various concentrations from 5, 10, and 15 mL was added separately and agitated at room temperature. Control treatment (without Silver nitrate, only plant extract and distilled water) was also run along with experimental flask. (Fig. 2) After 24, 48 and 72 hours of time interval culture filtrate and Silver nitrate solutions turned colourless to dark brown colour due to reduction of Silver nitrate to Silver ions.

#### Characterization of synthesized silver nanoparticles

##### UV-Visible spectroscopy

UV-Visible spectroscopy is simplest way to confirm the formation of nanoparticles. The reduction of Silver ions was confirmed by qualitative testing of supernatant by UV-Visible spectrophotometer. The UV-Visible spectroscopy measurements were performed on Elico spectral photometer as a resolution of 1nm from 200 to 800 nm with distilled water as blank reference.

##### XRD study

Powdered sample was used for X-ray diffraction; analysis for silver nanoparticles was performed by using monochromatic  $\text{Cu } \alpha$  radiation ( $\lambda=1.5406 \text{ \AA}$ ) operated at 40 kV and 30 mA at 2 $\theta$  angle pattern. The Coherently diffracting Crystallography domain size of the Silver nano particle was calculated from the width of the XRD peaks using scherrer formula.

##### TEM analysis

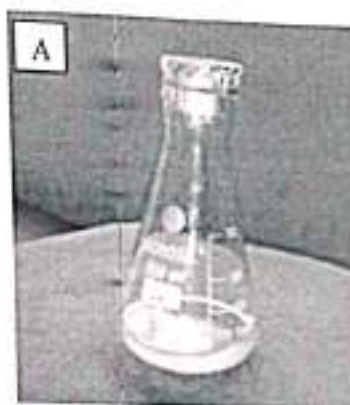
Samples were prepared for Transmission electron microscopic Analysis (IIT Mumbai) TEM Technique was employed to see the size and shape of the synthesized silver nanoparticles, the dilute drops of suspension were allowed to dry slowly on carbon-coated grids for TEM measurement

## RESULTS AND DISCUSSION

It was observed that there is variation in the particle sizes around 30% of particles in 25 nm range and 25% in 30 nm range and 20% in 35 nm ranges. The particles range from 12 nm least to 75 nm high, the TEM image suggests that the particles are polydispersed and are rounding spherical in shape.

Three different concentrations that are 5 ml, 10 ml, and 15 ml of *Annona squamosa* plant extracts screened for Biological synthesis of Silver nanoparticles. Plant extract was treated with 1 Mm Silver nitrate in 100 ml conical flask the reduction of silver ion into silver nanoparticles during exposure to plant extract was followed by changing color, colorless to dark brown. It is known that silver nanoparticles exhibits brown color in aqueous solution due to excitation of surface plasmon vibrations in Silver nanoparticles. Interestingly, 10 ml and 15 ml concentration plant extracts were changed the color within 24 hours from colorless to brown whereas 5 ml concentration plant extract changed the color within 72 hours (Fig. 3) the UV VIS-Spectroscopy of the synthesized silver nanoparticles were in the range of 420,425, and 430 respectively.





(A) 50ml plantextract

Fig 1: Aqueous plant extract of *Annona squamosa*

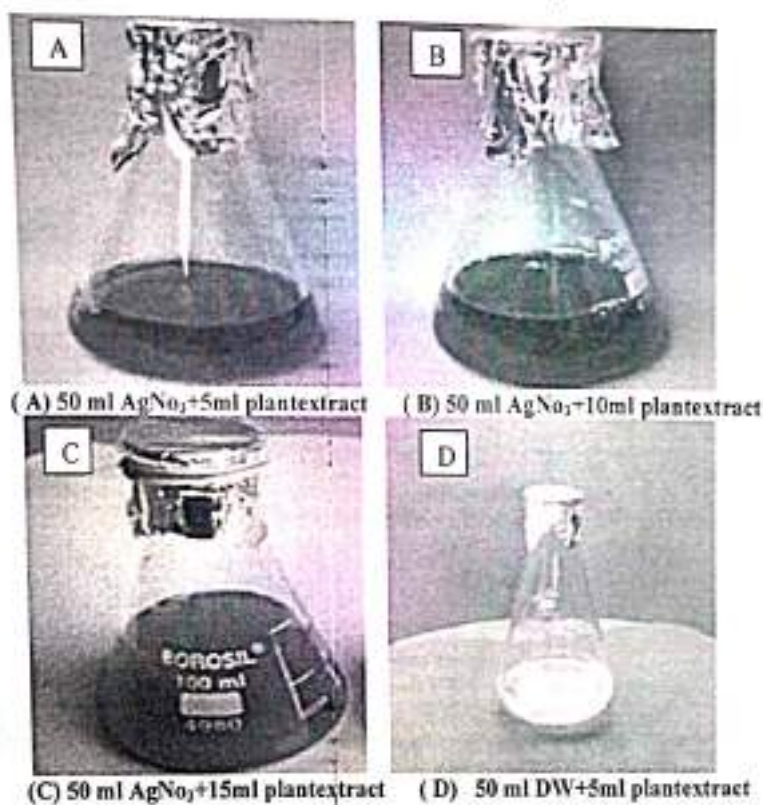


Fig 2: Biosynthesis of silver nanoparticles-color change reaction: conical flask containing the aqueous plant extract of *Annona squamosa* i

Research Article

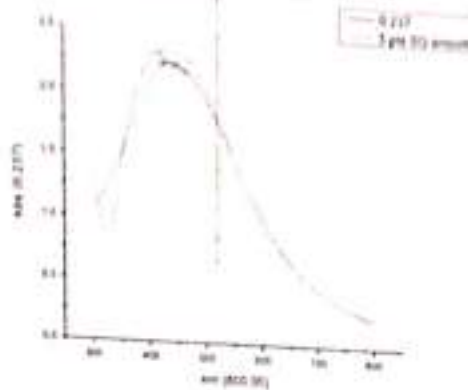


Fig 3: UV-Vis spectrum of silver nanoparticles synthesized using *Annona squamosa* plant extract. UV-Vis spectra recorded as function of time of reaction of an aqueous solution of 1mM silver nitrate solution with the plant filtrate. The time of reaction is indicated next to the respective curves.

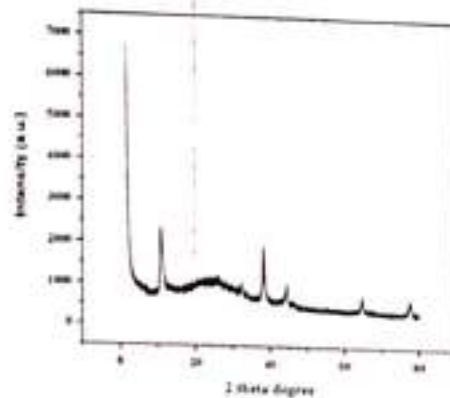


Fig 4: XRD analysis, peaks assigned to the corresponding diffraction signals (111), (200), (220), and (311) facets of Silver.



Fig 5: Transmission electron microscopic photographs of synthesized silver nanoparticles from *Annona squamosa*.



### Research Article

**Table 1: UV-VIS Spectrum analysis shows time interval for changing color of plant extracts.**

Plant extracts & concentration	Time taken for reduction	Uv – peaks in nm	Colour
<i>Annona squamosa</i> 5 ml	72 hours	430-490	Colorless- Brown
<i>Annona squamosa</i> 10 ml	24 hours	420-470	Colorless- Brown
<i>Annona squamosa</i> 15 ml	24 hours	420-470	Colorless- Brown

#### XRD study

Obtained Silver nanoparticles were purified by repeated centrifugation at 3000 rpm for 40 minutes by redispersing silver nanoparticles pellet into 10 ml double distilled water. After drying silver nanoparticles in room temperature structure and composition analysis was carried out by XRD (Fig. 4) The crystallite domain size was calculated by the width of the XRD peaks using Scherer formula  $D=0.96 \lambda/\beta \cos \theta$ , where D is crystalline domain size perpendicular to reflecting planes,  $\lambda$  is the x-ray wavelength,  $\beta$  is the full width at half maximum and  $\theta$  is the diffraction angle.

The average particle size was 30-35 nm. XRD analysis, peaks assigned to the corresponding diffraction signals (111), (200), (220), and (311) facets of Silver. The mean particle diameter of silver nanoparticles was calculated from the XRD pattern according to the line width of the (111) plane.

#### TEM Analysis

Sample was prepared for Transmission electron microscopic Analysis (IIT Mumbai) TEM Technique was employed to see the size and shape of the synthesized silver nanoparticles; it was observed that there is variation in the particle sizes around 30% of particles in 25 nm range and 25% in 30 nm range and 20% in 35 nm ranges. The particles range from 12 nm least to 75 nm high, the TEM image suggests that the particles are polydispersed (fig. 5) and are rounding spherical in shape.

#### Conclusion

In the present study Silver nanoparticles were Green synthesized using *Annona squamosa* plant extract. The plant extract in different concentration i.e. 5 ml 10 ml and 15 ml are challenged with 1mM Silver nitrate; change of mixture from color less to dark brown indicates the synthesis of Silver nanoparticles in the reaction mixture. And the crystallite domain size of synthesized silver nano particles was measured 30-35 nm by XRD analysis, shape and size of the silver nanoparticles was studied by TEM analysis. Results conclude that *Annona squamosa* plant extract is potential producer of Silver nano particles.

#### ACKNOWLEDGEMENT

Authors wish to thank to Gulbarga University Gulbarga, Karnataka, India. And also thankful to USIC and Physics departments (G.U.G) for UV spectrum and XRD analysis and IIT Mumbai for TEM analysis

#### REFERENCES

- Ju-Nam Y and Lead JR (2008). Manufactured nanoparticles: An overview of their chemistry, interactions and potential environmental implications. *Science of the total environment* **400**, 396-414.
- Kim K, Jun, B, Kim J and Kim W (2010). Effects of embedding non-absorbing nanoparticles in organic photovoltaics on power conversion efficiency. *Solar Energy Materials and Solar Cells* **94** 1835-1839.
- Parveen S, Misra R and Sahoo SK (2012). Nanoparticles: a boon to drug delivery, therapeutics, diagnostics and imaging. *Nanomedicine: Nanotechnology, Biology and Medicine* **8** 147-166.
- Phillips J, Bowen W, Cagin E, Wang W (2011). Electronic and Optoelectronic Devices Based on Semiconducting Zinc Oxide. *Comprehensive Semiconductor Science and Technology* **6** 101-127.
- Raveendran Shiju N and Guljants, VV (2009). Recent developments in catalysis using nanostructured materials. *Applied Catalysis A: General* **356** 1-17.



**Research Article**

- Ravindra B K., A H Rajasab (2014)** A comparative study on biosynthesis of silver nanoparticles using four different fungal species. *Academia: Science's IJPPS* 6(1)
- Song JY, Jang HK and Kim BS (2009)** Biological synthesis of gold nanoparticles using *Magnolia kobus* and *Diospyros Laki* leaf extracts. *Process Biochemistry* 44 1133-1138
- Van den Wildenberg W (2005)** Roadmap Report on Nanoparticles W&W Espusa s1 Avda Diagonal 361.



**Research Article**

## SYNTHESIS AND CHARACTERIZATION OF SILVER NANOPARTICLES USING *MANGIFERA INDICA* LEAVES

\*Ravindra B. K. and N. G. Patil

Department of P. G. Studies and Research in Botany,  
Gulbarga University, Gulbarga-585106, Karnataka, India  
\*Author for Correspondence: [ravindrakeluskar@gmail.com](mailto:ravindrakeluskar@gmail.com)

### ABSTRACT

*Mangifera indica* is a large tropical tree. It is commonly called as mango. The fruit is edible, is called as king of fruits. In the present study, the aqueous leaves extract of *Mangifera indica* was used to synthesize silver nanoparticles. 5 ml of aqueous leaf extract was added to 50 ml 1mM Silver nitrate. After 72 hours of incubation at room temperature, the formation of stable dark brown color indicated the synthesis of AgNPs. Synthesized silver nanoparticles were characterized using UV-VIS Spectroscopy, XRD, and TEM.

**Key words:** *AgNO<sub>3</sub>*, PDA, Bavistin, *Mangifera indica* leaves, and Mercuric chloride etc.

### INTRODUCTION

Nanoparticles, generally considered as particles with a size up to 100 nm, exhibit completely new or improved properties as compared to the bulk material that they are collected based on particular characteristics such as size, distribution, and morphology [Wildenberg 2005]. Nanoparticles of noble metals, such as gold, silver and platinum are broadly applied in many fields and also directly come in contact with the human body, such as shampoos, soaps, detergents, shoes, cosmetic products, and tooth paste, besides medical and pharmaceutical applications [Parveen *et al.*, 2012]. In present days, nanoparticles based on their electrical, optical, magnetic, chemical and mechanical properties are used in various areas, such as the medical sector for diagnosis, antimicrobial, drug delivery and also they are also used in the electronic and optoelectronic industry [Phillips *et al.*, 2011, Raveendran and Gulians 2009] in the chemical sector for catalysis [Ju-Nam and Lead 2008] for environmental protection [Kim *et al.*, 2010] and energy conversion [Ravindra and Rajasab 2014]. Nanoparticle synthesis is generally carried out by physical and chemical methods, such as laser ablation, pyrolysis, chemical or physical vapour deposition, lithography electro deposition, sol gel etc., which are costliest, human hazardous, and not eco friendly. Because of the use of toxic and hazardous reagents emits toxic byproducts in environment. Compared to physical and chemical methods, the green synthesis is low cost, ecofriendly, competent, and fast method for producing nanoparticles. Currently, there is a growing need to develop environmentally benevolent nanoparticles synthesis processes that do not use toxic chemicals in the synthesis protocol. So the researchers in the field of nanoparticles synthesis and assembly have turned to biological inspiration [Song *et al.*, 2009].

In biosynthesis, many prokaryotic and eukaryotic micro organisms such as bacteria, fungi, yeast, and macro organisms like plants are using for nanomaterial synthesis either intra or extracellularly. Compare to micro organisms' plants are the rich source of nature and are easily available in nature and also their enzymatic activity is more. Grounding on these potential properties we selected plant extract for synthesis of Silver nanoparticles. In the present work, we used *Mangifera indica* leaves extract for AgNPs synthesis. *Mangifera indica* leaves it is a large tropical tree belongs to family Anacardiaceae Plant is widely grown; its fruit is edible when fully ripe, tasting almost like almond. Because of its evergreen properties, easy availability and more metabolic rate we selected *Mangifera indica* for silver nanoparticles synthesis.


### MATERIALS AND METHODS

#### Materials

Silver nitrate ( $AgNO_3$ ), *Mangifera indica* leaves. Mercuric chloride

Centre for Info Bio Technology (CIBTech)

S. G. Gounbali  
Smt. V.G. Women's Degree College,  
KALABURAGI

  
PRINCIPAL  
Smt. V.G. Degree College for Women,  
KALABURAGI.

## Research Article

### Methodology

#### Sample collection

Fresh leaves of *Mangifera indica* were collected in sterilized polythene bag from kusnoor village which is just behind Gulbarga University kalaburagi. And brought to Mycology and Plant pathology Laboratory and stored in laboratory conditions for further studies.

#### Preparation of leaf extract

Collected sample *Mangifera indica* leaves were surface sterilized, and dried under shade. Dried leaves were cut into small pieces and grinded to powder. 10 gram of *Mangifera indica* leaf powder boiled in 200 ml of distilled water for 10 minutes then filtered it with whatman No.1 filter paper. (Fig. 1) The prepared plant extract solution was cooled at 4° C and stored in laboratory condition for further experimental work.

#### Green synthesis of silver nanoparticles

50 mL of 1 mM aqueous solution of silver nitrate ( $\text{AgNO}_3$ ) was taken in 100 mL conical flask. Then the prepared leaf extract solution with various concentrations from 5, 10, and 15 mL was added separately and agitated at room temperature. Control treatment (without Silver nitrate, only plant extract and distilled water) was also run along with experimental flask. After 24, 48 and 72 hours of time interval culture filtrate and Silver nitrate solutions turned colourless to dark brown colour due to reduction of Silver nitrate to Silver ions. (Fig. 2)

#### Characterization of synthesized silver nanoparticles

##### UV- Visible spectroscopy

UV-Visible spectroscopy is simplest way to confirm the formation of nanoparticles. The reduction of Silver ions was confirmed by qualitative testing of supernatant by UV- Visible spectrophotometer. The UV -Visible spectroscopy measurements were performed on Elico spectral photometer as a resolution of 1nm from 200 to 800 nm with distilled water as blank reference.

##### XRD study

Powdered sample was used for X-ray diffraction; analysis for silver nanoparticles was performed by using monochromatic Cu  $\text{K}\alpha$  radiation ( $\lambda=1.5406 \text{ \AA}$ ) operated at 40 kV and 30 mA at  $2\theta$  angle pattern. The Coherently diffracting Crystallography domain size of the Silver nano particle was calculated from the width of the XRD peaks using scherrer formula.

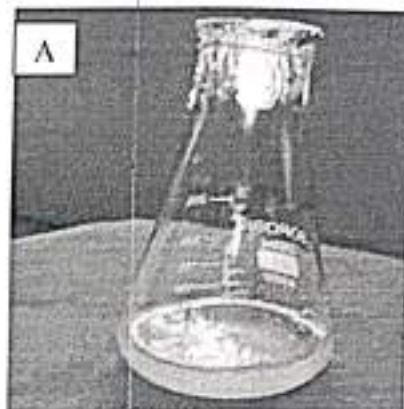
##### TEM analysis

Samples were prepared for Transmission electron microscopic Analysis (IIT Mumbai) TEM Technique was employed to see the size and shape of the synthesized silver nanoparticles, the dilute drops of suspension were allowed to dry slowly on carbon-coated grids for TEM measurement

## RESULTS AND DISCUSSION

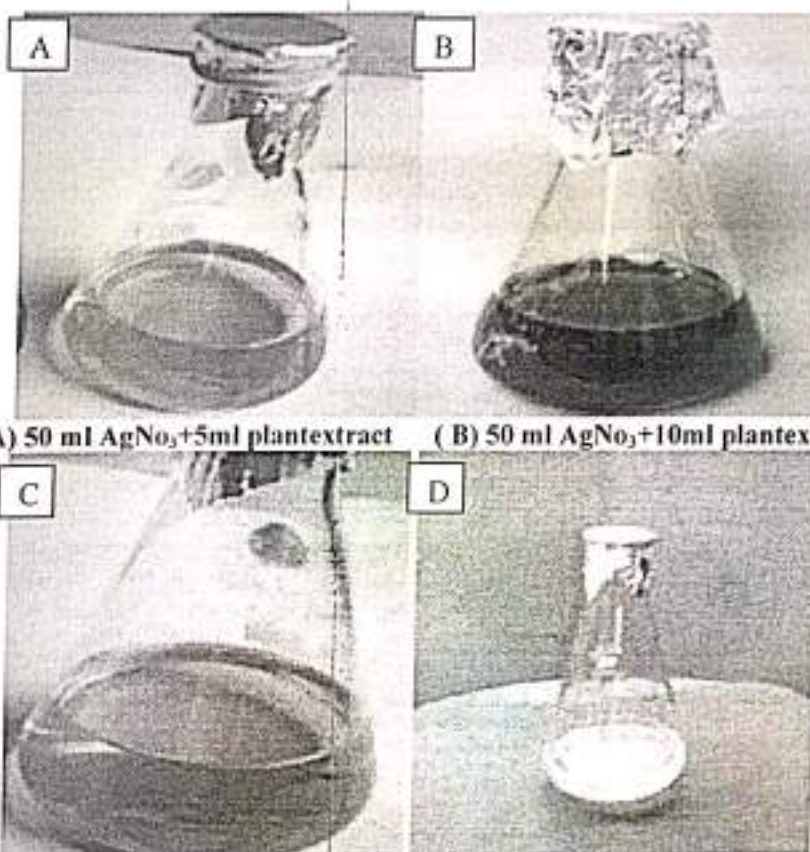
It was observed that there is variation in the particle sizes around 30% of particles in 25 nm range and 25% in 30 nm range and 20% in 35 nm ranges. The particles range from 12 nm least to 75 nm high, the TEM image suggests that the particles are polydispersed and are rounding spherical in shape.

Three different concentrations that are 5 ml, 10 ml, and 15 ml of *Mangifera indica* leaves extracts treated for Biological synthesis of Silver nanoparticles. Plant extract was treated with 1 Mm Silver nitrate in 100 ml conical flask the reduction of silver ion into silver nanoparticles during exposure to plant extract was followed by changing color, colorless to dark brown. It is known that silver nanoparticles exhibits brown color in aqueous solution due to excitation of surface plasmon vibrations in Silver nanoparticles. Interestingly, 10 ml and 15 ml concentration plant extracts were changed the color within 24 hours from colorless to brown whereas 5 ml concentration plant extract changed the color within 72 hours (Fig. 3) the UV VIS-Spectroscopy of the synthesized silver nanoparticles were in the range of 420,425, and 430 respectively.



(A) 50ml plantextract

Fig 1: Aqueous plant extract of *Mangifera indica*



(A) 50 ml  $AgNO_3$ +5ml plantextract    (B) 50 ml  $AgNO_3$ +10ml plantextrac

(C) 50 ml  $AgNO_3$ +15ml plantextract    (D) 50 ml DW+15ml plantextract

Fig 2: Biosynthesis of silver nanoparticles-color change reaction: conical flask containing the aqueous plant extract of *Mangifera indica*

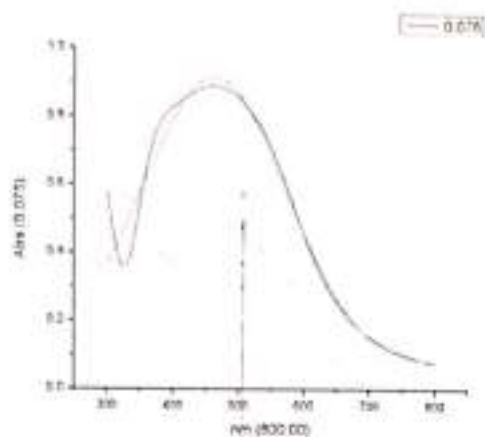


Fig 3: UV-Vis spectrum of silver nanoparticles synthesized using *Mangifera indica* plant extract. UV-Vis spectra recorded as function of time of reaction of an aqueous solution of 1mM silver nitrate solution with the plant filtrate. The time of reaction is indicated next to the respective curves.

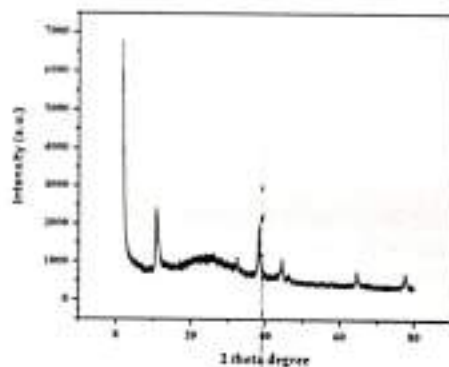


Fig 4: XRD analysis, peaks assigned to the corresponding diffraction signals (111), (200), (220), and (311) facets of Silver.





**Research Article**

**Fig 5: Transmission electron microscopic photographs of synthesized silver nanoparticles from Terminalia catapa.**

**Table 1: UV-VIS Spectrum analysis shows time interval for changing color of plant extracts.**

Plant extracts & concentration	Time taken for reduction	Uv – peaks in nm	Color
Mangifera indica 5 ml	72 hours	430-490	Colorless- Brown
Mangifera indica 10 ml	24 hours	420-470	Colorless- Brown
Mangifera indica 15 ml	24 hours	420-470	Colorless- Brown

**XRD study**

Obtained Silver nanoparticles were purified by repeated centrifugation at 3000 rpm for 40 minutes by redispersing silver nanoparticles pellet into 10 ml double distilled water. After drying silver nanoparticles in room temperature structure and composition analysis was carried out by XRD (Fig. 4) The crystallite domain size was calculated by the width of the XRD peaks using Scherer formula  $D=0.96 \lambda/\beta \cos \theta$ , where D is crystalline domain size perpendicular to reflecting planes,  $\lambda$  is the x-ray wavelength,  $\beta$  is the full width at half maximum and  $\theta$  is the diffraction angle.

The average particle size was 30-35 nm. XRD analysis, peaks assigned to the corresponding diffraction signals (111), (200), (220), and (311) facets of Silver. The mean particle diameter of silver nanoparticles was calculated from the XRD pattern according to the line width of the (111) plane.

**TEM Analysis**

Sample was prepared for Transmission electron microscopic Analysis (IIT Mumbai) TEM Technique was employed to see the size and shape of the synthesized silver nanoparticles; it was observed that there is variation in the particle sizes around 30% of particles in 25 nm range and 25% in 30 nm range and 20% in 35 nm ranges. The particles range from 12 nm least to 75 nm high, the TEM image suggests that the particles are polydispersed (fig. 5) and are rounding spherical in shape.

**Conclusion**

In the present study Silver nanoparticles were Green synthesized using *Mangifera indica* plant extract. The plant extract in different concentration i.e. 5 ml 10 ml and 15 ml are challenged with 1mM Silver nitrate; change of mixture from color less to dark brown indicates the synthesis of Silver nanoparticles in the reaction mixture. And the crystallite domain size of synthesized silver nanoparticles was measured 30-35 nm by XRD analysis, shape and size of the silver nanoparticles was studied by TEM analysis. Results conclude that citrus limon plant extract is potential producer of Silver nanoparticles

**ACKNOWLEDGEMENT**

Authors wish to thank to Gulbarga University Gulbarga, Karnataka, India. And also thankful to USIC and Physics departments (G.U.G) for UV spectrum and XRD analysis and IIT Mumbai for TEM analysis

**REFERENCES**

Ju-Nam Y and Lead JR (2008). Manufactured nanoparticles: An overview of their chemistry, interactions and potential environmental implications. *Science of the total environment* 400, 396-414.  
 Kim K, Jun, B, Kim J and Kim W (2010). Effects of embedding non-absorbing nanoparticles in organic photovoltaics on power conversion efficiency. *Solar Energy Materials and Solar Cells* 94 1835-1839.  
 Parveen S, Misra R and Sahoo SK (2012). Nanoparticles: a boon to drug delivery, therapeutics, diagnostics and imaging. *Nanomedicine: Nanotechnology, Biology and Medicine* 8 147-166.  
 Phillips J, Bowen W, Cagin E, Wang W (2011). Electronic and Optoelectronic Devices Based on Semiconducting Zinc Oxide. *Comprehensive Semiconductor Science and Technology* 6 101-127.  
 Raveendran Shiju N and Gulianti, VV (2009). Recent developments in catalysis using nanostructured materials. *Applied Catalysis A: General* 356 1-17.



*International Journal of Innovative Research and Review* ISSN: 2347 – 4424 (Online)

An Online International Journal Available at <http://www.cibtech.org/ijir.htm>

2017 Vol. 5 (3) July-September, pp.31-36/Ravindra and Patil

### **Research Article**

**Ravindra B K., A H Rajasab (2014).** A comparative study on biosynthesis of silver nanoparticles using four different fungal species. *Academic Sciences IJPPS* 6(1).

**Song JY, Jang HK and Kim BS (2009).** Biological synthesis of gold nanoparticles using *Magnolia kobus* and *Diospyros kaki* leaf extracts. *Process Biochemistry* 44 1133-1138.

**Van den Wildenberg W (2005).** Roadmap Report on Nanoparticles. W&W Espana s.l. Avda. Diagonal 361.



Research Article

## SYNTHESIS AND CHARACTERIZATION OF SILVER NANOPARTICLES USING *PHYLLANTHUS EMBLICA* LEAVES

\*Ravindra B. K., N. G. Patil

Department of P. G. Studies and Research in Botany,  
Gulbarga University, Gulbarga-585106, Karnataka, India

\*Author for Correspondence: [ravindrakeluskar@gmail.com](mailto:ravindrakeluskar@gmail.com)

### ABSTRACT

*Phyllanthus emblica* is a commercial plant cultivated for fruits. The fruit is traditionally used as medicine. The fruits are used in the preparation of pickle, in the present study, the aqueous leaves extract of *Phyllanthus emblica*, was used to synthesize silver nanoparticles. 5 ml of aqueous leaf extract was added to 50 ml 1mM Silver nitrate. After 72 hours of incubation at room temperature, the formation of stable dark brown color indicated the synthesis of AgNPs. Synthesized silver nanoparticles were characterized using UV-VIS Spectroscopy, XRD, and TEM.

**Keywords:** AgNO<sub>3</sub>, Plant Extract, XRD, TEM

### INTRODUCTION

Nanoparticles, generally considered as particles with a size up to 100 nm, exhibit completely new or improved properties as compared to the bulk material that they are collected based on particular characteristics such as size, distribution, and morphology [Wildenberg 2005]. Nanoparticles of noble metals, such as gold, silver and platinum are broadly applied in many fields and also directly come in contact with the human body, such as shampoos, soaps, detergents, shoes, cosmetic products, and tooth paste, besides medical and pharmaceutical applications [Parveen *et al.*, 2012]. In present days, nanoparticles based on their electrical, optical, magnetic, chemical and mechanical properties are used in various areas, such as the medical sector for diagnosis, antimicrobial, drug delivery and also they are also used in the electronic and optoelectronic industry [Phillips *et al.*, 2011, Raveendran and Gulians 2009] in the chemical sector for catalysis [Ju-Nam and Lead 2008] for environmental protection [Kim *et al.*, 2010] and energy conversion [Ravindra and Rajasab 2014]. Nanoparticle synthesis is generally carried out by physical and chemical methods, such as laser ablation, pyrolysis, chemical or physical vapour deposition, lithography electro deposition, sol gel etc., which are costliest, human hazardous, and not eco friendly. Because of the use of toxic and hazardous reagents emits toxic byproducts in environment. Compared to physical and chemical methods, the green synthesis is low cost, ecofriendly, competent, and fast method for producing nanoparticles. Currently, there is a growing need to develop environmentally benevolent nanoparticles synthesis processes that do not use toxic chemicals in the synthesis protocol. So the researchers in the field of nanoparticles synthesis and assembly have turned to biological inspiration [Song *et al.*, 2009].

In biosynthesis, many prokaryotic and eukaryotic micro organisms such as bacteria, fungi, yeast, and macro organisms like plants are using for nanomaterial synthesis either intra or extracellularly. Compare to micro organisms' plants are the rich source of nature and are easily available in nature and also their enzymatic activity is more. Grounding on these potential properties we selected plant extract for synthesis of Silver nanoparticles. In the present work, we used *Phyllanthus emblica*, leaves extract for AgNPs synthesis. *Phyllanthus emblica*, it is a small evergreen tree belongs to family *Phyllanthaceae*. Plant is widely grown, its fruit used for various purposes. Because of its evergreen properties, easy availability and more metabolic rate we selected *Phyllanthus emblica* for silver nanoparticles synthesis.


### MATERIALS AND METHODS

#### Materials

Silver nitrate (AgNO<sub>3</sub>), *Phyllanthus emblica*, leaves, and Mercuric chloride ect.

Centre for Info Bio Technology (CIBTech)

S. G. Gounbali  
IQAC Co-ordinator  
Smt. V.G. Women's Degree College,  
KALABURAGI.

  
PRINCIPAL  
Smt. V.G. Degree College for Women,  
KALABURAGI.



Research Article

## SYNTHESIS AND CHARACTERIZATION OF SILVER NANOPARTICLES USING *MORINGA OLEIFERA* LEAVES

\*Ravindra B. K. and N. G. Patil

Department of P. G. Studies and Research in Botany,  
Gulbarga University, Gulbarga-585106, Karnataka, India  
\*Author for Correspondence: [ravindrakeluskar@gmail.com](mailto:ravindrakeluskar@gmail.com)

### ABSTRACT

*Moringa oleifera* is a fast-growing, drought-resistant tree. It is commonly called as Drumstick tree from the appearance of the long, slender, triangular seed-pods. This plant grows in poor nutrient soil and it has tremendous potential for human use. In the present study, the aqueous leaves extract of *Moringa oleifera* was used to synthesize silver nanoparticles. 5 ml of aqueous leaf extract was added to 50 ml 1mM Silver nitrate. After 72 hours of incubation at room temperature, the formation of stable dark brown color indicated the synthesis of AgNPs. Synthesized silver nanoparticles were characterized using UV-VIS Spectroscopy, XRD, and TEM.

**Key words:** AgNO<sub>3</sub>, PDA, Bavistin, *Moringa oleifera* leaves, and Mercuric chloride etc.

### INTRODUCTION

Nanoparticles, generally considered as particles with a size up to 100 nm, exhibit completely new or improved properties as compared to the bulk material that they are collected based on particular characteristics such as size, distribution, and morphology [Wildenberg 2005]. Nanoparticles of noble metals, such as gold, silver and platinum are broadly applied in many fields and also directly come in contact with the human body, such as shampoos, soaps, detergents, shoes, cosmetic products, and tooth paste, besides medical and pharmaceutical applications [Parveen *et al.* 2012]. In present days, nanoparticles based on their electrical, optical, magnetic, chemical and mechanical properties are used in various areas, such as the medical sector for diagnosis, antimicrobial, drug delivery and also they are also used in the electronic and optoelectronic industry [Phillips *et al.* 2011, Raveendran and Gulians 2009] in the chemical sector for catalysis [Ju-Nam and Lead 2008] for environmental protection [Kim *et al.* 2010] and energy conversion [Ravindra and Rajasab 2014]. Nanoparticle synthesis is generally carried out by physical and chemical methods, such as laser ablation, pyrolysis, chemical or physical vapour deposition, lithography electro deposition, sol gel etc., which are costliest, human hazardous, and not eco friendly. Because of the use of toxic and hazardous reagents emits toxic byproducts in environment. Compared to physical and chemical methods, the green synthesis is low cost, ecofriendly, competent, and fast method for producing nanoparticles. Currently, there is a growing need to develop environmentally benevolent nanoparticles synthesis processes that do not use toxic chemicals in the synthesis protocol. So the researchers in the field of nanoparticles synthesis and assembly have turned to biological inspiration [Song *et al.* 2009].

In biosynthesis, many prokaryotic and eukaryotic micro organisms such as bacteria, fungi, yeast, and macro organisms like plants are using for nanomaterial synthesis either intra or extracellularly. Compare to micro organisms' plants are the rich source of nature and are easily available in nature and also their enzymatic activity is more. Grounding on these potential properties we selected plant extract for synthesis of Silver nanoparticles. In the present work, we used *Moringa oleifera* leaves extract for AgNPs synthesis. *Moringa oleifera* fast-growing, drought-resistant tree belongs to family moringaceae. Plant is widely grown in poor nutrient soil and it has tremendous potential for human use. Because of its ever green properties, easy availability and more metabolic rate we selected *Moringa oleifera* for silver nanoparticles synthesis.

**IQAC Co-ordinator**  
**Smt. V.G. Women's Degree Coll.**  
**KALABURAGI**

**PRINCIPAL**  
**Smt. V.G. Degree College for Women,**  
**KALABURAGI.**



Research Article

## PLASTIC DEGRADATION AND ANTIFUNGAL ACTIVITY OF SILVER NANOPARTICLES SYNTHESIZED USING *PHYLLANTHUS EMBLICA* LEAVES

\*Ravindra B. K. and N. G. Patil

Department of P. G. Studies and Research in Botany,  
Gulbarga University, Gulbarga-585106, Karnataka, India  
\*Author for Correspondence: [ravindrakechuskar@gmail.com](mailto:ravindrakechuskar@gmail.com)

### ABSTRACT

Plastic is using as substitute for almost all human utensils. Its dump in everywhere on earth leads pollution in environment, and effects on human health. Now a day's its decomposition is a major issue. In the present study, we used 100 ml aqueous solution of silver nanoparticle for degradation of 0.8 mm plastic material. Silver nanoparticles were synthesized using *Phyllanthus emblica* leaves extract, plant cultivated for fruits. The fruits are used in the preparation of pickle the plant is commercial cultivated for fruits. The fruits and leaves are traditionally used as medicine. Experiments were also conducted to test the efficacy of nanoparticles against pathogenic fungi. The fungal zone of inhibition was determined as compared to the standard drug bavistin. Green Synthesized silver nanoparticles were characterized using UV-VIS Spectroscopy, XRD, and TEM.

**Keywords:** Plastic, Decomposition, AgNO<sub>3</sub>, plant extract, XRD, and TEM etc.

### INTRODUCTION

Excessive use of plastics in domestic, industrial and agriculture sectors exert pressure on capacities available for plastic waste disposal which cause an additional burden on the environment (Akarsu *et al.*, 2006). Plastics including shopping bags, prepared from polyethylene, Water bottles, after their useful life, find their way to streets, sidewalks, beaches and water bodies ultimately to the block sewerage system which may serve as a suitable habitat for disease causing vectors including mosquitoes (Angulo-Sanchez *et al.*, 1994) and lead to the death of billions of marine animals by ingestion of the plastic debris or entanglement (Asapu *et al.*, 2011). A number of approaches have been proposed for dealing with the plastic waste. These include incineration, landfills, thermal degradation, bio-degradation, and photo-catalysis (Asghar *et al.*, 2011). Many of these are associated, however, with secondary problems. Uncontrolled burning of polyethylene produces vapors which includes many toxic compounds like ketones, acrolein, and methane and pollute the air which causes serious environmental hazards (Briassoulis 2006). Polyethylene wastes buried in soil cause negative effects to soil quality and may affect the drainage patterns leading to declined agricultural yield (Briassoulis *et al.*, 2004). In the plastic degradation studies reported so far Titania has been used in the form of nanoparticles. An option for using a larger surface area material, in the form of nanotubes (Da Silva *et al.*, 2014). Metal nanoparticles exhibit unique chemical and physical properties including large surface/volume ratio, which are useful in different fields such as electronics, photonics, biomedical, catalysis etc. (Ostuni *et al.*, 2001; Joannopoulos *et al.*, 2008; Guo *et al.*, 2013; and Arinstein *et al.*, 2007). Among the various noble metals, silver is the metal of first choice due to their diverse properties especially high antimicrobial and catalytic nature (Mashwani *et al.*, 2015; and Rostami-Vartooni *et al.*, 2016). Thus, researcher attention has been focused on alternative means of degrading the plastic material, in the present study; we used 50 ml aqueous solution of green synthesized silver nanoparticle for degradation of 0.8 mm plastic material. Silver nanoparticles shows positive effect in degradation of plastic material, AgNPs are synthesized using *Phyllanthus emblica* leaves extract, the plant is commercial cultivated for fruits. The fruit is traditionally used as medicine. Pathogenic fungal inhibiting Efficacy of silver nanoparticles is

Centre for Info Bio Technology (CIBTech)

S. G. Gounbali  
IQAC Co-ordinator  
Smt. V.G. Women's Degree College,  
KALABURAGI

  
PRINCIPAL  
Smt. V.G. Degree College for Women,  
KALABURAGI

## Research Article

tested by wells method. The fungal zone of inhibition was determined comparing with standard control bavistin. Green Synthesized AgNPs were characterized using UV-VIS Spectroscopy, XRD, and TEM.

## MATERIALS AND METHODS

### Materials:

Silver nitrate ( $\text{AgNO}_3$ ), *Phyllanthus emblica* leaves, plastic cut pieces of water bottle, *Fusarium udum*, bavistin, Mercuric chloride ect.

### Methodology:

#### Sample collection:

Fresh leaves of *Phyllanthus emblica* from kusnoor village which is just behind Gulbarga University, kalaburgi and used water bottle from foot way of Sedam road kalaburgi were collected in sterilized polythene bag, and brought to Mycology and Plant pathology Laboratory. Plastic bottle was cut into small pieces with surgical blade and stored in laboratory conditions for further studies.

#### Preparation of leaf extract:

Collected sample *Phyllanthus emblica*, leaves were surface sterilized, and dried under shade. Dried leaves were cut into small pieces and grinded to powder. 10 gram of *Phyllanthus emblica*, leaf powder boiled in 200 ml of distilled water for 10 minutes then filtered it with whatman No. 1 filter paper. The prepared plant extract solution was cooled at  $4^\circ\text{C}$  and stored in laboratory condition (Fig. 1) for further experimental work.

#### Green synthesis of silver nanoparticles:

100 mL of 1 mM aqueous solution of silver nitrate ( $\text{AgNO}_3$ ) was taken in conical flask. Then the prepared leaf extract solution with various concentrations from 5, 10, and 15 mL was added separately and agitated at room temperature. Control treatment (without Silver nitrate, only plant extract and distilled water) was also run along with experimental flask. After 24, 48 and 72 hours of time interval culture filtrate and Silver nitrate solutions turned colourless to dark brown colour due to reduction of Silver nitrate to Silver ions (Fig. 2)

#### Plastic degradation by Silver nanoparticles:

100 ml Synthesized Silver nanoparticles of *Phyllanthus emblica* was taken in 500 ml beaker. Then 5 Mg small cut pieces of plastic were added into the beaker and kept at room temperature. Along with experimental beaker, Control treatment (without Silver nitrate, only plant extract and distilled water Fig. 3) was also kept along with experimental beaker.

#### Isolation and inoculation:

Wilted stem of pigeon pea was surface sterilized by running water and broken longitudinal kept in the moist blotter for growth of the fungi, after two days associated fungi were isolated and identified as *Fusarium udum* with the help of published literature. An isolated fungus was further sub cultured on PDA plates (fig. 4) in order to obtain a pure culture.

#### Antifungal activity:

The antifungal activity of AgNPs was investigated by well diffusion method. Potato dextrose agar plates were prepared, sterilized and solidified, after solidification *Fusarium udum* was inoculated on the plates. 0.20 mg/ml, 0.30 mg/ml AgNPs and 0.20 mg/ml, 0.30 mg/ml, Bavitin and distilled water (control) were poured in the wells and kept for incubation at room temperature for five days. (Fig. 5) A zone of inhibition measured and compared with the standard bavistin and silver nitrate solution.

#### Characterization of synthesized AgNPs

##### UV-Visible spectroscopy:

The reduction of silver ions was confirmed by testing the supernatant by UV-visible spectrophotometer. (Fig. 6) The UV-visible spectroscopy measurements were performed on Elico spectral photometer as a resolution of 1 nm from 300 to 800 nm.

##### X-ray diffraction (XRD) study:

Powdered sample was used for XRD; The Coherently diffracting Crystallography domain size of the Silver nano particle was calculated from the width of the XRD peaks (Fig. 7) using scherrer formula.

### Research Article

#### Transmission electron microscopic (TEM) analysis:

The TEM analysis was performed at IIT Mumbai. (Fig. 8) TEM technique was employed to see the size and shape of the synthesized silver nanoparticles.

## RESULTS AND DISCUSSION

#### Plastic degradation:

50 ml Synthesized Silver nanoparticles from *Phyllanthus emblica* was taken in 500 ml beaker. Then 5 Mg small cut pieces of plastic were added into the beaker and kept at room temperature. Along with experimental beaker, Control treatment 5 mg plastic cut pieces with 50 ml plant extract and distilled water was also kept along with experimental beaker. The dependent variable is the amount of decomposition observed after 11 days. This is determined by using the digital weighing scale to measure the weight of the plastic before and after the 11 days. The total weight of the plastic is checked using the digital weight scale. The total weight of the plastic is subtracted by the weight of plastic material decomposed. The values are recorded in the table given below, the result confers that the synthesized Silver nanoparticles have strong efficacy to decompose plastic materials.

**Table 1: AgNPs shows degradation of Plastic.**

Solutions	Plastic decomposition after 11 days		
	Start weight (g)	Finish weight (g)	% Decomposition
50 ml AgNPs solution	5 Mg	1 Mg	20%
50 ml <i>Phyllanthus emblica</i> extract (control)	5 Mg	00 Mg	0%
50 ml Distilled water (control)	5 Mg	00 Mg	0%

#### Antifungal activity:

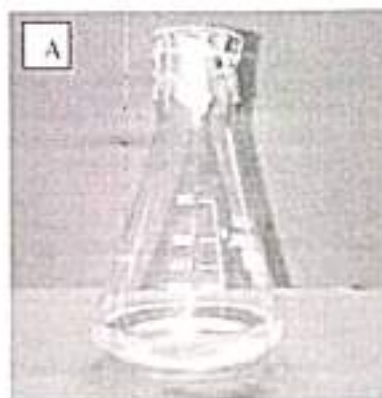
The AgNPs possess antifungal activity against isolated fungi at the concentrations of 2 mg/ml and 3 mg/ml. The AgNPs were compared favorably with standard bavistin at the concentrations of 0.20 and 0.30 ml. AgNPs exhibited positive effects inhibiting the growth of tested fungi, the MIC of AgNPs was tested against which varied from 0.20 to 0.30 mg/ml whereas bavistin showed 0.20 to 30 mg/ml. The results indicated that biosynthesized AgNPs has a positive antifungal effect.

**Table 2: AgNPs shows Antifungal Activity against *Fusarium udum***

Fungi	Zone of Inhibition					
	Silver nanoparticles.		Standard bavistin		Distilled water	
	0.20 mg/ml	0.30 mg/ml	0.20 mg/ml	0.30 mg/ml	0.20 ml	0.30 ml
<i>Fusarium udum</i>	42%	56%	41%	54%	-	-



**Research Article**

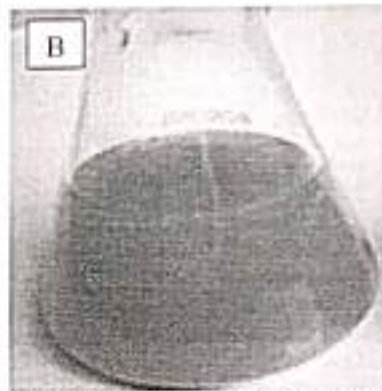


(A) 50ml plantextract

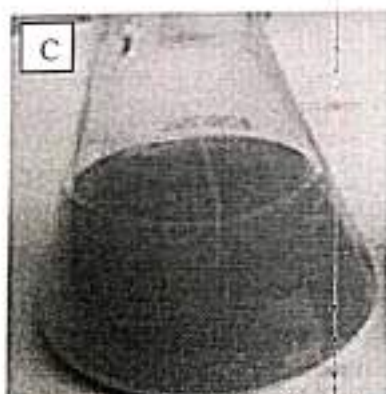
**Fig 1: Aqueous plant extract of *Phyllanthus emblica***



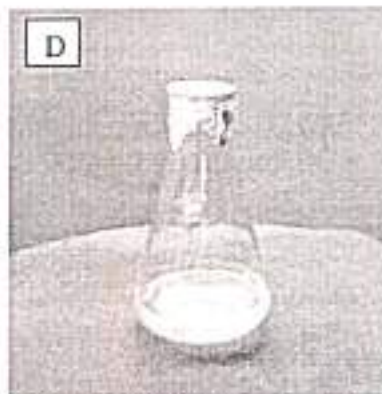
(A) 100 ml  $AgNO_3$ +5ml plantextract



(B) 1000 ml  $AgNO_3$ +10ml plantextract

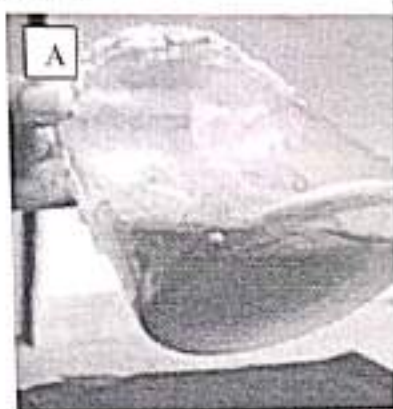


(C) 100 ml  $AgNO_3$ +15ml plantextract

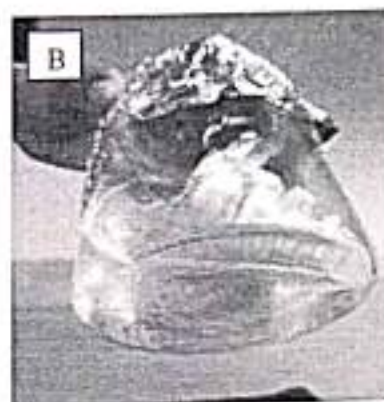


(D) 50 ml DW+5ml plantextract

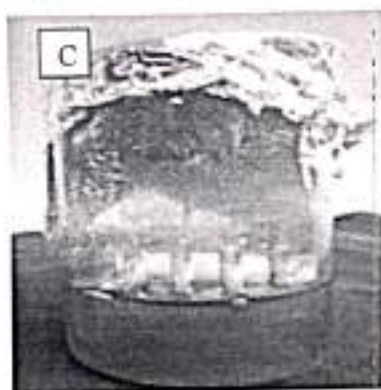
**Fig 2: Biosynthesis of silver nanoparticles-color change reaction: conical flask containing the aqueous plant extract of *Phyllanthus emblica***



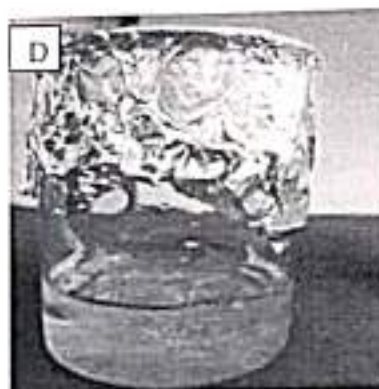
(A) 50 ml  $AgNO_3$  + 5mg plastic



(B) 50 ml D. water + 5mg plastic



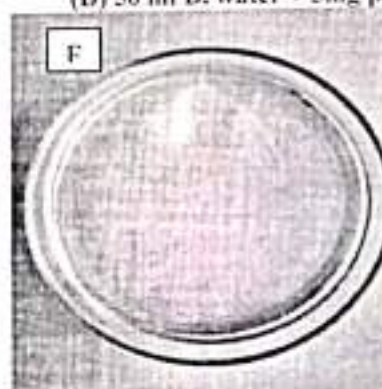
(C) 50 ml  $AgNO_3$  + 5mg plastic



(D) 50 ml D. water + 5mg plastic



(E) 1 mg decomposed plastic filterate



(F) 0 mg Control filterate

**Fig 3: Degradation of 0.8 mm water bottle's Plastic material employing Silver nanoparticle**



Fig. 4: colony morphology of *Fusarium udum*



CNP: *Phyllanthus emblica*, extract's Silver nanoparticles.  
 BVST: Bavistin standard control  
 DW: Distilled water

Fig. 5: Antifungal effect of AgNPs against *Fusarium udum* by well method

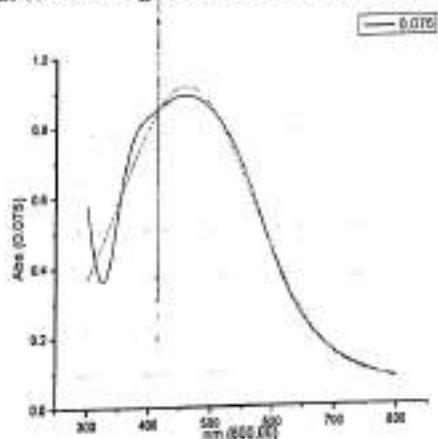


Fig 6: UV-Vis spectrum of silver nanoparticles synthesized using *Phyllanthus emblica* plant extract. UV-Vis spectra recorded as function of time of reaction of an aqueous solution of 1mM silver nitrate solution with the plant filtrate. The time of reaction is indicated next to the respective curves.

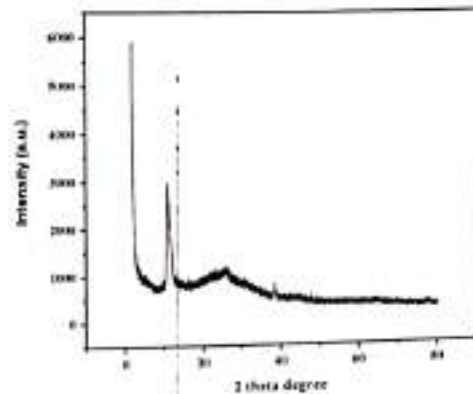


Fig 7: XRD analysis, peaks assigned to the corresponding diffraction signals (111), (200), (220), and (311) facets of Silver.



Fig 8: Transmission electron microscopic photographs of synthesized silver nanoparticles from *Phyllanthus emblica*.

**XRD study:**

Obtained Silver nanoparticles were purified by repeated centrifugation at 3000 rpm for 40 minutes by redispersing silver nanoparticles pellet into 10 ml double distilled water. After drying silver nanoparticles in room temperature structure and composition analysis was carried out by XRD (Fig. 4) The crystallite domain size was calculated by the width of the XRD peaks using Scherrer formula  $D=0.96 \lambda/\beta \cos \theta$ , where D is crystalline domain size perpendicular to reflecting planes,  $\lambda$  is the x-ray wavelength,  $\beta$  is the full width at half maximum and  $\theta$  is the diffraction angle.

The average particle size was 30-35 nm. XRD analysis, peaks assigned to the corresponding diffraction signals (111), (200), (220), and (311) facets of Silver. The mean particle diameter of silver nanoparticles was calculated from the XRD pattern according to the line width of the (111) plane.

**TEM Analysis:**

Sample was prepared for Transmission electron microscopic Analysis (IIT Mumbai) TEM Technique was employed to see the size and shape of the synthesized silver nanoparticles; it was observed that there is variation in the particle sizes around 30% of particles in 25 nm range and 25% in 30 nm range and 20% in



### Research Article

35 nm ranges. The particles range from 12 nm least to 75 nm high, the TEM image suggests that the particles are polydispersed (Fig. 5) and are rounding spherical in shape.

### Conclusion

In the present study Silver nanoparticles were Green synthesized using *Phyllanthus emblica* plant extract. The plant extract in different concentration i.e. 5 ml 10 ml and 15 ml are challenged with 1mM Silver nitrate; change of mixture from color less to dark brown indicates the synthesis of Silver nanoparticles in the reaction mixture. 100 ml of Synthesized Silver nanoparticles applied for the degradation of 0.8 mm plastic material, the dependent variable amount of decomposition observed after 11 days. Antifungal Efficacy of Synthesized AgNPs was tested against *Fusarium udum*. Zone of inhibition was observed. And the crystallite domain size of synthesized Silver nano particles was measured 30-35 nm by XRD analysis, shape and size of the silver nanoparticles was studied by TEM analysis. Results conclude that *Phyllanthus emblica*, plant extract is potential producer of Silver nano particles, and Silver nanoparticle have strong efficacy of plastic decomposition and also fungal inhibition.

### ACKNOWLEDGEMENT

Authors wish to thank to Gulbarga University, Gulbarga, Karnataka, India. And also thankful to USIC and Physics departments (G.U.G) for UV spectrum and XRD analysis and IIT Mumbai for TEM analysis

### REFERENCES

- Akarsu M, Asilturk M, Sayilkan F, Kiraz N, Arpac E and Sayilkan H (2006). A novel approach to the hydrothermal synthesis of anatase Titania nanoparticles and the photo catalytic degradation of rhodamine B. *Turkish Journal of Chemistry* 30(3) 333–343.
- Angulo-Sanchez JL, Ortega-Ortiz H, Sanchez-Valdes S (1994). Photo degradation of polyethylene films formulated with a titanium-based photo sensitizer and titanium dioxide pigment. *Journal of Applied Polymer Science* 53 (7) 847–856.
- Arinstein A, Burman M, Gendelman O and Zussman E (2007). Effect of supra molecular structure on polymer nanofibre elasticity. *Natural Nanotechnology* 2 59e62.
- Asapu R, Palla V M, Wang B, Guo Z, Sadu R and Chen DH (2011). Phosphorus-doped Titania nanotubes with enhanced photo catalytic activity. *Journal of Applied Polymer Science* 225 (1) 81–87.
- Asghar W, Qazi IA, Ilyas H, Khan AA, Awan MA and Aslam MR (2011). Comparative solid phase photo catalytic degradation of polythene films with doped and undoped TiO<sub>2</sub> nanoparticles. *Journal of Nanotechnology Materials* 12.
- Briassoulis D (2006). Mechanical behavior of biodegradable agricultural films under real field conditions. *Polymer Degradation and Stability* 91(6) 1256–1272.
- Briassoulis D, Aristopoulou A, Bonora M and Verloot I (2004). Degradation characterisation of agricultural low-density polyethylene films. *Biosystematic Engineering* 88 (2), 131–143.
- Da Silva KIM, Fernandes JA, Kohlrausch EC, Dupont J, Santos MJL and Gil MP (2014). Structural stability of photodegradable poly (l-lactic acid)/PE/TiO<sub>2</sub> nano composites through TiO<sub>2</sub> nanospheres and TiO<sub>2</sub> nanotubes incorporation. *Polymer Bulletin* 71 (5) 1205–1217.
- Guo X, Baumgarten M and Müllen K (2013). Designing p-conjugated polymers for organic electronics. *Progress in Polymer Science* 38 1832e908.
- Joannopoulos JD, Johnson SG, Winn JN and Meade RD (2008). Photonic Crystals: Molding the Flow of Light. 2nd ed. Princeton, NJ: Princeton University Press.
- Mashwani ZUR, Khan T, Khan MA and Nadhman A (2015). Synthesis in plants and plant extracts of silver nanoparticles with potent antimicrobial properties: current status and future prospects. *Applied Microbiology and Biotechnology* 99 9923e34.



*International Journal of Innovative Research and Review* ISSN: 2347 - 4424 (Online)  
An Online International Journal Available at <http://www.cibtech.org/ijrr.htm>  
2017 Vol. 5 (1) January-March, pp 28-36 Ravindra and Patil

**Research Article**

**Ostuni E, Chen CS, Ingber DE and Whitesides GM (2001).** Selective deposition of proteins and cells in arrays of micro wells. *Langmuir* 17 2828e34.

**Rostami-Vartooni A, Nasrollahzadeh M and Alizadeh M (2016).** Green synthesis of seashell supported silver nanoparticles using *Bunium persicum* seeds extract: application of the particles for catalytic reduction of organic dyes. *Journal of Colloid Interference Science* 470 268e75.



# FLUORESCENCE STUDIES ON ORGANIC ACIDS DOPED PANI-PVA THIN FILMS AND QUENCHING WITH PICRIC ACID

Parvathi Paul<sup>\*2</sup>, Lakshmidevi V.<sup>1,2</sup>, Sharmabasava V. Ganachari<sup>3</sup>, A. Venkataraman<sup>\*1,2</sup>

<sup>1</sup> Materials Chemistry Laboratory, Department of Materials Science, Gulbarga University Kalaburagi-585106, Karnataka.

<sup>2</sup> Department of Chemistry, Gulbarga University, Kalaburagi-585106, Karnataka

<sup>3</sup> Centre for Material Science, KLE Technological University, Hubballi-580031

\*Correspondence author email: raman.dms@gmail.com

E-mail for correspondence: raman.dms@gmail.com

## Abstract

The polyaniline poly (vinyl alcohol) (PANI/PVA) thin films were prepared by the chemical oxidative dispersion polymerization of aniline monomer in 0.2 M HCl aqueous media with the poly (vinyl alcohol) (PVA) and p-Toluenesulfonic acid (PTSA) as the stabilizer and dopant respectively. The PANI/PVA thin films were characterized by Fourier transform infrared spectroscopy (FTIR), Thermal gravimetric analysis (TGA), Scanning Electron microscopy (SEM). Fluorescence emission spectra of PTSA doped PANI/PVA thin films were investigated in different doping ratio of 0.1, 0.3 and 0.5. The present work the importance of fluorescence of p-Toluenesulfonic acid (PTSA) doped PANI/PVA thin films and the quenching phenomenon of the electron withdrawing groups such as nitro functionalized high energy materials called as nitroaromatics. The present report is on the fluorescence quenching study of picric acid.

**Keywords:** Fluorescence quenching, PTSA doped Polyaniline salt, Stern-Volmer plot.

## INTRODUCTION

Polyaniline is the most of the intensively studied conductive polymers which have been exposed for use in electronic and optical application. Polyaniline have been intensively studied of their potential for commercial applications seen as pole injection layers for flexible light emitting diodes (16) electromagnetic interface shielding (17) corrosion protection (18) etc. The protonation PANI emeraldine base (PANI-EB) or its



derivatives with organic acids can be used for the protonation of electrically conducting polymers with improved process ability (1-5). 5

In this study, we investigated the effects of the dopant and the solvent on the change transport properties in polyaniline systems for dopants we used BSA, TSA, CSA, PTSA, NSA. The emeraldine base for of polyaniline along with the dopant is dissolved in solvent like chloroform, BEOH, DMF, NMF, DMSO. In PANI extended conjugation intermolecular hydrogen bonds are formed between the amine and imine group of the adjacent chain and stacking.

Polyaniline shows fluorescence characteristics due to the extended conjugation and were used as selective fluorescence for the detection of electron deficient nitroaromatics (NACS) Nitroaromatic are the prominent high energy materials which are being used as explosives and detonators etc. the present studies are employed by doping PANI with PTSA different concentrations dissolving DMF solvent before going for fluorescence studies. The  $H^+$  ions were added upon protonation so that imine groups at the quinoid ring at as a charge delocalization of holes in the valence bond.

The electron withdrawing group ( $-NO_2$ ) of picric acid quenches the fluorescence showed by the PTSA-doped polyaniline base. The electron transitions are transfer from PTSA doped polyaniline base to electron withdrawing group of picric Acids. Quenching takes place and it is attracted much attention due to their high sensitivity and selectivity. The stacking in polymers which is responsible for sensitive fluorescence quenching is explained (8). The nitroaromatics are also in polymers films.

In this paper, we have reported the study on the effect of concentration of picric acid on the fluorescence intensity of PTSA-PANI employee DMF as a solvent and the study was carried out 0-50°C. the fluorescence of PTSA-PANI in difference concentrations has been quenched and quenching is in accordance with S-V relation. The S-V constant was obtained.

## EXPERIMENTAL

### Materials and Methods

Aniline ( $C_6H_5NH_2$ ), ammonium persulfate ( $(NH_4)_2S_2O_8$ ), p-Toluenesulfonic acid ( $CH_3C_6H_4SO_3H$ ), Poly (vinyl alcohol)  $[CH_2CH(OH)]_n$ , Hydrochloric acid (HCl), Dimethylformamide ( $C_3H_7NO$ ), methanol ( $CH_3OH$ ) and acetone ( $C_3H_6O$ ). All the





chemicals purchased were used as received and analytical reagent grade. Double distilled water was used in the experiment.

### **Synthesis of emeraldine salt**

15 ml of concentrated HCl (0.2M) and 12 ml of aniline (0.2M) was taken in a round bottom flask. 180 ml of distilled water (covered with ice cubes salt mixtures in maintain low polymerization temperature) equipped with electromagnetic stirrer. Then 13 gram (0.08M) ammonium persulfate in 100ml 0.2M HCl was abruptly added into the above solution. The polymerization temperature maintained for 2 hours to complete the reaction.

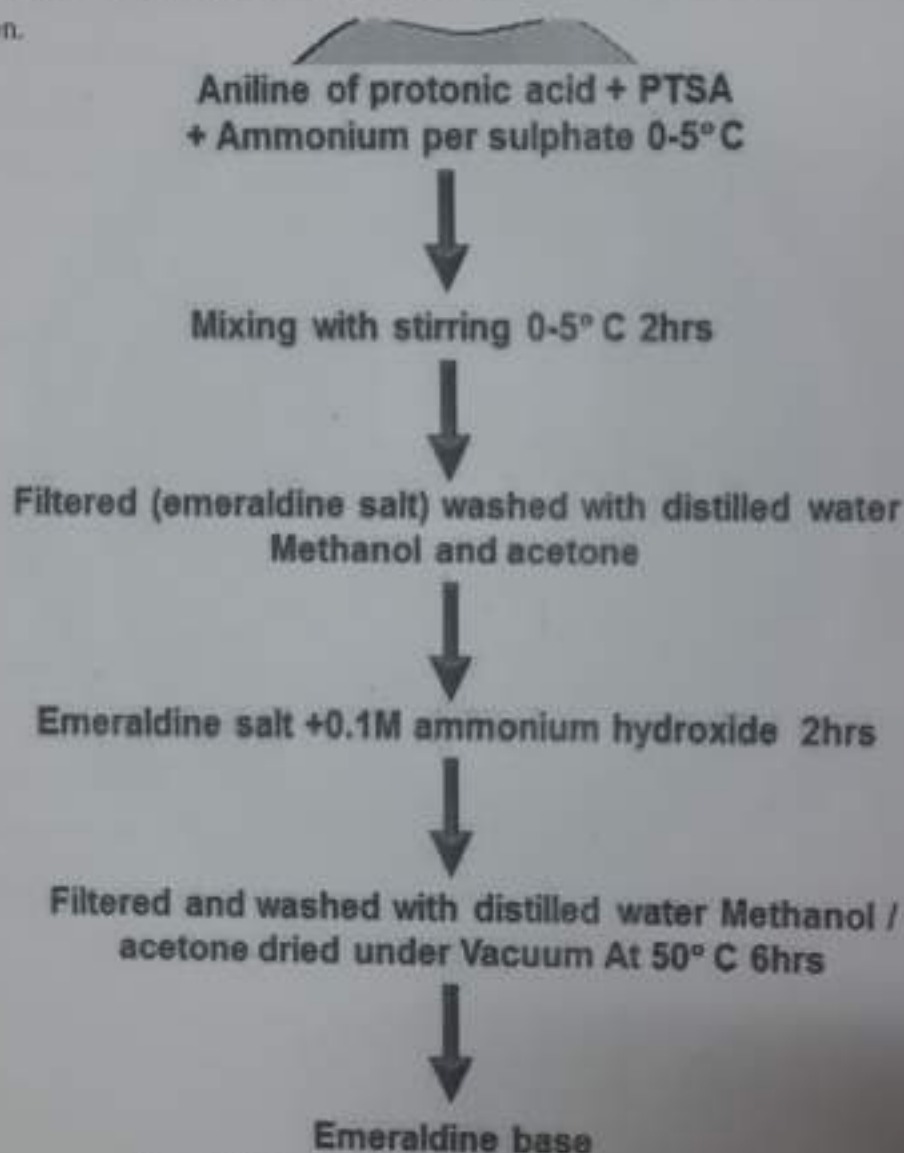


Figure 1. Flow chart of the preparation of emeraldine base

The precipitate emeraldine salt is filtered and washed with distilled water until the filtered is color less. It is then washed with methanol to remove oligomeric impurities. Finally, it is washed with acetone to remove water content and kept overnight for filtering.



The precipitated is collected in picker and dried under vacuum at 50°C for 6 hours then it is crushed into fine powder to get emeraldine salt. The emeraldine salt was taken in a round bottle flask contained 20ml of ammonia solution and 80ml of water stirred continuously for 24 hrs. The precipitate (blue emeraldine base) is filtered and washed with distilled water and finally with acetone. After keeping overnight, filtering the precipitate is then crushed into fine powder to get.

#### **Preparation of PTSA doped PANI**

PANI (EB) was synthesized by solid state reaction using experimental procedure reported by *Raghu et. Al.* [12]. PANI-PTSA was prepared by mixing 0.006M of emeraldine base with 0.0006M of PTSA using agate Mortar and pestle. Similarly, 0.006M of emeraldine base with 0.0018M of PTSA using agate Mortar and pestle. 0.006M of emeraldine base with 0.003M of PTSA using agate Mortar and pestle.

#### **Preparation of sample solutions**

Different concentration of dilute solution of PTSA-PANI in DMF are prepared to avoid absorption effects and the quencher concentration been varied. The 10 ppm PTSA doped polyaniline in DMF solution is prepared. The 5ppm of picric acid in DMF used as quencher.

#### **Preparation of polymer films**

The films of different doped polyaniline prepared by following procedure. A 0.07gm sample of doped PANI was mixed with 0.02 gram of PVA in 10ml of DMF and the solution was stirred for 12 hrs. Then 0.16ml each of the various doped polyaniline solution was cost on a glass slide and dried in a vacuum oven at 50-60°C for 12 hrs.

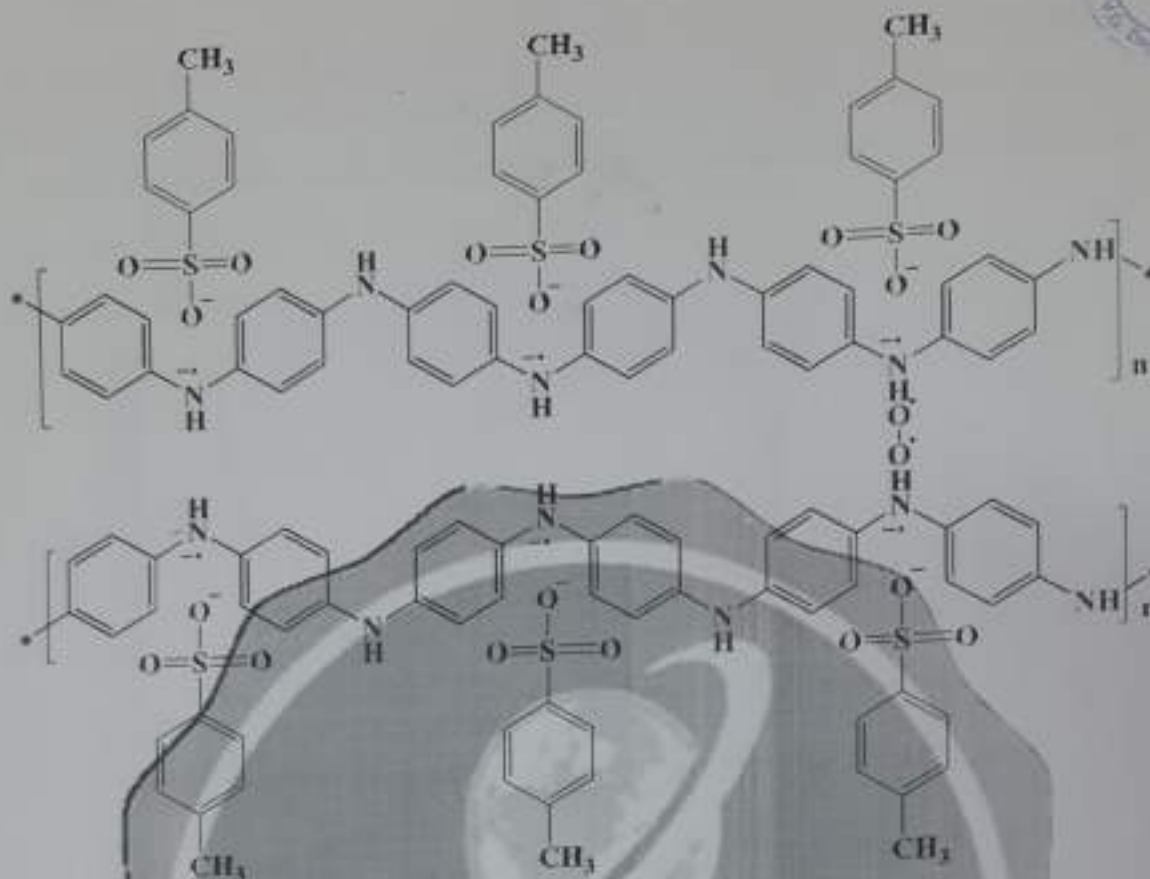


Figure 2. Chemical structure of emeraldine salt of PTSA doped PANI.

### Characterizations

**Fourier Transform Infra-Red spectrometer (FTIR):** The FTIR spectra of the polymers were recorded on a Thermo Nicolet, Avatar 370 instrument in the range 4000–400  $\text{cm}^{-1}$  at a resolution of 4  $\text{cm}^{-1}$  by making KBr pellets. **Scanning Electron Microscope (SEM):** The morphologies of the polymers were studied by using coupling JEOL Model JSM - 6390LV scanning electron microscope. The electron microscope was operated at 20 kV. **Thermal Gravimetric analysis:** The thermogravimetric analysis (TGA) measurements were made using a Perkin Elmer, Diamond System at a heating rate of 10°C per min under nitrogen atmosphere. **Fluorescence Spectrophotometer:** Fluorescence measurements are performed by employing ELICO-SL174 spectrophotometers equipped with a xenon arc lamp. The slit width for excitation and emission were fixed at 5 nm. All measurements were made using 1 cm Quartz Cuvette at room temperature.

### Quenching experiments

The emission spectra of PTSA-PANI are measured by fluorescence spectrophotometer. Studied spectroscopic data such as absorption and emission wavelength, fluorescence intensity and stokes shift. The concentration of PTSA –PANI



was kept constant and the concentration of P1 (0.1), P2 (0.3) and P3 (0.5). the quencher picric acid (PA) is take different concentration. The polymer solution showed a maximum excitation wavelength at different excitation and different emission wavelength was observed in P1 (0.1), P2 (0.3) and P3 (0.5) ( $\lambda_{em}$ )

### Results and discussion

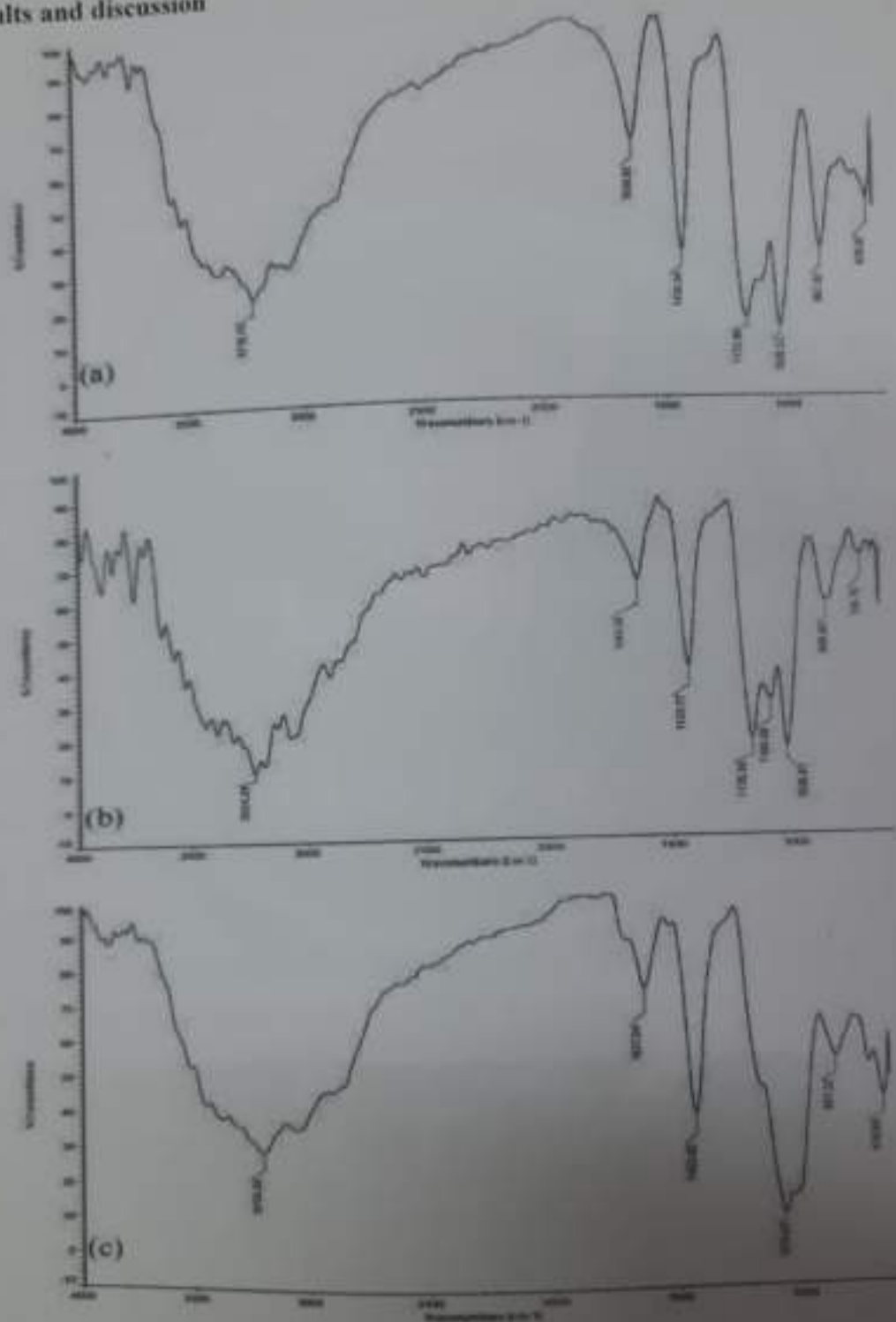


Figure 3. a) P1, b) P2 and c) P3 FTIR Spectra of PTSA doped PANI

### FTIR Spectra

The FTIR spectrum of PTSA doped different concentrations P 0.1, 0.3, 0.5 are shown in figure 3 (a), 3 (b) and 3 (c) respectively. The peaks at  $1560.30\text{ cm}^{-1}$  in all the three peaks shows the quinoid. The peaks at  $1693\text{ cm}^{-1}$ ,  $1636\text{ cm}^{-1}$ ,  $1640\text{ cm}^{-1}$  shows the Benzenoid ring respectively as shows the oxidation state of emeraldine salt of PANI.

A strong bond observed in  $1931\text{ cm}^{-1}$ ,  $1434\text{ cm}^{-1}$ ,  $1433\text{ cm}^{-1}$  in fig 3 (a, b, and c) described as the electronic light band. All the three spectra peak at about  $1171\text{ cm}^{-1}$ , is due to C-N stretching mode peaks about  $1172\text{ cm}^{-1}$ ,  $1178\text{ cm}^{-1}$  and  $667\text{ cm}^{-1}$  is usually assigned to the C-N stretch of secondary aromatic amine the peak at  $726\text{ cm}^{-1}$ ,  $1419.59\text{ cm}^{-1}$  in 4 and 5 figure are assigned to the aromatic C-H in plane bending modes. The peak at  $565.1\text{ cm}^{-1}$ ,  $567.03\text{ cm}^{-1}$ ,  $568.96\text{ cm}^{-1}$ , are usually assigned to an out of plane bending deformation of C-H. The peaks at  $798.47\text{ cm}^{-1}$ ,  $800.4\text{ cm}^{-1}$  in 3 and 4 usually assigned to para di substituted aromatic ring indication polymer formation. The peaks at  $1034\text{ cm}^{-1}$ ,  $1035\text{ cm}^{-1}$ ,  $1036\text{ cm}^{-1}$ , is assigned to  $\text{SO}_3$ -group of the dopant and PTSA.

### SEM Images

The SEM images powder displays highly agglomerated morphology made up of the petals like particle with  $20$  to  $30\text{ }\mu\text{m}$  in diameter and  $20\text{ }\mu\text{m}$  in length these particles are formed during low temperature in situ polymerization of aniline and maintain their morphology even after re doping with PTSA but agglomeration appeared due to strong intra and intermolecular ionic interactions between chains triggered by proto generated charge carried (i.e. polarons and bipolarons) in shown in figure 4(a). In figure 4(b) the images of PTSA doped PANI shows that high grown in hexagonal structure in the morphology all the crystal aligned in the same direction and the sulfonate groups in present in thickness the particle size  $40$  to  $60\text{ }\mu\text{m}$  diameter and  $100$ - $200\text{ }\mu\text{m}$  in length the vander walls interaction between the phenyl ring PTSA and solvent desorbed Lennard potential. This molecular interaction known to cause crystal and growth of PTSA.



Figure 4. a) P1, b) P2 and c) P3 SEM images of PTSA doped PANI



In figure 4 (c) shows that the images of cotton like structure and the particle size 80 to 90  $\mu\text{m}$  diameter and 200 to 300  $\mu\text{m}$  in length the fibers of particle size present sulfonate groups are very thickness and agglomerates deformation resulting in increasing adjacent the rigs due to PTSA ion bulky molecule and steric hindrance by electro static repARATION between doping ion and hydrogen of the imine sites.

### Thermal Analysis

Figure 5 (a) shows that thermal behavior of PTSA doped PANI is illustrated by DTG curve the weight loss in the first 15.2% attributed to the description superficial water molecular associated with the doped PANI-1.62 first stage. Figure 5(b) shows PTSA doped PANI than remains stable  $-98^\circ\text{C}$  the second step extending up to  $200^\circ\text{C}$  with weight loss of 56.7% indicates the loss of PTSA and the polymer is completely dedoped at  $-300^\circ\text{C}$

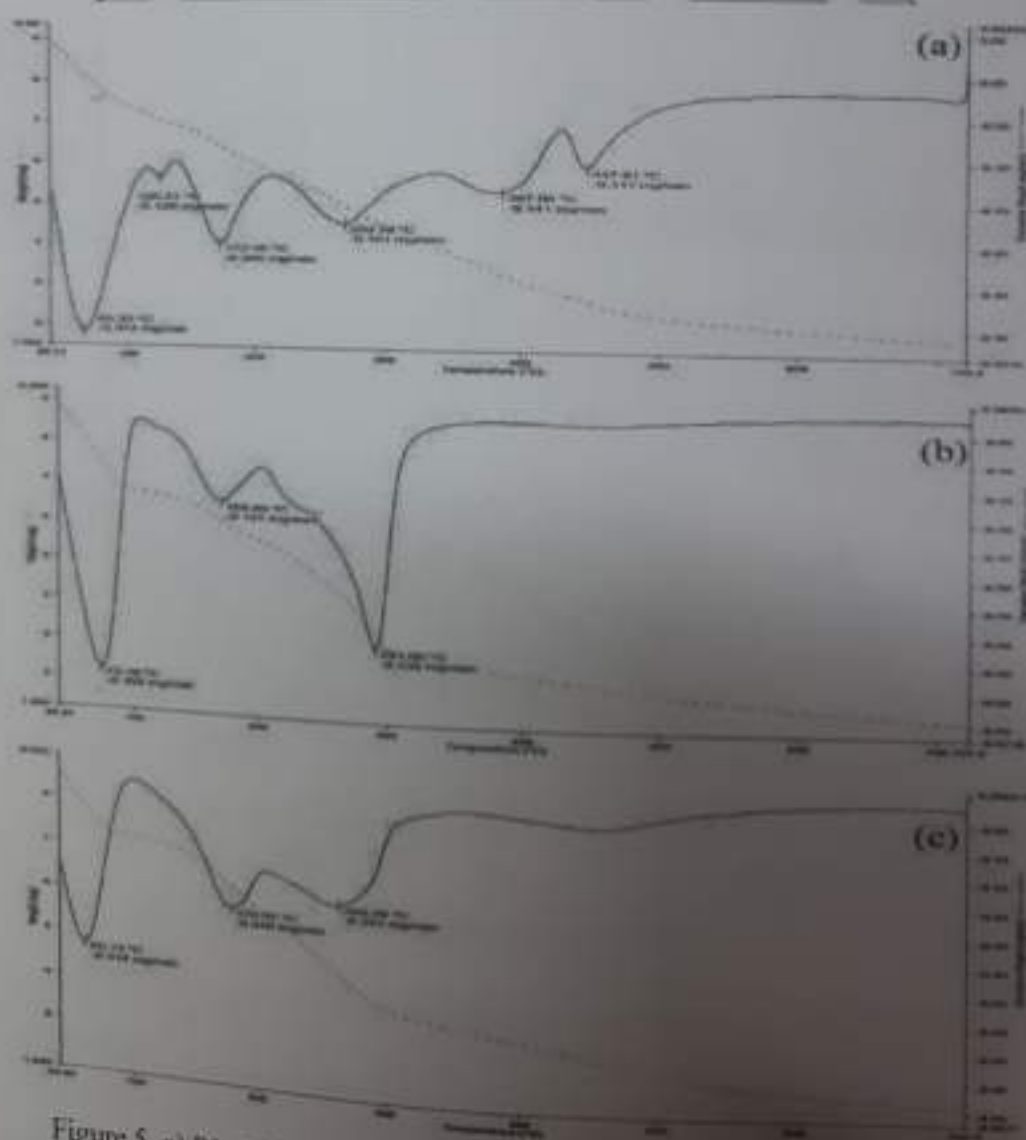


Figure 5. a) P1, b) P2 and c) P3 Thermal analysis of PTSA doped PANI



Figure 5(c) shows that stage extending up to 720°C in this stage sulphonate ions, were readily detached from the polymer backbone. The polymer backbone the polymer degradation stated. Move interestingly at 300°C, the acid was completely dedoped from the polymer and the total weight loss was found about -6.08% at higher temperature, it shows full scale polymer degradation. Conclusion PTSA doped PANI was successfully obtained via the in situ oxidative polymerization of aniline with doping level is determined. Spectroscopic and thermal properties of the polymers are found to be affected by the type of the dopant used. Fluorescent characteristic of polymer solution/ film upon exposure to a good potential to be exploited as sensing material for detection. A good repeatability and reproducibility of measurement were obtained. A complete regeneration cycle took about 17 minutes and 4 complete cycle were observed in 60 minutes of testing.

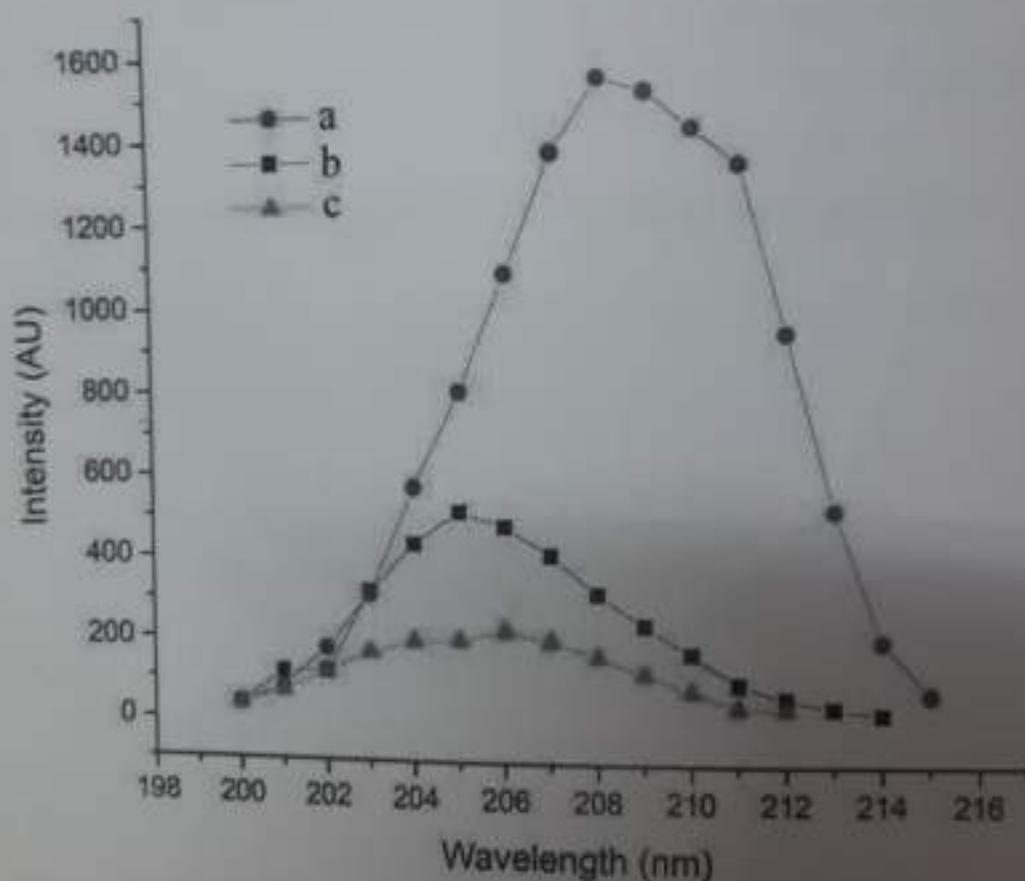


Figure 6. a) P1, b) P2 and c) P3 Fluorescence emission spectrum of PTSA doped PANI

#### Quenching studies

The self-quenching mechanism Covalently fluorophore pairs factors influencing efficiency of self-quenching are disassembled into four components as shown in figure 7 Quenching



of a fluorophore is significantly influenced by the molecular structure of the quencher. [17] in this study quenching by nitroaromatic compounds was evaluated to assist the molecular interaction between nitroaromatic molecules. Figure 6. a) P1, b) P2 and c) P3 shows the Fluorescence emission spectrum of PTSA doped PANI

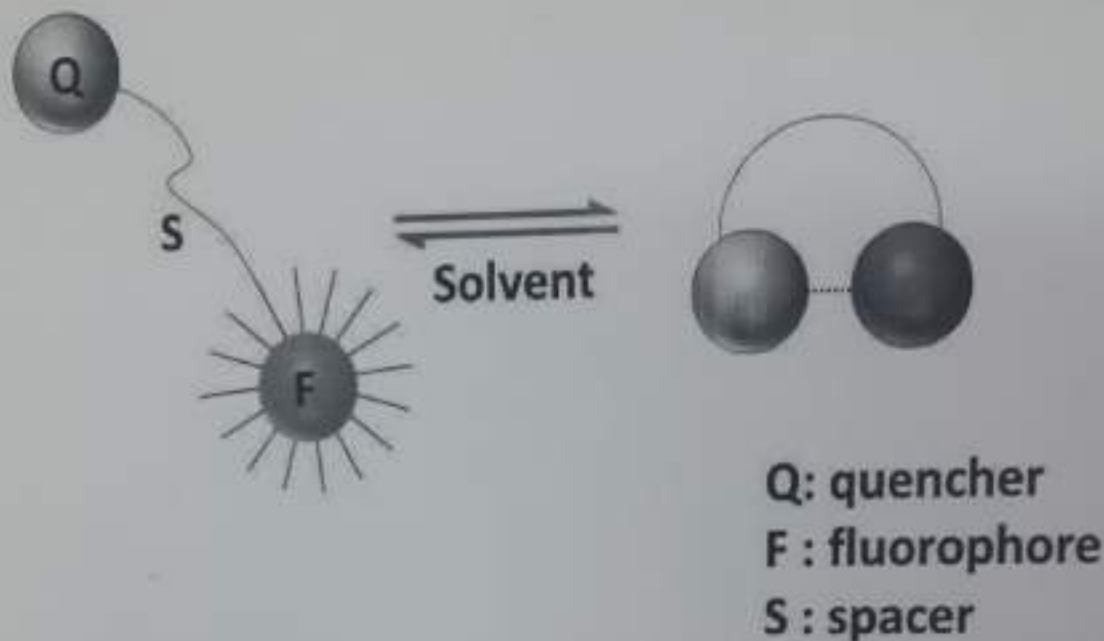


Figure 7. Quenching mechanism

The fluorophore interaction can be identified by examining the emission spectra using solvents. The emission spectra of PTSA doped PANI are measured. The spectroscopic data such as absorption and emission wavelength fluorescence intensity noted PANI is conjugated fluorescent polymer which exhibits  $\pi$  to  $\pi^*$  and  $n$  to  $\pi^*$  transitions. The emission spectra of Polymer solutions are mirror images of the excitation spectra upon photo excitation of a conjugated polymer. The electrons from the valance band are excited to the conduction band and then migrated along the polymer backbone

#### Conclusion

The fluorescence data of PTSA-PANI reveal that the nature and amount of shifts depend on the polarity of the solvents. It is concluded from the data that as the polarity of the solvent increases, PTSA-PANI shows a bathochromic shift for  $n-\pi$  and  $\pi-\pi^*$  transitions. Knowledge about the excited electronic state dipole moments of the solute molecules is quite useful in designing nonlinear materials and in elucidation of the nature of the excited state.

#### Acknowledgements





The author Parvathi Patil, acknowledges H. K. E. Society's Smt. Veeramma Gangasiri College for Women Kalaburagi, Karnataka, India for supporting throughout research work.

### Reference

- [1] A.J Hooger & J. Long, Jr optics and photonic news, August (1996) P-24 and references therein.
- [2] J.Joo and A.J Epstein in applied Physics lett. 65 – 2278 (1994)
- [3] P.J. Kinlen and C.R. Jeffreys Synth Met. To be published (1997)
- [4] Trivedi DC in Nalwa Its editor Hand Book of organic conducting molecules polymers Vol.2 Chichester UK Willey (1997), P-72
- [5] Mac Diarmid Ag, Epstein At Faraday Discuss Chem Soc. 1989, 88-317.
- [6] Steskal Japuria LMacromolecules 1989-31(17), 2218.
- [7] Cao, Y Smith P Heeger A.J Synthmet 1993-55-57; 3514
- [8] S.Shanmuga Raju, H.Jadhav, R.Karthik and P.S.Mukherjee RESC advances 2013, 3(15),4940,4950.
- [9] H.Swaruparani, S.Basavaraja, C.Basavaraja and A.Venkataraman Journal of applied polymer science 2010, 117, 1350.
- [10] The electronic structure of polyniline and doped phases studied by soft X-ray absorption and emission spectra copies M.Mangusoon T.H. and S.M. Butorin A, Agbi, C. Sathe, J.Nordgren, A.P. Monkman Journal of Chemical physics 1999, 111 (10), 4756-4761
- [11] Y.Safinas R.M Manez, M.D. marcos, F.Sancemon, A.M costero M.Parra and S.Gil Chem Soc. Rev. 2012, 41(3)
- [12] Raghu M and Heeger A-J Physical Review B 47(4):1758 (1993).
- [13] Yese J Wang Z.H Somack K.R. Epstein A.J; MacDiarmid A.G. J.Am chem. Soc. 1991, 113, 2665-2671.
- [14] Sinha.S.Bhadra S.Khastgir, D.J. Appl. Polym. Sci.2009, 112,3135-3140.
- [15] B.D.Gokcen, D.Bihter and B.Mehmet Chemical Communications 2013, 49, 6140-6142.
- [16] N.L.Sheela, S.M. Umesh, L.B. Swaminath V.A Prashant, R.P Shivajiroa and B.K. Govind Bull Chem. Soc. Ethip. 2009, 23(2) 231-238.
- [17] Gilat,S.L; Adronov, A ;Frechet,J. M.J. Angew. Chem.Ed. 1999, 38, 1422-1427

## Effect of solvent polarity on fluorescence spectra of camphor Sulphonic acid doped Polyaniline

Lakshmidhevi V. **Ranjith** and Venkataraman A. *Materials Chemistry Laboratory, Department of Materials Science, Gulbarga University, Kalaburagi-585106, Karnataka, India*  
*Department of Chemistry, Gulbarga University, kalaburagi-585106, Karnataka, India*

### Article Info

**\*Corresponding author:**  
**Venkataraman A.**  
 Department of Chemistry  
 Gulbarga University  
 kalaburagi-585106  
 Karnataka, India  
 Email: [raman.dms@gmail.com](mailto:raman.dms@gmail.com)  
 doi: 10.18689/mjai.2017-105

Received: January 09, 2017  
 Accepted: January 24, 2017  
 Published: January 27, 2017

Citation: Lakshmidhevi V. **Ranjith** and Venkataraman A. Effect of solvent polarity on fluorescence spectra of camphor Sulphonic acid doped Polyaniline. *Madridge J Anal sci instrum* 2016; 1(1): 21-24.

Copyright: © 2016 Venkataraman A et al. This work is licensed under a Creative Commons Attribution 4.0 International License, which permits unrestricted use, distribution, and reproduction in any medium, provided the original work is properly cited.

Published by Madridge Publishers

### Abstract

The Camphor sulphonic acid doped polyaniline (CSA-PANI) is synthesized by chemical polymerization method and then characterized by using UV-Visible and FTIR. The surface morphology is studied by SEM and AFM techniques. The degree of crystallinity of PANI is studied by XRD and redox behaviour by cyclic voltametry. Thermal stability of the doped polymer is investigated by TGA and DSC. The fluorescence emission spectra of CSA-PANI are investigated in different solvents such as dimethyl formamide (DMF), dimethyl sulphoxide (DMSO) and N-methyl-2-pyrrolidone (NMP). The fluorescence intensity decreases with increase of solvent polarity. A fluorescence study reveals that the nature (blue or red shift) and amount of the shifts of PANI depends on the solvents used. The significance of present study evolves a trend in solvatochromic shifts of PANI in different solvents.

**Keywords:** Conducting polymer, PANI, Dipole Moment, Fluorescence, Stokes shift, Solvatochromic Shift.

### Introduction

Conducting polymers were considered as the futuristic new materials that would lead to the next generation of electronics and optoelectronics devices. Among all conducting polymers PANI and its derivatives have attracted much attention worldwide because of chemical stability, simple preparation and high conductivity, low ionization potential, high electron affinity and the ability to be oxidized or reduced more reversibly than conventional polymer [1-3]. PANI has extended  $\pi$ -electron delocalization, which is responsible for fluorescence emission and it is a fluorescent conjugated polymer. The photoluminescence of PANI emeraldine salt was reported by Gong et al [4]. The extended conjugation also leads to intermolecular hydrogen bonds between the amine and imine group of the adjacent chain and  $\pi$  stacking. Hence the polymer chain becomes rigid which induces insolubility and infusibility to the polymer chain. The processability of PANI can be improved by using functionalized dopants like CSA or DBSA which was first reported by Cao et al [5]. The bulky dopants will reduce the mutual aggregation by increasing the solubility of PANI salt in non-polar and weakly polar solvent.

In recent years considerable effort has been made to design and to synthesize functional molecule that could serve as sensitive sensors for the analytical detection of chemically and biologically important ionic species. Fluorescence sensors have received a considerable attention for their potential applications to biochemical and medical analysis. The effect of solvents on spectral properties of molecules generally referred as solvatochromism has been investigated [6]. The study of solvent effects on fluorophore

*S.G. Gounhal*

has been the intensive area of research in recent years. Suming Chen et.al. Have studied the effect of local environment the fluorescent probe tyrosine under denaturation conditions [7]. Photophysical properties like Stokes shift and quantum yield are the subject of intensive investigation which have considerable importance in the photophysics and photochemistry. Fluorescence emission of a molecule is sensitive to environment and solvent polarity which are of significant interest due to their versatile applications in chemistry, biology and environmental science [8].

PANi doped with CSA was synthesized by chemical oxidation method and characterized by different techniques which are reported earlier. In this paper we focus on the investigation of Fluorescence studies of CSA-PANi in different solvents which sheds some light on the effect of polarity on the fluorescence spectra.

## Materials and methods

All chemicals and solvents used for synthesis and fluorescence measurements were of analytical grade and used as received.

Fluorescence measurements were done using Elico SL174 Spectro photometer equipped with a Xenon arc lamp. The slit width for excitation and emission were fixed at 5 nm. All measurements were made using 1 cm Quartz Cuvette at room temperature.

## Polymer Solution Preparation

5.0 ppm Polymer solution was prepared by dissolving 5.0 mg CSA- PANi in 1000 ml of solvents.

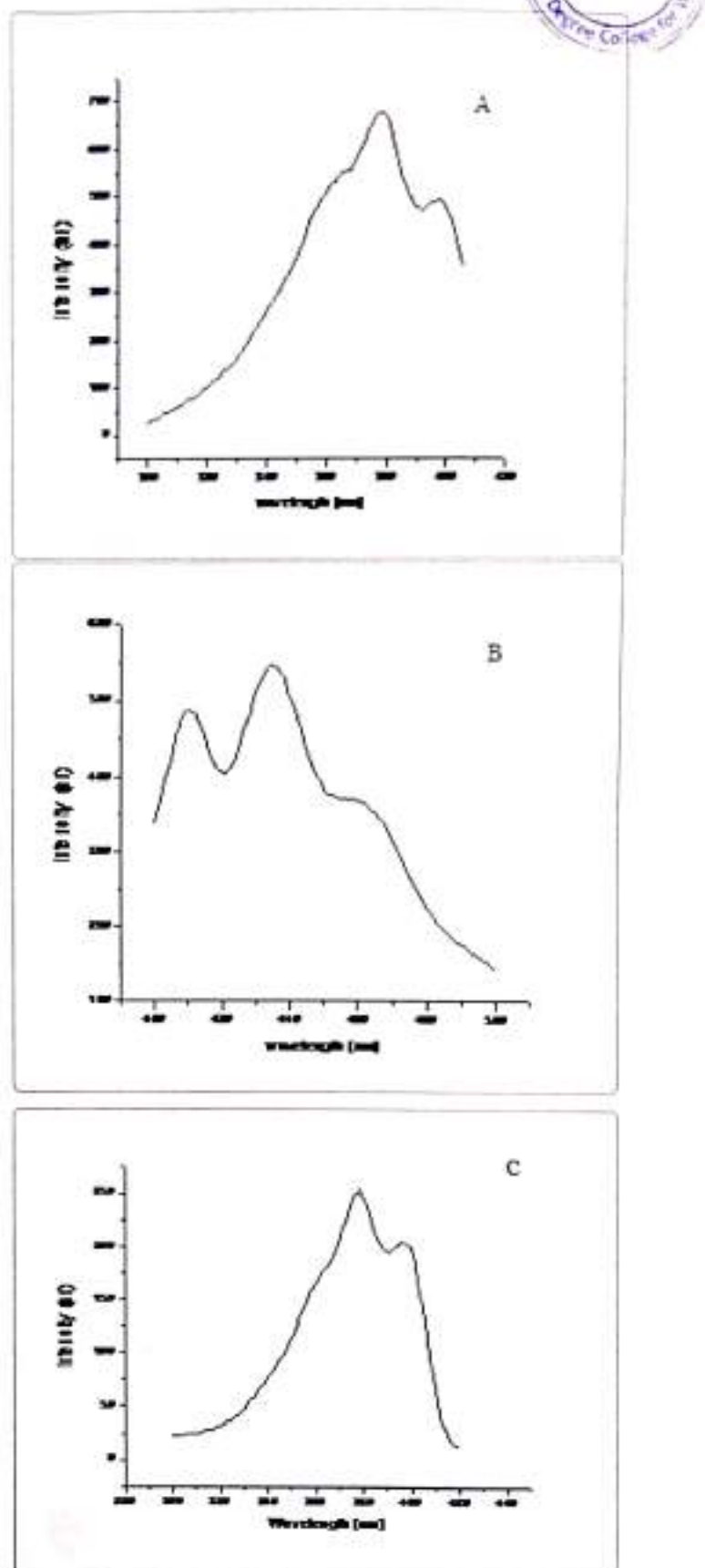
## Fluorescence Measurement

The effect of solvent polarity on the fluorescence of CSA-PANi solution was investigated using fixed concentration of PANi in different solvents of different polarities (viz.DMF, NMP and DMSO). The emission spectra of CSA-PANi are measured in polar solvents of different polarity at room temp. Spectroscopic data such as absorption, and emission wavelength, fluorescence intensity and stokes shift are shown in the Table.1

Solvent	Dipole moment (Debye)	Excitation wavelength (nm)	Intensity (Au)	Emission wavelength (nm)	Intensity (Au)	Stokes shift(nm)
DMF	12.7	378	674.08	409	486	31
DMSO	13.5	379	253	408	272	29
NMP	13.6	374	390.42	418	112	37

Table-1: Dipole moment, Excitation wavelength, Emission wavelength and Stokes shift of CSA- PANi in different solvents.

The emission spectra of the polymers solutions were mirror images of the excitation spectra as shown in the figure-1



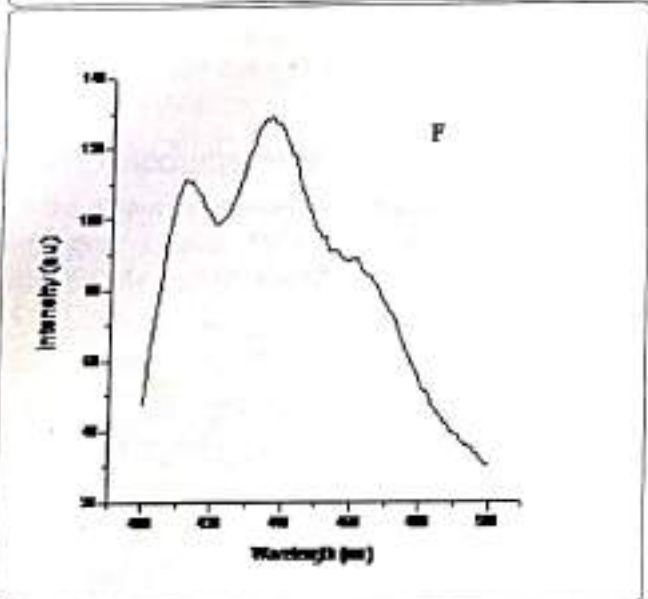
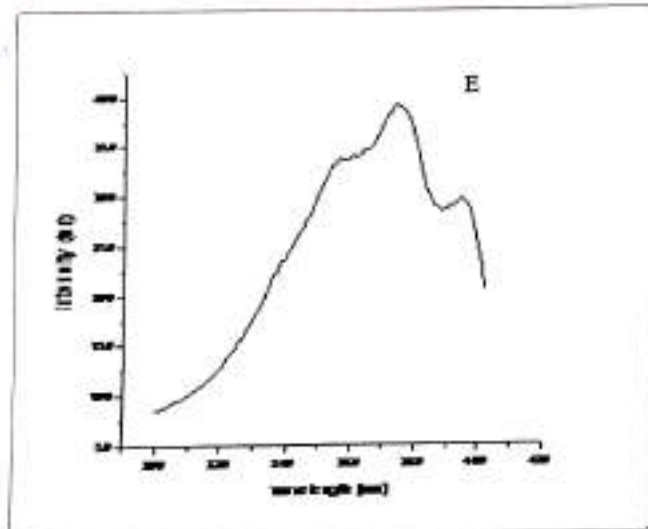
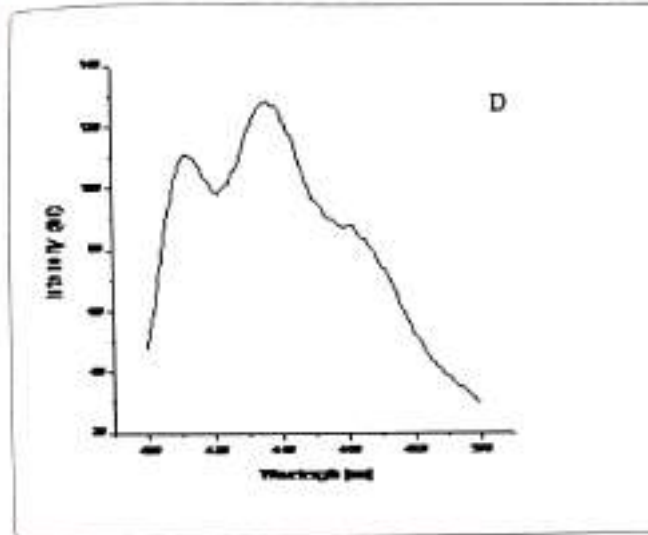


Figure-1 Fluorescence excitation and emission of CSA-PANI in different solvents

- A and B Excitation & Emission spectra of CSA-PANI in solvent DMF respectively.
- C and D Excitation & Emission spectra of CSA-PANI in solvent DMSO respectively.
- E and F Excitation & Emission spectra of CSA-PANI in solvent NMP respectively

## Results and Discussion

A variety of environmental factors affect fluorescence emission, including solvent polarity, inorganic and organic compounds, temperature, pH, and the localized concentration of the fluorescent species. The high degree of sensitivity in fluorescence is primarily due to interactions that occur in the local environment during the excited state lifetime. A fluorophore can be considered an entirely different molecule in the excited state (than in the ground state), and thus will display an alternate set of properties in regard to interactions with the environment. Polar solvent molecules surrounding fluorophore interact with the dipole moment of the fluorophore to yield an ordered distribution of solvent molecules around the fluorophore<sup>9</sup>.

The fluorescence emission CSA-PANI occurs in the range from 409 nm to 411 nm with maximum emission at 418 nm in DMSO [10]. The fluorescence emission spectra are shown in the figure 1. The emission peak of the compound exhibit a gradual shift from DMF to NMP.

From the table it is observed that as the polarity of the solvent increases, there is a spectral shift which increases with increase in the polarity of the solvent as shown in the figure-2. The emission peak wavelength of CSA-PANI in DMF is 409 nm but in DMSO it is 418 nm. This shift could be explained using solvent relaxation as shown in the figure-2.

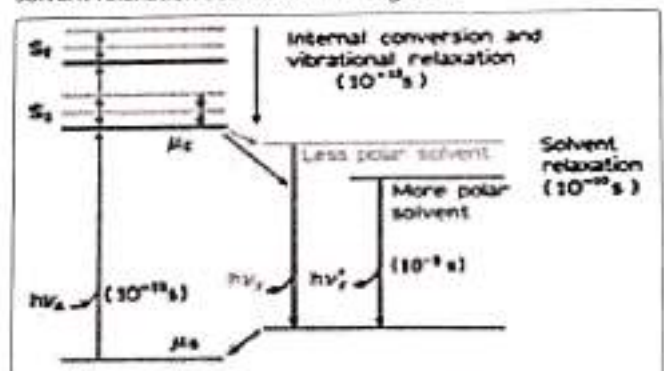


Figure-2 Schematics of solvent relaxation.

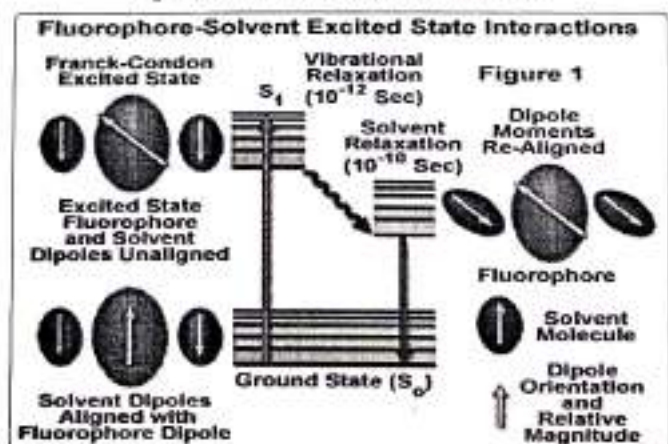


Figure-3 Fluorophore-solute excited state interactions<sup>10</sup>

### Fluorophore - Solvent Interactions

In a polymer solution, the fluorophore in the ground state is surrounded by polar solvent molecules having dipole moments that can interact with the dipole moment of the

fluorophore to yield an ordered distribution of solvent molecules around the fluorophore [11]. By the absorption of energy fluorophore is excited to higher energy level and there will be change in the dipole moment which ultimately induces a rearrangement or reorientation of surrounding solvent molecules around the fluorophore which lowers the energy of excited state of fluorophore. This is called solvent relaxation. Solvent molecules will reduce the energy gap between the ground state and excited state of the fluorophore which results in red shift or Bathochromic shift of the fluorescence emission. Increasing the solvent polarity produces a correspondingly larger reduction in the energy level of the excited state [12]. Fluorescent molecules have larger dipole moment in excited state than in the ground state. Therefore different solvents having different polarity may differently affect the energies of ground state and excited state for a molecule. In non-polar solvent like xylene the excited state of the fluorophore is not stabilized and the energy gap between the ground state and excited state of the molecule increases. Thus the emission peaks are shifted to shorter wavelength or blue shift is observed [13].

The Solubility of CSA-PANi is found to be dependent on the polarity of the solvent. The solubility is high in the highly polar solvents selected and decreases as the polarity of the solvent decreases.

## Conclusion

The fluorescence data of CSA-PANi reveal that the nature and amount of shifts depend on the polarity of the solvents. It is concluded from the data that as the polarity of the solvent increases, CSA-PANi shows a bathochromic shift for  $n-\pi$  and  $\pi-\pi^*$  transitions. Knowledge about the excited electronic state dipole moments of the solute molecules is quite useful in designing nonlinear materials and in elucidation of the nature of the excited state.

## Acknowledgements

The author Lakshmidevi V. acknowledges Government first grade college, Ramanagara, Karnataka, India for supporting throughout research work.

## References

1. Michael Jonas ad Silva, Alex Otávio Sanches, Luiz Francisco Malmonge, José Antonio Malmong. Electrical, mechanical and thermal analysis of natural rubber/Polyaniline-DBSA composite. *Mat.Res.* 2014;(17): 59-63.
2. Naader Alizadeh, Alireza Akbarinejad, Arash Ghoorchian. Photophysical Diversity of Water-Soluble Fluorescent Conjugated Polymers Induced by Surfactant Stabilizers for Rapid and Highly Selective Determination of 2,4,6-Trinitrotoluene Traces. *ACS Appl. Mater. Interfaces.* 2016,8(37):24901-24908. doi: 10.1021/acsami.6b08577
3. Swarnparani H, Basavaraja S, Basavaraja C, Venkataraman A. A new approach to soluble polyaniline and its copolymers with toluidenes. *Journal of Applied Polymer Science.* 2010; 117(3): 1350-1360. DOI 10.1002/app.31745
4. Jian G, Jianzhong Y, Yaguang C, Lunyu Q. Gas-Solid phase method to synthesize polyaniline doped with heteropoly acid. *Mater. Lett.* 2002; 57(3): 765-770. [http://dx.doi.org/10.1016/S0167-577X\(02\)00869-8](http://dx.doi.org/10.1016/S0167-577X(02)00869-8)
5. Cao Y, Smith P, Heeger AJ. Counter-ion induced processibility of conducting Polyaniline and of conducting polyblends of Polyaniline in bulk polymers. *Synth Met.* 1992; 48 (1): 91-97. [http://dx.doi.org/10.1016/0379-6779\(92\)90053-L](http://dx.doi.org/10.1016/0379-6779(92)90053-L)
6. H. Anton A, Dana O. D. Solvent Effects on the Electronic Absorption and Fluorescence Spectra. *Journal of Advanced Research in Physics* 2011;2(1): 1-9.
7. Chen S, Li X, Ma H. New approach for local structure analysis of the Tyrosine domain in proteins by using a site-specific and polarity-sensitive fluorescent probe. *Chembiochem.* 2009; 10 (7): 1200-1207. 10.1002/cbic.200900003
8. Ritesh N, Sethuraman S. Donor-acceptor substituted phenylethynyltriphenylene- excited state intramolecular charge transfer, solvatochromic absorption and fluorescence emission. *Beilstein J. Org. Chem.* 2010; 6: 992-1001. doi: 10.3762/bjoc.6.112
9. Richard S, Kenneth PG. Solvent effects on the fluorescence of coumaric acids. *Journal of photochemistry.* 1983; 22(4): 373-377 Olympus Microscopy Resource Centre, Florida University.
10. Yadigar GS, Isa S. Solvent effect on the absorption and fluorescence spectra of 7-acetoxy-6-(2,3-dibromopropyl)-4,8-dimethylcoumarin: Determination of ground and excited state dipole moment. *Spectrochimica Acta Part A: Molecular and Biomolecular Spectroscopy.* 2013;102: 286-296. <http://dx.doi.org/10.1016/j.saa.2012.10.018>
11. Hrdovic P, Donovalova J, Starkovicova H, Gaplovsky A. Influence of Polarity of Solvents on the Spectral Properties of Bichromophoric Coumarins. *Molecules* 2010; 15(12): 8915-8932. doi: 10.3390/molecules15128915.
12. Haidekker MA, Brady TP, Lichlyter D, Theodorakis EA. Effects of solvent polarity and solvent viscosity on the fluorescent properties of molecular rotors and related probes. *Bioorg Chem.* 2005; 33(6):415-25. doi: 10.1016/j.bioorg.2005.07.005



## नवजागरण के विकास काल में दलित कवियों का योगदान

❖ डॉ. प्रेमचन्द चव्हाण

सहायक प्राध्यापक, हिन्दी विभाग

एम. एम. डगनी महाविद्यालय, गुलबर्गा

स्वतंत्रता के बाद राष्ट्र की विशेष उपलब्धी यही रही है कि पिछड़ी जाति के दलित जन समूह बदलते हुए परिवेश के वैचारिक धरातल पर सचेत हो गए हैं। शोषित यह जन समूह शिक्षित एवं आत्मनिर्भर होकर अपना हक अपना स्थान-मान पहचानने लगे हैं।

इसलिए मैं ने "नवजागरण के विकास काल में दलित कवियों का योगदान" इस बहुमूल्य आलेख को प्रस्तुत करने का प्रयास किया है।

**दलित काव्य की पृष्ठभूमि :**

दलितों का शोषण एवं उत्पीड़न सदियों पुराना है ठीक उसी प्रकार दलितोत्थान के प्रयास भी सदियों पूर्व प्रारंभ हो गये थे। उसकी प्रमुख झाकियाँ इस प्रकार हैं। दलित के लिए वेदों में प्रयुक्त शब्द 'शूद्र' की उत्पत्ति के बारे में (ऋग्वेद के सर्ग 10-10-12) में लिखा है -

"ब्रह्मणोऽस्य मुखमसीद् बाहू रजस्यः कृतः

उरु तदस्य यद् वैश्यः पदभ्यां शूद्रो जायत"

अर्थात्-ब्राह्मण मुख से, क्षत्रिय बाहु से, वैश्य जंघा से, और शूद्र पैर से उत्पन्न हुये हैं। वेदों में आर्यों-अनार्यों के संघर्ष के उदाहरण -

1. दै इन्द्र ! तुमने शम्बर नामक दस्यु के 100 पुरों को ध्वस्त किया। (ऋग्वेद-6-20,10)
2. दै इन्द्र ! तुमने शगदासुर को सात परिवारों को बला से चूर्ण कर दिया। (ऋग्वेद-3, 12,6)

**वेदों / ब्राह्मणों/उपनिषदों/पुराणों/ मनस्मृति में लगाये गये प्रतिबंध :**

1. ऋग्वेद के अनुसार शूद्र सबसे नीचे की श्रेणी में आता है। (10, 12, 10)
2. यज्ञ करने समय शूद्र से बान नहीं करनी चाहिए न शूद्र की उपस्थिति में यज्ञ करना चाहिए। (शुद्धाचार ब्राह्मण 3, 19,10)

S. G. Gounbali

IOAC Coordinator  
Smt. Veeramma Gangasiri  
College for Women  
Kalaburagi - 585 102

PRINCIPAL  
Smt. Veeramma Gangasiri  
College for Women  
Kalaburagi - 585 102



3. जो अच्छे काम करते हैं वे ब्राह्मण क्षत्रिय, वैश्य इन अच्छी जातियों को प्राप्त करते हैं और जो अशुभ काम करते हैं वे कुत्ते, सुअर या शूद्र जाति को प्राप्त करते हैं। (छन्दोग्य उपनिषद -5, 10, 7)  
सामान्य में हम देखते हैं
4. शम्भूक ऋषि के शूद्र होने पर भी तपस्या करने पर राजा रामचंद्र द्वारा उसका वध। महाभारत में हम पाते हैं
5. शिक्षा न देने पर भी गुरु दक्षिणा के रूप में गुरु द्रोणाचार्य द्वारा एकलव्यका दायाँ अंगूठा कटवा लेना।

सिद्ध, नाथ और संतों आदि योगियों द्वारा भेद भाव का निवारण :

1. सिद्ध सरहपाद दोहाकोश (1-3,141) में लिखते हैं -  
“ब्राह्मण न जानते भेद। यों ही पढ़े ये चारों वेद  
म टी, पानी, कुश लई पठंत। घर ही बैठी अग्नि होमंत  
एक दण्डी त्रिदण्डी भागवा भेसे। ज्ञानी होके हँस उपदेसे  
मिथ्ये ही जग वह भूले धर्म-अधर्म न जनत तूलथे।”
2. गोरखनाथ - मंदिर मसजिद विग्रह के संबंध में कहते हैं  
“हिन्दू ग्यावे देहरा मुसलमान मसीत  
जोगी घ्यावै परम पद जहाँ देहरा न मसीत।”

3. संत कबीर का कथन है -

“एक-एक ज्योति थे उतपना, कौन ब्राह्मण कौन सूदा  
माटी एक वेष धरि नाना सब में ब्रह्म समाना।”

“जल में कुम्भ कुम्भ में जल है बाहरि-भीतरीपानी  
फूटा कुम्भ जल जलहि समाना यह तत कथै गियानी।”

4. गुरुनानक का कथन है

“एक बूंद एक मल मूतर एक चाम अरु गूदा  
एक ज्योति से सब ही जनमै को ब्राह्मन को सूदा  
नीचा अन्दरि नीच जाति नीची हूँ अति नीच  
नानक जिनके संग साथ बडिया सीधु किया रीस।”

साठोत्तरी काल और दलित काव्य :

साठोत्तर काल में अनेक कवियों और कवयित्रियों ने व्यवस्था के शोषण का शिकार दलितों को संघर्ष के लिए ललकारते हुए, दलित व शोषितों को सचेत करते हुए, शोषितों में

जागृत होती चेतना को लेकर तथा नवजागरण को लेकर अपने बहुमूल्य विचारों को प्रकट किये हैं। वह इस प्रकार है।

5. जगदीश गुप्त-शम्बूक :

दलितोत्थान से संबंधित पुराणों की कथाओं के आधार पर रचित काव्य शम्बूक में जगदीश गुप्तजी ने इस प्रकार कहा है -

"जो व्यवस्था  
 व्यक्ति के सतर्कम को भी मान ले अप्राथ  
 जो व्यवस्था फूल को खिलने न दे निर्बाध  
 जो व्यवस्था वर्ग सीमित स्वार्थ से हो ग्रस्थ  
 वह विषम घातक व्यवस्था, शीघ्र हीहो अस्त ।"

6. जनपद कवि नागार्जुन - कर दो वमन नामक कविता में समाज का नग्न और बीभत्स चित्रण करते हुए कहते हैं -

"प्रभु तुम कर दो वमन ! होगा मेरी क्षुधा का शमन  
 स्वीकृत हो करुणामय  
 अजीर्ण अन्न भोजी अपंगों का नमन ।"

7. केदारनाथसिंह - दलितों को संघर्ष के लिए ललकारते हुए तथा नव जागरण के लिए प्रेरणा देते हुए संबोधन करते हैं -

"उठो मेरे सोये हुए धागों उठो  
 उठो झाड़न में मोजों में टाट में दुमियों में दबे हुए धागे उठो  
 उठो कहीं छ गलत हो गया है  
 उठो की इस दुनियाका सारा कपडा  
 फिर से बुनना होगा उठो मेरे टूटे हुए धागों उठो  
 उठो की बुनने का समय हो रहा है ।"

8. सर्वेश्वर दयाल सक्सेना :

क्रांतिकारी चेतना की अभिव्यक्ति करते हुए इस प्रकार कहते हैं -

"तुम्हारे पास रोशनी तो होगी ? मैं पूछता हूँ  
 कड़कति विजली है दिलों में, बस  
 अन्धेरा खुद रोशनी को जनम देता है,  
 अन्धेरे में निकल पडो  
 तो अन्धेरा-अन्धेरा नहीं रह जाता है ।"

9. धूमिल :

छोटे वडों में समानता लाने के लिए धूमिल कहते हैं



“रौंपी से उठी हुयी आँखों ने मुझे क्षण भर टटोला  
 और जैसे पतियाये हुए स्वर में वह हँसते हुए बोला  
 बाबुजी ! सच कहूँ मेरी निगाह में न कोई छोटा है  
 न बडा है मेरे लिए, हर आदमी एक जोड़ीजूता है  
 जो मेरे सामने परम्मत के लिए खडा है ।”

10. लीलाधर जगूडी

लीलाधर जगूडी ‘उदासी के खिलाफ’ कविता में दलित व शोषित वर्गों को सचेत करते हुए इस प्रकार कहा है -

“उदास लोगों ! उठो और नामंजूर करो  
 उठो और विरोध करो उठो और चोट करो  
 उदास लोगों ! उठो और फैसला दो  
 उठो और जिसने कल तुम्हें कुचला था  
 उसे घोंडे की नाल बना लो ।”

11. हरिवंशराय बच्चन अरे देश के भूखों जागो

नामक कविता में असहायक गरीब भूखों को जागृत करते हुए कहा है -

“मुझसे सून लो  
 नहीं स्वर्ग से अन्न गिरेगा  
 नहीं गिरेकी नभ से रोटी  
 ..... उठा भाग अपना मांगो  
 अरे देशके भूखों जागो ।

12. रामविलास शर्मा - कार्यक्षेत्र धूल से भरा किसान एवं गरीब इन्सान की दयनीय स्थितियों को देखकर ‘कार्यक्षेत्र’ नामक कविता में कवि लिखते हैं -

“धरती के पुत्र की होगी कौन जाति  
 कौन मत, कहो कौन धर्म  
 धूलि भरा धरती का पुत्र है  
 जोतताहै, बोता है, किस न किस धरतीको  
 मिट्टी को पुतलाहै, विचित्र विश्व की  
 रूढ़ियों को नियमों की, अस्पष्ट विचारों की  
 चिन्हित है प्रेत रूप छाया, मटीले मुँह पर ।”



दलित काव्य को महिला कवयत्रियों का योगदान :

13. सुभद्रा कुमारी चौहान- प्रभु तुम मेरे मन को जानो नामक कविता में कवयित्री छूआ-छूत का निवारण को लेकर ईश्वर से प्रार्थना करती है -

“मैं अछूत हूँ मन्थिर में आने का मुझको अधिकार नहीं है  
किन्तु देवता यह न समझनातुमपर मेरा प्यार नहीं है  
प्यार असीम अमिट है फिर भीपास तुम्हारे आ न सकूंगी  
इसलिए इस अन्धकार में मैं छिपती-छिपति आयी हूँ  
तुम देखो पहचान सको तो मेरे मन को पहचानो  
जग न भले ही समझो मेरे , प्रभु तुम मेरा पहचानो ।”

14. धनदेवी-पुकार नामक कविता में दलितोंपर हो रहे शोषण एवं-अत्याचार का यथार्थ का परिचय कराती हुए उन्हें जागृत होने की प्रेरणा देती हुई लिखती है -

“आये दिन होत रहते हैं, दलितों पर जुल्मों के वार  
अन्त कहें होगा इन सबका, बढ़ता जाये अत्याचार  
कब तक खून बहेगा अपना ? हत्या होगी कितनी बार?  
कितने होंगे बलात्कार !  
कदम उठाओ, मत घबराओ, नहीं सहेंगे दुर्व्यवहार  
जुल्म सितम का करो सामना, लेकर रहेंगे स्वाधिकार  
नहीं बचे अन्याय भूमिपर, करें ऐसा चमत्कार  
रहे चमकता कीर्ती सूर्य, जागो दलितों सुन पुकार ।”

15. अबला-सबला : अबल-सबला नारी शोषण के प्रति कवयित्री ने कहा है  
“एक तथ्य-मजदूरीन हो/या दफतरन की बवुआइन  
पुरुष से अधिक ही पिसती है नारी  
सबला बेचारी ।”

एकप्रश्न :

“कल की अबला ने / आज की सबला को  
किस तरकीब से झोंका / दहेज की आग में ?  
आश्चर्य है -  
किस बहु ने / किसी सास को जलाया  
यह समाचार/किसी अखबार में  
क्यों नहीं आया !



Impact Factor: 3.1703

ISSN: 2319-1027 Vol. V Issue I Aug. 2016 - Jan. 2017

संदर्भ सूची :

1. ऋग्वेद सर्ग-6,19,1220.
2. शतपथ ब्राह्मण-3,10,19.
3. हिन्दीकी श्रेष्ठ आधुनिक कविताएँ .

S.G. Goumbali

**IQAC Coordinator**  
Smt. Veeramma Gangasiri  
College for Women  
Kalaburagi - 585 102

M. Suresh

**PRINCIPAL**  
Smt. Veeramma Gangasiri  
College for Women  
Kalaburagi - 585 102



# Radioactivity measurements of Soil samples from Devadurga and Lingasugur of Raichur District of Karnataka, India

S. Rajesh<sup>1</sup>, B. R. Kerur<sup>1\*</sup> and S. Anilkumar<sup>2</sup>

<sup>1</sup>Department of Physics, Gulbarga University, Gulbarga, Karnataka-585 106, INDIA

<sup>2</sup>Radiation Safety Systems Division, BARC, Mumbai-400 085, INDIA

(Corresponding Author: Email: [kerurbek@yahoo.com](mailto:kerurbek@yahoo.com))

**Abstract.** Naturally occurring radioactivity measurement, radiation monitoring of the region, dose assessment and interpretation of radiological related parameters are crucial aspects from the public awareness and environmental safety point of view. The ionizing radiations ( $\gamma$ -rays) emitted from radionuclides such as  $^{226}\text{Ra}$ ,  $^{232}\text{Th}$  and  $^{40}\text{K}$  present in environmental materials contributes significantly to the radiation dose received by the public. Gamma spectrometry based high efficiency 4"X4" NaI(Tl) detector was employed for estimating activity concentrations of the gamma emitting radionuclides. The spectra from the detector were recorded using a PC based 1k multichannel analyzer system (WinTMCA 32). Each sample spectra was acquired for a counting period of 60,000 sec (16.67 h). Assuming the daughter products of  $^{226}\text{Ra}$  and  $^{232}\text{Th}$  in equilibrium, the activity concentration of these radionuclides were estimated by using the prominent gamma photo peaks of daughter products. Using these activity dose related radiological parameters were calculated for all the samples. The activity concentrations of the radionuclides and the dose related parameters for the samples were found to be comparable with the global literature values. The data generated from our study will contribute to the base line radiological data of the region.

**Index Terms:** Absorbed dose, Activity, Natural radioactivity, Radionuclides and Scintillation detector.

## I Introduction

Radiations are present everywhere and human beings have always been continuously exposed to radiations knowingly or unknowingly, nature itself being one of the important sources of radiations. The studies have shown that the important source of radiations are the naturally occurring radionuclides such as  $^{232}\text{U}$ ,  $^{235}\text{U}$ ,  $^{238}\text{U}$  decay series and singly occurring  $^{87}\text{Rb}$ ,  $^{40}\text{K}$  etc [1, 2]. Gamma radiations emitted from naturally occurring radioisotopes, such as  $^{40}\text{K}$  and  $^{238}\text{U}$ ,  $^{232}\text{Th}$  and their decay products that are present in environmental materials such as soil, rock, water, granite, building materials etc., constitute the terrestrial background radiation and are a significant source of collective dose for the human beings [3]. The contribution of other nuclides to the total activity is negligible. Once present in the environment, these radionuclides, whether natural or artificial, are available for uptake by plants and animals and so make their way into the food chain [4]. The contribution of radiation from sediment to human exposure can either be whole body due to external radiation originating directly from primordial radionuclides present in sediment or internal due to inhalation [5]. Soil is an important environmental material which is used for many purposes such as building raw materials and products, for land filling in playgrounds, for streets etc. contains natural radionuclides contributing to the indoor and outdoor exposure. Therefore, measurement of

radionuclides in soil samples of the study area is necessary as the data produced in this paper may be used as baseline data for future environmental assessments. The present study estimates the external gamma dose rate, which creates a public awareness about the radiation and provides the necessary information about the radiological protection.

## II Study Area

The study has been carried out over two talukas of the Raichur district namely Devadurga and Lingasugur, covering an approximate area of 2500 square kilometers between 16.02 and 16.50 north latitude and 76.55 and 76.92 east longitude. The study area has been divided into four sampling stations for administrative convenience. Devadurga and Lingasugur forms part of Krishna catchment in northern part, while southern part forms the Lower Tungabhadra catchment area and is perennial in nature. Geomorphologically, continuous range of hills are absent in the district but a few cluster of hills are seen towards east, west, northwest, centre and southwest. Study area can be broadly classified into three major zones viz, (a) The northern rugged plateau, (b) The southern lower plains with inselbergs and isolated hillocks and (c) Valley fills [6]. The northern part of the district is characterized by expanses of level and treeless surface punctuated and there by flat and undulating hillocks, black soils and basaltic rocks are observable. The average elevation of the study area is 430 m above mean sea level. The change in the environmental radioactivity level contributes to the collective radiation dose to the general population. Therefore, an accurate assessment of possible radiological risks to human health of this region is essential. Hence, the measurement of the activity concentration levels of naturally occurring radionuclides in soils, building materials etc. and their assessment has been carried out and presented in the present paper.

## III Materials and methods

### Sample collection and preparation

Forty samples were collected from nine sampling stations of the study region. The ASTM standard procedure was followed for soil sample collection and preparation where surface soil over an area 50 cm \* 50 cm and 5 cm depth was mixed thoroughly and about 2-3 kg of each sample was collected. The geographic coordinates and elevation was recorded with a Garmin portable hand held GPS. After collection of sample pebbles, dried leaves, roots and other mixed materials were removed. The samples were placed in a hot air oven for drying

S. G. Gowballi  
IQAC Co-ordinator  
Smt. V.G. Women's Degree College  
KALABURAGI

PRINCIPAL  
Smt. V.G. Degree College for Women  
GULBARGA



at 110°C for 24 h to ensure that the moisture is completely removed. All samples were pulverized to get fine powder and unevenly sieved through a 200-mesh sieve to separate the crushed soil particles. Each pulverized sieved sample was then transferred to a 250 mL cylindrical Plastic (PVC) box. The boxes were filled fully, sealed with an adhesive, coded, weighed and then stored for a period of four to five weeks to attain secular equilibrium of radon ( $^{222}\text{Rn}$ ) and its daughter products before subjecting to gamma spectrometric analysis.

#### Gamma Spectrometric Analysis

Measurements of gamma activity were performed with a 4"X4" NaI (Tl) scintillation detector based gamma ray spectrometer. The detector is enclosed in a 3" thick lead shield to reduce background radiations originating from the surrounding and cosmic rays. The gamma ray spectrum was recorded using 1k PC based multichannel analyzer (winTMCA 32) with a built in spectroscopy amplifier. Efficiency calibration for the system was carried out using the standards (uranium, thorium and potassium) procured from International Atomic Energy Agency (IAEA). These standard materials were packed and sealed in a 250 mL cylindrical container, the same geometry as that for samples. The analysis of complex gamma spectra of samples from the detector due to  $^{238}\text{U}$ ,  $^{232}\text{Th}$  and  $^{40}\text{K}$  was carried out by least squares method. The determination of radionuclide activity in the soil sample was based on the, 1764 keV, 2614 keV and 1460 keV gamma photo peaks emitted from  $^{214}\text{Bi}$ ,  $^{208}\text{Tl}$  and  $^{40}\text{K}$ , respectively. The samples are counted for a period of 60,000 s to obtain gamma spectra of good statistics. Background gamma spectrum also was recorded and subtracted to get the net count rate for each sample. The activity concentrations of the sample were calculated from the peak intensity (cps) of each gamma line and the efficiency of the detector using the relation

$$\text{Activity (Bq)} = \frac{\text{Net Area under the photopeak (cps)}}{\text{Efficiency (\%)}}$$

#### IV Results and discussion

##### Activity concentration

The estimated activity concentrations of the three primordial radionuclides  $^{238}\text{U}$ ,  $^{232}\text{Th}$ , and  $^{40}\text{K}$  obtained for each of the samples collected from the study region are summarized in table 1. The activity of  $^{238}\text{U}$ ,  $^{232}\text{Th}$  and  $^{40}\text{K}$  for all the samples was found to lie in the range from 10- 85 Bq/kg, 18-285 Bq/kg and 135-1646 Bq/kg respectively. In almost all the soil samples the thorium concentration was observed to be higher compared to that of  $^{238}\text{U}$ . This is because radium is more susceptible to solubility, whereas thorium is less soluble hence adsorbed to soil [7]. Some soil samples showed a high activity of  $^{40}\text{K}$ . It may be due to the fact that the samples were collected from areas near the cultivated lands. The potassium activity for the soil samples was also comparable with the world median values. The estimated values of mean activities of  $^{238}\text{U}$ ,  $^{232}\text{Th}$  and  $^{40}\text{K}$  in soil were found to be comparable within the range of worldwide values [8]. A comparison of the values obtained in the present work with other literature data are shown in table 2 and shows the activity concentration of

the primordial radionuclides for the soil samples from Devadurga and Lingasugur are well within the national and world average values as presented in the UNSCEAR. In accordance with it some soil samples of the study area showed low activity and some high and moderate activity. To represent the activity levels of  $^{238}\text{U}$ ,  $^{232}\text{Th}$  and  $^{40}\text{K}$  by a single quantity, a common radiological index called radium equivalent activity has been introduced and calculated by the relation [9]

$$Ra_{eq} = C_{Ra} + AC_{Th} + BC_K$$

Where  $C_{Ra}$ ,  $C_{Th}$  and  $C_K$  are the activity concentrations of  $^{238}\text{U}$ ,  $^{232}\text{Th}$  and  $^{40}\text{K}$  in Bqkg<sup>-1</sup> respectively and A, B are constants 1.43, 0.077 respectively. It is observed from the present study that the radium equivalent activity for the soils of study region is well below the recommended limit of 370 Bq/kg. The value of  $Ra_{eq}$  greater than 370 Bq/kg shows a higher gamma dose rate

##### Absorbed gamma dose rate assessment

The absorbed gamma dose rates due to the primordial radionuclide concentrations were calculated for all the samples. The absorbed gamma dose rates due to terrestrial gamma rays at 1 m above the earth's surface were calculated from the concentrations of  $^{238}\text{U}$ ,  $^{232}\text{Th}$  and  $^{40}\text{K}$  and the conversion factors of 0.604, 0.462 and 0.0417 respectively were used as given by [UNSCEAR]

$$D = (0.604C_{Th} + 0.462C_{Ra} + 0.0417C_K) \mu\text{Gy h}^{-1}$$

where  $C_{Th}$ ,  $C_{Ra}$  and  $C_K$  are the average activity concentration of  $^{232}\text{Th}$ ,  $^{238}\text{U}$  and  $^{40}\text{K}$  respectively. The estimated absorbed gamma dose rates for all the samples are shown in table 1. The annual effective dose can be estimated using the conversion factor of 0.7 SvGy<sup>-1</sup> to absorbed dose rate as given by UNSCEAR.

$$AED = D \times 8760 \times 0.7$$

The calculated results are presented in table 1. The mean absorbed gamma dose rate was found to lie in the range 27-279 nGy h<sup>-1</sup>. The annual effective dose associated for all the samples was estimated. These values are within the permissible dose equivalent limit of 1 mSv y<sup>-1</sup> for the general public [10].

#### V Conclusions

Main sources of external radiation exposure are Uranium and Thorium, their decay products and  $^{40}\text{K}$ . The internal exposure is due to radon and its radioactive daughters, present in the environment, which has the maximum contribution towards the average effective dose received by human beings. Devadurga and Lingasugur sampling station shows the higher activity among the sampling station. If the annual gamma dose rate from soil samples is less than 1 mSv and  $Ra_{eq}$  is less than 370 Bq/kg, Relative contributions to the  $Ra_{eq}$  rate owing to  $^{238}\text{U}$ ,  $^{232}\text{Th}$  and  $^{40}\text{K}$  for the samples is shown in fig 1. Then the external hazard index ( $H_{ex}$ ) is always less than one. For insignificant radiation hazard the indices should be less than unity. The internal exposure to radon ( $^{222}\text{Rn}$ ), an inert gas enters through inhalation and affects the respiratory system. The present study is well in accordance with the condition of



unity and pose that the soil of the study area is safe to be used for construction purposes. Further measurements over more environmental samples of this region are being continued. And the present study showed a wide distribution of  $^{238}\text{U}$ ,  $^{232}\text{Th}$  and  $^{40}\text{K}$  activity concentration among the samples. The concentration of  $^{238}\text{U}$ ,  $^{232}\text{Th}$  and  $^{40}\text{K}$  in the soil samples were found to be little higher values in comparison to other places of India and world literature values. Similarly, the health hazard indices for all the samples were within the limits. The present study reveals that the radiological parameters estimated were due to activity of natural radionuclides and

well comparable with the national and international values. The data produced in the present work can be used as baseline radiological data for future investigations and programs.

#### Acknowledgements

The authors express their deep sense of gratitude to Board of Research in Nuclear Sciences (BRNS) for providing the financial support to carry out this work. The authors are also thankful to Dr. D N Sharma, Ex Director, HS&E Group and Dr. Pradeepkumar, Head, RSSD, BARC, Mumbai for the continuous guidance and encouragement for the work.

#### References

1. Ramola R.C., Gustin G.S., Manjari Badoni, Yogesh Prasad, Ganesh Prasad and Ramachandran T.V.,  $^{238}\text{Ra}$ ,  $^{232}\text{Th}$ ,  $^{40}\text{K}$  contents in soil samples from Garhwal Himalaya, India, and its radiological implications, *J. Radiol. Prot.*, 28, 379-385, 2008.
2. Has an M. Khan, Ismail M., Khalid Khan and Perveen Akhter, Measurement of Radionuclides and Gamma-Ray Dose Rate in Soil and Transfer of Radionuclides from Soil to Vegetation, Vegetable of Some Northern Area of Pakistan Using  $\gamma$ -Ray Spectrometry, *Water Air Soil Pollut.*, DOI: 10.1007/s11270-010-0693-5, 2010.
3. El-Arabi A.M.,  $^{238}\text{Ra}$ ,  $^{232}\text{Th}$  and  $^{40}\text{K}$  concentrations in igneous rocks from eastern desert, Egypt and its radiological implications *Radiat. Meas.*, 42, 94-100, 2007.
4. K. A. Kabir, S. M. Islam and M. Rahman, "Distribution of Radionuclides in Surface Soil and Bottom Sediment in the District of Jessore, Bangladesh and Evaluation of Radiation Hazard," *Journal of Bangladesh Academy of Sciences*, Vol. 33, No. 1, 2009, pp. 117-130.
5. Jibiri and Okeyode, N.N. Jibiri, I.C. Okeyode Evaluation of radiological hazards in the sediments of Ogun river, South-Western Nigeria, *Radiation Physics and Chemistry*, 81 (2012), pp. 1829-1835.
6. Radhakrishna B.P., Vaidyanathan R., *Geology of Karnataka* 2<sup>nd</sup> edn. Geological society of India, Bangalore, 123-126, 1997.
7. Tsai Tsey-Lin, Lin Chun-Chih, Wang Tzu-Wen and Tseh-Chi Chu, Radioactivity concentrations and dose assessment for soil samples around nuclear power plant IV in Taiwan. *J. Radiol. Prot.* 28, 347-360, 2008.
8. UNSCEAR, United Nations Scientific Committee of the Effect of Atomic Radiation Sources and effects of ionizing radiations United Nations, New York, 2000.
9. Beretka J, Mathew P J (1985) *Health Phys* 48(1):87-95, DOI 10.1097/00004032-198501000-00007.
10. ICRP, Recommendations of the international commission on radiological protection. In: *Annals of the ICRP*. ICRP Publication 60, Pergamon press, Oxford, 1990.
11. S. Rajesh, Avinash P R, B. R. Kerur and S. S. Anilkumar. Assessment of Natural radioactivity levels in soil samples of Bidar district by Gamma Spectrometry. ISBN 978-81-929777-0-6
12. Shiva Prasad NG, Nagaiah N, Ashok GV, Karanukara N. Concentrations of Ra-226, Th-232 and K-40 in the soils of Bangalore Environment, South India, *Health Physics*, 94(3):264-271, *Health Phys* 94(3):264-27, 2008.
13. Selvasekarapandian S., Sivakumar R., Munikandan N.M., Meenakshisundaram V., Raghunath V.M. and Gajendran V. Natural radionuclide distribution in soils of Gudalora, India. *Appl. Radiat. Isot.* 52, 299-306, 2000.
14. Kamath R.R., Menon M.R., Shukla V.K., Sadasivan S. and Nambi K.S.V., Natural and fallout radioactivity measurement of Indian soils by gamma spectrometric technique. Proceedings of the fifth national symposium on environment Saha institute of nuclear physics Calcutta, India, 56-60, 1996.
15. Oladele Samuel Ajayi, Measurement of activity concentrations of  $^{40}\text{K}$ ,  $^{238}\text{Ra}$ , and  $^{232}\text{Th}$  for assessment of radiation hazards from soils of the south western region of Nigeria. *Radiat. Environ. Biophys.* 48, 323-332, 2009.

S.G. Gounhalis

IQAC Co-ordinator  
Smt. V.G. Women's Degree College  
KALABURAGI

PRINCIPAL  
Smt. V.G. Degree College for Women  
GUI BARGA



Table 1: Activity concentrations of  $^{238}\text{U}$ ,  $^{232}\text{Th}$  and  $^{40}\text{K}$ , and dose rate

SL No	Sampling Station	Activity (Bq kg <sup>-1</sup> )			Absorbed Dose (nGyh <sup>-1</sup> )	Range AED Outdoor (mSvy <sup>-1</sup> )	
		$^{238}\text{U}$	$^{232}\text{Th}$	$^{40}\text{K}$		Estimated	Measured
1	Devadurga (10)	14 - 85	22-285	256-1646	63 -279	0.078 - 0.343	0.069-0.315
2	Kavital (10)	14 - 52	30 - 72	190-1550	35-132	0.044 - 0.162	0.052-0.154
3	Lingasnugur (10)	10 - 33	18 - 47	241 - 799	34 - 55	0.042 - 0.068	0.052-0.069
4	Mudgal (10)	13 - 58	25-138	135-1118	27-138	0.034 - 0.170	0.035-0.154

Table 2. Comparison of radionuclides concentrations (Bq/ kg) for soil samples of present study with other literature data

Location (Soil samples)	Activity (Bq/kg)		
	$^{238}\text{U}$	$^{232}\text{Th}$	$^{40}\text{K}$
Present Study	30.9	60.6	551.5
Bidar [11]	32.45	37.21	251.61
Bangalore[12]	26.2	53.1	635.1
Gudalore, Tamilnadu [13]	17-62	19-272	78-596
All India [14]	31	63	394
Southwestern Region(Nigeria)[15]	54.5	91.1	286.5
China [8]	2 - 690	1 - 360	9 - 1800
USA [8]	4-140	4 - 130	100-700
World Average [8]	35	45	420

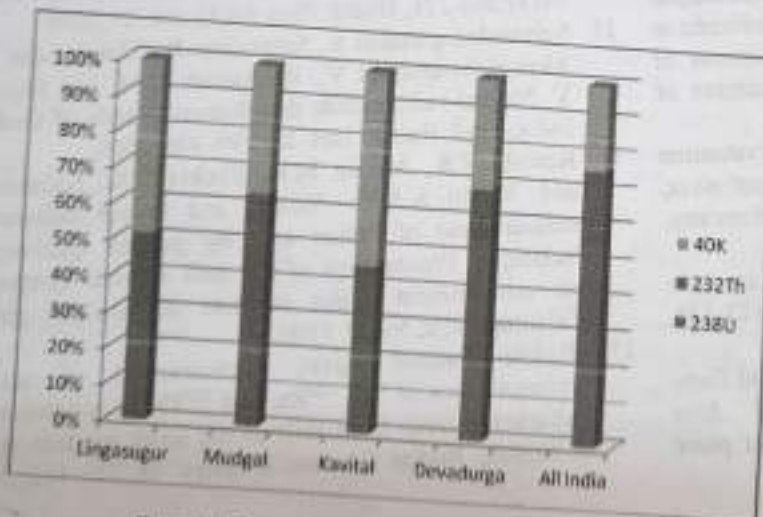


Figure 1 Comparison of Relative contributions to the  $R_{ext}$  rate owing to  $^{238}\text{U}$ ,  $^{232}\text{Th}$  and  $^{40}\text{K}$  for the all the sampling stations and Indian value.



## Determination of Mass Attenuation Coefficients, Effective atomic number and Electron Density of Lumefantrine in the Energy Range 1 keV – 100 GeV

Ingalagondi. P. K<sup>1</sup>, Omnath Patil<sup>1</sup>, G. B. Mathapati<sup>1</sup>, Shivraj G. G<sup>2</sup>,  
T. Sankarappa<sup>1</sup> and S. M. Hanagodimath<sup>1</sup>

<sup>1</sup>Department of Physics, Gulbarga University, Kalaburagi – 585 106

<sup>2</sup>Department of Physics, VG Women's College, Kalaburagi – 585 102

Email: [prabhu762udag@gmail.com](mailto:prabhu762udag@gmail.com)

### Abstract

The effective atomic number and electron density of Lumefantrine(LU) have been calculated for total and partial photon interactions by the direct method in the wide energy range of 1 keV – 100 GeV using WinXCOM. The values of these parameters have been found to change with energy. The variations of effective atomic number and electron density with energy are calculated and shown graphically.

**Keywords:** LU; Mass attenuation coefficients; Effective atomic number; Electron density.

### 1. Introduction

Mass Attenuation Coefficients ( $\mu/p$ ), Effective atomic number ( $Z_{eff}$ ) and Electron Density ( $N_e$ ) are important parameters in determining the interactions of X-rays and gamma photons in matter (Manohara & Hanagodimath, 2007). By the large applications and extensive use of gamma-active isotopes in medicine, industry and agriculture, the study of absorption of gamma rays with biological materials is essential in radiation medicine and in the medical field. Mass attenuation coefficient is a measure of how strongly a substance absorbs or scatters radiation at a given wavelength per unit mass per unit area. The knowledge of mass attenuation coefficients of X-rays and gamma photons in biological and other important materials is of significant interest for industrial, biological, agricultural and medical applications (Jackson & Hawkes, 1981). In composite materials, the energy delivered through the photon interactions, a single number cannot represent the atomic number uniquely across the entire energy range, as in case of pure elements. This number for composite materials is known as "effective atomic number" ( $Z_{eff}$ ) and it varies with energy as pointed out by G. J. Hyne (Hyne, 1952). On the other hand, the concept of z-dependence of photon attenuation coefficient has been utilized in many applications of radiation studies. And it is very important to evaluate the amount of radiation especially in medical Physics (Shivalinge Gowda et al. 2004).

In this study we used the computational technique developed by the Manohara S. R. (Manohara et al. 2008 "a") using the interpolation program WinXCom (Gerward et al. 2001) and its underlying cross-section database for calculating the  $Z_{eff}$  of biomolecules. This prompted us to undertake a rigorous and exhaustive investigation of  $Z_{eff}$  and  $N_e$  over an extended energy range 1 keV – 100 GeV. The energy absorption in a given medium can be calculated if certain constants are known, these necessary constants are  $Z_{eff}$  and  $N_e$  of the medium. The importance of this paper from diagnostic or therapeutic point of view is that while calculating the  $Z_{eff}$  of the compound, especially when the photon energy is close to the binding energy of the electron present in the compound, it gives correct information about corrections to be added while calculating the dose to the patient. In such cases the experimental determined  $Z_{eff}$  may not be agreeable with the theoretical values. In this paper we reported the results on  $Z_{eff}$  and  $N_e$  for LU in the extended energy range from 1 keV – 100 GeV.

### 2. Computational method and theoretical basis

UGC JOURNAL NO. 45204;

[https://www.ugc.ac.in/journalist/ugc\\_admin\\_journal\\_report.aspx?oid=NDUyMDQ=](https://www.ugc.ac.in/journalist/ugc_admin_journal_report.aspx?oid=NDUyMDQ=)

IMPACT FACTOR: 4.977

Page | 42

S. G. Gounbali  
IQAC Co-ordinator  
Smt. V.G. Women's Degree College  
KALABURAGI

PRINCIPAL  
Smt. V.G. Degree College for Women  
KALABURAGI





## 2.1. Calculation of effective atomic number and electron density.

The total cross-section ( $\sigma$ ) per atom in turn can be related as the sum of partial cross sections,

$$\sigma = \sigma_{pe} + \sigma_{phr} + \sigma_{coh} + \sigma_{incoh} + \sigma_{nlp} + \sigma_{phn} \quad (1)$$

Where  $\sigma_{pe}$  (or  $\tau$ ),  $\sigma_{incoh}$  and  $\sigma_{coh}$  are the photoelectric cross section, incoherent (Compton) and coherent (Rayleigh) cross sections respectively.  $\sigma_{nlp}$  (or  $k_e$ ) and  $\sigma_{phn}$  (or  $k_p$ ) are the cross sections for electron-positron pair production (creation) in the field of nucleus and in the field of atomic electrons ('triplet production'), respectively.  $\sigma_{phn}$  is the photo nuclear cross section.

$$\sigma_m = \sum_i n_i \sigma_i \quad (2)$$

where,  $\sigma_i$  and  $n_i$  are the number of atoms and atomic cross section of the  $i^{th}$  constituent element present in a molecule.  $\sigma_i$  is the mass attenuation coefficient,  $(\mu/\rho)_i$  through

$$\sigma_i = \frac{A_i}{N_A} \left( \frac{\mu}{\rho} \right)_i \quad (3)$$

where,  $N_A$  is the Avogadro constant and  $A_i$  is the atomic mass of the  $i^{th}$  element present in a molecule.

The cross section per molecule can be written in terms of an effective (average) cross section per atom,  $\sigma_a$ , and an effective (average) cross section per electron,  $\sigma_e$ , as

$$\sigma_m = n \sigma_a = n Z_{eff} \sigma_e \quad (4)$$

Where,  $Z_{eff}$  is the effective atomic number and  $n = \sum_i n_i$  is the total number of atoms present in a molecule.

Equ. (4) can be regarded as the definition of the effective atomic number. Essentially it is assumed that the actual atoms of the molecule can be replaced by the same number of identical (average) atoms, each having  $Z_{eff}$  is given by

$$Z_{eff} = \frac{\sum_i n_i A_i \left( \frac{\mu}{\rho} \right)_i}{\sum_i n_i \frac{A_i}{Z_i} \left( \frac{\mu}{\rho} \right)_i} \quad (5)$$

where,  $Z_i$  is the atomic number of the  $i^{th}$  element present in a molecule.

The effective electron density,  $N_e$  can be expressed in the number of electrons per unit mass is closely related to the  $Z_{eff}$ . for a chemical element, the electron density is given by  $N_e = N_A (Z/A)$ , this expression can be generalized to a compound, and one has

$$N_e = N_A \frac{n Z_{eff}}{\sum_i n_i A_i} = N_A \frac{Z_{eff}}{\langle A \rangle} \quad (6)$$

where,  $\langle A \rangle$  average atomic mass of the compound.

In the present work, we have calculated mass attenuation coefficient and photon-interaction cross sections in the energy range from 1 keV to 100 GeV using WinXCom (Gerward et al. 2004). This program uses the same underlying cross-sectional database as the well known tabulation of Hubbell and Seltzer (1995). WinXCom makes it possible to export the cross-sectional data to a

UGC JOURNAL NO. 45204;

[https://www.ugc.ac.in/journalist/ugc\\_admin\\_journal\\_report.aspx?eid=NDUyMDQ=](https://www.ugc.ac.in/journalist/ugc_admin_journal_report.aspx?eid=NDUyMDQ=)

IMPACT FACTOR: 4.977

Page | 43



predefined MS Excel template, a feature that greatly facilitates the subsequent and numerical data analysis.

Table 1. Compound studied in the present work.  $\langle Z \rangle$  is the mean atomic number calculated from the chemical formula. SN is the sample number.

SN	Compound	$\langle Z \rangle$
1	LU	3.52

## 2. Results and Discussion

### 2.1. Total photon interaction (with coherent).

The mass attenuation coefficients values for LU are calculated at photon energies 1keV -100 GeV. Fig-1 shows the variation of mass attenuation coefficients of LU with photon energy in the range 1 keV to 100 GeV. From Fig-1,

- We can see that there are three energy ranges where photo electric absorption, Compton scattering, and pair production respectively, are the dominating attenuation processes. It is seen that the  $(\mu/\rho)_c$  values are large and show a decreasing trend with strong energy dependence in the low incident photon energy range of 1 keV- 25 keV. In the intermediate (25 keV ) and high (1 MeV) energy regions,
- $(\mu/\rho)_c$  values show less energy dependent behavior and gradually decrease with increasing incident photon energy is due to the coherent scattering which varies as Z (Shastry & Jnananda, 1958). In the inter mediate energy region, where incoherent scattering is the most dominant process, the mass attenuation coefficient is found to be constant and is due to the linear z-dependence of incoherent scattering and insignificant role played by pair production. In the higher region the variation of mass attenuation coefficient is due to the z dependence of pair production (El-Kateb & Abdul Hamid, 1991).

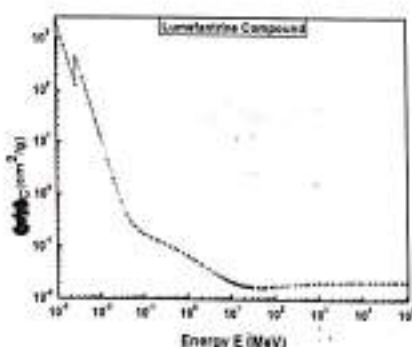


Figure-1. Variation of photon mass attenuation coefficient  $(\mu/\rho)_c$  of LU with photon energy for total photon interaction (Coherent).

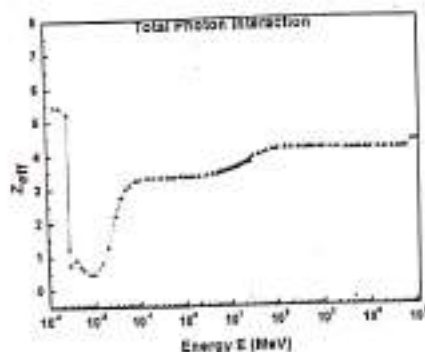


Figure-2. Variation of effective atomic number  $Z_{eff}$  of LU with photon energy for total photon interaction (Coherent).

### 2.2. Photo electric absorption

The variation of  $Z_{eff}$  with photon energy for photoelectric absorption is as shown in Fig.3 which indicates that  $Z_{eff}$  is almost independent of photon energy and remains constant. This is due to the fact that Photoelectric effect process is predominant at low energies (<1 MeV) and for materials of higher atomic numbers than for low Z materials. Similar results were also obtained by Perumallu et al (Perumallu et al. 1985) in multi element materials of biological importance. The variation of  $Z_{eff}$  is almost independent of energy. This is because of the fact that LU consist of elements which are close to atomic number and are same in number.

### 2.3. Incoherent (Compton) scattering

The variation of  $Z_{eff}$  with photon energy for incoherent scattering is as shown in Fig.4 which indicates that  $Z_{eff}$  increases slowly with increase in energy in the region 1-400 keV. Beyond 400 keV,  $Z_{eff}$  is independent of photon energy. Most of the elements in a composite material have a value of Z/A of about 0.5 where as hydrogen has a value of 1.0, which effects Compton scattering. This result is similar to the results obtained by S. R. Manohara et al. (Manohara & Hanagodimath, 2007). Khayyoom and Parthasaradhi have also studied  $Z_{eff}$  of some alloys; their experimental results suggest that in incoherent scattering  $Z_{eff}$  is independent of photon energy from 20 to 800 keV. In our findings  $Z_{eff}$  is independent of photon energy only above 400 keV but depends on photon energy below 400 keV. The variation of  $Z_{eff}$  depends on respective proportion and range of atomic numbers of the elements of LU.

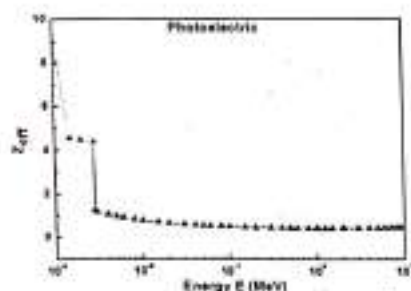


Figure-3. Variation of effective atomic number  $Z_{eff}$  of LU with photon energy for photoelectric absorption.

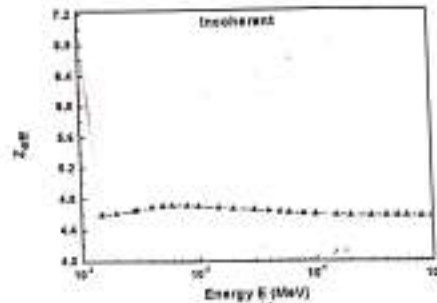


Figure-4. Variation of effective atomic number  $Z_{eff}$  of LU with photon energy for incoherent scattering.

#### 2. 4. Coherent (Rayleigh) scattering

The variation of  $Z_{eff}$  with photon energy for coherent scattering is as shown in Fig 5. From this figure it is clear that  $Z_{eff}$  increases with increase in energy from 1 keV to 300 keV, beyond 300 keV  $Z_{eff}$  is independent of energy i.e. remains invariable with the increase in energy. Whereas at 200 keV there is a slight steady state and further increase with increase in energy this is due to the presence of sulfur. Our results are in good agreement with the results shown by (Manohara & Hanagodimath, 2007).

#### 2. 5. Pair production (Nuclear field)

The variation of  $Z_{eff}$  with photon energy for pair production is as shown in Fig 6. With reference to the figure it is clear that  $Z_{eff}$  decreases more with increase of photon energy from 1.1 to 100 MeV, this is because of the large number of atomic numbers, beyond 100 MeV there is a slight increase in  $Z_{eff}$  with increase in photon energy and again there is a decrease in  $Z_{eff}$  with increase in photon energy up to 200 MeV and then it remains invariant i.e. independent of photon energy.

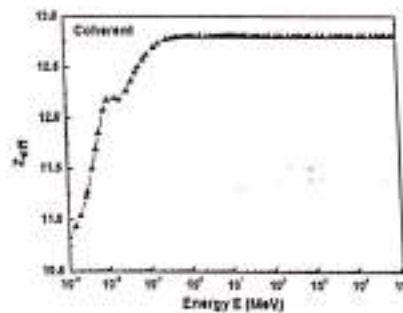


Figure-5. Variation of effective atomic number  $Z_{eff}$  of LU with photon energy for coherent scattering.

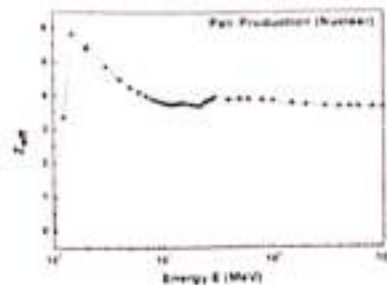


Figure-6 Variation of effective atomic number  $Z_{eff}$  of LU with photon energy for pair production in nuclear field

## 2.6. Pair production (Electric field)

The variation of  $Z_{eff}$  with photon energy for pair production is as shown in Fig 7. From the figure it is clear that  $Z_{eff}$  slightly decreases 1.1 MeV to 120 MeV and is remains invariant i.e. independent of photon energies from 120 MeV. The variations of  $N_e$  with photon energy in LU for partial and total interaction processes are similar to that of  $Z_{eff}$  and can be explain on the similar manner as that of  $Z_{eff}$  and are as shown in Figs.8-13.

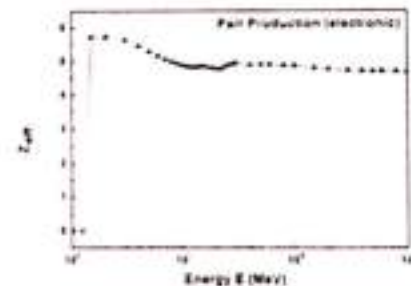


Figure-7. Variation of effective atomic number  $Z_{eff}$  of LU with photon energy for pair production in electric field

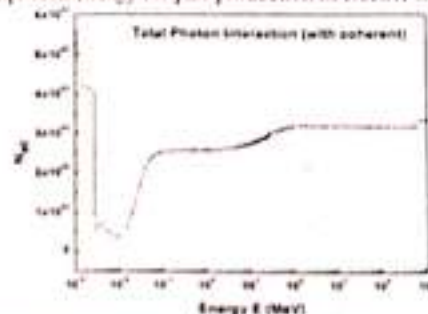


Figure-8. Variation of electron density  $N_e$  of LU with photon energy for total photon interaction (with coherent)

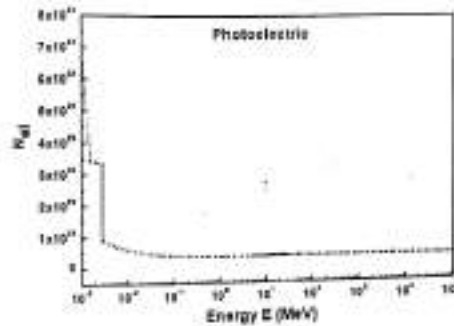


Figure-9. Variation of electron density  $N_{ei}$  of LU with photon energy for photoelectric absorption.

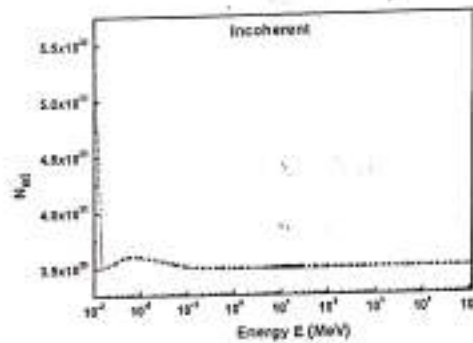


Figure-10. Variation of electron density  $N_{ei}$  of LU with photon energy for incoherent scattering.

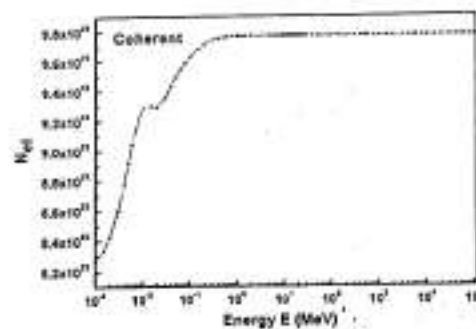


Figure-11. Variation of electron density  $N_{ei}$  of LU with photon energy for coherent scattering.

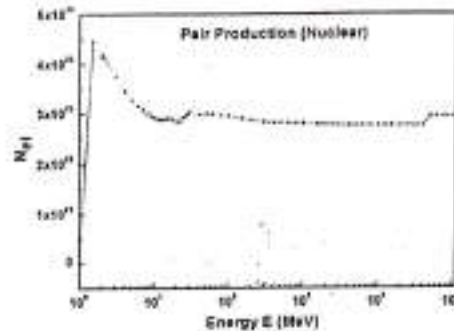


Figure-12. Variation of electron density  $N_e$  of LU with photon energy for pair production in nuclear field.

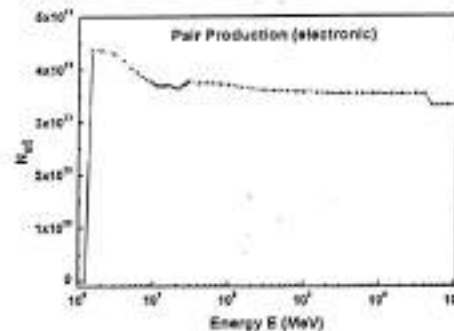


Figure-13. Variation of electron density  $N_e$  of LU with photon energy for pair production in electric field.

### 3. Conclusions

- 1) The  $Z_{eff}$  and the corresponding  $N_e$  of LU have been calculated in the energy region from 1 keV to 100 GeV using WinXcom (Gerward et al. 2001, 2004) and its underlying database of atomic photon interaction cross-sections. We have used a comprehensive and consistent set of formulae i.e. valid for all types of materials and for all energies greater than 1 keV (Manohara et al. 2008 "a").
- 2) One can distinguish three energy regions of a LU. The three energy regions are approximately  $E < 0.1$  MeV,  $0.1$  MeV  $< E < 100$  MeV and  $E > 100$  MeV. The main photon interaction processes in these regions are photoelectric absorption, incoherent (Compton) scattering and pair production, respectively. Between these energy regions there are transition regions with a rapid variation of  $Z_{eff}$  and  $N_e$ .
- 3) The K-absorption edge is found at 2.82 keV with  $Z_{eff} = 5.23$  in the photoelectric absorption region.
- 4)  $Z_{eff}$  and  $N_e$  are increases for low energies and remains constants for higher energies in coherent scattering. Whereas they decreases for low energies and remains constant for higher energies in case of photoelectric absorption and incoherent scattering respectively.



#### 4. Acknowledgement

One of the authors viz., Ingalagsudi P. K., thankful to Dr. P. M. Veeresha Sharma, Founder, Chemogenesis Research and Development Centre, Hubli, Karnataka, India, for providing the dye.

#### References

1. El-Kateb, A. H., & Abdul Hamid, A. S. (1991). Photon attenuation coefficient study of some materials containing hydrogen, carbon and oxygen, *Applied Radiation Isotopes*, 42, 303-307.
2. Gerward, L., Gilbert, N., Jensen, K. B., & Leving, H. (2001). WinXCom-a program for calculating X-ray attenuation coefficients, *Radiation Physics and Chemistry*, 60, 23.
3. Gerward, L., Gilbert, N., Jensen, K. B., & Leving, H. (2004). WinXCom-a program for calculating X-ray attenuation coefficients *Radiation Physics and Chemistry*, 71, 653-654.
4. Hyne, G. J. (1952). The effective atomic numbers of materials for various  $\gamma$ -ray interactions, *Physics Review*, 85, 725.
5. Jackson, D. F., & Hawkes, D. J. (1981). X-ray attenuation coefficients of elements and mixtures *Physics Report*, 70, 169.
6. Manohara, S. R., & Hanagodimath, S. M. (2007). Studies on effective atomic numbers and electron densities of essential amino acids in the energy range 1 keV- 100 GeV. *Nuclear instruments and methods in physics research B*, 258, 321-328.
7. Manohara, S. R., Hanagodimath, S. M., & Gerward, L. (2008a). Energy dependence of effective atomic numbers for photon energy absorption and photon interaction: studies on some biological molecules in the energy range 1 keV-20 MeV. *Medical Physics*, 35, 388-402.
8. Perumallu, A., Nageshwararao, A. S., & Krishnarao, G. (1985). Z-dependence of photon interactions in multi-element materials, *Physica B+C*, 132C, 388-394.
9. Shivalinge Gowda, Krishnaveni, S., Yashoda, T., Umesh, T.K., & Ramakrishna Gowda (2004). Photon mass attenuation coefficients, effective atomic numbers and electron densities of some thermo luminescent dosimetric compounds, *PRAMANA*, 63, 529-41.
10. Shastry, K. S. R., & Jnanananda, S. (1958). *Journal of Scientific and Industrial Research*, 17B, 389.





## FLUORESCENCE QUENCHING STUDIES OF BSA DOPED POLYANILINE

Sharanabasava Ganochari<sup>1</sup>, Venkataraman A.<sup>1,2\*</sup><sup>1</sup> Materials Chemistry Laboratory, Department of Materials Science, Gulbarga University, Kalaburagi-585106, Karnataka<sup>2</sup> Department of Chemistry, Gulbarga University, Kalaburagi-585106, Karnataka<sup>3</sup> Centre for Material Science, KLE Technological University, Hubballi-580031, Karnataka

**Abstract** — Polyaniline (PANI) was synthesized by chemical oxidation polymerization method in the presence of ammonium persulfate as oxidant and benzeno sulphonic acid (BSA) as dopant. In this study, fluorescence characteristics of polyaniline doped with BSA is soluble in Dimethyl sulfoxide (DMSO) in terms of fluorescence quenching reported in this paper. The synthesized BSA-PANI is characterized for its structural and morphological behaviour. The detection of quencher is studied through the observed intense quenching of fluorescence signals in the emission spectra of the BSA-PANI solution. The preparation of polymer solution is found to be 100 ppm in a 100 ppm solution of BSA-PANI solution.

**Keywords**- Polyaniline, fluorescence quenching, sulphonic acid dopant, X-ray diffraction, Scanning electron microscope.

## I. INTRODUCTION

Polyaniline (PANI) is one of the utmost promising conjugated conducting polymer which have fascinated more attention because of its economical low cost, superior electrochemical performance, mechanical flexibility and relative ease of processing [1-4]. Hence Polyaniline and its similarities find use in the field of sensors, actuators, super-capacitors, electromagnetic-shielding, corrosion protection, as well as electronic, electroluminescence and electro chromic devices [5-9]. Because of this prolonged conjugation inter-molecular hydrogen bonds are formed between the NH<sub>2</sub> and NH-R group of the head-to-head chain and  $\pi$  stacking occurs. The polymer chain converts rigid which induces insolubility in most dynamic solvents. The processability of PANI can be enhanced by using functionalized dopants like Benzeno sulfonic acid (BSA), Camphor sulfonic acid (CSA) or Dodecyl Benzeno Sulphonic Acid (DBSA) etc. The bulky dopants will reduce the common aggregation by cumulative the solubility of PANI salt [10-13]. Polyaniline shows fluorescence characteristics due to the extended conjugation and were used as selective fluorescence for the detection of electron deficient nitroaromatics (NACS). Nitroaromatic are the prominent high energy materials which are being used as explosive materials and detonators etc.

The present studies are employed by doping PANI with BSA dissolving DMSO solvent before going for fluorescence studies. Fluorescence occurs when the molecule returns to the electronic ground state, from the excited singlet state, by emission of a photon. If a molecule which absorbs UV radiation does not fluoresce it means that it must have lost its energy some other way. The term quenching usually refers to non-radiative energy transfer from an excited species to other molecules. Meanwhile, fluorescence quenching is a process of decreasing in fluorescence intensity for a fluorescing species.

## II. EXPERIMENTAL

## 2.1 Materials and Methods:

The BSA doped PANI is synthesised by chemical oxidation method employing ammonium per sulphate as the oxidising agent. The quencher and solvent DMSO were of analytical grade and were used as received.

## 2.2 Preparation of BSA- PANI:

0.2 M solution of BSA- PANI (0.5: 1) in DMSO are prepared to avoid self-absorption effects and the quencher concentration has been varied. A 100 ppm BSA-PANI in DMSO solution has been prepared by diluting the stock solution of 100 ppm. The 100 ppm quencher in DMSO is used. Below Figure 1. Shows Flow chart of the preparation of emeraldine base

## 2.3 Preparation of polymer films

The films of BSA doped polyaniline prepared by following procedure. 0.07gm sample of doped PANI was mixed with 0.02 gram of PPVA in 10ml of DMF and the solution was stirred for 12 hrs. Then 0.16ml each of the various doped polymer solution was cast on a glass slide and dried in a vacuum over at 50-60 °C for 12 hrs.

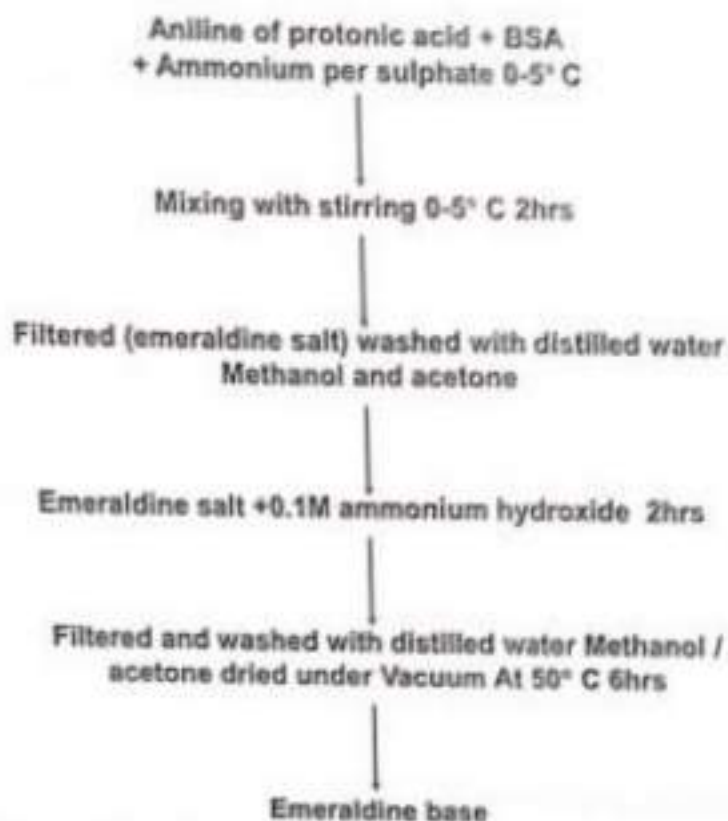


Figure 1. Flow chart of the preparation of emeraldine base

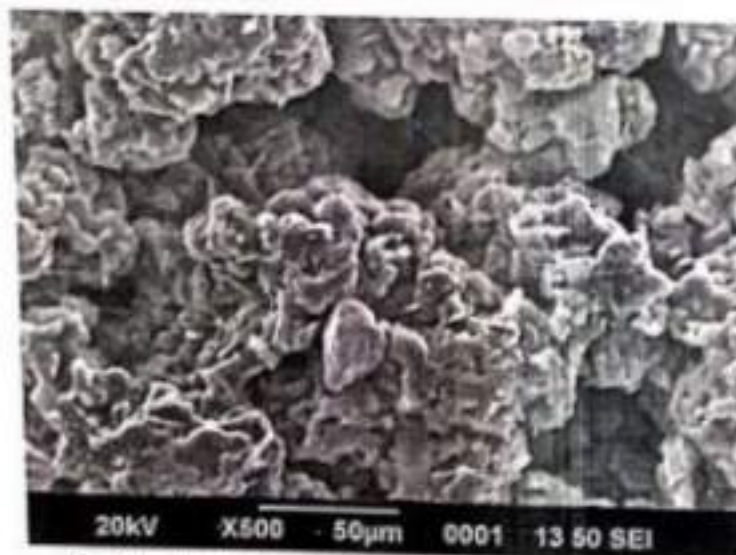


Figure 2. scanning electron microscope image of BSA doped PANI

#### Characterizations

Scanning Electron Microscope (SEM) The morphologies of the polymers were studied by using coupling JEOL Model JSM -6390LV scanning electron microscope. The electron microscope was operated at 20 kV. X-ray diffraction (XRD) Phillips-2710 powder X-ray diffractometer in the 2 $\theta$  range 10° to 100° using CuK $\alpha$  radiation ( $\lambda$ =1.54056 Å).



### III. RESULTS AND DISCUSSION

#### 3.1 Scanning Electron Microscope

BSA-PANI particles are shown in Fig. 2. It is observed clearly that the agglomerated spherical particles were formed when the feeding ratio of PANI-BSA was 1: 0.5 ratios the spherical and uneven arrangement of particles were observed.

#### 3.2 X-ray diffraction

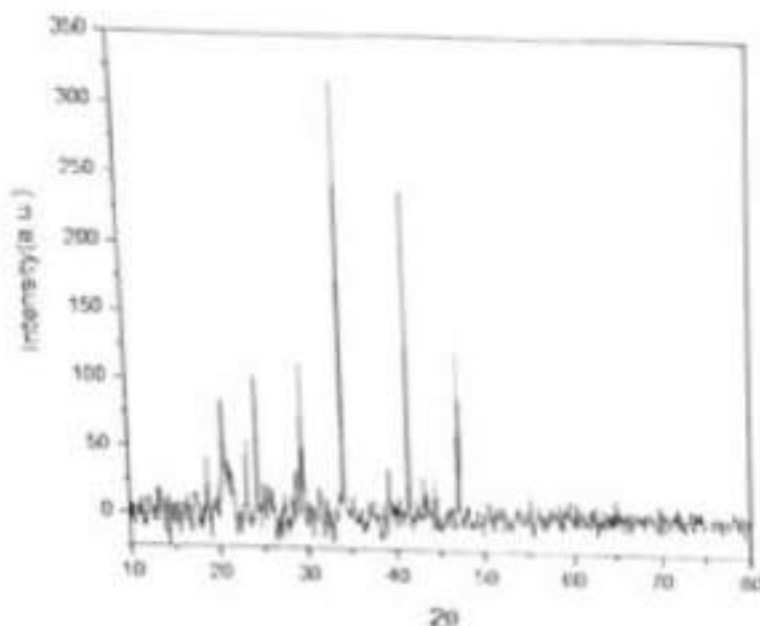


Figure 3. X-ray diffraction pattern of BSA doped PANI

XRD patterns of BSA-PANI-PVA, PANI is shown in Fig. 3, the crystalline peaks of BSA-PANI appeared at  $2\theta$  22.5°, 25°, 30°, 35°, 39°, 42° and 48° are accredited to the periodicity perpendicular to the BSA-PANI chain in its crystalline salt form, representative that BSA doped PANI-PVA was partly crystalline (crystalline and amorphous). For the PANI/PVA, the broadest peaks at around  $2\theta$  20° were due to the P-PVA crystallites, and the diffraction peaks at about 20°-25° were related to the partially crystalline PANI/PVA.

#### 3.3 Fluorescence quenching studies

Figures 4 shows the fluorescence quenching of BSA-PANI with meta diazo benzene (MIBZ). From the figure it is observed that the fluorescence intensity of the fluorophore reduced regularly with increasing concentration of quencher but no change in the emission wavelength of BSA-PANI is observed. This is due to quenching. The degree of quenching depends on the quantity of quencher in a homogeneous solution. This indicates that the non-radiative energy transfer between the excited donor (fluorophore) and the acceptor (quencher).

### IV. CONCLUSIONS

BSA doped PANI-PVA thin films prepared and reveal that agglomerated uneven arrangement of particles shows in SEM partial crystallinity shows in XRD. Quenching studies of BSA-PANI reveal that the intensity decrease the electron are excited to ground state to excited state, a molecule in a high vibrational level of the excited state will quickly fall to the low vibrational level of the state by losing energy to other molecule through collision the form of quenching usually refers to non-radiative energy transfer from excited species to other molecules.

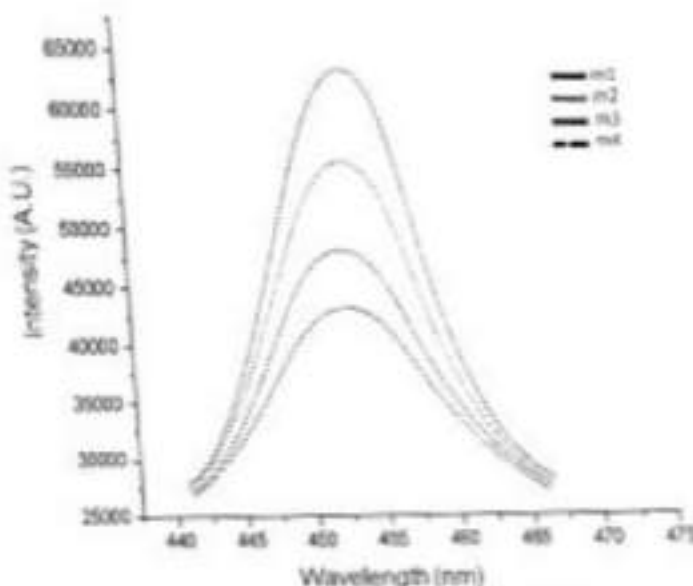


Figure 4: Fluorescence emission spectrum 100 ppm BSA-PAN] with 100 ppm quencher

#### ACKNOWLEDGEMENTS

The author Parvathi Patil, acknowledges H. K. E. Society's Smt. Veeramma Gangasiri College for Women Kalaburagi, Karnataka, India for supporting throughout research work.

#### REFERENCES

- [1] H. Swarnarani, S. Basavaraja, C. Basavaraja and A. Venkatesamas, *Journal of Applied Polymer Science*, 2010, 117, 1350.
- [2] Q. Zhou and T.M. Swager, *J.Am.chem.soc.* 1995, 117,7017-7018
- [3] P.K. Khol, K.K. Satheesh Kumar, S. Geetha and D.C. Trivedi, *Synthetic Metals*, 2003, 139, 191-200
- [4] Yolanda S., Marta V.S., Rebecca E.S., Karina R.L., Jess L., Ian O.J., Ramon M.M., Felix S., M. Dolores Marcos, Pedro Amorin, Carmen Guillen, *Chemistry A European Journal*, 2014, 20, 855-866.
- [5] S. Shanmugaraja, H. Jadhav, R. Karthik and P. S. Mukherjee, *RSC Advances*, 2013, 3(13), 4940-4950.
- [6] T. A. Skotheim and J. R. Reynolds, *Handbook of Conducting Polymers*, 3rd ed., CRC Press, (Taylor and Francis Group) 2007
- [7] N. L. Shoela, S. M. Umesh, L. B. Swaminath, V. A. Prashant, R. P. Shivajirao and B. K. Govind, *Bull. Chem. Soc. Ethiop.* 2009, 23(2), 231-238.
- [8] A. Airinei, R. I Tigniani, E. Russo and D. O. Doroboi, *Digest journal of Nanomaterials and Biostructures*, 2011, 6(3), 1265-1272.
- [9] Parvathi Patil, Lakshmidevi V., Sharasabasava V. G., A. Venkatesamas, *International Journal of Advance Research and Innovative Ideas in Education* 2017, 3, 3 page 3259-3269
- [10] B. D. Gokcen, D. Bilir and B. Mehmet, *Chemical Communications*, 2013, 49, 6140-6142.
- [11] Radhakrishnan, S., Siju, C.R., Mahanta, D., Paul, S. and Madras, G., *Electrochim. Acta*, 2009, 54: 1249
- [12] Lin, H.K. and Chen, S.A., *Macromolecules*, 2000, 33: 8117
- [13] Li, X.G., Huang, M.R., Feng, W. and Chen, Y.M., *Polymer*, 2004, 45: 101
- [14] Ahmed, S.M. and Ahmed, S.A., *Eur. Polym. J.* 2002, 38: 25
- [15] Laika, J. and Wilfars, J., *Synth. Met.*, 2003, 135: 261
- [16] Gill, M. and Armes, S.P., *Langmuir* 1992, 8: 2178
- [17] Jan, L.S. and Siddig, M.A., *Chinese J. Polym. Sci.*, 2011, 29(2): 181
- [18] Sonani, P.R., *Mater. Chem. Phys.*, 2002, 77: 81
- [19] Riedt, A., Stejkal, J. and Heilmann, M., *Synth. Met.*, 2001, 121: 1763
- [20] Banerjee, P. and Moudal, B.M., *Macromolecules*, 1993, 28: 3940
- [21] Mirmohseni, A. and Wallace, G.G., *Polymer*, 2003, 44: 3523
- [22] Giménez, V., Reina, J.A., Martínez, A. and Cádiz, V., *Polymer*, 1999, 40: 2759
- [23] An, Y., Koyama, T., Haruhisa, K., Shirai, H., Wada, J., Yonemitsu, H. and Itoh, T., *Polymer*, 1993, 36: 2297

- [24] Suzuki, M., Yoshida, T., Koyama, T., Kobayashi, S., Kimura, M., Hanabusa, K. and Shirai, H., *Polymer*, 2000, 41: 4531
- [25] Li, X.H., Wang, L.F., Zhuang, L.Q. and Luo, Z.H., *J. Natural Gas Chem.*, 1998, 7: 273
- [26] Chen, F. and Liu, P., *AIChE J.*, 2011, 57: 599
- [27] Chattopadhyay, D. and Manda, B.M., *Langmuir*, 1996, 12: 1585
- [28] Hino, T., Namiki, T. and Kuramoto, N., *Synth. Met.*, 2006, 15: 1327



RESEARCH ARTICLE OPEN ACCESS

# Non-Newtonian Visco-elastic Heat Transfer Flow Past a Stretching Sheet with Convective Boundary Condition

P H Veena, D Vinuta, V K Pravin

Dept. of Mathematics, Smt. V.G. College for Women, Gulbarga, Karnataka, India  
Dept. of Mathematics, Gulbarga University, Gulbarga, Karnataka, India  
Dept. of Mech. Engg., P.D.A. College of Engg., Gulbarga, Karnataka, India

### ABSTRACT

In this paper two dimensional flow of a viscoelastic fluid due to stretching surface is considered. Flow analysis is carried out by using closed form solution of fourth order differential equation of motion of viscoelastic fluid. Further (Walters' liquid B' model) heat transfer analysis is carried out using convective surface condition. The governing equations of flow and heat transfer are non-linear partial differential equations which are unable to solve analytically hence are solved using Runge-Kutta Numerical Method with efficient shooting technique. The flow and heat transfer characteristics are studied through plots drawn. Numerical values of Wall temperature are calculated and presented in the table and compared with earlier published results which are in good agreement

**Key Words:** Visco-elastic (Walters' liquid B') fluid, stretching sheet, convective boundary condition, heat transfer, flow analysis

### Nomenclature

- b stretching rate
- x horizontal coordinate
- y vertical coordinate
- u horizontal velocity component
- v vertical velocity component
- T temperature
- c<sub>p</sub> specific heat
- f dimensionless stream function
- Pr Prandtl number
- l Characteristic length
- k<sub>1</sub> viscoelastic parameter
- λ<sub>e</sub> the co-efficient of elasticity,
- T<sub>s</sub> the temperature of the sheet.
- B<sub>1</sub> Biot number
- differentiation with respect to η

### Greek symbols

- η similarity variable
- θ dimensionless temperature
- k thermal conductivity
- μ viscosity
- ν kinematic viscosity
- ρ density
- α root value

### Subscripts

- w properties at the plate
- ∞ free stream condition

### I. INTRODUCTION

In reality most of the liquids are non-Newtonian in nature and are used abundantly in many engineering applications, such as plastic film manufacture, artificial fibers manufacture, aerodynamic extrusion of plastic sheets, cooling of metallic sheets in a cooling bath on process, in Geothermal reservoirs and in petroleum industries. Hence the study of viscoelastic non-Newtonian fluid flow and heat transfer phenomena is much more important as considered to the study of Newtonian fluids. Many researchers worked on the flow and heat transfer problems of viscoelastic fluids. Some of them are discussed below.

As we study the literature, Sakiadis [1] was a first researcher among all other investigators to study the phenomena considering boundary layer flow of viscous fluid over moving rigid surfaces. It is more appropriate to consider non-Newtonian behavior of all those fluids in the analysis of boundary layer flow and heat transfer characteristics as most of the fluids such as plastic films, and artificial fibers in industrial applications are strictly Newtonian. But these were restricted to flow and heat transfer in non-porous media. In recent years a great deal of interest has focused on the rheological effects of non-Newtonian flow through porous media.

Rajagopal et al [2] studied the flow of viscoelastic fluid over a stretching sheet. Siddappa and Abel [3] studied the flow analysis and heat transfer characteristics of viscoelastic fluid due to stretching plate in presence of suction and



injection. Further the same authors Siddappa and Abel [4] studied the viscoelastic fluid flow analysis due to stretching sheet. They obtained the analytical solution for the problem. Dandapat and Gupta [5] studied the flow and heat transfer characteristics in a visco-elastic fluid over a stretching sheet. Lawrence and Rao [6] investigated the heat transfer analysis in the flow of a visco-elastic fluid over a stretching sheet. Cortell [7] studied the similarity solutions of the flow and heat transfer analysis of visco-elastic fluid due to a stretching sheet. Sonth et.al [8] analyzed the heat and mass transfer effects in viscoelastic fluid flow over on accelerating surface with effect of heat source/sink and viscous dissipation. Khan and Sanjayanand [9] investigated the visco-elastic fluid flow and heat transfer analysis using an exponential stretching sheet. Bhattacharya et.al [10] studied the heat transfer of a visco-elastic fluid over a stretching surface.

Nataraja et.al [11] investigated the non-Similar solutions for flow and heat transfer problem considering a viscoelastic fluid over a stretching sheet. Abel et.al [12] investigated the flow and Heat transfer characteristics in a viscoelastic boundary layer flow over a stretching sheet with viscous dissipation and non-uniform heat source. They obtained an analytical solution for the problem in terms of Kummer's function. Aziz [13] has given a similarity solution for laminar thermal boundary layer over flat plate with a convective boundary condition for the viscous fluid. Makinde and Aziz [14] investigated the mixed convection on MHD flow of viscous fluid from a vertical plate embedded in a porous medium with a convective boundary condition is used to study the heat transfer analysis.

$$\frac{\partial u}{\partial x} + \frac{\partial v}{\partial y} = 0,$$

$$(1) u \frac{\partial u}{\partial x} + v \frac{\partial v}{\partial y} = \nu \frac{\partial^2 u}{\partial y^2} - k_1 \left\{ u \frac{\partial^3 u}{\partial x \partial y^2} + v \frac{\partial^3 u}{\partial y^3} + \frac{\partial u}{\partial x} \frac{\partial^2 u}{\partial y^2} - \frac{\partial u}{\partial y} \frac{\partial^2 u}{\partial x \partial y} \right\}, \quad (2)$$

$$\rho c_p \left( u \frac{\partial T}{\partial x} + v \frac{\partial T}{\partial y} \right) = k \frac{\partial^2 T}{\partial y^2}, \quad (3)$$

Here in above equations,  $\rho$  is the density,  $T$  is the temperature,  $\nu$  is the kinematic viscosity,  $k_1$  is the co-efficient of elasticity,  $k$  is coefficient of thermal conductivity,  $c_p$  is specific heat at constant pressure, The other quantities have their usual meaning. It is to be emphasized here that Eq.

Makinde and Olanrewaju [15] investigated the Buoyancy effects on the thermal boundary layer over flow due to a vertical plate with a convective surface boundary condition for heat transfer analysis. Yao and Fang [16] investigated the heat transfer analysis of a generalized stretching /shrinking wall problem with convective boundary conditions. Makinde and Aziz [17] studied boundary layer flow of a nano-fluid past a stretching sheet with a convective boundary condition.

On observing above there are studies of heat transfer analysis of viscous fluids with convective heating conditions, but there are no studies in heat transfer analysis of viscoelastic fluids with convective heating condition as it has more practical application in the field of engineering and industries. Hence in the present paper the investigation of flow and heat transfer analysis of viscoelastic fluid with convective heating boundary condition is studied.

## II. MATHEMATICAL FORMULATION

Here it is considered the two-dimensional laminar boundary layer flow of an incompressible, visco-elastic fluid (Walters' liquid B' model) due to a stretching sheet as it has created due to two equal and opposite forces applied along the x-axis, so that the sheet is stretched, keeping the origin fixed. Under the boundary layer approximations and the assumptions that the contribution due to the normal stress is of the same order of magnitude as the shear stress - the basic boundary layer equations governing the flow of Walters' Liquid B', heat transfer in presence of non-uniform heat generation can be written as:

(2) is one order higher than the Navier-Stokes equation and this would require an additional boundary condition. Since we are considering a semi-infinite region such a boundary condition may be assumed in the form of an asymptotic condition at infinity. This is reflected in the following boundary conditions;



$$\left. \begin{aligned} u &= bx, & v &= 0, \\ -k \frac{\partial T}{\partial y} &= h_s (T_s - T) \end{aligned} \right\} \text{ at } y = 0, \quad (4)$$

$$\left. \begin{aligned} u &\rightarrow 0, & \frac{\partial u}{\partial y} &\rightarrow 0, & T &\rightarrow T_\infty \end{aligned} \right\} \text{ at } y \rightarrow \infty$$

Here  $u$  and  $v$  are the velocity components along  $x$  - and  $y$ -directions respectively, where  $T_\infty$  is the temperature of the fluid far away from the sheet (temperature of ambient cold fluid)  $T$  is the uniform temperature on the top surface of the plate. Hence we have  $T_s > T > T_\infty$ .

### III. FLOW ANALYSIS

Now introducing the similarity transformations in the form,

$$u = bx f_\eta(\eta), \quad v = -\sqrt{b\nu} f(\eta) \quad (5)$$

where  $\eta = \sqrt{\frac{b}{\nu}} y$  is dimensionless normal distance

Eq.(1) is identically satisfied with these change of variables and Eq.(2) is transformed to:

$$f_\eta^2 - f f_{\eta\eta} = f_{\eta\eta\eta} - k_1 \{ 2f_\eta - f f_{\eta\eta\eta} - f_{\eta\eta}^2 \} \quad (6)$$

where

$$k_1 = \frac{k_s b}{\nu} \quad (7)$$

the subscript  $\eta$  denotes the differentiation with respect to  $\eta$ ,  $k_1$  is the non-dimensional visco-elastic parameter. The governing boundary conditions on velocity Eq.(4) take the following form as:

$$f = 0, \quad f_\eta = 1 \quad \text{at } \eta = 0, \quad (8)$$

$$f_\eta \rightarrow 0, \quad f_{\eta\eta} \rightarrow 0 \quad \text{as } \eta \rightarrow \infty,$$

The solution of Eq.(6) corresponding to the boundary conditions (8) is obtained as

$$f(\eta) = \frac{1 - e^{-\alpha\eta}}{\alpha} \quad (9)$$

where

$$\alpha = \sqrt{\frac{1}{1 - k_1}} \quad (10)$$

The velocity components  $u$  &  $v$  become

$$u = bx e^{-\alpha y}, \quad v = -\sqrt{b\nu} \left( \frac{1 - e^{-\alpha y}}{\alpha} \right) \quad (11)$$

where  $b > 0$  and  $\alpha$  is given by Eq. (10).

### IV. SKIN FRICTION

The local skin friction coefficient or frictional drag coefficient is given by

$$C_f = \frac{\tau_w}{\mu b x \sqrt{\frac{b}{\nu}}} = \alpha \quad (12)$$

where  $\tau_w = -\mu \left( \frac{\partial u}{\partial y} \right)_{y=0} = \mu b x \alpha \sqrt{\frac{b}{\nu}}$ , is the wall shearing stress on the surface of the stretching sheet,  $\mu$  is the dynamic viscosity of fluid and  $\alpha$  is given by Eq.(12).

### V. HEAT TRANSFER ANALYSIS

In this section the convective boundary condition with constant surface temperature for the heating process is considered. To solve heat equation (3) Defining the non-dimensional temperature  $\theta(\eta)$  as:

$$\theta(\eta) = \frac{T - T_\infty}{T_s - T_\infty} \quad (13)$$

where  $T_s$  the temperature of the sheet.

Using Eqn. (13), Eqs. (3) and (4) can be converted to

$$\theta'' + Pr f \theta' = 0, \quad (14)$$

$$\left. \begin{aligned} \theta'(\eta) &= B_1 (1 - \theta(\eta)) & \text{at } \eta &= 0, \\ \theta(\eta) &\rightarrow 0 & \text{as } \eta &\rightarrow \infty. \end{aligned} \right\} \quad (15)$$



where

$$Pr = \frac{\mu C_p}{k}$$

is the Prandtl number.

$$Bi = \frac{h \sqrt{a}}{k}$$

is the thermal Biot number

Here Biot number  $Bi$ , is the dimensionless parameter and it plays the fundamental role in conduction problems that involves surface convection effects. Biot number parameter provides the measure of temperature drop in the solid relative to the temperature difference between the surface and fluid.

For  $Bi \ll 1$  shows the resistance to conduction within the solid is much less than the resistance to the convection across the fluid boundary layer, hence assumption of uniform temperature is reasonable. Whereas  $Bi \gg 1$  says the temperature difference across the solid is much larger than that between surface and fluid.

## VI. NUMERICAL SOLUTION

In this section we are explaining about the method of Numerical Solution used to solve the boundary value problems of considered study. The Governing equations of motion and heat transfer are highly non-linear so it is very difficult to solve, hence the partial differential equations are converted into ordinary differential equations by means of similarity transformation. The exponential exact solution of momentum equation is obtained and is used to find the solution of energy equation (14) with respect to the boundary conditions (15). The Boundary value problem considered is converted into initial value problem then by using Newton-Rapson method, the missing condition is found and then using Runge-Kutta integration scheme the solution of temperature boundary value problem is obtained. The step size is chosen as 0.001 and the accuracy of result is maintained upto 10<sup>-6</sup>.

## VII. RESULTS AND DISCUSSION

After obtaining the solution of boundary value problem, various plots of flow, velocity and temperature are plotted to analyze the effect of various governing parameters.

Fig.1. is the representation of physical sketch of considered problem. It shows how the stretching sheet problem is constructed.

Fig.2. Is plotted for the flow profiles as well as the velocity profiles for different values of viscoelastic parameter  $k_1$ . Which show that, both the profiles decrease with increase in the parametric values of viscoelastic parameter which

happens throughout the boundary layer which is obvious.

Fig.3. is Plotted for the temperature profile which shows the effect of viscoelastic parameter. On observing the plot one can see that the temperature is increasing with increase in the parametric value of viscoelastic parameter. This is due to the fact that an increase of viscoelastic normal stress give rise to thickening of the thermal boundary layer.

Fig. 4 shows that, the temperature profile decreases with an increase in the parametric value of Prandtl number, which shows that the viscoelastic boundary layer is thicker than the thermal boundary layer.

Fig. 5 shows the effect of Biot number parameter on the temperature profile. On observing the graph it depicts the fact that temperature is increases with increase in the parametric value of Biot number as the stronger convection results in higher surface temperatures, which causes the thermal effect to penetrate strongly deeper into the fluid.

## VIII. CONCLUSIONS

- Analytical Solutions for flow and numerical solution of convective heat transfer problem are obtained.
- The effects viscoelastic parameter is to decrease the flow and velocity, which was quite opposite on temperature.
- The thermal boundary layer thickness decreases with increasing Prandtl number in convective heat transfer phenomenon
- When viscoelastic parameter  $k_1$  tends to zero, results are reduced to the Newtonian case.

## REFERENCES

- Sakiadis BC; Boundary layer behavior on continuous solid surfaces AICHEJ 1961;7:26-8.
- Rajagopal KR, Na TY, Gupta AS; Flow of a viscoelastic fluid over a stretching sheet Rheol Acta 1984;23:213-5.
- Siddappa B, Subhas Abel; Visco-elastic boundary layer flow past a stretching plate with suction and heat transfer. Rheol Acta, 1985(23):815-16.
- Siddappa B, Subhas Abel; Non-Newtonian flow past a stretching plate, ZAMP, 1985(36) 890-892.
- Dandapat BS, Gupta AS; Flow and Heat transfer in a visco-elastic fluid over a stretching sheet. Int J.Non-linear Mech.1989 ;24(93):21 5-9

- [6] Lawrence PS, Rao BN; Heat transfer in the flow of a visco-elastic fluid over a stretching sheet Acta Mech 1992 ,( 93), 53-61.
- [7] Cortell R; Similarity solutions for flow and heat transfer of visco-elastic fluid over a stretching sheet Int J Non-linear Mech 1994 29(2) 155-61
- [8] Sonth RM, Khan SK, Abel MS, Prasad KV; Heat and mass transfer in viscoelastic fluid flow over an accelerating surface with heat source/sink and viscous dissipation Heat Mass Transfer 2002;38 213-20.
- [9] Khan SK, Sanjayanand E; Visco-elastic boundary layer flow and heat transfer over an exponential stretching sheet Int J Heat Mass Transfer 2005 48 1534-42
- [10] Bhattacharya S, Pal A, Gupta A S, Heat transfer in the flow of a visco-elastic fluid over a stretching surface Heat Mass Transfer 34(1998)41-45.
- [11] Nataraja H.R., Sharma M.S., Nageshwar Rao B, Non-Similar solutions for flow and heat transfer in a visco-elastic fluid over a stretching sheet Int J non-linear mech.33 (1998)357-361.
- [12] Abel, Siddheshwar M.S, PG, Mahantesh M.Nandeppanavar, Heat transfer in a viscoelastic boundary layer flow over a stretching sheet with viscous dissipation and non-uniform heat source. Int. J. Heat Mass Transfer 2007;50 960-6
- [13] Aziz A; A similarity solution for laminar thermal boundary layer over flat plate with a convective boundary condition. Commun. Non-linear Sci, Numer. Simulat 14(2009) 1064-1068
- [14] Makinde O D, Aziz A; MHD mixed convection from a vertical plate embedded in a porous medium with a convective boundary condition. Int J Ther Sci.49 (2010)1813-1820
- [15] Makinde O D, Olanrewaju P O, Buoyancy effects on thermal boundary layer over a vertical plate with a convective surface boundary condition Trans ASME-J Fluid Eng 132(2010)044502(1-4)
- [16] Yao S, Fang T, Heat transfer of a generalized stretching/shrinking wall problem with convective boundary conditions Commun Non-linear Sci Numer, simulatz 16 (2011)752-760
- [17] Makinde O D, Aziz A, Boundary layer flow of a nanofluid past a stretching sheet with a convective boundary condition. Int J Therm Sci 50 (2011)1326-1332.

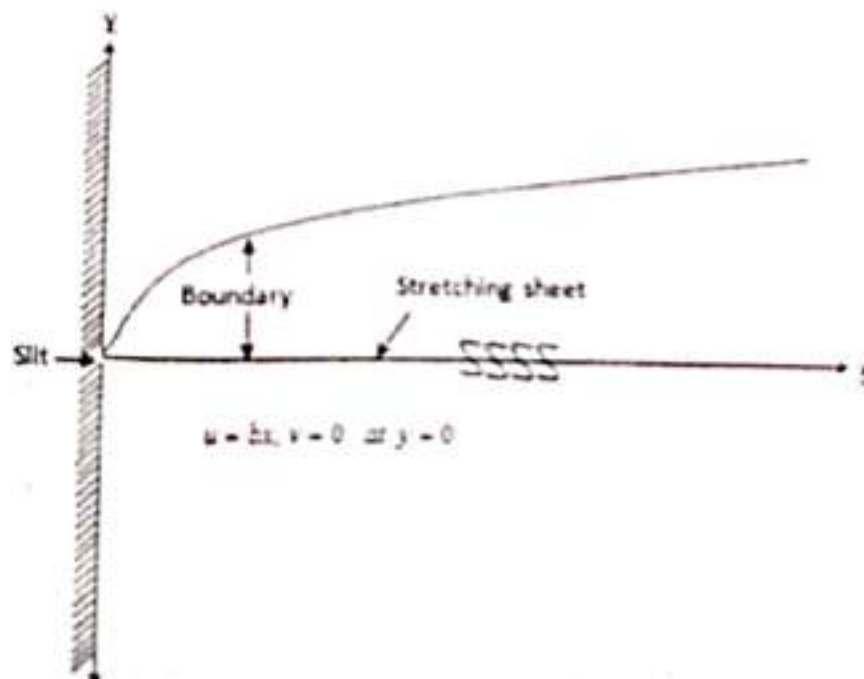


Fig. 1. Schematic diagram of linear stretching sheet

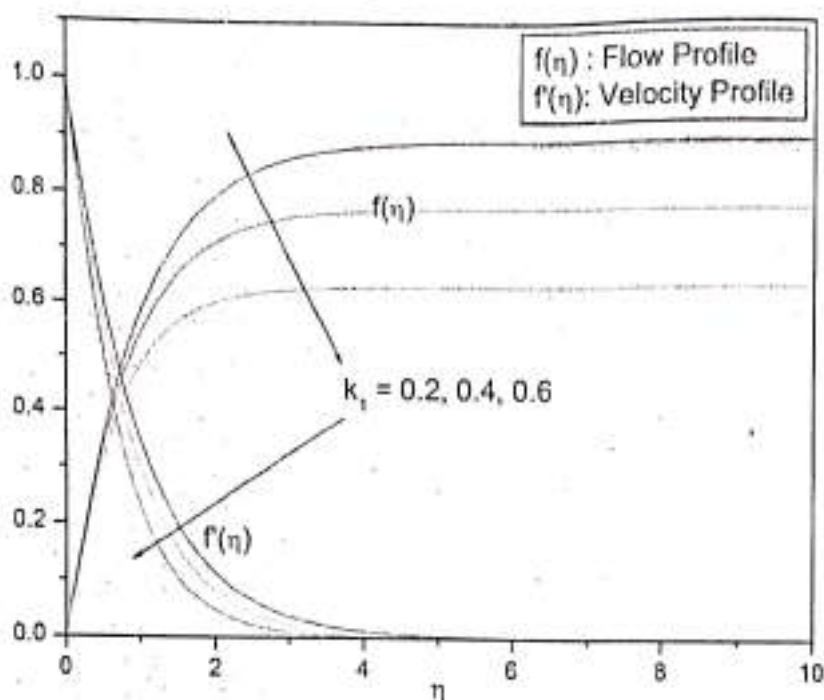


Fig.2. Flow and Velocity profile for different values of viscoelastic parameter

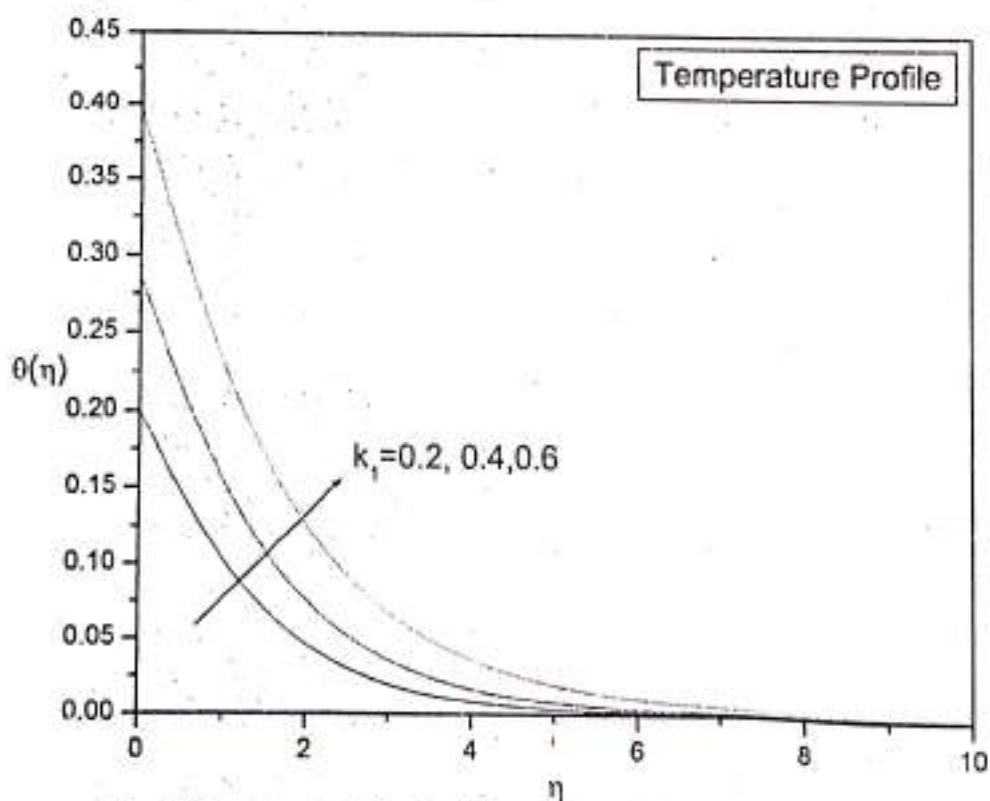


Fig.3. Temperature profiles for different values of visco-elastic parameter

69



# Mass Transfer and Radiative Heat Transfer Flow of MHD Casson Fluid with Temperature Gradient Dependent Heat Sink and Internal Mass Diffusion in a Vertical Channel with Stretching Porous Walls

N. Raveendra<sup>1</sup> P.H. Veena<sup>2</sup> V.K. Pravin<sup>3</sup>

- 1. Asst. Prof. RajaRajeswari College of Engineering, Ramohalli Cross, Bangalore-560074, Karnataka
- 2. Asso. Prof. Dept. of Mathematics, Smt. V.G. College for Women, Kalaburagi-585102, Karnataka
- 3. Prof. Dept. of Mechanical Engg., P.D.A. College of Engg., Kalaburagi-585102, Karnataka, India

### Abstract

In the present paper an investigation of the flow, heat and mass transfer characteristics of a MHD Casson fluid in a parallel plate channel with stretching walls with respect to a uniform magnetic field and porous media is carried out. Similarity transformation technique is used to transform the system of partial differential equations into ordinary differential equations. The governing non-linear differential equations are solved numerically using Runge-Kutta method of fourth order via shooting technique. Graphs for the velocity, temperature and concentration are plotted to analyze the behavior of the flow with different physical parameters. The skin friction, Nusselt number and Sherwood numbers are computed and tabulated

**Keywords:** Casson Fluid, Porous Media, MHD, Heat and Mass Transfer, Stretching Walls

### Nomenclature:

$u$ and $v$	Velocity Components in $x$ and $y$ Directions
$\rho$	Density
$p$	Pressure
$\nu$	Kinematic Viscosity
$\sigma$	Electrical Conductivity
$B_0$	Strength of the Magnetic Field
$T$	Temperature at the Plate
$c_p$	Specific Heat
$q$	Radiative Heat Flux
$C$	Concentration of Fluid
$D$	Mass Diffusivity
$\sigma^*$	Stephan-Boltzman Constant
$k^*$	Mean Absorption Coefficient
$\mu_p$	Plastic Dynamic Viscosity of the Non-Newtonian Fluid
$\tau_y$	Yield Stress of the Fluid
$\pi$	Product Component of Deformation Rate with Itself
$e_{ij}$	( $i,j$ )th Component of Deformation Rate
$\pi_c$	Critical Value of $\pi$ Based on Non-Newtonian Model
$\beta$	non-Newtonian Casson Parameter
$Q'$	Temperature Gradient Dependent Heat Sink/Source Parameter
$K$	Chemical Reaction Parameter
$k_2$	Permeability parameter
$Re$	Stretching Reynolds Number
$Mn$	Hartman Number
$Sc$	Schmidt Number
$Pr$	Prandtl Number
$Sh$	Sherwood Number
$Nu$	Nusselt Number

S.G. Gounkals

**IQAC Co-ordinator**  
Smt. V.G. Women's Degree College  
KALABURAGI

**PRINCIPAL**  
Smt. V.G. Degree College for Women,  
KALABURAGI

## Introduction

Many researchers' interest is to know the varied applications of boundary layer flow behaviors of non-Newtonian fluids in natural sciences, engineering sciences and industry. The mutual coordination between motion of the fluid and magnetic field is required feature of the physical situation in the MHD fluid flow problems. Principles of MHD are required in the design of power generators, pumps, radar systems and flow meters. MHD parameter is one of the most important required parameter by which the cooling rate can be controlled. Besides non-Newtonian fluid have variety of applications in industry and engineering moreover in the extraction of crude oil from petroleum products.

In this regard Bhattacharyya and Layek [1] have investigated the slip effect on diffusion of chemically reactive species in boundary layer flow over a vertical stretching sheet with suction or blowing. Awad et al. [2] have studied heat and mass transfer in unsteady rotating fluid flow with binary chemical reaction and activation energy. Boyd et al. [3] have discussed the analysis of the Casson and current yasuda non-Newtonian blood models in steady and oscillatory flow using the lattice Boltzmann method. Makinde [4] has studied MHD mixed-convection interaction with thermal radiation and  $n$ th order chemical reaction past a vertical porous plate embedded in a porous medium. Misra et al. [5] have analyzed the flow and heat transfer of a MHD viscoelastic fluid flow and heat transfer in a channel with a stretching wall: some applications to haemodynamics. Ashraf et al. [6] have studied MHD non-Newtonian micro-polar fluid flow and heat transfer in a channel with stretching walls. Raftari and Vajravelu [7] have made use of homotopy analysis method to study MHD viscoelastic fluid flow and heat transfer in a channel with a stretching wall. Anjalidevi and Kandasamy [8] have investigated the effects of chemical reaction, heat and mass transfer on laminar flow along a semi-infinite horizontal plate. Hayat et al. [9] have discussed MHD flow and mass transfer of a Jeffery fluid over a nonlinear stretching surface. Shehzad et al. [10] have analyzed the effects of mass transfer on MHD flow of Casson fluid with chemical reaction and suction. Shaw and Sibanda [11] have studied thermal instability in a non-Darcy porous medium saturated with a Nano fluid and with a convective boundary condition. Bhattacharyya et al. [12] have discussed the analytic solution for magneto hydrodynamic boundary layer flow of Casson fluid over a stretching /shrinking sheet with wall mass transfer. Nadeem et al. [13] have studied MHD three dimensional Casson fluid flows past a porous linearly stretching sheet. Kirubhashankar [14] has analyzed the Casson fluid flow and heat transfer over an unsteady porous stretching surface. Hasanuzzaman [15] has made a study on similarity solution of unsteady combined free and forced convective laminar boundary layer flow about a vertical porous surface with suction and blowing. Kameswaran et al. [16] have examined a new algorithm for internal heat generation in Nano fluid flow due to a stretching sheet in a porous medium. Sibanda et al. [17] have studied the dual solutions of Casson fluid flow over a stretching or shrinking sheet. Hayat et al. [18] have studied three dimensional stretched flow of Jeffrey fluid with variable thermal conductivity and thermal radiation. Islam et al. [19] have analyzed the MHD free convection and mass transfer flow with heat generation through an inclined plate. Rahman et al. [20] have examined the thermophoresis effect on MHD forced convection on a fluid over a continuous linear stretching sheet in presence of heat generation and power-law wall temperature. Khalid et al. [21] have studied unsteady MHD free convection flow of Casson fluid past over an oscillating vertical plate embedded in a porous medium. Thiagarajan and Senthilkumar [22] have observed the DTM-Pade approximations of MHD boundary layer flow of a Casson fluid over a shrinking sheet. Nadeem et al. [23] have made an investigation on MHD three dimensional Casson fluid flows past a linearly stretching sheet. Rizwan et al. [24] have studied the convective heat transfer and MHD effects on Casson Nano fluid flow over a shrinking sheet. Akbar [25] has examined the influence of magnetic field on peristaltic flow of a Casson fluid in an asymmetric channel: application in crude oil refinement. Sinha and Shit [26] have studied electro magneto hydrodynamic flow of blood and heat transfer in a capillary with thermal radiation. Swati Mukhopadhyaya [27] has investigated the effects of thermal radiation on Casson fluid flow and heat transfer over an unsteady stretching surface subjected to suction/ blowing. Mukhopadhyaya et al. [28] have investigated MHD boundary layer flow of Casson fluid passing through an exponentially stretching permeable surface with thermal radiation. Khalid et al. [29] have analyzed the exact solutions for unsteady free convection flow of a Casson Nano fluid past a linearly stretching sheet with convective boundary conditions. Nadeem et al. [30] have studied MHD three dimensional boundary layer flow of Casson Nano fluid past a linearly stretching sheet with convective boundary conditions. Riwuz Ul Haq et al. [31] have studied the convective heat transfer in MHD slip flow over a stretching surface in the presence of carbon Nano tubes. Khalid [32] has investigated the exact solutions for unsteady free convection flow of a Casson fluid over an oscillating vertical plate with constant wall temperature.

## Mathematical Model

Consider the two dimensional steady laminar flow of a Casson fluid in a parallel plate channel with stretching walls in the presence of a transverse magnetic field. The magnetic Reynolds number is assumed to be small so that the induced magnetic field can be neglected. The constitutive equation for the Casson fluid can be written





$$\tau_{ij} = \begin{cases} 2\left(\mu_B + \frac{\tau_y}{\sqrt{2\pi}}\right) e_{ij}, & \pi > \pi_c \\ 2\left(\mu_B + \frac{\tau_y}{\sqrt{2\pi}}\right) e_{ij}, & \pi < \pi_c \end{cases} \quad (1)$$

Using equation (1) the governing equations of the flow heat and mass transfer are

$$u \frac{\partial u}{\partial x} + v \frac{\partial v}{\partial y} = 0 \quad (2)$$

$$u \frac{\partial u}{\partial x} + v \frac{\partial u}{\partial y} = -\frac{1}{\rho} \frac{\partial p}{\partial x} + \nu \left(1 + \frac{1}{\beta}\right) \frac{\partial^2 u}{\partial y^2} - \frac{\sigma B_0^2}{\rho} u - \frac{\nu}{k} u \quad (3)$$

$$u \frac{\partial v}{\partial x} + v \frac{\partial v}{\partial y} = -\frac{1}{\rho} \frac{\partial p}{\partial y} + \nu \left(1 + \frac{1}{\beta}\right) \frac{\partial^2 v}{\partial y^2} \quad (4)$$

$$u \frac{\partial T}{\partial x} + v \frac{\partial T}{\partial y} = \frac{k}{\rho C_p} \frac{\partial^2 T}{\partial y^2} - \frac{1}{\rho C_p} \frac{\partial q_r}{\partial y} + Q' \frac{\partial T}{\partial y} \quad (5)$$

$$u \frac{\partial C}{\partial x} + v \frac{\partial C}{\partial y} = D \frac{\partial^2 C}{\partial y^2} - k_1(c - c_2) \quad (6)$$

The boundary conditions are

$$\begin{aligned} u = bx, \quad v = 0, \quad T = T_1, \quad C = C_1, \quad y = 0 \\ u = bx, \quad v = 0, \quad T = T_2, \quad C = C_2, \quad y = \infty \end{aligned} \quad (7)$$

Where  $b > 0$  is for the stretch of the channel walls.

Using Roseland approximation the radiative heat flux can be taken as  $q_r = \frac{-4\sigma^* \partial T^4}{3k^* \partial y}$  (8)

Now assuming that the temperature difference within the flow is such that  $T^4$  can be expressed as linear function of temperature. With Taylor series expansion about  $T_\infty$  and neglecting higher order terms we get

$$T^4 \approx 4T_\infty^3 T - T_\infty^4 \quad (9)$$

Now introduce the following similarity variables to convert the governing partial differential equations into ordinary differential equations

$$u = bx f'(\eta), \quad v = -ab f(\eta), \quad \eta = \frac{y}{a} \quad (10a)$$

$$\theta(\eta) = \frac{T - T_2}{T_1 - T_2}, \quad \varphi(\eta) = \frac{C - C_2}{C_1 - C_2} \quad (10b)$$

Eliminating pressure gradient from (2) and (3) and using (8) - (10b), equations (2) - (6) are reduced to the following form

$$\left(1 + \frac{1}{\beta}\right) f'''' = \text{Re} \left\{ (f')^2 - f f'' \right\} - (M_a^2 + k_2) f' \quad (11)$$

$$(1 + Nr) \theta'' + \text{Re Pr} \theta' (f + Q') = 0 \quad (12)$$

$$\varphi'' - \text{Sc Re} (K\varphi - f\varphi') = 0 \quad (13)$$

The corresponding boundary conditions are  $f(0) = 0, f'(0) = 1, \theta(0) = 1, \varphi(0) = 1, \text{ as } y = 0$  (14a)

$f(\infty) = 0, \theta(\infty) = 0, \varphi(\infty) = 0, \text{ as } y = \infty$  (14b)

Where  $\beta = \mu_B \frac{\sqrt{2\pi} \epsilon}{\rho \gamma}, \text{ Re} = \frac{a^2 b}{\nu}, \text{ Nr} = \frac{16\sigma^* T_\infty^3}{3kk^*}, M_a^2 = \frac{\sigma}{\mu} B_0^2 a^2, \text{ Pr} = \frac{\mu C_p}{k}$

$$k_2 = \frac{\nu}{k'}, \quad Sc = \frac{\nu}{D}, \quad K = \frac{k_1}{b}$$

#### Skin Friction Coefficient

The skin friction that arises owing to the viscous drag in the vicinity of the plate is calculated as

$$C_f = \frac{\tau_w}{\mu \frac{bx}{a}} = f''(-1), \quad \text{where } \tau_w = \mu \left( \frac{\partial u}{\partial y} \right)_{y=0} = \mu \frac{bx}{a} f''(-1) \quad (15)$$

#### Heat Transfer Coefficient

The rate of heat transfer between the fluid and the walls is evaluated through the non-dimensional Nusselt number.

The Nusselt number is given by

$$Nu = \frac{q_w}{\frac{k}{a}(T_1 - T_2)} = \theta'(-1) \quad \text{Where } q_w = k \left( \frac{\partial T}{\partial y} \right)_{y=0} = \frac{k}{a}(T_1 - T_2)\theta'(-1) \quad (16)$$

#### Mass Transfer Coefficient

The rate of mass transfer coefficient between the fluid and the walls is derived and calculated in terms of Sherwood number which is given by

$$Sh = \frac{m_w}{\frac{D}{a}(C_1 - C_2)} = \varphi(-1), \quad \text{where } m_w = D \left( \frac{\partial C}{\partial y} \right)_{y=0} = \frac{D}{a}(C_1 - C_2)\varphi(-1) \quad (17)$$

The governing equations (11) – (13) along with the boundary conditions 14(a) and 14(b) are solved numerically by using Runge-Kutta method of fourth order along with shooting technique.

#### Results and Discussion

Effect of Reynolds number  $Re$  on the velocity profile is shown in fig. 1. It has been clearly observed from graph that, the velocity decreases with increasing values of Reynolds number  $Re$ . In Fig. 2 the effect of non-Newtonian casson parameter  $\beta$  on the velocity profile is shown. It is noticed from the graph that thickness of the boundary layer decreases with increasing values of casson parameter  $\beta$ . Variation of velocity profile for different values of magnetic parameter  $Mn$  is shown in fig. 3. It is observed from the graph that, the velocity decreases with increasing values of magnetic parameter  $Mn$ . Graph of temperature profile for different values of temperature gradient parameter  $Q'$  is shown in fig. 4. It is noticed from the figure that, thickness of the boundary layer decreases with increasing values of temperature gradient. Variation of temperature profile for different values of Prandtl number  $Pr$  is shown in fig. 5. With increasing values of Prandtl number  $Pr$  the temperature profile decreases. Fig. 6 depicts the effect of temperature profile for different values of radiation parameter  $Nr$ . As we increase the values of radiation parameter  $Nr$ , the temperature profile increases. Fig. 7 illustrates the variation of temperature profile for different values of Reynolds number  $Re$ . It has been noticed from graph that, the temperature profile decreases with an increasing value of Reynolds number  $Re$ . Effect of concentration profile for different values of Reynolds number  $Re$  is shown in fig. 8. It is clearly observed from graph that, the thickness of boundary layer decreases with an increasing value of Reynolds number  $Re$ . Changes in concentration profile for different values of Schmidt number  $Sc$  is shown in fig. 9. Concentration profile increases with an increasing value of Schmidt number  $Sc$ . Variation of concentration field for different values of chemical reaction parameter  $K$  is shown in fig.10. As we increase the chemical reaction parameter  $K$  the concentration profile decreases.



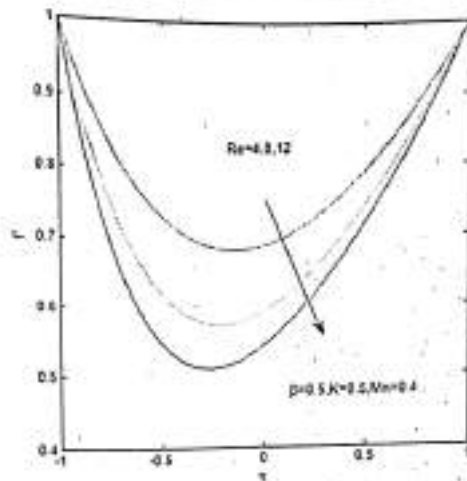


Fig.1 Velocity Profiles for Different Values of Reynolds Number  $Re$

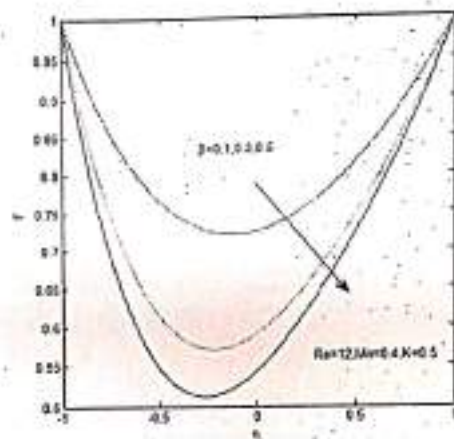


Fig.2 Velocity Profiles for Different Values of Casson Parameter  $\beta$

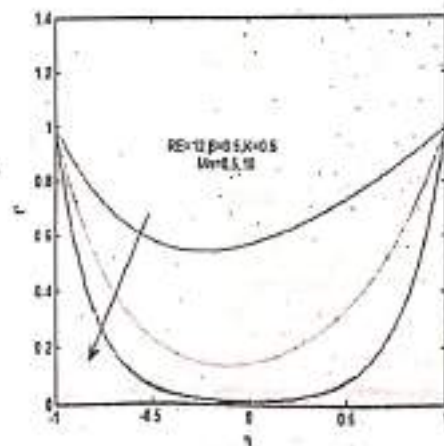


Fig.3 Velocity Profiles for Different Values of Magnetic Parameter  $Mn$



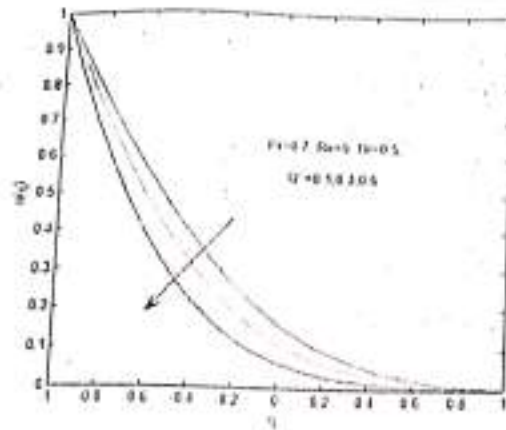


Fig.4. Temperature Profiles for Different Values of Temperature Gradient Heat Sink Parameter

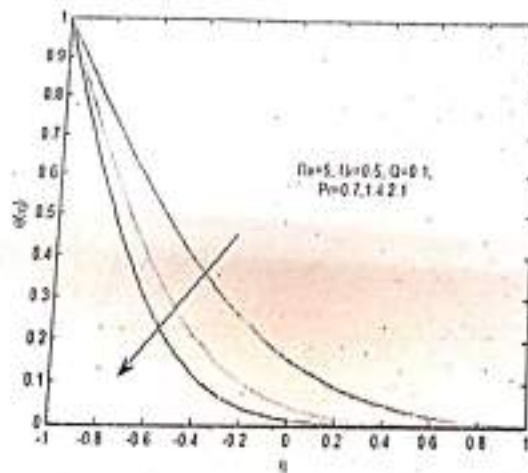


Fig.5 Temperature Profiles for Different Values of Prandtl Number Pr

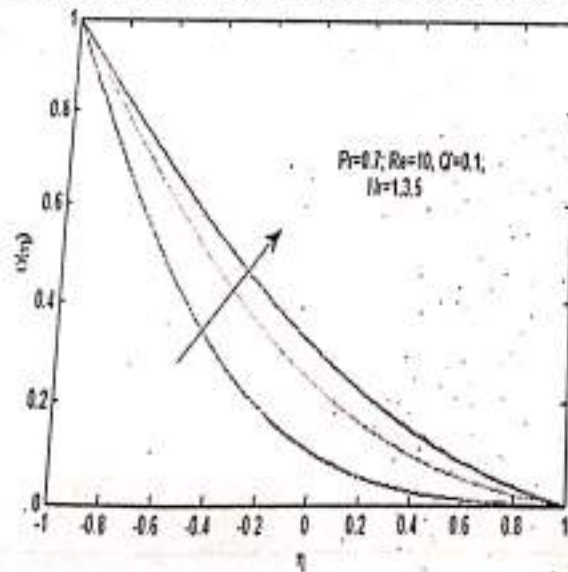


Fig.6. Temperature Profiles for Different Values of Radiation Parameter Nr



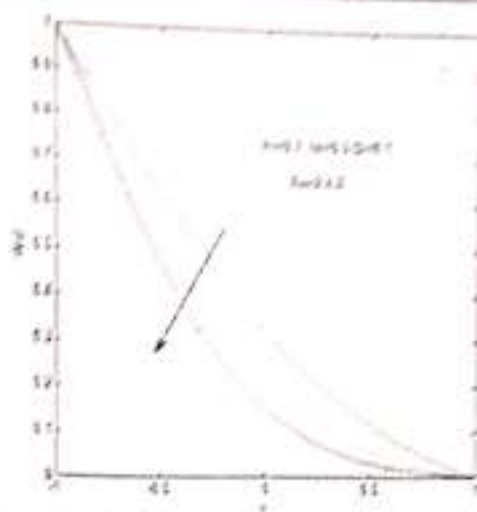


Fig.7. Temperature Profiles for Different Values of Reynolds Number Re

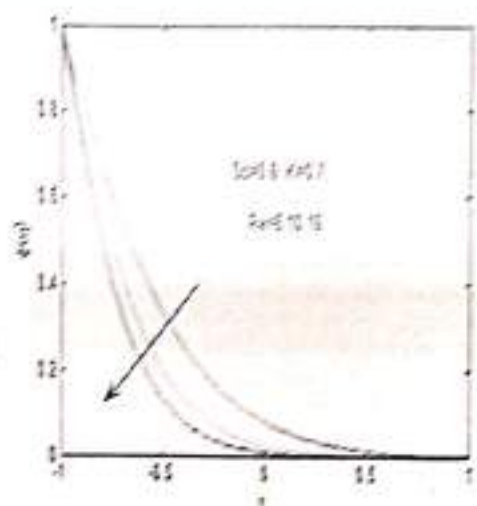


Fig.8. Concentration Profiles for Different Values of Reynolds Number Re

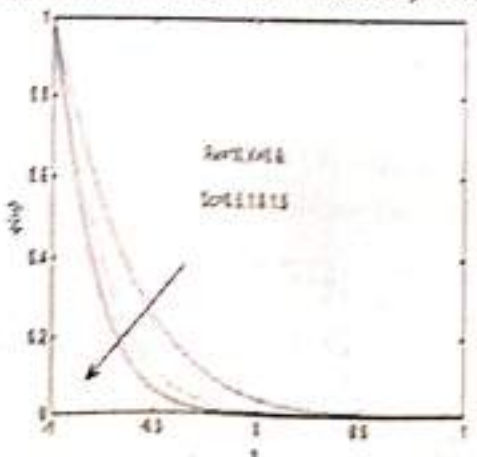


Fig.9. Concentration Profiles for Different Values of Schmidt Number Sc

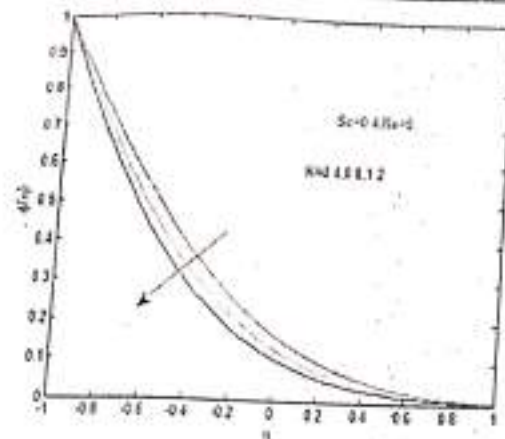


Fig.10 Concentration Profiles for Different Values of Chemical Reaction Parameter K

Table 1. The values of skin friction, Nusselt number and Sherwood number on the lower wall for different parameters.

Re	$\beta$	M	Nr	Pr	Sc	K	Q	K2	$f''(-1)$	$\theta'(-1)$	$\varphi'(-1)$
5											
10	0.6	0.5	0.1	0.7	0.5	0.6	0.1	0.1	-1.156	-1.4677	-1.6288
15									-1.7577	-2.1593	-2.2773
									-2.2223	-2.746	-2.7754
10	0.1	0.5	0.1	0.7	0.5	0.6	0.1	0.1	-0.6864	-2.3235	-2.3695
	0.3								-1.2997	-2.2273	-2.3143
	0.5								-1.6362	-2.1769	-2.2868
10	0.6	0	0.1	0.7	0.5	0.6	0.1	0.1	-1.7273	-2.1648	-2.2802
		5							-3.6539	-1.8093	-2.1198
		10							-6.4517	-1.4992	-2.004
10	0.6	0.5	0.1	0.7	0.5	0.6	0.1	0.1	-1.7577	-2.1593	-2.2773
			0.3						-1.7577	-1.9389	-2.2773
			0.6						-1.7577	-1.6991	-2.2773
10	0.6	0.5	0.1	0.7	0.5	0.6	0.1	0.1		-2.1593	
				1.4						-3.4119	
				2.1						-4.4933	
10	0.6	0.5	0.1	0.7	0.3	0.6	0.1	0.1		-2.1593	
					0.6					-2.1593	
10	0.6	0.5	0.1	0.7	0.5	0.5	0.1	0.1			-2.1658
						1					-2.6794
						1.5					-21.59
10	0.6	0.5	0.1	0.7	0.5	0.6	0.1	0.1			-2.2773
							0.3				-2.2773
							0.6				-2.2773

**Conclusions**

An analysis of MHD flow of Casson fluid in vertical channel and the associated problem of heat and mass





transfer have been investigated with internal mass diffusion and radiative temperature gradient dependent heat sink/source.

The velocity decreases with an increasing values of  $Re$ ,  $Mn$ ,  $\beta$  and velocity attains same position with an increasing the values of  $Pr$ ,  $Nr$ ,  $Sc$  and  $K$ .

The temperature decreases with an increasing values of  $Re$ ,  $Pr$ , and temperature increases with an increasing values of  $Nr$ ,  $Mn$ ,  $Q'$ ,  $\beta$  and attains uniform thickness of the boundary layer for  $Sc$  and  $K$ .

#### References:

1. K. Bhattacharyya and G.C. Layek, Slip effect on diffusion of chemically reactive species in boundary layer flow over a vertical stretching sheet with suction or blowing. *Chemical Eng. Commun.*, 198, p.1354 (2011).
2. F.G. Awad, S. Motsa, M. Khumalo, Heat and mass transfer in unsteady rotating fluid flow with binary chemical reaction and activation energy. *PLOS ONE* 9 (2014) CL07622.
3. J. Boyd, J. M. Buick and S. Green, Analysis of the Casson and Carreau Yasuda non-Newtonian blood models in steady and oscillatory flow using the lattice Boltzmann method. *Phys. Fluids*, 19, p.93 (2007).
4. O.D. Makinde, MHD mixed-convection interaction with thermal radiation and nth order chemical reaction past a vertical porous plate embedded in a porous medium. *Chem. Eng. Commun.*, 198, p.1354 (2011).
5. J.C. Misra, G.C. Shit and H.J. Rath, Flow and Heat Transfer of a MHD viscoelastic fluid flow and heat transfer in a channel with a stretching walls: some applications to Haemodynamics. *ZARM* 2010; 1-26.
6. M. Ashraf, N. Jameel and K. Ali, MHD non-Newtonian micro-polar fluid flow and heat transfer in a channel with stretching walls. *Appl. Math. Mech. - Engl. Ed.*, 34 (10), 1263-1276 (2013).
7. B. Raftari, K. Vajravelu, Homotopy analysis method for MHD viscoelastic fluid flow and heat transfer in a channel with a stretching wall. *Commun. Nonlinear Sci. Numer. Simulat* 17 (2012) 4149-4162.
8. S.P. Anjalidevi and R. Kandasamy, Effects of chemical reaction, heat and mass transfer on laminar flow along a semi-infinite horizontal plate. *Heat and Mass Transfer*, Vol. 35, pp. 465-467, 1999.
9. T. Hayat, M. Qasim, Z. Abbas and A.A. Hendi, MHD flow and mass transfer of a Jeffery fluid over a nonlinear stretching surface. *Z. Naturforsch. A*, 64a, p.1111 (2010).
10. S.A. Shehzad, T. Hayat, M. Qasim and S. Asghar (2013) Effects of mass transfer on MHD flow of casson fluid with chemical reaction and suction. *Brazilian Journal of Chemical Engineering*, 30,187-195
11. S. Shaw and P. Sibanda, Thermal instability in a non-Darcy porous medium saturated with a Nano fluid and with a convective boundary condition. *Bound Value Probl.* 1 (2013) 185
12. K. Bhattacharyya, T. Hayat and A. Alsaedi (2013) Analytic solution for magneto hydrodynamic boundary layer flow of casson fluid over a stretching /shrinking sheet with wall mass transfer. *Chinese Physics B*, 22, Article ID: 024702
13. S. Nadeem, Rizwan Ul Haq, Noreen Sher Akbar and Z.H Khan, MHD three dimensional casson fluid flows past a porous linearly stretching sheet. *Alex. Eng. J.* 52(2013) 577-682.
14. C.K. Kirubhaskar, S. Ganesh and A. Mohamed Ismail, Casson fluid flow and heat transfer over an unsteady porous stretching surface. *Appl. Math. Sci.* 9(7) (2015) 345-351
15. M. Hasanuzzaman, B Mandal and M.M.T. Hossain, A study of similarity solution of unsteady combined free and forced convective laminar boundary layer flow about a vertical porous surface with suction and blowing. *Annals of Pure and Applied Mathematics*, 6(1) (2014) 85-97
16. P.K. Kameswaran, Z.G. Makukula, P. Sibanda, S.S Motsa and P.V.S.N Murthy, A new algorithm for internal heat generation in nano-fluid flow due to a stretching sheet in a porous medium. *Int. J. Numer. Math. Heat and Fluid Flow* 24(2014) 1020-1043.
17. P.K. Kameswaran, S. Shaw and P. Sibanda, Dual solutions of casson fluid flow over a stretching or shrinking sheet. *Sadhana* 39(2014) 1573-1583.
18. T. Hayat, S.A. Shehzad and A. Alsaedi, Three dimensional stretched flow of Jeffery fluid with variable thermal conductivity and thermal radiation. *Appl. Math. Mech.* 34(2013) 823-833.
19. M.S. Islam, M. Samsuzzoha, S. Ara and P. Dey, MHD free convection and mass transfer flow with heat generation through an inclined plate. *Annals of Pure and Applied Mathematics*, 3(2) (2013) 129-141.
20. M.A. Rahman, M.A. Alim and M.J. Islam, Thermophoresis effect on MHD forced convection on a fluid over a continuous linear stretching sheet in presence of heat generation and power-law wall temperature. *Annals of Pure and Applied Mathematics*, 4(2) (2013) 192-204.
21. A. Khalid, I. Khan, A. Khan and S. Shafiq, Unsteady MHD free convection flow of casson fluid past over an oscillating vertical plate embedded in a porous medium. *Eng. Sci. Technol. Int. J.* (2015).
22. M. Thiagarajan, K. Senthilkumar, DTM-Pade approximations of MHD boundary layer flow of a casson fluid over a shrinking sheet. *USA Res. J.* 1 (2013) 1-7.
23. S. Nadeem, R.U. Haq, N.S Akbar and Z.H. Khan, MHD three dimensional casson fluid flows past a linearly stretching sheet. *Alexandria Engineering Journal*, 52(2013) 577-582.



24. Rizwan Ul Haq, Sohail Nadeem, Zafar Hayyat Khan, Toyin Gideon Okedayo, Convective heat transfer and MHD effects on casson Nano fluid flow over a stretching sheet. *J. Cent. Eur. J. Phys.* 12(12) (2014) 862-871.
25. N. Akbar, Influence of magnetic field on peristaltic flow of a casson fluid in an asymmetric channel: application in crude oil refinement. *J. Magnet Magnet Mater.* 278 (2015) 463-468.
26. A. Sinha, G.C. Saha, Electromagnet hydrodynamic flow of blood and heat transfer in a capillary with thermal radiation. *J. Magnet Magnet Mater.* 278 (2014) 1020-1043.
27. Swati Mukhopadhyaya, "Effects of thermal radiation on casson fluid flow and heat transfer over an unsteady stretching surface subjected to suction blowing." *Chin. Phys. B* Vol. 22, No.11 (2013) 114702.
28. S. Mukhopadhyaya, I.C. Meinda and T. Hayat, MHD boundary layer flow of casson fluid passing through an exponentially stretching permeable surface with thermal radiation. *Chin. Phys. B* 23 (2014) 1056-1074.
29. A. Khalid, I. Khan, S. Shafiq, Exact solutions for unsteady free convection flow of a casson Nano fluid past a linearly stretching sheet with convective boundary conditions. *IEEE Trans. Nanotechnol.* 13(10) (2014) 109-115.
30. S. Nadeem, R.L. Haq and N.S. Akbar, MHD three dimensional boundary layer flow of casson Nano fluid past a linearly stretching sheet with convective boundary conditions. *IEEE Trans. Nanotechnol.* 13 (1) (2014) 109-115.
31. Rizwan Ul Haq, Sohail Nadeem, Zafar Hayyat Khan, Convective heat transfer in MHD slip flow over a stretching surface in the presence of carbon nanotubes. *Phys. B: Condens. Matter* 457(15) (2015) 40-47.
32. A. Khalid, I. Khan, S. Shafiq, Exact solutions for unsteady free convection flow of a casson fluid over an oscillating vertical plate with constant wall temperature. *Abstr. Appl. Anal.* (15) (2015) 946330.

67



International Journal of Mechanical Engineering and Technology (IJMET)  
Volume 8, Issue 2, February 2017, pp. 16-26, Article ID: IJMET\_08\_02\_003  
Available online at <http://www.iaeme.com/ijmet/issues.asp?JType=IJMET&VType=8&IType=2>  
ISSN Print: 0976-6340 and ISSN Online: 0976-6359  
© IAEME Publication

# MHD CASSON FLUID FLOW AND HEAT TRANSFER WITH PST AND PHF HEATING CONDITIONS DUE TO A STRETCHING SHEET

P H Veena

Department of Mathematics, Smt. V.G. College for Women,  
Gulbarga, Karnataka, India

D Vinuta

Department of Mathematics, Gulbarga University,  
Gulbarga, Karnataka, India

V K Pravin

Department of Mechanical Engineering,  
P.D.A. College of Engineering Gulbarga, Karnataka, India

## ABSTRACT

In the present paper two-dimensional flow of non-Newtonian MHD flow of Casson fluid heat transfer with PST & PHF is considered. Using Navier Stoke's Equations of Motion the momentum and energy equations of Casson fluid are derived. These governing equations of motion and temperature are non-linear partial differential equations which are tedious to solve as they are, hence these partial differential equations are converted into Ordinary differential equations using suitable similarity transformations. These ODE's are then solved numerically by the efficient Runge Kutta Fehlberg method. Effects of various governing parameters on the flow and heat transfer profiles are analyzed. Further the numerical Values of Wall temperature and Wall temperature Profiles are calculated and discussed in detail through graphs in both the cases of PST and PHF.

**Key words:** Convective Heat transfer, Casson fluid, BVP, IVP, Numerical Solution.

**Cite this Article:** P H Veena, D Vinuta and V K Pravin. MHD Casson Fluid Flow and Heat Transfer with PST and PHF Heating Conditions due to a Stretching Sheet. *International Journal of Mechanical Engineering and Technology*, 8(2), 2017, pp. 16-26.  
<http://www.iaeme.com/ijmet/issues.asp?JType=IJMET&VType=8&IType=2>

## Nomenclature

- b stretching rate
- x horizontal coordinate
- y vertical coordinate
- u horizontal velocity component

S. G. Gaurbally  
IQAC Co-ordinator  
Smt. V.G. Women's Degree College,  
KALABURAGI  
[www.iaeme.com/IJMET/index.asp](http://www.iaeme.com/IJMET/index.asp)

16

PRINCIPAL  
Smt. V.G. Degree College for Women,  
KALABURAGI



$v_z$	vertical velocity component
$T$	temperature
$c_p$	specific heat
$f$	dimensionless stream function
$Pr$	Prandtl number
$l$	Characteristic length
$Mn$	Magnetic parameter
$\frac{d}{d\eta}$	differentiation with respect to $\eta$

### Greek Symbols

$\eta$	similarity variable
$\theta$	dimensionless temperature
$k$	thermal conductivity
$\mu$	viscosity
$\nu$	kinematic viscosity
$\rho$	density
$\alpha$	thermal diffusivity
$\beta$	Casson parameter

### Subscripts

$w$	properties at the plate
$\infty$	free stream condition

## 1. INTRODUCTION

On analyzing the various studies on boundary layer flow and Heat transfer of continuous moving surface, it is came to know that, boundary layer flow is an important type of flow occurring in many engineering applications. Some of them are, in an Aerodynamic extrusion of plastic sheets, the boundary layer along a liquid film in condensation process and a polymer sheet or filament extruded continuously from a die are examples of practical applications of continuous moving surfaces. Besides, cooling of an infinite metallic plate in a cooling path, Gas blowing, continuous casting and spinning of fibers also involve the flow due to a stretching sheet. We have looked towards some important studies as mentioned below:

Crane [1] investigated the flow due to a stretching sheet. First time stretching sheet concept is used by Crane [1], which is very helpful in various engineering industries and this work is considered for a viscous fluid in his study. But as considered with the applications of Newtonian fluids, the applications of non-Newtonian fluids are more hence many researchers have worked on flow, heat and mass transfer analysis of non-Newtonian fluids. Hayat et.al [2] studied Soret and Dufour effects on the magneto hydrodynamics of Casson fluids. Nadeem et. al [3] made a focus on the MHD flow of non-Newtonian Casson fluid due to an exponential shrinking sheet. Pramanik [4] analysed the flow analysis and heat transport analysis of Casson fluid using porous stretching sheet, and phenomena investigated the effects of suction and blowing effect on flow and heat transfer. Bhattacharya et, al [5] investigated flow analysis of Casson fluid over non-porous stretching sheet with the slip effect. Swati et, al [6] investigated the effect of unsteadiness on flow and heat transfer analysis. Qasim and Nooreer [7] made an analysis of Flow of Casson fluid due to permeable shrinking sheet with viscous dissipation. Rizwan et.al [8] focused on the Study of the Flow of MHD Casson nano fluid due to a shrinking sheet. Hussain et, al [9] studied the flow analysis of Casson nanofluid with viscous dissipation and convective boundary conditions. Kamehswaran et.al [10] obtained



dual solutions for Flow analysis of Casson fluid due to stretching or shrinking sheet. Nandeppanavar [11] carried out the work on the flow and heat transfer analysis with two heating conditions. Considering the non-Newtonian Casson fluid due to linear stretching sheet. The solution they obtained is by a power series method analytically, further Nandeppanavar [12-13] also investigated the heat transfer analysis of Casson fluid due to stretching sheet with convective heating condition both Numerical and analytical results in terms of Kummer's function and Runge-Kutta fourth order method with shooting technique. Attia and Ahmed [14] were proposed to study the transient Couette flow analysis of Casson fluid between parallel plates with heat transfer analysis. Bhattacharyya et. al [15] have given an analytical solution for magneto hydrodynamic boundary layer flow of Casson fluid, they also studied the effect of wall mass transfer analysis too. Swati [16] showed the effect of thermal radiation on the flow and heat transfer analysis of Casson fluid over an unsteady stretching sheet with effect of suction and blowing. Shehzad et.al [17] investigated the mass transfer of magnetohydrodynamic flow of Casson fluid with chemical reaction.

Considering all above works, in the present paper, the flow and Heat transfer analysis with two heating conditions (Prescribed surface temperature and Prescribed Wall heat flux) with Numerical Solution is undertaken and the effects of all governing parameters are analysed on the flow and heat transfer analysis.

## 2. MATHEMATICAL FORMULATION

Assuming rheological equation of non-Newtonian Casson fluid as

$$\tau_{ij} = \left[ \mu_p + \left( \frac{P_c}{\sqrt{2\pi}} \right)^2 \right] \dot{\epsilon}_{ij} \quad (1)$$

Here  $\mu$  is the dynamic viscosity,  $\mu_p$  is the plastic dynamic viscosity of Casson fluid,  $P_c$  is the stress of Casson fluid.  $\pi = \epsilon_{ij} \epsilon_{ij}$ ,  $\epsilon_{ij}$  is the (i,j) the component of the deformation rate Casson fluid ( $\pi$  is the product of the component of deformation rate with itself). Considering  $n \geq 1$  we have many applications.

Considering above rheology of Casson fluid. The governing equations of the fluid with MHD are:

$$\frac{\partial u}{\partial x} + \frac{\partial v}{\partial y} = 0 \quad (2)$$

$$u \frac{\partial u}{\partial x} + v \frac{\partial u}{\partial y} = \nu \left( 1 + \frac{1}{\beta} \right) \frac{\partial^2 u}{\partial y^2} - \frac{\sigma B_0^2 u}{\rho} \quad (3)$$

where  $u$  and  $v$  are the components of velocity in  $x$  and  $y$  axis respectively.  $\nu$  is the kinematic viscosity &  $\beta = \mu_p \sqrt{2\pi} / P_c$  is Casson parameter which is non-Newtonian.

The corresponding boundary conditions for the momentum transfer are

$$\left. \begin{aligned} u_x(x) = bx, v = 0, \quad y = 0 \\ u \rightarrow 0, \quad \text{as} \quad y \rightarrow \infty \end{aligned} \right\} \quad (4)$$

with  $b > 0$ , the stretching rate. Equations (2) and (3), subjected to the boundary conditions (4), admit a self-similar solution in terms of the similarity function  $f$  and the similarity variable  $\eta$  defined by

$$u = bx f(\eta), v = -\sqrt{bx} f(\eta), \eta = \sqrt{\frac{b}{\nu}} y \quad (5)$$





It can be easily verified that Eq. (2) is identically satisfied and substituting the above transformations in Eq. (3) we obtain

$$f''^2 - ff'' = \left(1 + \frac{1}{\beta}\right) f'' - M_\infty f' \quad (6)$$

Similarly the boundary conditions (4) are converted to:

$$\left. \begin{aligned} f'(\eta) = 1, \quad f(\eta) = 0 & \quad \text{at } \eta = 0 \\ f'(\eta) \rightarrow 0, & \quad \text{as } \eta \rightarrow \infty \end{aligned} \right\} \quad (7)$$

where

$$M_\infty = \frac{\sigma B_0^2}{\rho b} = \text{magnetic parameter}$$

### 3. HEAT TRANSFER ANALYSIS

The Energy equations with boundary layer approximations can be considered as:

$$\rho C_p \left( u \frac{\partial T}{\partial x} + v \frac{\partial T}{\partial y} \right) = k \frac{\partial^2 T}{\partial y^2} \quad (8)$$

where  $k$  is the thermal conductivity,  $\rho$  is the density of the fluid,  $C_p$  is the specific heat at constant pressure. The heat transfer analysis is carried out due to following two heating conditions:

**Case A:** Prescribed surface temperature (PST Case): In this case

The boundary conditions are:

$$\left. \begin{aligned} T = A \left( \frac{x}{l} \right)^2, & \quad \text{at } y = 0 \\ T \rightarrow T_\infty & \quad \text{as } y \rightarrow \infty \end{aligned} \right\} \quad (9)$$

where  $T_\infty$  is the temperature of the fluid far away from the sheet. Defining the non-dimensional temperature  $\theta(\eta)$  as

$$\theta(\eta) = \frac{T - T_\infty}{T_w - T_\infty} \quad (10)$$

Where  $T_w$  the temperature of the sheet at the wall.

Using Eqn. (10), Eqs. (8) and (9) can be converted to

$$\theta'' + Pr f \theta' - 2f Pr \theta = 0 \quad (11)$$

$$\left. \begin{aligned} \theta(\eta) = 1 & \quad \text{at } \eta = 0, \\ \theta(\eta) \rightarrow 0 & \quad \text{as } \eta \rightarrow \infty. \end{aligned} \right\} \quad (12)$$

Where

$$Pr = \frac{\mu C_p}{k} \quad \text{is the Prandtl number.}$$



**Case B:** Prescribed Surface Wall Heat Flux (PHF Case):

The power law heat flux on the wall surface is considered as:

$$\left. \begin{aligned} -k \frac{\partial T}{\partial y} &= B \left( \frac{x}{l} \right)^2 \quad \text{at } y=0 \\ T &\rightarrow T_{\infty} \quad \text{at } y \rightarrow \infty \end{aligned} \right\} \quad (13)$$

where B is a constant. The scaled temperature is defined as:

$$g(\eta) = \frac{T - T_{\infty}}{T_w - T_{\infty}} \quad (14)$$

Making use of the transformation (14) into Eqn (8) and (13) the following non-dimensional equations for temperature and corresponding boundary conditions are obtained

$$g'' + \text{Pr} f g' - 2f \text{Pr} g = 0 \quad (15)$$

$$\left. \begin{aligned} g'(\eta) &= -1 \quad \text{at } \eta = 0, \\ g(\eta) &\rightarrow 0 \quad \text{as } \eta \rightarrow \infty, \end{aligned} \right\} \quad (16)$$

#### 4. NUMERICAL SOLUTION

The set of non-linear differential equations (6 and 11) subject to the boundary conditions (5 and 12) are integrated numerically using a very efficient method known as Runge-Kutta Fehlberg method with shooting technique.

The most important factor of this method is to choose the appropriate finite values of  $\eta \rightarrow \infty$  in order to determine  $\eta_{\infty}$  for the boundary value problem stated by Eq.(5 & 11), we start with some initial guess value for some particular set of physical parameters to obtain  $f''(0)$  &  $\theta''(0)$ . The solution procedure is repeated with another large value of  $\eta_{\infty}$  until two successive values of  $f''(0)$  &  $\theta''(0)$  differ only by the specified significant digit. The last value of  $\eta_{\infty}$  is finally chosen to be the most appropriate value of the limit  $\eta \rightarrow \infty$  for that particular set of parameters. The value of  $\eta$  may change for another set of physical parameters. Once the finite value of  $\eta$  is determined then the coupled boundary value problem given by Eq. (6) - (11) are solved numerically using the method of superposition. In this method the third order Non-linear Eq. (6) and second order Eq. (11) have been reduced to five simultaneously ordinary differential equations as follows:

Let us call

$$\left. \begin{aligned} y_1 &= f \\ y_2 &= f' \\ y_3 &= f'' \\ y_4 &= \theta \\ y_5 &= \theta' \end{aligned} \right\} \quad (13)$$

The Boundary value problem is given by



$$\begin{aligned}
 \frac{dy_1}{d\eta} &= y_1 \\
 \frac{dy_2}{d\eta} &= y_2 \\
 \frac{dy_3}{d\eta} &= \frac{(y_1^2 - y_2 y_3) + M y_3}{(1 + \frac{1}{\beta})} \\
 \frac{dy_4}{d\eta} &= y_4 \\
 \frac{dy_5}{d\eta} &= -Pr y_4 y_5
 \end{aligned} \tag{14}$$

The boundary conditions now become:

$$y_1(0) = 0, y_2(0) = 1, y_3(0) = x_1, y_4(0) = 1, y_5(0) = x_2, y_1(\infty) = 0, y_2(\infty) = 0, y_3(\infty) = 0 \tag{15}$$

Where  $x_1$  &  $x_2$  are determined such that it satisfied  $y_1(\infty) = 0$  &  $y_2(\infty) = 0$ . Thus, to solve this resultant system, we need five initial conditions, but we have only two initial conditions on  $f$  and one initial condition on  $\theta$ . The third condition on  $f$  (i. e.  $f'(0)$ ) and second condition on  $\theta$  (i.e.  $\theta(0)$ ) are not prescribed which are to be determined by shooting method by using the initial guess values  $x_1$  &  $x_2$  until the boundary conditions  $f_1(\infty) = 0, f_2(\infty) = 0$  (or  $y_1(\infty) = 0, y_2(\infty) = 0$ ) are satisfied. In this way, we employ shooting technique with Runge-Kutta Fehlberg scheme to determine two more unknowns in order to convert the boundary value problem to initial value problem. Once all the five initial conditions are determined the resulting differential equations can then be easily integrated, without any iteration by initial value solver. For this purpose, Runge kutta scheme has been used.

The Same procedure is followed to find the solution of Eq (15) with PHF boundary conditions.

To study the behavior of the velocity and temperature profiles, various curves are drawn for various values of the physical parameters that describe the flow.

## 5. RESULTS AND DISCUSSION

We have considered the flow and heat transfer of MHD Casson fluid due to linear stretching sheet. Here we have considered two types of heating conditions they are namely, Prescribed Surface Temperature (PST) and Prescribed wall Heat Flux (PHF). The Governing boundary layer equations are solved numerically using Runge-Kutta method with efficient shooting technique by converting partial differential equations into ordinary differential equations by means of suitable similarity transformations.

Fig1: shows the geometry of the considered problem, which shows the heated plate, flow direction etc.

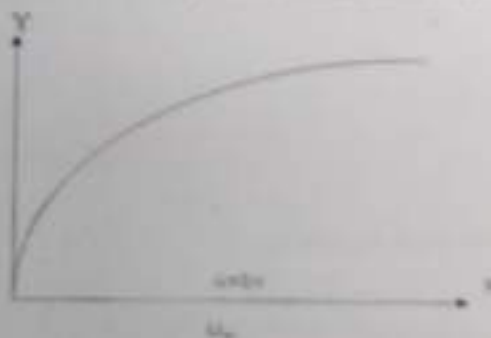


Figure 1 Physical Configuration of Considered Problem



$$\left. \begin{aligned}
 \frac{dy_1}{d\eta} &= y_2 \\
 \frac{dy_2}{d\eta} &= y_3 \\
 \frac{dy_3}{d\eta} &= \frac{(y_1^2 - y_1 y_3) + M y_1}{(1 + \frac{1}{\beta})} \\
 \frac{dy_4}{d\eta} &= y_5 \\
 \frac{dy_5}{d\eta} &= -Pr y_4 y_5
 \end{aligned} \right\} \quad (14)$$

The boundary conditions now become:

$$y_1(0) = 0, y_2(0) = 1, y_3(0) = s_1, y_4(0) = 1, y_5(0) = s_2, y_2(\infty) = 0, y_4(\infty) = 0 \quad (15)$$

Where  $s_1$  &  $s_2$  are determined such that it satisfied  $y_2(\infty) = 0$  &  $y_4(\infty) = 0$ . Thus, to solve this resultant system, we need five initial conditions, but we have only two initial conditions on  $f$  and one initial condition on  $\theta$ . The third condition on  $f$  (i. e.  $f''(0)$ ) and second condition on  $\theta$  (i.e.  $\theta'(0)$ ) are not prescribed which are to be determined by shooting method by using the initial guess values  $s_1$  &  $s_2$  until the boundary conditions  $f_2(\infty) = 0, f_4(\infty) = 0$  (or  $y_2(\infty) = 0, y_4(\infty) = 0$ ) are satisfied. In this way, we employ shooting technique with Runge-Kutta Fehlberg scheme to determine two more unknowns in order to convert the boundary value problem to initial value problem. Once all the five initial conditions are determined the resulting differential equations can then be easily integrated, without any iteration by initial value solver. For this purpose, Runge kutta scheme has been used.

The Same procedure is followed to find the solution of Eq.(15) with PHF boundary conditions.

To study the behavior of the velocity and temperature profiles, various curves are drawn for various values of the physical parameters that describe the flow.

## 5. RESULTS AND DISCUSSION

We have considered the flow and heat transfer of MHD Casson fluid due to linear stretching sheet. Here we have considered two types of heating conditions they are namely, Prescribed Surface Temperature (PST) and Prescribed wall Heat Flux (PHF). The Governing boundary layer equations are solved numerically using Runge-Kutta method with efficient shooting technique by converting partial differential equations into ordinary differential equations by means of suitable similarity transformations.

Fig1: shows the geometry of the considered problem, which shows the heated plate, flow direction etc.

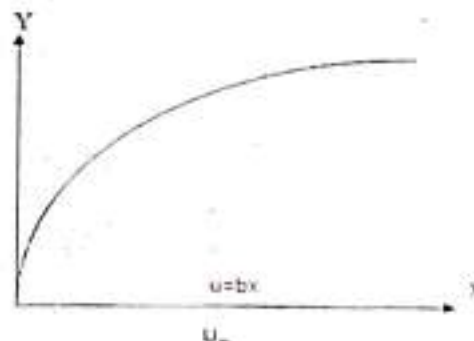


Figure 1 Physical Configuration of Considered Problem

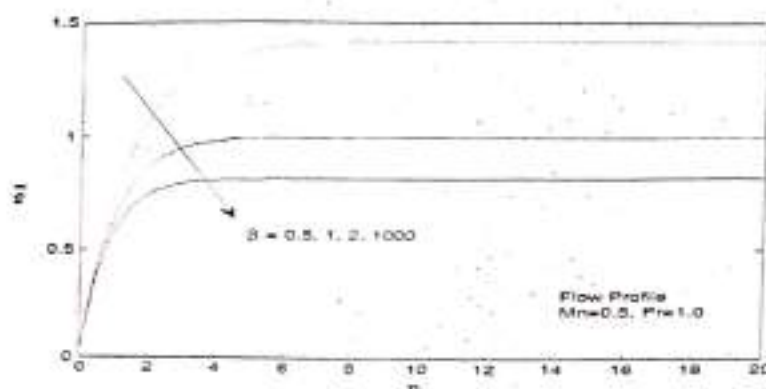


Figure 2 Flow Profile for different values of Casson parameter

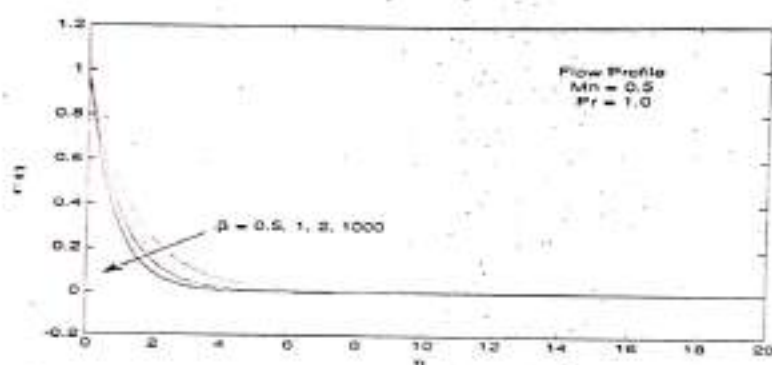


Figure 3 Velocity Profile for different values of Casson parameter

Fig.2: shows the influence of Casson parameter  $\beta$  on flow profile. We observe that the magnitude of flow in the boundary layer decreases with an increase in the Casson fluid parameter  $\beta$ . Also the effect of Casson parameter on velocity is seen in Fig 3. Which depicts that, when Casson parameter  $\beta$  approaches infinity, the problem will reduce to a Newtonian case. Hence increasing value of Casson parameter  $\beta$ , decreases the velocity and boundary layer thickness. Hence velocity decreases with an increase in parametric value of Casson parameter  $\beta$  because of resistance created by Casson parameter in the fluid flow.

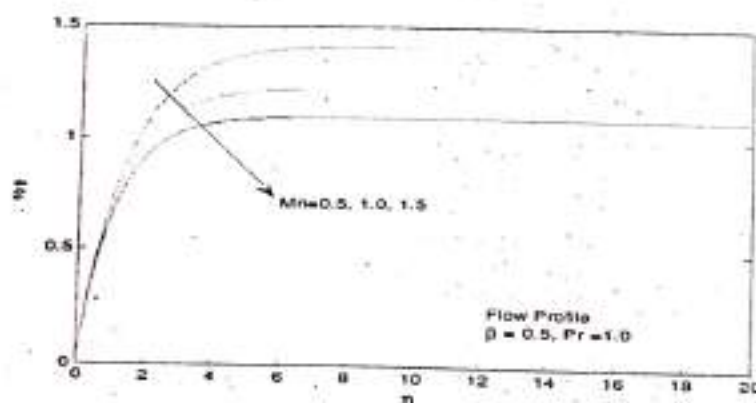


Figure 4 Flow Profile for Different values of Magnetic field parameter

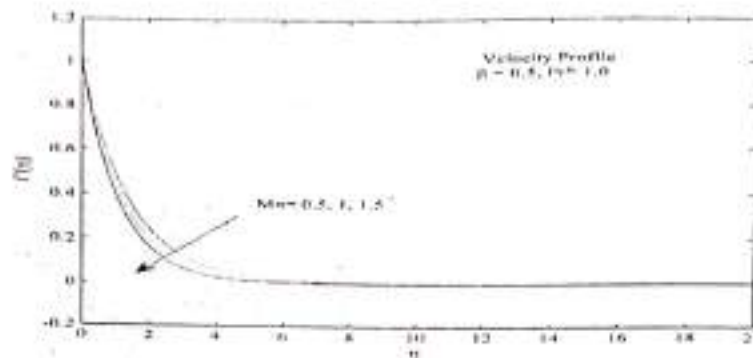


Figure 5 Velocity Profile for Different values of Magnetic field parameter

Figures (4) and (5) show the effect of magnetic parameter  $Mn$  on the flow and velocity profiles respectively, on observing them we can notice that the effect of the magnetic parameter  $Mn$  on flow and the velocity profiles. As the magnetic parameter  $Mn$  increases, the flow and the velocity decreases. Thus the presence of the magnetic field reduces the momentum boundary layer thickness. Physically, the presence of a transverse magnetic (applied normally) field gives rise to a drag force which results in the flow and velocity retardation.

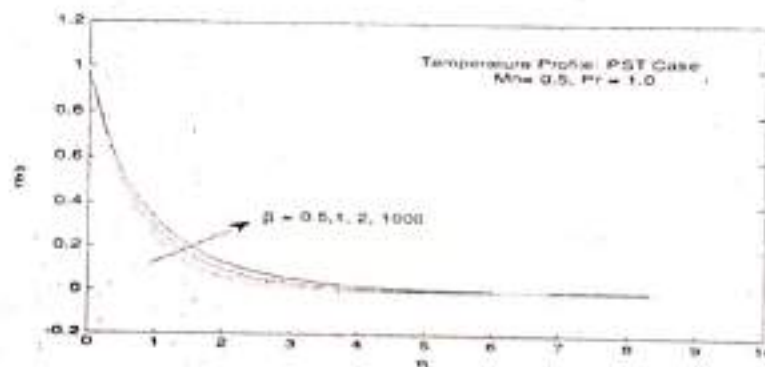


Figure 6 Temperature Profile for different values of Casson parameter in PST Case

Fig.(6): shows the effect of Casson parameter  $\beta$  on the temperature distribution in PST case. The effect of increasing Casson parameter leads to the enhancement of the temperature due to increase in the velocity stress parameter, the same effect is observed in fig (9) for PHF case too.

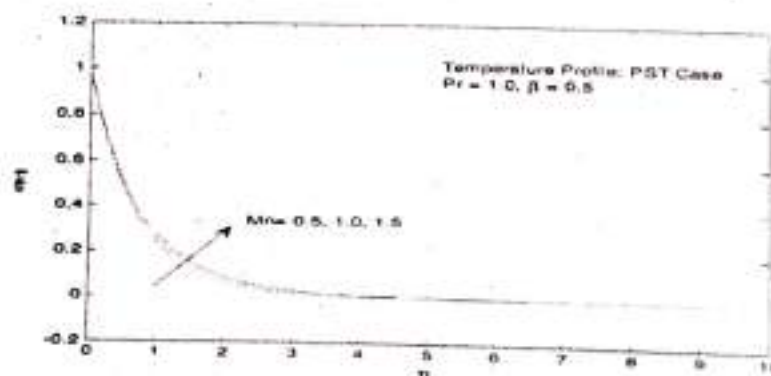


Figure 7 Temperature Profile for different values of Magnetic field parameter in PST Case



In Fig (7), The increase in magnetic field parameter  $Mn$  then it reduces the boundary layer thickness and hence it enhances the temperature profile. Same effect is observed in fig (10) for PHF case too.

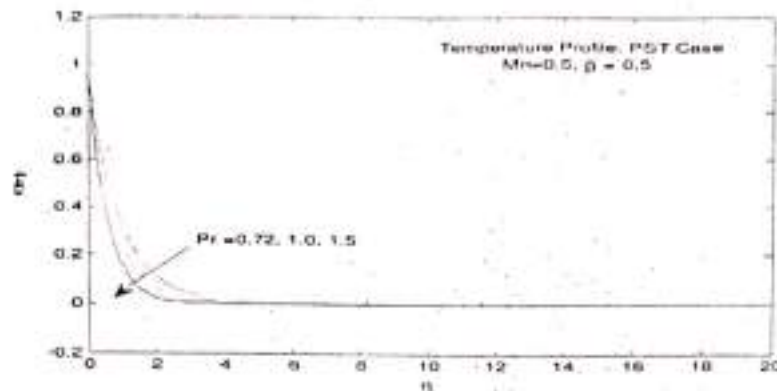


Figure 8 Temperature Profile for different values of Prandtl number parameter in PST Case

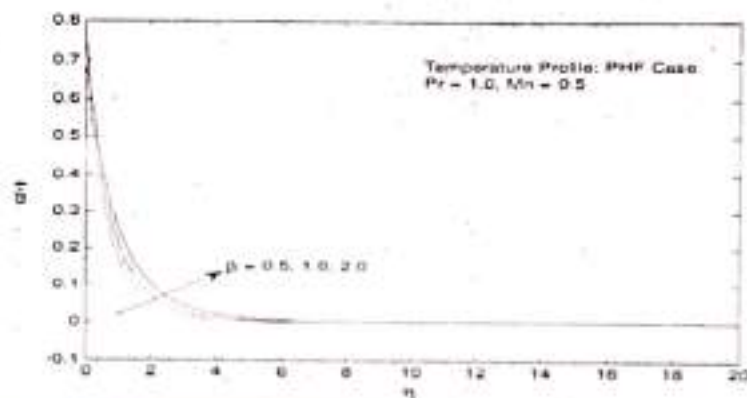


Figure 9 Temperature Profile for different values of Casson parameter in PHF Case

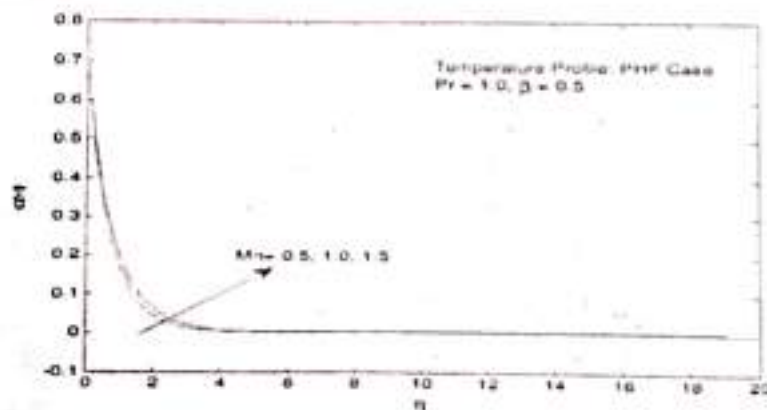


Figure 10 Temperature Profile for different values of Magnetic field parameter in PHF case

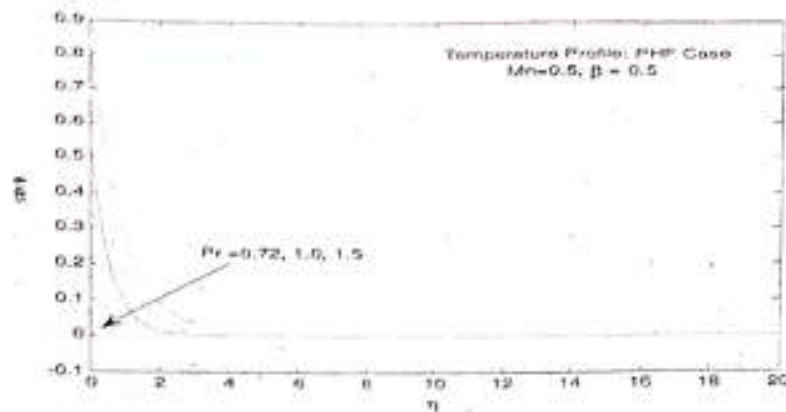


Figure 11 Temperature Profile for different values of Prandtl number parameter in PHF Case

Fig (8) shows the effect of the Prandtl number  $Pr$  on temperature profile. On observing this plot we can conclude that the temperature and the thermal boundary layer thickness decrease as the Prandtl number increases. Same effect is observed in fig (11) for PHF case too.

## 6. CONCLUSIONS

- Here numerical Solutions for MHD flow Casson fluid and heat transfer problems (for PST and PHF cases) are obtained.
- The effect of the Casson fluid parameter  $\beta$  on velocity and temperature are quite opposite.
- The thermal boundary layer thickness decreases with increasing Prandtl number in heat transfer phenomenon for both PST and PHF cases.
- When  $\beta$  tends to infinity, it reduce to the results of Newtonian case

## REFERENCES

- [1] L J Crane; Flow past a stretching plate. *J. Appl. Math. Phy (ZAMP)*, 21 (1970) 645-647.
- [2] T Hayat, S A Shehzad, A Alsaedi, Soret and Dufour; Effects on magneto hydrodynamic flow of Casson fluid, *Appl.Math.Mech*, 33(2012) 1301-1312.
- [3] S Nadeem, U H Rizwan, C Lee; MHD flow of a Casson fluid over an exponentially shrinking sheet, *Scientia Iranica B*, 19(2012),1550-1553.
- [4] S Pramanik; Casson fluid flow and heat transfer past an exponentially porous stretching surface in presence of thermal radiation, *Ain Shams Engg.J (2013) (Article in Press)*
- [5] K Bhattacharya, K Vajravelu, T Hayat; Slip effect on parametric space and the solution for the boundary layer flow of Casson fluid over a non-porous stretching/shrinking sheet. *Int. J. Fluid Mech. Research* 40(2013)482-493
- [6] S Mukhopadhyay, P Ranjan De, K Bhattacharyya, G C Layek; Casson fluid flow over an unsteady stretching surface., *Ain. Shams. Engineering Journal* 2013(4) 933-938.
- [7] M Qasim, S Noreen; Heat transfer in the boundary layer flow of a Casson fluid over a permeable shrinking sheet with viscous dissipation, *Eur.Phys.J.Plus7 (2014) 129*.
- [8] Rizwan-Ul-Haq, S Nadeem, Z H Khan, T G Okedayo; Convective Heat transfer and MHD effects On Casson nano fluid over a shrinking sheet *cent.Eur.J.Phys* 12(12).2014.862-871.
- [9] T Hussain, S A Shehzeb, A Alsaedi, T Hayat, M Ramzon; "Flow of Casson Nano fluid with viscous dissipation and convective conditions. A mathematical model *J Cent.SouthUni*. 22(2015)1132-1140.





- [10] P K Kameshwaran, S Shaw, P Sibanda; Dual solutions of Casson fluid flow over Stretching or Shrinking sheet. *Sadhana* 39(6):2014, 1573-1583.
- [11] Mahantesh M Nandeppanavar; Flow and Heat transfer analysis of Casson fluid due to a stretching sheet. *Advances in Physics Theories and Applications*, (2015) 50:27-34
- [12] Mahantesh M Nandeppanavar; Convective Heat Transfer Analysis of Non-Newtonian Fluid due to a Linear Stretching Sheet, *Chemical and Process Engineering Research* 41 (2016) 1-8.
- [13] Mahantesh M Nandeppanavar; Flow and Heat transfer of Casson fluid due to stretching sheet with convective boundary condition: an analytical solution, *Chemical and Process Engineering Research*, 41 (2016) 10-22.
- [14] H A Attia, M E S Ahmed; Transient MHD Couette flow of a Casson fluid between parallel flow with heat transfer, *Italian J.Pure Appl.Math.* 27(2010)19-38.
- [15] K Bhattacharyya, T Hayat, A Alsaedi; Analytical solution for magnetohydrodynamic boundary layer flow Casson fluid over stretching sheet with wall mass transfer. *Chin.Phys.B* 22(2013)024702.
- [16] S S Mukhopadhyay; Effect of thermal radiation on Casson fluid flow and heat transfer over unsteady stretching surface subject to suction/blowing. *Chin.Phys.B* 22 (2013)114702(pp 1-7).
- [17] S A Shehzad, T Hayat, M Qasim and S Aaghar; Effect of mass transfer on MHD flow of Casson Fluid with chemical reaction and suction, *Brazilian J.Chemical Engineering* 30(2013)187-195.
- [18] B.Lakshmi, G.V.Pradeep, K.Rama Narasimha and K.R.Jaya Kumar, Steady Mixed Convection MHD Boundary Layer Flow and Heat Transfer of Casson Fluid in Presence of Suction and Blowing. *International Journal of Mechanical Engineering and Technology*, 7(5), 2016, pp. 18-30.
- [19] Suresh, P.H. Veena and V. K. Pravin, Study of Performance Evaluation of Domestic Refrigerator working with Mixture of Propane, butane and isobutene Refrigerant (LPG). *International Journal of Mechanical Engineering and Technology*, 7(3), 2016, pp. 161-169.

70



International Journal of Advanced Research in Engineering and Technology (IJARET)  
Volume 8, Issue 1, January- February 2017, pp. 17-33, Article ID: IJARET\_08\_01\_003  
Available online at <http://www.iaeme.com/IJARET/issues.asp?JType=IJARET&VType=8&ITType=1>  
ISSN Print: 0976-6480 and ISSN Online: 0976-6499  
© IAEME Publication

# MIXED CONVECTIVE HEAT AND MASS TRANSFER MHD FLOW PAST AN UNSTEADY STRETCHING SHEET WITH INTERNAL HEAT GENERATION, VISCIOUS DISSIPATION, INTERNAL MASS DIFFUSION INCLUDING SORET AND DOFOUR EFFECTS

N. Raveendra

Assistant Professor, Raja Rajeswari College of Engineering,  
Ramohalli Cross, Bangalore, Karnataka, India

P.H. Veena

Associate Professor, Department of Mathematics,  
Smt. V.G. College for Women, Kalaburagi, Karnataka, India

V.K. Pravin

Professor, Department of Mechanical Engineering,  
P.D.A College of Engineering, Kalaburagi, Karnataka, India

## ABSTRACT

Mixed two dimensional convection heat and mass transfer flow with suction, viscous dissipation, heat source/sink effect, mass diffusion including Soret and Dufour effects due to an unsteady porous stretching sheet is studied in the present analysis. The flow is subjected to magnetic field normal to the vertical plate in a saturated porous medium. The governing non-linear partial differential equations have been reduced to ordinary differential equations using suitable similarity transformation variables. The resultant equations which are coupled and highly non-linear are solved by standard Runge-Kutta fourth order numerical technique via shooting method. The momentum, temperature and concentration field distributions are analyzed and discussed numerically and presented pictorially through graphs. Numerical values for skin friction coefficient, local Nusselt number and Sherwood number at the plate in the presence of magnetic field and porous medium are derived and discussed for various values of physical parameters and are presented in table. Finally the present results are compared with previously published results and found to be well in agreement.

**Key words:** Mixed Convection, Heat and Mass Transfer, Heat Source/Sink, MHD, Porosity, Stretching Sheet.

PRINCIPAL  
Smt. V.G. Degree College for Women,  
KALABURAGI.

S.G. Gouhalli  
IQAC Co-ordinator

Smt. V.G. Women's Degree College,  
KALABURAGI  
[www.iaeme.com/IJARET/index.asp](http://www.iaeme.com/IJARET/index.asp)





**Cite this Article:** N. Raveendra, P.H. Veena and V.K. Pravin, Mixed Convective Heat and Mass Transfer MHD Flow Past an Unsteady Stretching Sheet with Internal Heat Generation, Viscous Dissipation, Internal Mass Diffusion Including Soret and Dofour Effects. *International Journal of Advanced Research in Engineering and Technology*, 8(1), 2017, pp 17-33.  
<http://www.iaeme.com/IJARET/issues.asp?JType=IJARET&VType=8&IType=1>

## NOMENCLATURE

- $u, v, T$  and  $C$  are the fluid  $x$  and  $y$  components of velocity, temperature and concentration
- $\nu$  Fluid Kinematic Viscosity
- $\rho$  Density
- $\sigma$  Electric Conductivity of the Fluid
- $\beta_T$  and  $\beta_C$  Coefficients of Thermal and Concentration
- $\alpha$  Thermal Conductivity
- $C_\infty$  Free Stream Concentration
- $B_0$  Magnetic Induction
- $U$  Free Stream Velocity
- $D_m$  Mass Diffusivity
- $T_w$  Temperature of the Hot Fluid at the Left Surface of the Plate
- $C_w$  Species Concentration at the Plate Surface.
- $\eta$  Similarity Variable
- $f$  Dimensionless Stream Function
- $\theta$  Dimensionless Temperature
- $\phi$  Dimensionless Concentration
- $M$  Magnetic Field Parameter
- $Gr$  Thermal Grashof number
- $Gc$  Solutal Grashof Number
- $D_f$  Dufour Number
- $S_r$  Soret Number
- $Q$  Heat Generation/Absorption Parameter
- $P_r$  Prandtl Number
- $S_c$  Schmidt Number
- $A_1$  Unsteady Parameter
- $f_w$  Suction Parameter
- $K$  Chemical Reaction Parameter
- $k_2$  Permeability Parameter





## 1. INTRODUCTION

Mixed convection is often observed in very high power output devices where the forced convection is insufficient to dissipate all of the heat necessary. At this situation combining natural convection with forced convection will often give good results. Nuclear Reactor technology and some electronic cooling devices play an important role in this. Heat and Mass transfer phenomena play an important role in manufacturing industries for the design of steel rolling and, nuclear power plants, gas turbines and various propulsion devices for furnace design, energy utilization and temperature measurements. Study of heat transfer with visco-elastic flow induced by heated stretching surfaces is often encountered in many engineering applications, such as materials manufactured by extrusion process, wire and fiber coating, cooling of metallic sheets or electronic chips, crystal growing.

In this regard Loganathan [1] Analyzed about the study of thermal conductivity on unsteady MHD free convective flow over a semi infinite vertical plate. Vidyasagar and Bala [2] studied the MHD convective heat and mass transfer flow over a permeable stretching surface with suction and internal heat generation/absorption. Krishna et al. [3] Investigated the effects of radiation and chemical reaction on MHD convective flow over a permeable stretching a surface with suction and heat generation. Ramana et al. [4] studied the Thermal Diffusion and chemical reaction effects on unsteady MHD dusty viscous flow. Bhattacharyya and Mukhopadhyay [5] Studied similarity solutions of mixed convective boundary layer slip flow over a vertical plate. Makinde [6] made a study on MHD heat and mass transfer flow over a moving vertical plate with a convective surface boundary condition. Usman and Uwanta [7] analysed the Effect of thermal conductivity on MHD heat and mass transfer flow past an infinite vertical plate with Soret and Dufour effects. Makinde [8] made Computational modeling of MHD unsteady flow and heat transfer toward a flat plate with navier slip and newtonian heating. Olanrewaju [9] investigated the Effects of thermal-diffusion, diffusion-thermo, magnetic field and viscous dissipation on unsteady mixed convection flow past a porous plate moving through a binary mixture of chemically reacting fluid. Singh [10] studied MHD slip flow of viscous fluid over an isothermal reactive stretching sheet. Shankar [11] made an analysis on Radiation and mass transfer effects on MHD free convection fluid flow embedded in a porous medium with heat generation/absorption. Mohammed and Bhaskar [12] studied the Similarity solutions of heat and mass transfer for natural convection over a moving vertical plate with internal heat generation and a convective boundary condition in the presence of thermal radiation, viscous dissipation and chemical reaction. Sharma and Borgohain [13] Studied the influence of chemical reaction, Soret and Dufour effects on heat and mass transfer of a binary fluid mixture in porous medium over a rotating disk. Ibrahim [14] found out the Effects of chemical reaction on dissipative radiative MHD flow through a porous medium over a non-isothermal stretching sheet. Ali-Chamkha and Mansour [15] worked on Unsteady MHD free convective heat and mass transfer from a vertical porous plate with hall current, thermal radiation and chemical reaction effects. Ambreen et al. [16] stressed on the Effects of variable viscosity on the flow of non-Newtonian fluid through a porous medium in an inclined channel with slip conditions. Hassan and Soleiman [17] examined the Effects of MHD and temperature dependent viscosity on the flow of non-Newtonian nanofluid in pipe: analytical solutions. Mohammed and Nourazar [18] have studied the conjugated forced convection heat transfer from a heated flat plate of finite thickness and temperature dependent thermal conductivity. Shakhaoath et al. [19] made a study on possessions of chemical reaction of MHD heat and mass transfer of nanofluid flow on a continuously moving surface. Ali et al. [20] Studied on the solution of characteristic value problems arising in linear stability analysis; semi-analytical approach. Shyam et al. [21] investigated the MHD free convection radiation interaction along a vertical surface embedded in darcian porous medium in presence of soret and dufour effects. Salem [22] studied the effects of variable viscosity, viscous dissipation and chemical reaction on heat and mass transfer flow of MHD micro-polar fluid along a permeable stretching sheet in a non-Darcian porous medium. Oahimire and Olajuwon [23] Effect of hall current and thermal radiation on heat and mass transfer of a chemically reacting MHD flow of a micro-polar fluid through a porous medium. Sarya Narayana et al. [24] Effects of hall current and radiation absorption on MHD micro-polar fluid in a rotating system. Adeniyani



and Adigun [25] Transient MHD boundary-layer slip-flow of heat and mass transfer over a stretching surface embedded in porous medium with waste discharge concentration and convective boundary conditions. Srinivasacharya and Ram Reddy [26] Soret and Dufour effects on mixed convection from an exponentially stretching surface. Al-Odat and Al-Ghamdi [27] Dufour and Soret effects on unsteady MHD natural convection flow past vertical plate embedded in non-Darcy porous medium. Magyari and Keller [28] studied heat and mass transfer in the boundary layers on an exponentially stretching continuous surface. Srinivasacharya and Ram Reddy [29] investigated the effects of Soret and Dufour on mixed convection from an exponentially stretching surface. Subhakar and Gangadhar [30] analyzed the effects of Soret and Dufour on MHD free convection heat and mass transfer flow over a stretching vertical plate with suction and heat source/sink.

## 2. FORMULATION OF THE PROBLEM

The governing equations under unsteady condition are represented by:

$$\frac{\partial u}{\partial x} + \frac{\partial v}{\partial y} = 0 \quad (1)$$

$$\frac{\partial u}{\partial t} + u \frac{\partial u}{\partial x} + v \frac{\partial u}{\partial y} = \nu \frac{\partial^2 u}{\partial y^2} - \frac{\sigma B_0^2}{\rho} u + g\beta_T(T - T_\infty) + g\beta_c(C - C_\infty) - \frac{\nu}{k} u \quad (2)$$

$$\frac{\partial T}{\partial t} + u \frac{\partial T}{\partial x} + v \frac{\partial T}{\partial y} = \alpha \frac{\partial^2 T}{\partial y^2} + \frac{D_m K_T}{c_s c_p} \frac{\partial^2 C}{\partial y^2} + q(T - T_\infty) + \frac{\mu}{\rho c_p} \left( \frac{\partial u}{\partial y} \right)^2 \quad (3)$$

$$\frac{\partial C}{\partial t} + u \frac{\partial C}{\partial x} + v \frac{\partial C}{\partial y} = D_m \frac{\partial^2 C}{\partial y^2} + \frac{D_m K_T}{T_\infty} \frac{\partial^2 T}{\partial y^2} - k_1(C - C_\infty) \quad (4)$$

The boundary conditions for the velocity, temperature and concentration fields are

$$\begin{aligned} u = U, \quad v = V_w, \quad T = T_w, \quad C = C_w \quad \text{at} \quad y = 0 \\ u \rightarrow 0, \quad T \rightarrow T_\infty, \quad C \rightarrow C_\infty, \quad \text{as for} \quad t > 0 \end{aligned} \quad (5)$$

The mass concentration equation (1) is satisfied by the Cauchy-Riemann equations

$$u = \frac{\partial \psi}{\partial y}, \quad v = -\frac{\partial \psi}{\partial x} \quad (6)$$

Where  $\psi(x, y)$  is the stream function.

To transform (2) – (4) into a set of ordinary differential equations, the following similarity transformations and dimensionless variables are introduced

$$\begin{aligned} \eta = y \sqrt{\frac{c}{\nu(1-\lambda t)}}, \quad \psi = x \sqrt{\frac{c\nu}{(1-\lambda t)}} f(\eta) \\ T = T_\infty + T_w \left[ \frac{cx}{2\nu(1-\lambda t)^2} \right] \theta(\eta), \quad C = C_\infty + C_w \left[ \frac{cx}{2\nu(1-\lambda t)^2} \right] \phi(\eta) \\ M = \frac{\sigma B_0^2(1-\lambda t)}{\rho c}, \quad Gr = \frac{g\beta_T T_w}{2c\nu}, \quad Gc = \frac{g\beta_c C_w}{2c\nu}, \quad D_f = \frac{D_m k_T C_w}{\nu c_s c_p T_w}, \quad Sr = \frac{D_m k_T C_w}{\nu T_w C_w} \end{aligned}$$

$$Pr = \frac{\nu}{\alpha}, Sc = \frac{\nu}{D_m}, A = \frac{\lambda}{c}, Ec = \frac{2cx\nu}{T_w c_p}, K = \frac{k_1}{c} (1 - \lambda t)$$

Making use of (7), the continuity (1) is automatically satisfied and equations (2) - (4) reduce to

$$f'''(\eta) + f(\eta)f''(\eta) - \frac{A}{2}\eta f''(\eta) + Gr\theta(\eta) + Gc\phi(\eta) - (f'(\eta))^2 - (M + A - K)f'(\eta) = 0 \quad (8)$$

$$\theta''(\eta) + Pr \left[ f(\eta)\theta'(\eta) - \frac{A}{2}\eta\theta'(\eta) - \theta'(\eta) + D_f\phi''(\eta) - 2A\theta + K\theta + Ec(f''(\eta))^2 \right] = 0 \quad (9)$$

$$\phi''(\eta) + Sc \left[ f(\eta)\phi'(\eta) - \frac{A}{2}\eta\phi'(\eta) - \phi(\eta)f'(\eta) + Sr\theta'(\eta) - 2A\phi \right] = 0 \quad (10)$$

The corresponding boundary conditions (5) converted to

$$\begin{aligned} f = fw, \quad f' = \theta, \quad \phi = 1 \quad \text{at} \quad y = 0 \\ f' = 0, \quad \theta = 0, \quad \phi = 0 \quad \text{as} \quad y \rightarrow \infty \end{aligned} \quad (11)$$

Where prime denotes derivative w.r.t  $\eta$  and  $fw$  is the suction parameter.

The local skin friction coefficient, the local Nusselt number and Sherwood number which are respectively proportional to  $f''(0)$ ,  $-\theta'(0)$  and  $-\phi'(0)$  are derived and their numerical values are presented in a tabular form.

### 3. SOLUTION OF THE PROBLEM

Higher order non-linear differential equations (8) - (10) are converted into initial value problems by using shooting technique and then set of coupled non-linear governing boundary layer equations are solved numerically using Runge-Kutta method of fourth order.

### 4. RESULT AND DISCUSSION

Numerical calculations have been carried out for different values of  $\beta$ ,  $Nr$ ,  $Pr$ ,  $K$ ,  $Sc$ ,  $Gr$ ,  $Gc$ ,  $A$ ,  $D_f$ ,  $Sr$ ,  $Ec$ ,  $M$ . The effect of magnetic parameter on the velocity field for  $Pr=0.7, Sc=0.2, Gr=0.5, Gc=0.5, A=0, D_f=0.5, Sr=0, K=0.5$  and  $Ec=1$  are shown in fig.1. It is seen from this figure that the velocity profiles decrease monotonically with an increase of magnetic parameter. The effect of suction parameter on the velocity field is shown in fig. 2. It is seen from the figure that the velocity profiles decrease gradually with an increase of suction parameter which indicating the usual fact that suction stabilizes the boundary layer growth. The effect of Grashof number on the velocity field is shown in fig.3. It is observed that from the figure as the Grashof number increases the velocity profile increases. The variation of Solutal Grashof number on the velocity profiles are shown in fig.4. It is noticed from the figure that with increase in Solutal Grashof number velocity profile also increases. Fig. 5 illustrates the effect of unsteady parameter on the velocity. It is found that the velocity boundary layer thickness decreases with increasing in the unsteady parameter. Fig. 6 shows the variation of velocity boundary layer with the Soret number. It is found that the velocity boundary layer thickness decreases with an increase in the Soret number. Figure 7 shows the variation of velocity profiles for different values of Eckert number. It is found that the velocity increases with increasing the values of Eckert number. The effect of suction parameter on temperature profile is shown in fig.8. It is clearly shows that as we increase suction parameter  $fw$  by keeping all other parameters as constants, the temperature also decreases. The effect of magnetic field strength on the temperature profile is shown in fig.9. It is found from the graph that as we increase magnetic field strength parameter  $M$  the temperature profile increases. Fig.10 shows the variation of temperature profiles for different values of  $Gr$ . It is seen from the figure that temperature profile



decreases with an increasing of Grashof number  $Gr$ . The influences of Schmidt parameter  $Sc$  on the temperature profile across the boundary layer are presented in fig.11. It is obvious that the influence of Schmidt parameter increasing values of  $Sc$ , the temperature distribution across the boundary layer increases. The effect of Solutal Grashof number on the temperature profile is shown in fig. 12. From this figure, it is noticed that the temperature profile decreases with an increasing the values of Solutal Grashof number  $Gc$ . Fig.13 illustrates the effect of the Prandtl number  $Pr$  on the temperature . It is observed that as the Prandtl number increases, the temperature decreases. The variation of thermal boundary layer with Dufour number  $Df$  is shown in fig.14. It is observed from the graph that thermal boundary layer increases with an increase in the Dufour number. The variation of unsteadiness parameter  $A1$  on the temperature field is shown in fig.15. The thermal boundary layer decreases with an increasing the values of unsteadiness parameter. The effect of chemical reaction parameter on the temperature field is shown in fig.16. It is noticed from the figure that the temperature profile increases with increasing the values of chemical reaction parameter  $K$ . Fig-17 shows the effect of Eckert number  $Ec$  on the temperature field. It is observed from the graph that the thermal boundary layer increases with increasing values of  $Ec$ . The influence of suction parameter  $fw$  on the temperature field is shown in fig.18. As the suction parameter increases the concentration increases. The variation of buoyancy parameter  $Gr$  on the concentration field is shown in fig.19. It is observed that the concentration boundary layer thickness decreases with an increase in the thermal Grashof number. The variation of Schmidt number  $Sc$  on the concentration field is shown in fig.20. It is observed that as the Schmidt number increases, there is a decreasing trend in the concentration field. The effect of Solutal Grashof number  $Gc$  on the concentration field is shown in fig.21. It is noticed that the concentration boundary layer thickness decreases with an increase in the Solutal Grashof number. The variation of Soret number  $Sr$  on the concentration field is shown in fig.22. It is noticed that the concentration boundary layer thickness decreases with an increase in the Soret number  $Sr$ . The effect of unsteadiness parameter  $A1$  on the concentration field is shown in fig.23. It is observed that there is decreasing trend in the concentration boundary layer as the unsteadiness parameter  $A1$  increases. The effect of Dufour number  $Df$  on the concentration field is shown in fig.24. There is an increasing trend in the concentration boundary layer thickness as the Dufour number  $Df$  increases. The variation of chemical reaction parameter on the concentration field is shown in fig.25. It is noticed from the figure that concentration boundary layer thickness increases with increasing values of chemical reaction parameter  $K$ . The effect of Eckert number  $Ec$  on the concentration field is shown in fig.26. It is observed that as the Eckert number  $Ec$  increases there is an increase in the boundary layer thickness. The effect of Magnetic field  $M$  on the concentration boundary layer is shown in fig.27. It is noticed that as the magnetic parameter increases the thickness of concentration boundary layer increases.

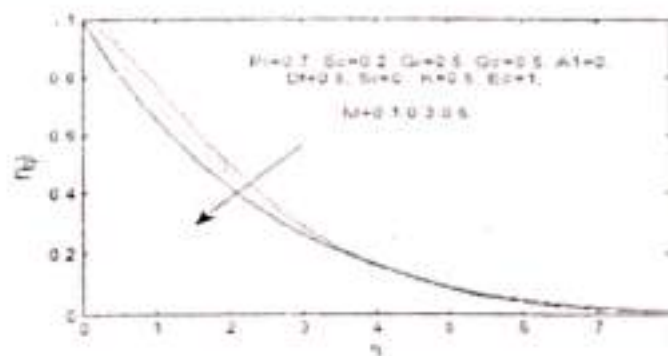


Figure 1 Longitudinal Velocity Profiles for Different Values of Magnetic Parameter  $M$

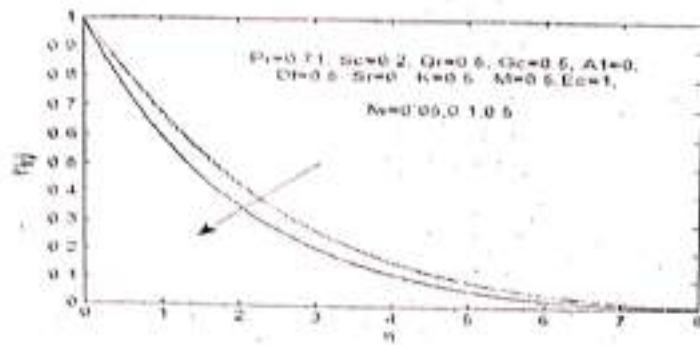


Figure 2 Longitudinal Velocity Profiles for Different Values of Suction Parameter  $f_w$

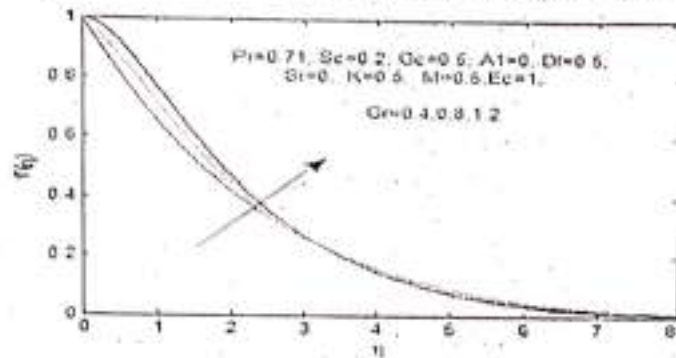


Figure 3 Velocity Profiles for Different Values of Grashof Number  $Gr$

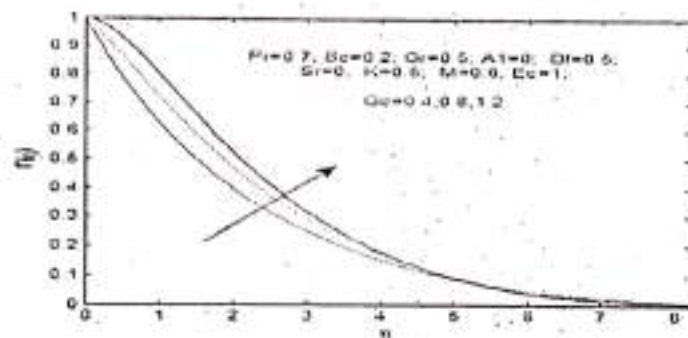


Figure 4 Velocity Profiles for Different Values of Modified Grashof Number  $G_c$

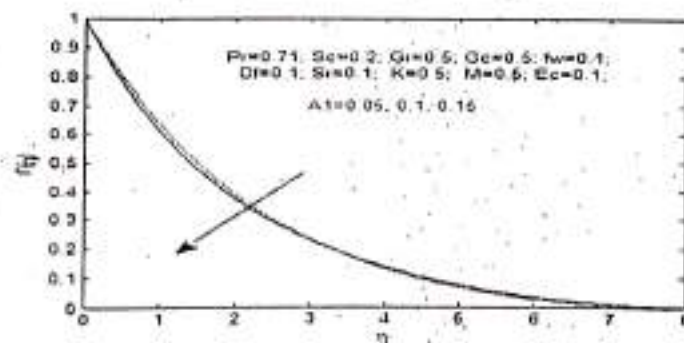


Figure 5 Velocity Profiles for Different Values of Unsteady Parameter  $A_1$





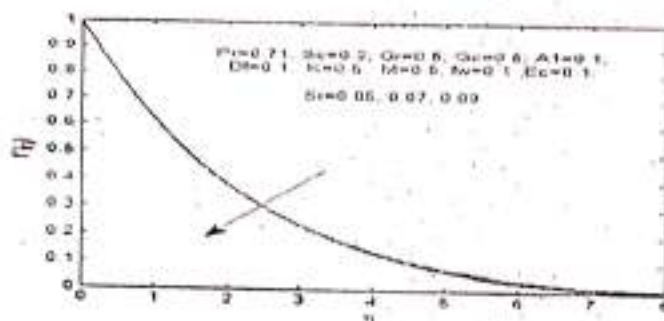


Figure 6 Velocity Profiles for Different Values of Soret Number  $Sr$

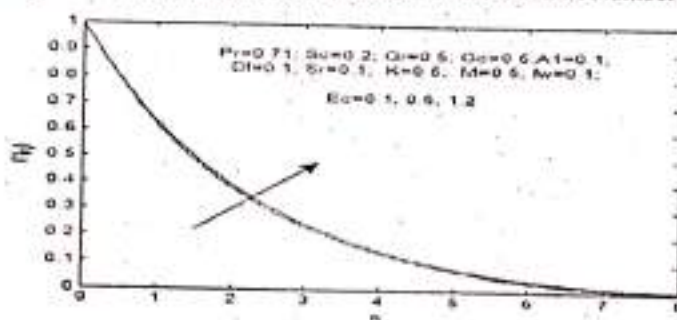


Figure 7 Velocity Profiles for Different Values of Eckert Number  $Ec$

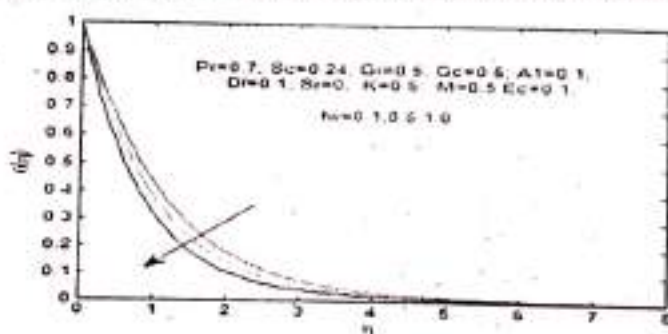


Figure 8 Temperature Profiles for Different Values of Suction Parameter  $fw$

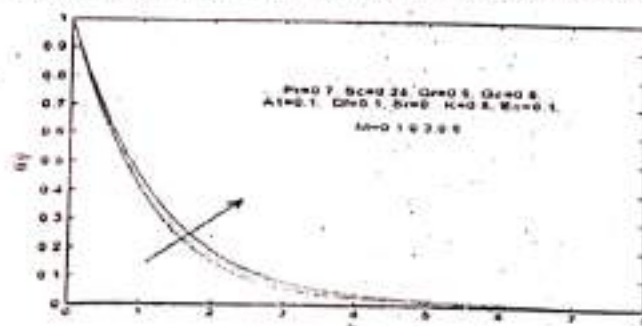


Figure 9 Temperature Profile for Different Values of Magnetic Parameter  $M$

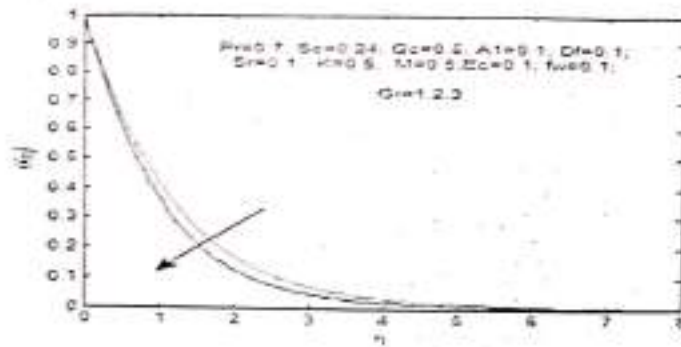


Figure 10 Temperature Profiles for Different Values of Thermal Grashof Number Gr

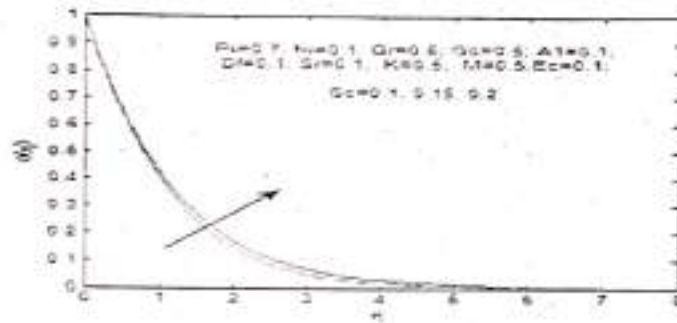


Figure 11 Temperature Profiles for Different Values of Schmidt Number Sc

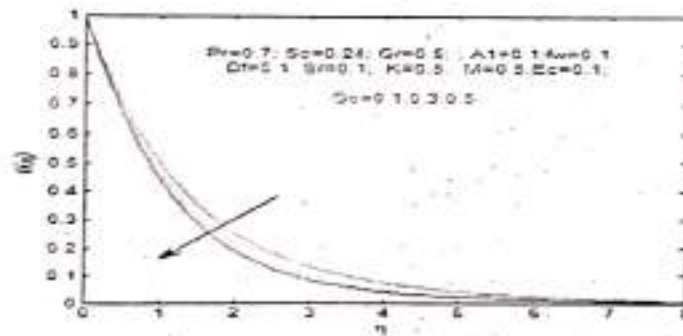


Figure 12 Temperature Profiles for Different Values of Solutal Grashof Number Gc

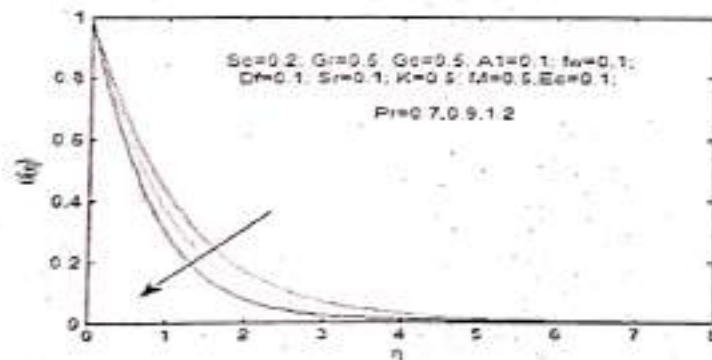


Figure 13 Temperature Profiles for Different Values of Prandtl Number Pr

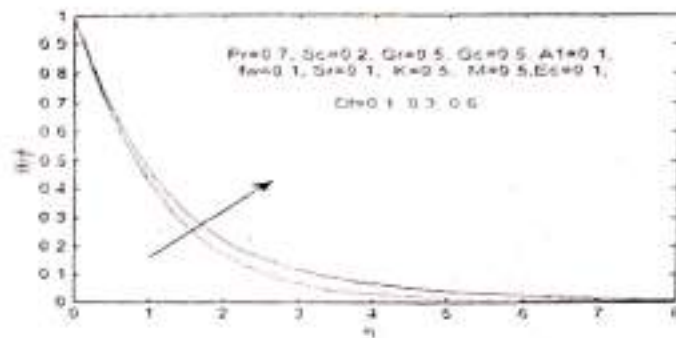


Figure 14 Temperature Profiles for Different Values of Dufour Number Df

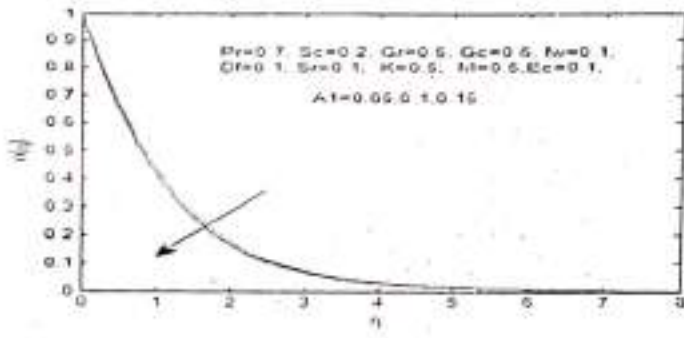


Figure 15 Temperature Profiles for Different Values of Unsteady Parameter A1

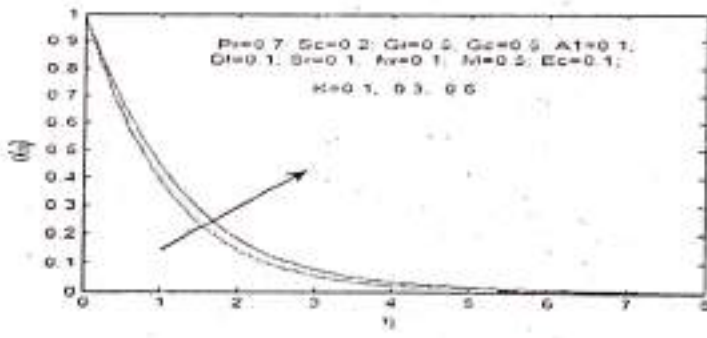


Figure 16 Temperature Profiles for Different Values of Chemical Reaction Parameter K

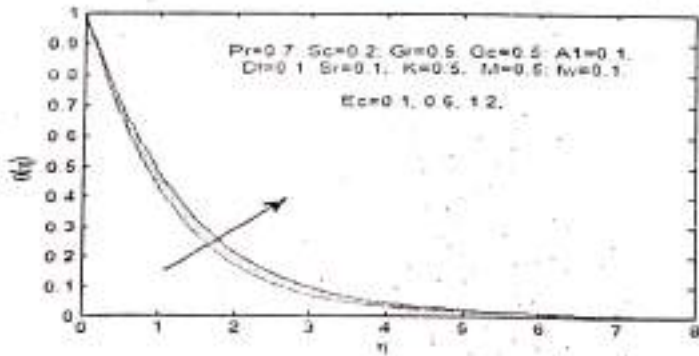


Figure 17 Temperature Profiles for Different Values of Eckert Number Ec

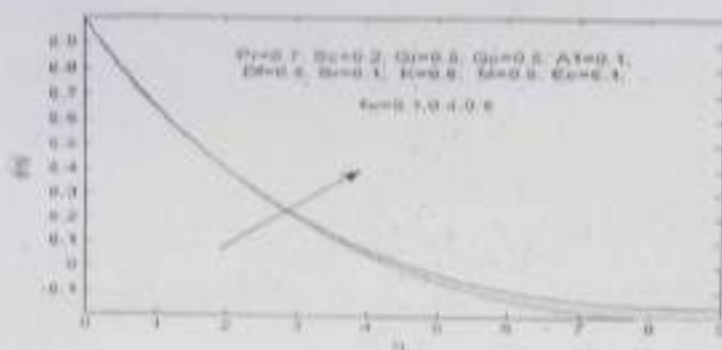


Figure 18 Concentration Profiles for Different Values of Suction Parameter  $f_w$

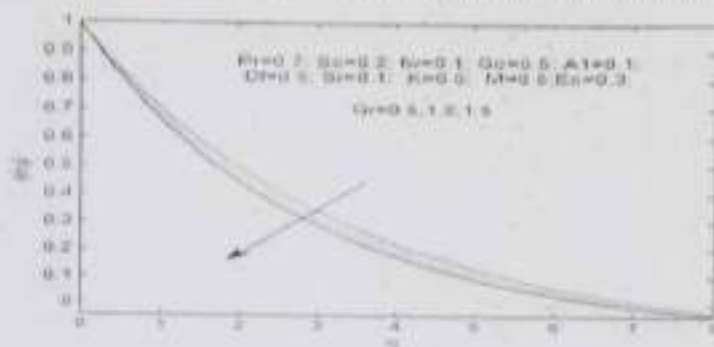


Figure 19 Concentration Profiles for Different Values of Thermal Grashof Number  $Gr$

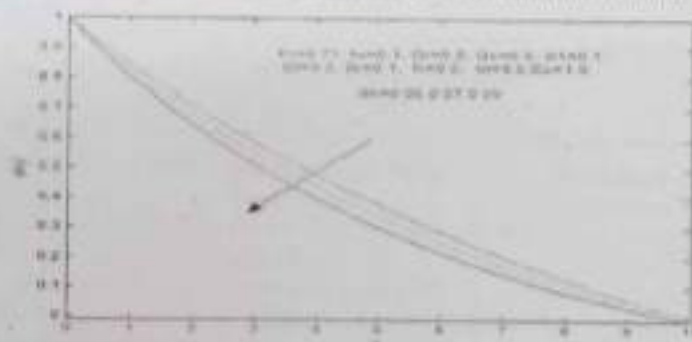


Figure 20 Concentration Profiles for Different Values of Schmidt Number  $Sc$

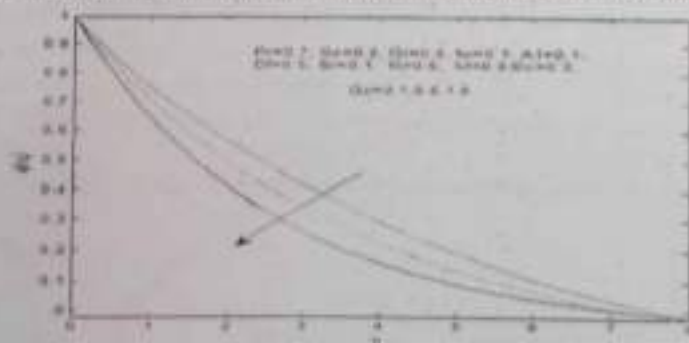


Figure 21 Concentration Profiles for Different Values of Solutal Grashof Number  $G_c$

61



## Influence of Porosity and Magnetic Field with Dissipative Heat Transfer Flow over a Stretching Surface through UCM Fluid

N. Raveendra<sup>1</sup> P.H. Veena<sup>2</sup> V.K. Pravin<sup>3</sup>

1. Asst. Prof. RajaRajeswari College of Engineering, Ramohalli Cross, Bengaluru-560074, Karnataka

2. Asso. Prof. Dept. of Mathematics, Smt. V.G. College for Women, Kalaburgi-585102, Karnataka

3. Prof. Dept. of Mechanical Engg. P.D.A College of Engg, Kalaburgi-585102, Karnataka

### Abstract

The purpose of present analysis is to examine the effects of transverse magnetic field within a boundary layer of an upper-Convected Maxwell (UCM) fluid over a stretching surface through porous media. The requisite partial differential equations are converted into ordinary differential equations by using similarity transformations. Resultant equations are highly non-linear which cannot be solved analytically. Hence those equations are solved numerically by using efficient numerical shooting technique with fourth order Runge-Kutta method. The main aim of the present work is to analyze the effect of elastic parameter  $\beta$ , magnetic parameter  $Mn$  and thermal conductivity  $k_2$  on the temperature field above the sheet. The previous results are compared with our present results and are shown in tabulation and represented graphically

**Keywords:** Upper-Convected Maxwell fluid, Boundary layer, Stretching surface, Similarity transformation, Magnetic parameter, Porous media, Viscous dissipation.

### Nomenclature:

$u$	Velocity in x direction
$v$	Velocity in y direction
$B_0$	Strength of the magnetic field
$\nu$	Kinematic viscosity of the fluid
$\lambda$	Relaxation time parameter of the fluid
$T_w$	Wall Temperature
$T_\infty$	Temperature far away from the sheet.
$T_0$	Melt Temperature at the die exit
$T-T_0$	Melt solidification temperature
$L$	Distance between the die exit and the point which the melt solidifies
$k_2$	Thermal conductivity of the fluid
$b$	Constant whose value also depends on the fluid
$Mn$	Magnetic parameter
$\beta$	Elastic parameter
$Ec$	Eckert number
$Pr$	Prandtl number
$\rho$	Density
$\mu$	Dynamic viscosity
$C_p$	Specific constant pressure
$f$	Dimensionless stream function
$g$	Acceleration due to gravity
$c$	Stretching parameter

### Introduction

In recent years behaviors of non-Newtonian fluids have been studied due to the wide range of engineering and industrial applications. The dynamics of non-Newtonian fluids is a popular area of research owing to its ever increasing applications in chemical and process engineering. Hence several constitutive equations of non-Newtonian fluids have been presented over the past decades.

In view of these applications Hayat et al. [1] have studied about melting heat transfer in a boundary layer flow of a second grade fluid under Soret and Dufour effects. Pop et al. [2] have discussed MHD flow and heat transfer of a UCM fluid over stretching surface with variable thermo physical properties. Vimsala and Loganathan [3] have analyzed the MHD flow of nano-fluids over an exponentially stretching sheet embedded in a stratified medium with suction and radiation effects. Shateyi and Marewo [4] have attained the numerical approach of MHD flow, heat and mass transfer for the UCM fluid over a stretching surface in the presence of thermal radiation. Rahman and Salabuddin [5] have experimented through hydro magnetic field, heat and mass transfer flow over an inclined heated surface with variable viscosity. Prasad et al. [6] have investigated the effect

S.G. Gowda  
IQAC Co-ordinator  
Smt. V.G. Women's Degree College,  
KALABURAGI

Smt. V.G. Degree College for Women,  
KALABURAGI.



of variable viscosity on MHD viscoelastic fluid flow and heat transfer over a stretching sheet. Pohni et al. [7] have investigated the flow and heat transfer over an unsteady shrinking sheet with suction in nano-fluids. Ishak et al. [8] have discussed heat transfer in nanofluids. Hayat et al. [9] have elaborated an unsteady boundary layer flow and heat transfer of a porous fluid over a permeable shrinking sheet. Singh et al. [10] have illustrated the influence of thermal radiation and magnetic field on unsteady stretching permeable sheet in presence of free stream velocity. Motin [11] has studied on a new spectral local linearization method for non-linear boundary layer flow problems. Mahian et al. [12] have studied the applications of nano fluids in solar energy systems. Anjumana [13] has studied porous fluid flow of variable viscosity and thermal conductivity along exponentially stretching surface. Aldam et al. [14] have analyzed the MHD boundary layer flow of an UCM fluid through porous channel. Rahman and Eltayeb [15] have made a study on radiative heat transfer in a hydro magnetic flow nano-fluid past a non linear stretching surface with convective boundary condition. Abel et al. [16] have analyzed MHD flow and heat transfer for the UCM fluid over a stretching sheet. Prasad et al. [17] have examined the influence of internal heat generation/absorption, thermal radiation, magnetic field, variable fluid property and viscous dissipation on heat transfer characteristics of a Maxwell fluid over a stretching sheet. Mahmoud and Megahed [18] have studied the non uniform heat generation effect on heat transfer of a non-Newtonian power-law fluid over a non linearly stretching sheet. Bhattacharyya Krishnaudu [19] have discussed in their experiment that the boundary layer flow and heat transfer over an exponentially shrinking sheet. Sastri et al. [20] have made study on spectral relaxation method for entropy generation on a MHD flow and heat transfer of a Maxwell fluid.

**Mathematical Formulation:**

The governing equations of continuity, momentum and energy for the magneto hydro dynamic flow of an incompressible Upper Convected Maxwell fluid over the stretching surface through porous media are presented as

$$\frac{\partial u}{\partial x} + \frac{\partial v}{\partial y} = 0 \tag{1}$$

$$u \frac{\partial u}{\partial x} + v \frac{\partial u}{\partial y} - \nu \frac{\partial^2 u}{\partial y^2} - \lambda \left[ u^2 \frac{\partial^2 u}{\partial x^2} + v^2 \frac{\partial^2 u}{\partial y^2} + 2uv \frac{\partial^2 u}{\partial x \partial y} \right] - \frac{\sigma B_0^2}{\rho} u - \frac{\nu}{k} u \tag{2}$$

$$u \frac{\partial T}{\partial x} + v \frac{\partial T}{\partial y} = \frac{k}{\rho C_p} \frac{\partial^2 T}{\partial y^2} + Q(T - T_\infty) + \mu \left( \frac{\partial u}{\partial y} \right)^2 \tag{3}$$

Here adopted two kinds of heating boundary conditions namely PST & PHF

(i) **Prescribed Power-Law Surface Temperature (PST):** In this case the respective boundary conditions are as follows.

$$u = Bx; \quad v = 0; \quad T = T_w(x) = T_\infty - T_s \left( \frac{x}{L} \right)^2 \quad \text{at} \quad y = 0$$

$$u \rightarrow 0; \quad T \rightarrow T_\infty \quad \text{as} \quad y \rightarrow \infty;$$

(ii) **Prescribed Power-Law Heat Flux (PHF):** In this case the boundary conditions are

$$u = Bx; \quad q_w = -k \left( \frac{\partial T}{\partial y} \right)_w = b \left( \frac{x}{L} \right)^2 \quad \text{at} \quad y = 0$$

$$u \rightarrow 0; \quad T \rightarrow T_\infty \quad \text{as} \quad y \rightarrow \infty \tag{4}$$

**Method of Solution**

Introducing the following dimensionless similarity variables

$$u = Bx f'(\eta), \quad v = \sqrt{bB} f(\eta), \quad \eta = \sqrt{\frac{B}{\nu}} y, \quad \theta(\eta) = \frac{T - T_\infty}{T_w - T_\infty}, \quad g(\eta) = \frac{T - T_\infty}{b \left( \frac{x}{L} \right)^2 \frac{1}{k} \frac{\nu}{b}} \tag{5}$$

Governing equations (1)-(3) can be transformed exactly into a set of ordinary differential equations as

$$f^{(4)} - M \eta f' - (f'')^2 + f f^{(3)} + \beta (2 f f' f'' - f^2 f''') - k_2 f^3 = 0 \tag{6}$$



$$\theta'' = Pr[2f'\theta - f\theta' - \beta\theta - Ec(f'')^2] \quad \text{in PST case} \quad (7)$$

$$g'' = Pr[2f'g - fg' - \beta g - Ec(f'')^2] \quad \text{in PIIW case} \quad (8)$$

And their associated boundary conditions are

$$f = 0; f' = 1; \quad \theta = 1; \quad g' = -1, \quad \text{at} \quad \eta = 0 \quad (9)$$

$$f'' = 0; \quad \theta = 0; \quad g = 0, \quad \text{as} \quad \eta \rightarrow \infty \quad (10)$$

Where  $Mn = \frac{\sigma B_0^2}{\rho B}$  is a Magnetic parameter and  $\beta = 2B$  is the elastic parameter,

$k_2 = \frac{\nu}{k}$  is the porous parameter. The non-linear differential equations (6), (7) and (8) of with appropriate boundary conditions given in (9) and (10) are first decomposed into a system of first order differential equations. The resulting initial value problem (IVP) then can be solved numerically by the shooting technique. The convergence criterion largely depends on fairly good guesses of the initial conditions in the shooting technique. Once the convergence is achieved then integrating the resultant ordinary differential equations using standard Runge-Kutta method with the given set of parameters to obtain the required solution.

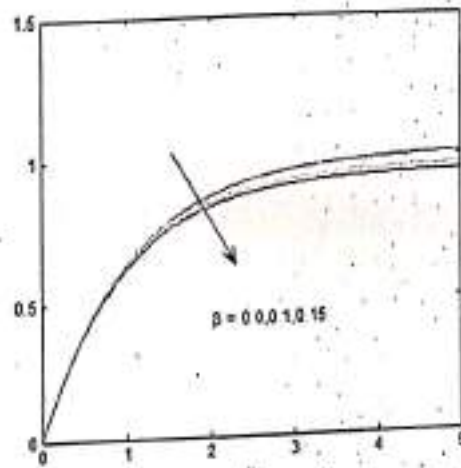


Fig.1. Transverse Velocity Profiles for Different Values of Elastic Parameter  $\beta$  and  $k_2=0.2$

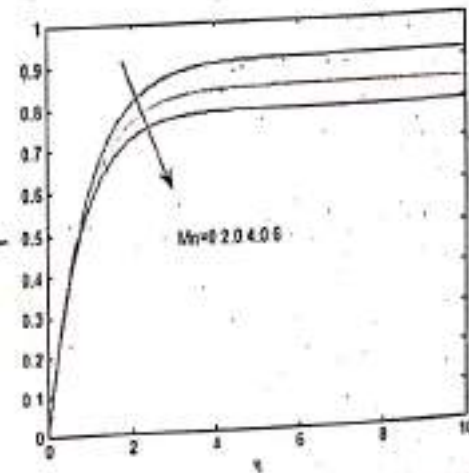


Fig.2. Transverse Velocity Profiles for Fixed Values of  $\beta = 0.05$  and Different Values of Mn

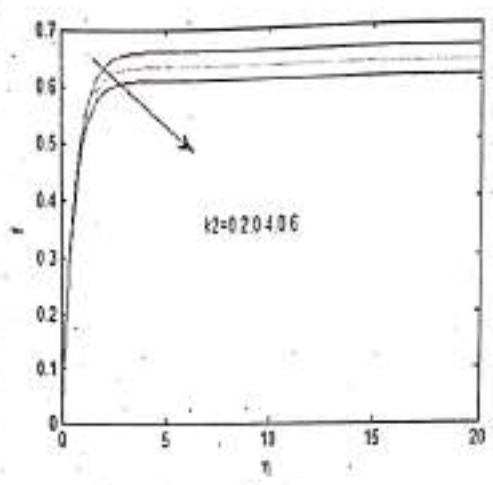


Fig.3, Transverse Velocity Profiles for Fixed Value of  $Mn=0.2$ ,  $\beta=0.05$  & Different Values of  $k_2$

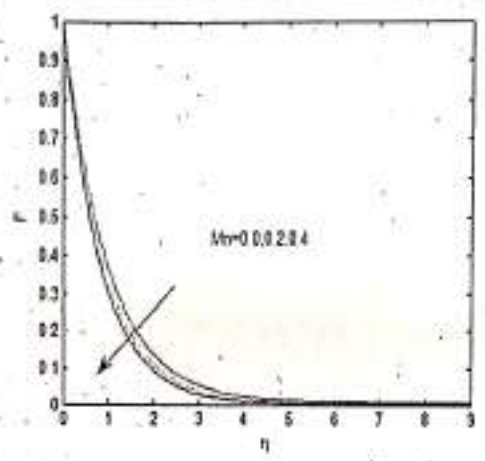


Fig.4 Longitudinal Velocity Profiles for Fixed Value of  $\beta=0.05$ ,  $k_2=0.2$  & Different Values of  $Mn$

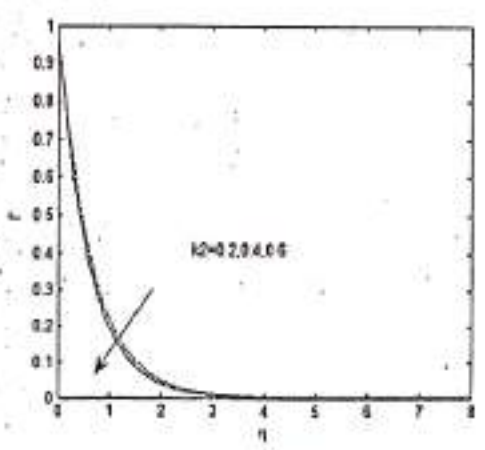


Fig.5, Longitudinal Velocity Profiles for Fixed Values of  $Mn=0.1$  and Different Values of  $k_2$



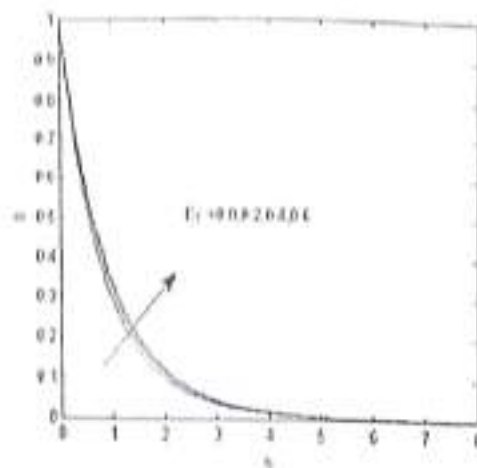


Fig.6. Temperature Profiles for Fixed Value of  $Pr=1$  and Different Values of  $Ec$

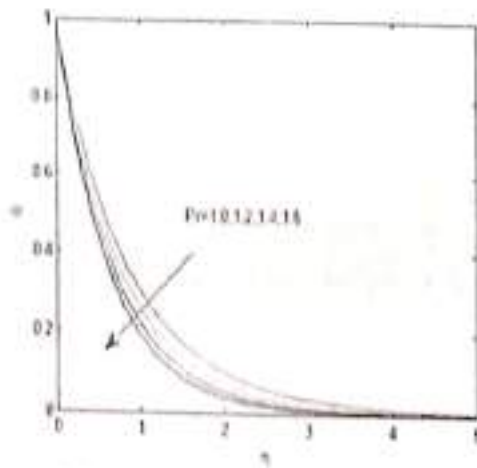


Fig.7. Temperature Profiles for Fixed Value of  $Ec=0.2$  and Different Values of  $Pr$

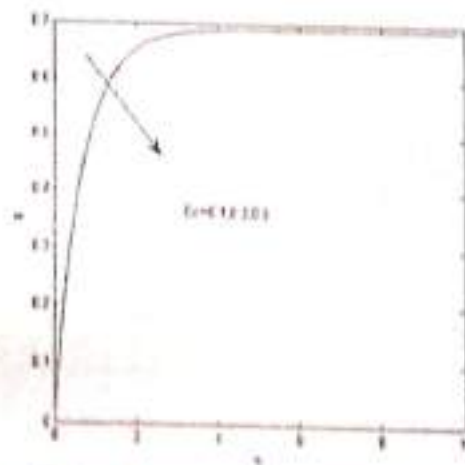


Fig.8. Temperature Profiles for Fixed Value of  $Pr=3$  and for Different Values of  $Ec$

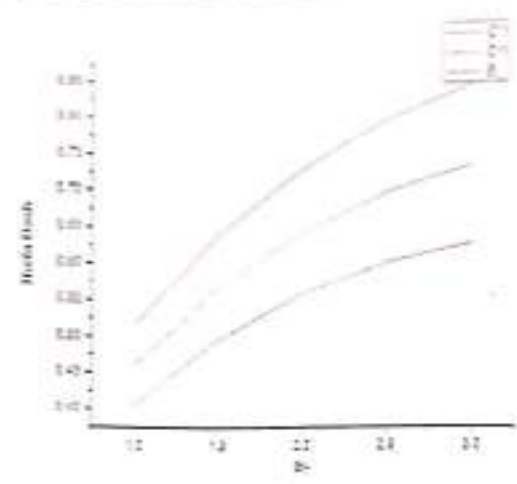


Fig. 9. Temperature Gradient in the PST case for  $Ec=1$ ,  $\beta=0.1$ ,  $Mn=1$  and for Different Values of  $Pr$

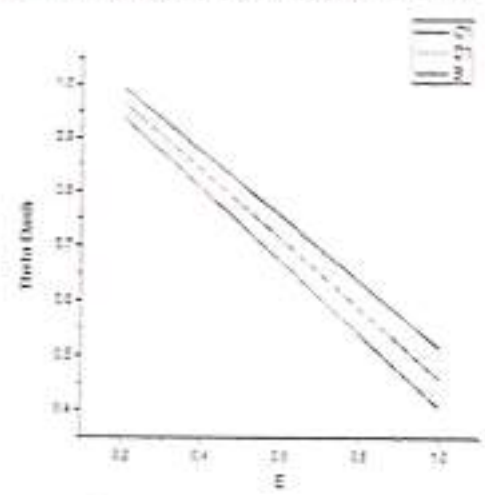


Fig. 10. Distribution of Wall Temp. in PHF Case for  $Mn=1$ ,  $\beta=0.1$ ,  $Pr=1$  and Different Values of  $Ec$

**Results and Discussions**

The study of ordinary differential equations (6)-(8) subject to the boundary conditions are solved numerically by Runge-Kutta fourth-fifth order method. Higher order non-linear differential equations (6) – (8) are converted into simultaneous linear differential equations of first order and they are transformed into initial value problem by applying shooting technique. The numerical calculation for the distribution of velocity, temperature and concentration across the boundary layer for different values of parameters are carried out.

The effect of elastic parameter  $\beta$  on the velocity profiles is shown in fig.1. It is observed from the graph that, the velocity decreases with increasing values of  $\beta$ . Effect of magnetic parameter  $Mn$  on the velocity profile is shown in fig. 2 with constant values elastic parameter  $\beta$ . It is noticed from the graph that, velocity decreases with increasing values of  $Mn$ . Fig.3 shows the variation of velocity for different values of permeability parameter  $k_1$ . The velocity boundary layer thickness decreases with increasing values of  $k_1$ . Longitudinal velocity profile is shown for different values of magnetic parameter  $Mn$  in fig.4. Variation of magnetic parameter  $Mn$  and other values keeping as constant, thickness of the boundary layer decreases. Fig.5 depicts longitudinal velocity profile for different values of  $k_1$ . As we increase the values of permeability parameter  $k_1$ , velocity profile decreases. Fig.6 illustrates the effect of Eckert number  $Ec$  on the temperature field. With increasing the values of Eckert number  $Ec$ , the boundary layer thickness increases. The effect of Prandtl number  $Pr$  on the temperature profile is shown in fig.7. It is observed from the graph that, thickness of the boundary layer decreases with increasing values of  $Pr$ . Temperature profile is shown for different values of Eckert number  $Ec$  in fig.8. It is noticed from the graph that, the boundary layer thickness decreases with increasing the values of



Eckert number  $Ec$ . The graphs of skin friction for different values of Prandtl number  $Pr$  are shown in fig.3-fig.4. It is observed from two graphs that the skin friction increases and decreases with increasing the values of  $Pr$  and  $Ec$ .

### Conclusions

In the present study of the flow, the effects of transverse magnetic field within a secondary layer of an UCM fluid over a stretching surface through porous media is analyzed. The resulting partial differential equations are converted into ordinary differential equations by using suitable transformations. These equations are highly non-linear which cannot be solved analytically. Therefore, employing ordinary differential equations are first solved numerically by using efficient numerical technique like fourth order Runge-Kutta method. The effects of various parameters on velocity, temperature profiles are discussed and presented graphically. The conclusions are as follows:

- The magnetic field parameter has a positive influence on skin friction coefficient.
- An increase in viscosity dissipation parameter enhances the thermal boundary layer.
- An increase in porosity number decreases the temperature profile.

### References

- Hayat T, Russaid M, Awais M and Shafiq S. Melting heat transfer in a secondary layer flow of a second grade fluid under stress and Joule effects. *Int. J. Numerical Methods for Heat and Fluid Flow* 16 (2013) 1489-1503.
- Pop I, Sujan A, Vajravelu K and Prasad K.V. MHD Flow and heat transfer of a fluid over stretching surface with variable thermo physical properties. *Mechanics* 47 (2012) 205-212.
- Vimala C and Loganathan P. MHD flow of nanofluid over an exponentially stretching sheet embedded in stratified medium with suction and radiation effects. *Journal of Applied Fluid Mechanics* 3 (2010) 33-39.
- Shateyi S and Mawoo G.T. A new numerical approach of MHD flow, heat and mass transfer for the fluid over a stretching surface in the presence of thermal radiation. *Mathematical Problems in Engineering*, Volume 2013, 1-8.
- Rahman M.M, Isahakuddin K.M. Study of hydro magnetic heat and mass transfer flow over an inclined heated surface with variable viscosity and electric conductivity. *Commun. Nonlinear Sci. Numer. Simulat.* (2011) 331-344.
- Prasad K.V, Pal Dular, Umesh V,PrasannaRao N.S. The effect of variable viscosity on MHD viscoelastic fluid flow and heat transfer over a stretching sheet. *Commun. Nonlinear Sci. Numer. Simulat.* (2011) 3073-3085.
- Rohati A.M, Ahmad S and Pop I. Flow and heat transfer over an unsteady stretching sheet with suction in nanofluid. *Int. J. Heat Mass Transfer* 55, 1899-1905 (2012).
- Jaluria Y,Manoj G, Paulosekian D, Vafai K and Wang L. Heat transfer in nano-fluids. *Adv. Mech. Eng. Article ID* 972973, 1-2 (2012).
- Bachok N, Ismail A and Pop I. Unsteady boundary layer flow and heat transfer of a nano-fluid over a permeable stretching shrinking sheet. *Int. J. Heat Mass Transfer* 55, 2032-2039 (2012).
- Singh P, Jangid A, Thiner N.S and Saha D. Effects of thermal radiation and magnetic field on unsteady stretching permeable sheet in presence of free stream velocity. *International Journal of Information and Mathematical Sciences* 9(1) 56-58 (2012).
- Motta S.S. A new spectral local linearization method for non-linear boundary layer flow problems. *Journal of Applied Mathematics*, Volume 2013, Article ID 429528, 1-15.
- Mahian O, Khamfari A, Kalogirou S.A, Pop I and Wangwong S. Review of the applications of nano fluids in solar energy. *Int. J. Heat Mass Transfer* 57, 506-524 (2013).
- Azizmanan I.I. Casson fluid flow of variable viscosity and thermal conductivity along exponentially stretching sheet embedded in a thermally stratified medium with exponentially heat generation. *Journal of Heat and Mass Transfer Research*, 1, (in press) (2013).
- Abbas Z, Sajid M and Hayat T. MHD boundary layer flow of an UCM fluid in a system channel. *Theoretical and Computational Fluid Dynamics*, 20-223-233 (2014).
- Rahman M. M and Eltayeb I.A. Radiative heat transfer in hydro magnetic nano fluid past a non-linear stretching surface with convective boundary condition. *Mechanics* 48, 401-415 (2013).
- Abel M.S, Tarwat I.V and Chandrashekar M.M. MHD flow and heat transfer for the UCM fluid over a stretching sheet. *Mechanics* 47, 385-393 (2012).
- Prasad K.V, Vajravelu K and Sujan A. Influence of internal heat generation, radiation, magnetic field, variable fluid property and viscous dissipation on heat transfer characteristics of a Maxwell fluid over a stretching sheet. *Journal of Applied Mechanics*, 6, 204-214, (2011).

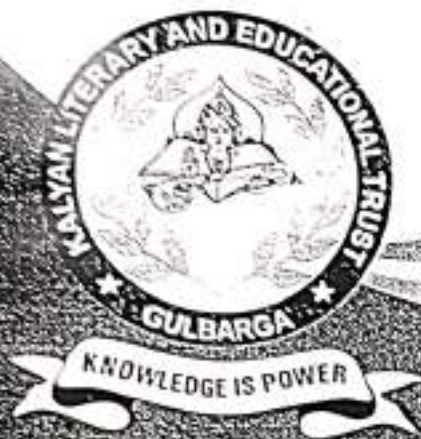
- Mahmoud M.A.A and Megahed A.M. Non-uniform heat generation effect on heat transfer of a non-Newtonian power-law fluid over a non-linearly stretching sheet. *Meccanica* 47, 1131-1139 (2012).
- Bhattacharyya Krishnendu, boundary layer flow and heat transfer over an exponentially shrinking sheet. *Chin. Phys. Lett.* 28(7) - (2011), 074701(1-4). (2013).
- Shateyi S, Motsa S.S and Makukula Z. On spectral relaxation method for entropy generation on a MHD flow and heat transfer of a Maxwell fluid. *Journal of Applied Fluid Mechanics*, 8, 21-31.(2015)

B-6

www.deccanjournal.com  
ISSN - 2321-0818



Impact Factor - 2.3



# INDIAN CHRONICLE OF ENGLISH LITERATURE

Indexed with International  
ISSN Directory, Paris

VOLUME : 5 • ISSUE : 7 • DEC 2017

Chief-Editor : Dr. B. O. Satyanarayana Reddy

Editor-in-Chief : Dr. U. S. Patil

IQAC Coordinator  
Smt. Veeramma Gangasiri  
College for Women  
Kalaburagi - 585102

PRINCIPAL  
Smt. Veeramma Gangasiri  
College for Women  
Kalaburagi - 585102



Reg. No. KAR.10/2-2012-TC

ISSN - 2321-0612

Indian Chronicle of English Literature is the official organ of Kalyan Literary and Educational Trust © to promote Literary, Cultural, Humanistic and Historic values among human beings and published bi-annually. It aims at recording and preserving through publishing the important critical and creative writings and events of English Literature of any nation of the world. It invites original and unpublished research papers and reports on a wide range of subjects, issues, trends, concepts, genres and related activities in English Literature including local literatures translated into English language.

Indian Chronicle of English Literature is a non-political, ideologically non-partisan journal, which gives importance to publish the papers and reports that present unbiased, objective, intellectual and humanistic opinions and ideas. All material published in Indian Chronicle of English Literature is exclusive to the journal and cannot be reprinted without the prior written permission of the publisher and the editor.

Copyright©: Publisher

The Editor reserves right to reprint/ reproduce the papers/ submission in any form. The journal is for restricted circulation only.

The Opinions expressed by the authors in their research papers, reviews etc., in the journal are their own. The editor is not responsible for them. All disputes concerning the journal shall be settled in the court at Kalburgi Dist. Karnataka State, India.

Printed and Published by Dr. H. S. Matti on behalf of Kalyan Literary & Educational Trust © KAR 10/2-2012-TC Printer : Bhagavathi Printer, Subedar Complex, Near Court, Kalaburgi Karnataka, India

Editorial Office:

**Dr. D T.ANGADI**

Krishna Krupa, Plot.No.26,  
Shree Hari Nagar, Jewargi Road,  
Kalaburgi-585102.

Cell No.: 09886045485, 9449133601

E-mail : [deccanliteraryjournal@gmail.com](mailto:deccanliteraryjournal@gmail.com)

[dtangadi2010@gmail.com](mailto:dtangadi2010@gmail.com)

[hosreddy@gmail.com](mailto:hosreddy@gmail.com)

ISSN 2321-0612



Printed and Published by Dr. H. S. Matti on Behalf of Kalyan Literary & Educational Trust © at "Krishna Krupa" Plot No. 26, Shree Harinagar, Jawargi Road, Kalaburgi, Karnataka, India

Edited by Dr. B.O. Satyanarayana Reddy

Printed at: Bhagavathi Printer, Subedar Complex, Near Court, Kalaburgi, Karnataka, India

IOAC ©  
Smt. Veeramma Gangasiri  
College for Women  
Kalaburagi - 585 102

PRINCIPAL  
Smt. Veeramma Gangasiri  
College for Women  
Kalaburagi - 585 102